This is to certify that the

thesis entitled
MECHANICAL BEHAVIOR OF
FIBROUS ORGANIC SOILS

presented by

Anwar S. Khattak

has been accepted towards fulfillment
of the requirements for

the PhD degree in Civil Engineering

O. B. Andersland

Major professor

Date Oct. 9, 1978

MECHANICAL BEHAVIOR OF FIBROUS ORGANIC SOILS

By

Anwar S. Khattak

A DISSERTATION

Submitted to
Michigan State University
in partial fulfillment of the requirements
for the degree of

DOCTOR OF PHILOSOPHY

Department of Civil Engineering

1978

ABSTRACT

MECHANICAL BEHAVIOR OF
FIBROUS ORGANIC SOILS

By

Anwar S. Khattak

It has been common practice for engineers to avoid organic soil deposits when constructing building foundations and highway embankments. Lack of information on the mechanical behavior of these soils and the potential for decomposition have been the major reasons. This study has been directed to the influence which organic fibers have on the stress-deformation and strength behavior of a model soil prepared from kaolinite and cellulose pulp fibers. Experimental work has included compression tests to evaluate the compressibility, direct shear and triaxial tests to observe the stress-strain response and to measure the shear strength parameters.

Various combinations of kaolinite and fiber were studied so as to encompass the full range of possible mechanical behavior. To provide data for comparison, compression and shear strength tests on kaolinite and fiber samples have been included. Physical properties of both clay and pulp fibers were determined prior to beginning the test program. Methods available from the pulp and paper industry were adopted for measurements of a weighted average fiber length. Surface area of fiber per gram of dry material was determined using methods

employed by soil scientists. The porous structure common to cellulose fibers was observed with the help of a scanning electron microscope.

The model soil can be considered to be a skeleton of clay particles and fibers enclosing both macro- and microvoids. Air and/or water fill the voids. When the model soil is subjected to an external load, compression of the sample occurs due to 1) compression of the solid matter, 2) compression of the gas and 3) drainage of water from the sample. Using compressive loads ranging from about 2 up to 350 kg/cm^2, the soil compressibility was observed in terms of change in void ratio for increasing stresses. A plot of void ratio versus logarithm of stress gives a linear curve which is typical for kaolinite. The kaolinite/fiber mixtures show a nonlinear relationship. The compression index or slope of these curves is a function of the soil organic content and the stress level. An immediate practical result concerns use of the compression index on field projects and the relationship it has to organic content and stress level.

Placement of normal or shear loads on the model soil produces first an elastic compression or displacement, and when the strength of the material is reached a compressive rupture or excessive shear displacement. The shear displacement results primarily from slippage between particles. Direct shear tests conducted on fiber samples showed that shear resistance continued to increase with shear displacement up to the limits of the test equipment. Shear resistance also increased with increase in normal stress suggesting a frictional type behavior. Triaxial tests on cylindrical samples included both drained ($\overline{CID}$) and consolidated-undrained tests ($\overline{CIU}$) on kaolinite, kaolinite/fiber mixtures, and all fiber samples. For undrained tests

on high fiber content samples excess pore pressures reached values equal to cell pressures at about 15+ percent axial strain. The stress difference continued to increase raising questions as to what stage of the test should be defined as failure. Use of the peak stress difference and/or 20 percent axial strain gave shear strength parameters (ϕ') which increased from 20 degrees for kaolinte to more than 80 degrees for all fiber samples. A new failure criterion, based on the peak value of the stress path defined by the maximum ratio of shear stress to effective normal stress, gave lower values of ϕ'. Consolidated-drained tests and failure based on 20 percent axial strain gave the lowest ϕ' values which ranged from 20 degrees for kaolinite up to 31 degrees for all fiber samples.

Availability of field data for an experimental slope failure in a fibrous papermill sludge with properties similar to the kaolinite/fiber mixtures permitted recomputation of the factor of safety. Use of ϕ' given by the consolidated-undrained tests and failure defined by the peak stress difference and/or 20 percent axial strain gave a factor of safety close to unity. This agreement with field behavior suggests that the shear strength parameter obtained from the $\overline{CIU}$ test appears to be best suited for field analysis problems relative to organic soils.

ACKNOWLEDGMENTS

The writer wishes to express his appreciation to his major professor, Dr. O. B. Andersland, Professor of Civil Engineering, for his encouragement, guidance and aid throughout the writer's doctoral studies. The writer wishes to acknowledge his gratitude to the other members of the doctoral committee: Dr. G. Y. Baladi, Assistant Professor of Civil Engineering; Dr. W. A. Bradley, Professor of Civil Engineering; Dr. M. M. Mortland, Professor of Soil Science and Dr. R. J. Kunze, Professor of Soil Science. The writer also wishes to express his appreciation to his colleague R. W. Lentz for his interest and suggestions.

Thanks are also extended to the National Science Foundation, the National Council of the Paper Industry for Air and Stream Improvement, and the Division of Engineering Research at Michigan State University for the financial assistance which made this research possible.

TABLE OF CONTENTS

LIST OF TABLES

LIST OF FIGURES

LIST OF SYMBOLS

A = Pore pressure coefficient

A_f = Pore pressure coefficient at failure

a = Contact area

a^* = Unit contact area

$a1$ = Cross-sectional area of a water molecule

B = Pore pressure coefficient.

b = Absorption coefficient

β_o = Constant

s = Compressibility of solids

C = Volume compressibility

c' = Shear strength parameter (cohesion)

C_s = Volume compressibility of solids.

C_v = Coefficient of consolidation

D_p = Particle density

d, d_w = Water density at different temperatures

e = Void ratio

e_o = Initial void ratio

F = Safety factor

G = Specific gravity

h_p = Hydrostatic pressure head

$k1$ = Boltzman constant

K_f ___ line = Line through $\bar{p}$ versus q

L = Weighted average length

l = Length

M = Molecular weight

m = Mass

N = Avogadro's number

n = Number

p = Pressure

p' = Pressure, effective stress basis

p_o = Saturation pressure

$\bar{p} = 1/2(\bar{\sigma}_1 + \bar{\sigma}_3)$

q, q_1, q_2 = Heat quantity

$\bar{q} = 1/2(\bar{\sigma}_1 - \bar{\sigma}_3)$

R = Molar gas constant

s, s_1 = Number of gas molecules

T = Absolute temperature

$t_1, t_2 \ldots t_i$ = Adsorption time

U = Pore pressure

U_f = Pore pressure, at failure

V = Volume

V_o = Initial volume

v = volume absorbed

v_m = Monolayer capacity

W = Total weight

w_1, w_2, w_3, w_4, w_5 = Weight

w_s, w_a, w_w, w_{sw} = Weight

X = Weight of moisture

α, α_o = Condensation coefficient

α = Inclination angle of force

α' = Slope of $\bar{p}$ versus q

β_o = Constant

β_s = Compressibility of solids

γ_s = Unit Weight, soil solids

γ_w = Unit weight, water

γ_{s_o} = Unit weight, soil solids at atmospheric pressure

Δu = Pore pressure increment

$\Delta p'$ = Pressure increment, effective stress basis

ΔV = Volume change

Δh = Change in height

Δx = Slice width

η_o = Constant

$\theta_o, \theta, \theta_1 \ldots \theta_i$ = Fraction of surface area

μ = Rate at which molecules strike a surface

ν, $\nu_1, \ldots \nu_i$ = Rate of departure of molecules

σ = Normal stress

$\bar{\sigma}$ = Effective normal stress

$\bar{\sigma}_{ff}$ = Normal stress on failure surface at failure

σ_1, σ_2, σ_3 = Principal stresses

τ_{ff} = Shear stress on failure surface at failure

$\tau_{\beta f}$ = Shear stress on the plane of maximum obliquity

τ_{tf} = Shear stress on the plane of tangency

τ_{mf} = Maximum shear stress at failure

τ = Time a molecule stays on surface

τ_i = Intrinsic line

τd = Failure envelope

$\bar{\phi}$ = Shear strength parameter, based on effective stresses

ψ = Inclination of intrinsic line

CHAPTER I

INTRODUCTION

One of the major problems facing the industrialized nations is the need for better utilization of land. In certain areas constructed facilities must now be designed for placement on organic soil deposits. Questions arise immediately as to how much settlement may occur and will the foundation be stable. In other areas shipping channels must be excavated through thick organic soil sediments. There is concern over stability of the side slopes as ships traverse the channel. Papermill operations are finding that their high ash sludge deposits occupy expensive land area which they now wish to use for other purposes. These sludge deposits are similar to organic soils and consist primarily of kaolinite and organic material. Questions arise as to compressibility, shear strength, and the potential for future decomposition of the organic component. This project is concerned with the mechanical behavior of these fibrous organic soils.

Much of the experimental work reported in the literature has been done on samples of peat, muskeg, or high ash papermill sludges. The investigators have been somewhat limited as to how they could vary the organic content, being restricted to field samples. In some cases organic content was not included with data reported on the mechanical behavior. Research on high ash papermill sludge showed that organic content had a very significant effect on both consolidation behavior

and shear strength. To provide an overall picture of how the organic component influences the mechanical behavior, it was decided to prepare a model organic soil from kaolinite and pulp fibers. The fibers, almost pure cellulose, are produced from soft or hard wood for the manufacture of paper. The physical nature of these cellulose fibers depend upon the type of wood (hard or soft) from which fibers are extracted. Cellulose fibers are by nature hydrophyllic and therefore highly compressible.

The weighted average fiber length and fiber particle specific surface area were measured using special tests common to paper technologists and soil scientists, respectively. Other physical properties of the pulp fiber and kaolinite were determined by standard tests. The kaolinite-fiber combinations resembled organic soils with high compressibility and low shear strength at the usual high water contents. The model soil mixtures were in most cases prepared by combining dry fluffed fiber with dry clay in the selected proportions and combining them with water. Stress history was accounted for during drainage to insure normal consolidation of triaxial samples. Compressibility of the model soil was observed using a special compression cylinder. Triaxial tests, both consolidated undrained and drained conditions, were run to determine the stress-strain behavior and shear strength parameters. Details are given in the appropriate sections.

The experimental results confirm that compressibility is highly dependent on organic content and stress level. For large stress changes the compression index is not constant as compared to kaolinite. Consolidation tests on samples from field sites is an appropriate means to determine the consolidation parameters for use in prediction of field settlements.

Strength tests on organic soils can be misleading. For undrained tests on high fiber content samples, excess pore pressures reached values equal to cell pressures at about 15 percent axial strain. The stress difference continued to increase raising questions as to what stage in the triaxial test should be considered failure. Use of the peak stress difference and/or 20 percent axial strain gave shear strength parameters (ϕ') which increased from 20 degrees for kaolinite to over 80 degrees for all fiber samples. A new failure criterion, based on the peak values of the stress path defined by the maximum ratio of shear stress to effective normal stress gave lower values of ϕ'. Consolidated-drained tests and failure based on 20 percent axial strain gave the lowest ϕ' values which ranged from 20 degrees for kaolinite up to 31 degrees for all fiber samples.

These experimental results did not answer the question as to which shear strength parameters are most suitable for field problems. Availability of field data on an experimental slope failure in a fibrous papermill sludge which is similar to the kaolinite/fiber mixtures permitted recomputation of the factor of safety. Using ϕ' from the consolidated-undrained test results corresponding to the organic content of the papermill sludge and extrapolation of field pore pressure data to the failure surface gave a factor of safety close to unity. This agreement between field behavior and the stability analysis suggests that ϕ' based on consolidated-undrained tests is most suitable for use on field problems which involve organic soils.

CHAPTER II

LITERATURE REVIEW

Information on the mechanical behavior of fibrous organic soils is limited. Often in the past it was easier and more economical to avoid these deposits or to replace them with select fill material. Recently due to the need for better utilization of land, much research has been conducted on the mechanical behavior of high ash papermill sludges. These materials are very similar to fibrous organic soils, hence much information is drawn from published research on these materials.

This literature review attempts to summarize the available information appropriate for this project on the mechanical behavior of organic soils. It is presented under the following headings: organic soils, physical properties of organic soils, surface area determination of small particles, compressibility of organic soils, and shear strength of organic soils.

2.1 Organic Soils

Organic soils are reviewed under the headings of natural deposits and landfills.

2.1.1 Natural Deposits

Organic soils consist of solids which are predominantly derived from plant matter in various stages of decomposition. The common designation is bog, muskeg, peat and muck. Muck has a higher degree of decomposition compared to peat which has plant remains relatively

well preserved (Winterkorn and Fang, 1975). The occurrence of organic soils depends upon the topographical and hydrological conditions of the terrain. Standing water and areas with rising water table are favorable conditions. Environment and plant ecologic factors have a significant influence on these soils which are best considered as organic terrain (Muskeg) and are classified according to the genetic principles as has been done by the Muskeg Subcommittee of the National Research Council of Canada (MacFarlane, 1969).

Identification is based on the organic content (Winterkorn and Fang, 1975), muck consists of thoroughly decomposed organic material with considerable amounts of mineral soil and some fiberous remains. When considerable fiberous material is present it may be classified as peat. The plant remains can sometimes be easily recognized. Color ranges from brown to black. Muck occurs in lowlands and swamps and has high shrinkage upon drying (Winterkorn and Fang, 1975).

The composition of peats is predominantly fiberous with a sponge-like nature which is related to their ability to have high natural water contents. The water content may vary from 50 percent to as high as 2000 percent. Void ratios are also high having an approximate range of 5 to 15. In certain cases a void ratio as high as 25 has been encountered. It has high drying shrinkage, up to 50 percent, low bearing capacity and high compressibility. The specific gravity of peat ranges from 1.1 to 2 and values above 2 indicate the presence of mineral matter which may be ascertained by the determination of ash content. The permeability of natural peat deposits varies widely and depends upon the effective size of the voids. It also depends upon the water that is held physicochemically on the external and the internal surfaces.

Permeability is usually greater in the horizontal direction than in the vertical (Winterkorn and Fang, 1975).

Low specific gravity of organic matter and water leads to low unit weights of peat. Tensile and shear strength of peat is provided in their natural state by the felt-like interwoven fibrous material. This is the reason why the tensile and shear strength do not always increase with decreasing water content. Peat will not display its original high water content after it has been once dried upon rewetting. Natural peat shows a decrease in strength once its natural structure is disturbed. The sensitivity of peat varies from 1.5 to 10 (Winterkorn and Fang, 1975).

2.1.2 Landfills

The paper industry removes a large percentage of the suspended and dissolved matter from their effluent streams. In the United States an estimated 2,500,000 dry tons (2.300×10^6kg) of waste solids, having a volume close to 200,000,000 cubic yards ($150 \times 10^6 m^3$) are removed annually (Gillespie, Mazzola, and Gillman, 1970). Today, disposal of these large volumes of pulp and papermill sludges presents a major problem for the paper industry. More than 1,100 acres ($4,450,000 m^2$) of land are used as depositories for these man-made waste materials. Disposal to date has been accomplished by some type of landfill operation, usually lacking rationale and being only a temporary measure. The procedure has been to purchase conveniently located waste land such as an abandoned gravel pit, fill this area to the elevation of the surrounding area, then cover the sludge with a layer of soil and move the operation to a different area. Only in a limited number of

cases has any attempt been made to place the sludge in an embankment above ground and then it has been mixed with sand and gravel. Bacon (1967) has suggested the possibility of using sludge as an economical method for land reclamation, especially in marginal lands, coal mining areas, etc. A survey conducted by Gillespie (1969) indicated that landfills are in wide use for the disposal of papermill waste solids throughout the United States. However, landfills are not necessarily an inexpensive or trouble-free means of disposal. Many land disposal sites have experienced difficulties with the waste. Part of these difficulties arise due to the lack of understanding of both the engineering properties and field behavior of these materials. In order to use this material safely in the form of embankments or foundation material for structures the behavior of the material from an engineering point of view must be understood. Since the composition of these sludges is very similar to that of peat or muskeg it is assumed that the behavior would approximate that of highly organic soils.

2.2 Physical Properties of Organic Soils

Physical properties of organic soils characterize, to some extent, the quality of the material relative to engineering purposes. The properties discussed below include the description and structure, density, and swelling properties.

2.2.1 Description and Structure

The term cellulose represents a group of high molecular weight substances. The most reliable molecular weight values have been obtained by the ultracentrifugal method (West and Todd, 1955). This method gives the average molecular weight of native cellulose as about

570,000 and for pure cellulose which is partly broken down as 150,000 to 500,000. The structure of the repeating units of the cellulose chain is expressed as follows.

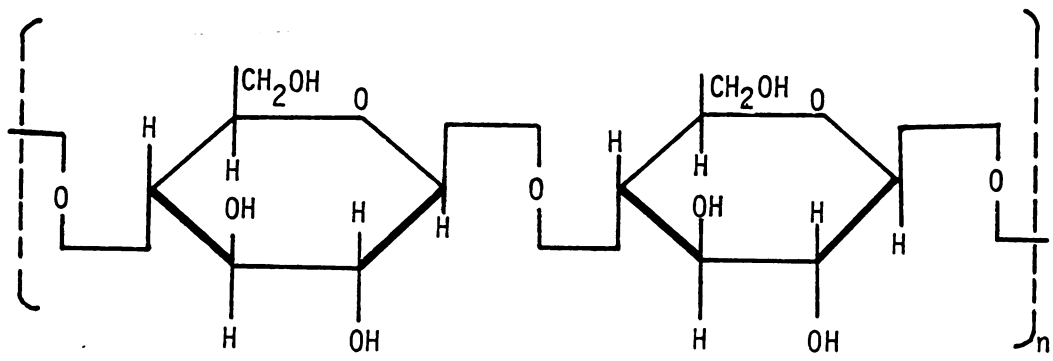

Figure 2.1. Repeating celluboise unit of cellulose (White, Handler and Smith, 1964).

Cellulose fibers are composed of amorphous and crystalline regions. X-ray analysis of cellulose fibers reveal that they consist of bundles of cellulose chains running parallel. These chains are held together horizontally by hydrogen bonds between the alcoholic hydroxyl groups. The cell wall, for example, may be thought of as a finely interwoven network of cellulose strands of varying complexity and size. The smallest structural units of the cell wall are called the elementary fibrils or micelles. These micelles consist of approximately 100 individual chains of cellulose and have an estimated cross-sectional area of 3000$\mathring{A}^2$. The next larger strand called the microfibril is thought to be composed of approximately 20 micelles and the cross-sectional area is about 62500$\mathring{A}^2$. The individual cellulose molecular chains cannot be observed with the scanning electron microscope but the micelles and the microfibrils are clearly discernable when viewed under the electron microscope. A combination of approximately 250

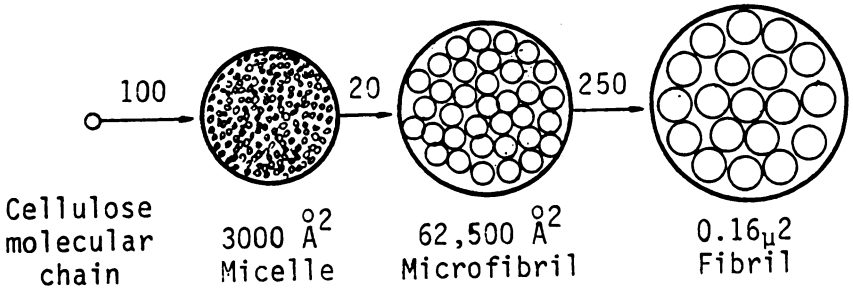

Figure 2.2 Diagrammatic representation of the association of molecular cellulose strands showing the approximate cross-sectional area (after Denlin, 1966).

microfibrils will make a microscopic fibril having a cross-sectional area of about $0.16\mu^2$. A cotton fiber which is easily visible to the unaided eye may contain as many as 1,500 fibrils. A simple calculation will show that there are about 7.5×10^8 individual molecular cellulose chains in one macroscopic cotton fiber which is 90 percent cellulose, for example (Figure 2.2).

$100 \times 20 \times 250 \times 1500 = 7.5 \times 10^8$ chains.

2.2.2 Density

Cellulose fibers are considered a porous body with large inner surfaces. The body of the fiber is considered porous due to existence of minute internal voids. In order to determine the density a buoyancy medium which may be a liquid or a gas is required. The true volume of a porous body is understood to be the external volume of the body minus the volume of the internal voids. The true density therefore depends upon the true volume. The results of density determination obviously depend upon the penetrating capability of the buoyancy medium into all voids in the porous body. If the pores are not completely filled the density values determined will be too low whereas higher values of density can be obtained for the same porous material if the buoyancy medium used is such that it could get compressed within the pores of the body. This has been found (Hermans, 1949) to be the case when gases such as hydrogen and air are used in porous carbon. According to Hermans (1949) Williams reported that with ceramics, and Cude et al (1920) with charcoal, the density found depends upon the displacement medium used. Varying values of carbon density were obtained using different organic liquids and

these values were smaller than the values obtained utilizing X-rays. When gases, such as air, were used the values of density obtained were higher since air was absorbed by the carbon and compressed (Hermans, 1949). According to Hermans (1949), Howard and Hullet utilized helium as the buoyancy medium for the density determination of carbon and reported values of density close to the true values because helium was not absorbed by the carbon. These findings were adopted to cellulose fibers by Heertjes (1938). Table 2.1 shows the values of cellulose densities obtained by using helium, toluene, and water as a buoyancy medium. Note that density values obtained are lower in organic liquids compared to those obtaining using water which are higher than values determined using helium. According to Hermans (1949), Davidson also discovered that equal values are obtained when benzene, tuluene, chloroform and nitrobenzene are used as the displacement medium. Organic liquids produced density values which are too low because these liquids failed to penetrate the small voids in the cellulose fiber. Water has the capability of penetrating the pores of the cellulose fiber therefore producing a higher value of the density. Small helium atoms, on the other hand, can penetrate the pores without any resistence and fill the pores entirely. Density and porosity are typically macroscopic concepts. This property is of practical value only if applied to bodies or voids with physical dimensions which are very large compared to molecular dimensions.

Neither volume nor density can be defined in the usual sense without taking into account the relative dimensions and shape of the molecules of the substance and the buoyancy medium. Consider a pile of spheres, the bulk density of which is required to be determined by

TABLE 2.1. DENSITIES OF CELLULOSE FIBERS IN VARIOUS BUOYANCY AGENTS (AFTER HERMANS, 1949)

Author and object	Buoyancy medium used		
	Helium	Toluene	Water
G. F. Davidson			
Native cotton			
American Upland	1.567	1.550	1.6095
Sea Island	1.558	1.548	1.6038
Sakel	1.563	1.550	1.6061
Mercerized cotton			
American Upland	1.550	1.536	1.6066
Sea Island	1.546	1.531	1.6017
Sakel	1.550	1.536	1.6041
Viscose rayon	1.548	1.534[1]	1.6081
Cuprammonium rayon	1.531	1.522	1.6005
Nitrocellulose rayon	1.543	1.529	1.6149
W. Biltz		Heptane	
Native cotton	---	1.540	---
Viscose rayon	---	1.516	---
H. L. Bredée		Benzene	
Viscose rayon, little orientated	---	1.513	1.604
better orientated	---	1.519	1.608
greatly stretched	---	1.522	---
Lilienfeld rayon	---	1.534	1.594

[1]This value of Davidson's is undeniably far too high. In all later investigations lower figures were found for rayon.

using a medium which consists of smaller spheres. The result would depend upon the relative dimensions of the spheres and will follow the rules of spherical packing. If the spheres of the medium are small enough to penetrate the voids between the larger spheres the density values obtained will be suddenly increased compared to the density values obtained by utilizing a medium consisting of larger spheres unable to penetrate the voids. The same principle applies to porous bodies and the density values obtained would depend as to how accessible the pores are to the molecules of the displacement medium. The

ease with which a buoyancy medium can penetrate a porous body would also depend to a certain extent upon the molecular coarseness of the pore walls (Hermans, 1949). Contraction resulting from mixing two types of spheres can also be explained on the basis of geometrical reasons if the molecules of one liquid like water penetrate and settle themselves in the voids between the molecules of some other substance. The macroscopic density of a substance is greater in the crystallized state when compared to the same substance in its amorphous state with few exceptions of which water is one. The reason is the less orderly arrangement of molecules in the amorphous state resulting in larger empty spaces between the molecules. Since cellulose fibers consist of a mixture of crystalline and amorphous regions (Eirich, 1958) obviously the density would depend upon the quantitative distribution of the crystalline and amorphous parts. The high density values of cellulose in water are considered normal results of the homogeneous mixing of water and cellulose in the amorphous portion (Hermans, 1949). The bulk density can be determined using a liquid which does not penetrate into the fiber substance but envelops it. The density obtained in this fashion would be the macroscopic or bulk density.

2.2.3 Swelling Properties

When water is accessible to fibers, absorption starts and fibers commence to swell. The first stage of swelling consists of the formation of hydrates. More and more water is attracted resulting in further covering of the chains in the amorphous regions. Swelling accompanied by the formation of thick layers of water continues. This last stage is termed "capillary condensation" with capillaries forming after

swelling takes place (Hermans, 1949). According to Hermans (1949), the end value of swelling should not be associated directly with the percentage of the amorphous substance present. The final swelling value probably depends upon the structure of the micellar system or in other words the extent to which the geometrical structure can expand while absorbing water without giving rise to resistance caused by excessive strain. Swelling characteristics can be substantially affected by introducing a slight change in the gel structure. Swelling in rubber can be reduced by vulcanization and the extent of this reduction depends upon the number of cross linkages (Hermans, 1949) introduced in the structure. It is obvious that the structure and the swelling characteristics, especially of artificial fibers, will depend upon the conditions under which these fibers were manufactured. Depending upon the history of drying, causing the introduction of cross linkages, the swelling characteristics of fresh fibers and fibers subjected to drying should be expected to be different. According to Hermans (1949) an interesting observation made by Risch, after treating rayon filaments for three hours under pressure with water vapor at 103° to 115°, was that water absorption dropped to approximately one-half of the initial value while swelling. In its dry state, the cellulose fiber is brittle and nonflexible. Cohesive forces in the micellar system are so powerful at all points that it becomes rigid. Thus water is a typical softener to cellulose (Hermans, 1949).

Attention should be given to the dual function of the hydroxyl groups in cellulose. The firm cohesion between molecules in a cellulose gel and the insolubility of cellulose in water is a result of the powerful forces between OH groups which are also responsible for

the hydrophyllic nature of cellulose. This duality can be explained as follows. The first function is due to those hydroxyl groups which are reciprocally bound by hydrogen bonds and the second function is because of the presence of free OH present in other locations (Hermans, 1949). Hydrogen bonds form where the chains are very close to each other and where the maximum degree of order exists. Whenever the hydroxyl groups of the neighboring chains are not in close proximity they remain free due to their inability to act at large distances.

One of the more important facts (Hermans, 1949) relative to swelling of fibers is the change in dimensions revealing the anisotropy of fibers. Almost all the dimensional changes take place widthwise with relatively negligible change lengthwise. This behavior is due to molecular chains which are oriented in the direction of the fiber axis. Water can only penetrate the fiber laterally between the chains or between the crystalline regions. According to Hermans (1949), Urquhart reports that volume change due to swelling of cotton in water is approximately 45 percent. Lengthwise swelling is less than 1 percent. Artificial fibers from cellulose swell by 70 to 100 percent with only 2 to 5 percent longitudinal swelling.

2.3. Surface Area Determination of Small Particles

Surface area of small particles provides the geotechnical engineer with information that helps explain the mechanical behavior of the material. Some knowledge of the methods used to measure surface area provides a background for discussion in later sections. A review of absorption, the solid-gas interface, the Langmuir and B.E.T. (Brunauer, Emmett, and Teller, 1938) equations are presented since sorption of

nitrogen and water vapor have been used to determine surface area of the pulp fibers.

2.3.1 Adsorption

Part of the gas or vapor is taken up by an evacuated solid when they are allowed to come in contact with each other. If this process is allowed to occur at constant volume the pressure will drop or if the pressure is kept constant a reduction in volume will result. The gas molecules lost to the solid from the gas phase either penetrate inside the solid or settle on the surface of the solid. The former phenomenon is termed absorption and the latter adsorption.

Absorption and adsorption often occur simultaneously. The total uptake of the gas by the solid is called sorption. In order to study adsorption the experiments must be conducted at temperatures, pressures and concentrations at which either the absorption of the gas is negligible or the two processes can be isolated with an acceptable degree of accuracy. Adsorbent is defined as the solid that takes up the gas. The gas or vapor attached to the surface of the solid is designated as the adsorbate. It is usually difficult to distinguish whether the gas or vapor molecules are inside or on the surface of the solid. Most solids are highly porous bodies having large internal surface areas. The external surface, studied under the best microscope, is only a small fraction of the large total surface. Gas molecules are considered to be on the outside even if they are adsorbed on the internal surface of solid as long as they do not penetrate into the field of force that exists between atoms, ions or molecules inside the solid.

If the gas penetrates the inside of the adsorbent there are two possibilities that might result: the gas dissolves in the solid forming a solid solution or a compound may result due to the reaction between the gas and the solid. If the gas molecules settle on the surface of the solid, again, there are two events that could happen: a weak interaction may take place between solid and gas similar to condensation or a strong interaction like chemical reaction may result. The first weak interaction is defined as physical adsorption and the strong interaction is called chemical adsorption or chemisorption (Brunauer, 1943).

2.3.2 The Solid-Gas Interface

The surface of the adsorbent is the place where gas and solid come in contact with each other. The molecules and atoms in the solid are firmly held in place due to the existence of several active forces like, electrostatic, Van der Waals, etc. In solids several of these forces are in action simultaneously with one or the other predominating. An atom located inside the solid is subjected to an equal force from every direction regardless of the nature of the operative forces. An atom situated in the plane of the surface is under the action of an inward pull and therefore under unbalanced forces resulting in a tendency of volume shrinkage and a decrease of surface. A solid has surface tension just like a liquid. The surface tensions of solids are much greater than those of liquids. The surface tension of benzene at 20°C is 28.8 dyne/cm while that of Barium Sulphate is 310 dyne/cm (Brunauer, 1943).

The free surface energy is defined as the product of the surface

tension and the surface area. Any process which carries a tendency to decrease the free surface energy proceeds spontaneously. The molecule or atom of the gas adsorbed by the solid relieves some of the unbalanced surface tension force. Therefore, all adsorption phenomenon that may be physical or chemical are spontaneous and cause a decrease of the free energy of the system (Brunauer, 1943).

The adsorbed molecules are either held rigidly to the surface or they can shift over the surface freely in two dimensions. Before adsorption gas molecules were free to move in all three directions, therefore the adsorption process is also associated with a decrease in entropy. All adsorption processes are exothermic. The decrease in the heat content of the system is called the heat of adsorption. The heat of the physical adsorption of nitrogen on an iron catalyst is about 2000-3000 calories per mole. The heat of chemisorption of nitrogen on the same surface is 35,000 calories per mole (Brunauer, 1943). In the former case nitrogen is adsorbed in the molecular form while in the latter case it dissocates into atoms. Only one chemisorbed layer results since the surface iron atoms and nitrogen atoms mutually saturate each others free valence forces. In physical adsorption adsorbed nitrogen molecules on the iron surface can absorb a second layer of nitrogen molecules and these in turn can attract a third layer and so on. Single layer adsorption on the surface is called unimolecular or monomolecular adsorption. More than one layer is designated as multimolecular.

2.3.3 The Langmuir Equation

There was no satisfactory theoretical treatment available that could be applied to surface adsorption until the year 1914. In the year 1915, according to Brunauer (1943), Polanyi and Langmuir presented their independent theories. The approach taken by each individual was different. Langmuir believed that the adsorption phenomenon was a chemical process and the adsorbed layer was a single layer which is termed a monomolecular layer or unimolecular layer. Polanyi on the other hand claimed that the adsorption was a physical process and the adsorbed molecules formed several layers on the surface of adsorption. Both of these approaches are correct within their limitations. Polanyi's theory applies to Van der Waals adsorption whereas Langmuir's theory can be applied to both physical and chemical adsorption. There are at present several isotherm equations (Brunauer, 1943) that have been developed which fit satisfactorily the experimental data but in most of their derivations the starting point is the Langmuir equation. For this reason the Langmuir equation is considered to be the most important equation in the field of adsorption and therefore the original kinetic derivation of Langmuir will be reviewed.

The kinetic derivation (Brunauer, 1943) assumes that the molecules of gas and vapor are in constant agitation. When these molecules are allowed to come in contact with a solid surface, two things can happen. The collisions taking place between the molecules and the solid surface may be an elastic collision, i.e., rebounding the molecules into the gas phase or inelastic collision where the molecule rests on the solid surface for a certain length of time. No exchange of energy

takes place between the surface and the gas molecules during elastic collision whereas energy exchange does take place during inelastic collision since the molecule stays in contact with the surface for a certain period of time before it leaves the surface and returns to the gas phase. Langmuir (1918) believed that this time lag was responsible for the phenomenon of adsorption. Ordinarily, the collision is inelastic, however, very infrequently elastic collisions may occur. At high temperatures the time of stay of the molecules on the surface is very short and therefore thermal equilibrium is not reached. On the other hand in chemisorption which involves strong binding between the molecules and the surface the time lag may be long.

Langmuir let the rate at which the molecules strike the surface be denoted by μ and let the rate of departure of the molecules from the surface be denoted by ν. The net rate of adsorption is therefore given by (Brunauer, 1943)

$$\frac{ds}{dt} = \alpha\mu - \nu \qquad (2.1)$$

where s denotes the number of gas molecules adsorbed per unit area, say, per square centimeter surface. The ratio of the number of molecules that condense on the surface to the total number of molecules that strike the surface is termed the condensation coefficient and in the above equation it is denoted by α. As mentioned earlier, the elastic collisions are infrequent, therefore the numerical value of α is always close to unity. When equilibrium is established the number of molecules adsorbed equals the number of molecules that are departed, therefore,

$$\frac{ds}{dt} = 0, \text{ and} \tag{2.2}$$

$$\alpha\mu = \nu \tag{2.3}$$

which is the isotherm equation in its most general form. From the kinetic theory of gases the value of μ for a unit surface is obtained from the following relationship (Brunauer, 1943)

$$\mu = \frac{p}{(2\pi mkT)^{\frac{1}{2}}} \tag{2.4}$$

where m denotes the mass of the gas and k denotes the Boltzmann's constant. The value of ν is a function of the binding strength between the solid surface and the molecules of the adsorbate. If q is the quantity of heat that is released during the adsorption of a single molecule then the molecules that would desorb will be the ones which require heat equal or greater than q. The rate of evaporation will then be given by (Brunauer, 1943)

$$\nu = k_o e^{-q/kT} \tag{2.5}$$

The average probability of evaporation per second for a single molecule is obtained if ν is divided by s, i.e., the number of molecules that leave a unit area of surface per second by the total number of molecules adsorbed on a unit area of surface. The reciprocal of this quantity (ν/s) will yield the average time that a molecule stays on the surface,therefore

$$\tau = s/\nu \tag{2.6}$$

The prevalent forces during the adsorption process are effective only through short distances. The effectiveness of the forces dies down with distance. Valence forces decrease exponentially with increasing

distance between the surface atoms and the molecules of the adsorbed molecules and the Van der waals forces decrease with the seventh power of the distance (Brunauer, 1943). Because of this very rapid decay of force with distance it is very unlikely that a surface covered with a single layer of adsorbed molecules will still have sufficient residual effective force left to provoke the settlement of a second layer of molecules on top of the first layer. But a second layer may form if the force of interaction between the molecules adsorbed on the surface and the molecules in the gas phase are sufficiently strong. The equation $\nu = k_o e^{-q/kT}$ indicates that a small change in the heat quantity q can cause a large change in the rate of evaporation. Let q_1 be the heat of adsorption in the first layer and q_2 be the heat of adsorption in the second layer. Langmuir (1932) has discussed the two cases, $q_1 < q_2$ and $q_1 > q_2$. When $q_2 > q_1$, i.e., when the forces between the molecules of the adsorbate are greater than the forces between the molecules of the gas and the molecules of the surface, the molecules of the adsorbate will adsorb on the surface in clusters. On top of these single layer clusters, a second, third or higher layers of molecules may form before the monomolecular layer on the surface is complete. For example, when molecules of iodine, cadmium or mercury condense on a glass surface at not too low temperatures, crystals of the condensed substance are formed, clearly demonstrating that the force between two iodine molecules is larger than the force between an iodine molecule and molecules of the glass surface (Brunauer, 1943). Langmuir (1932) believed that when $q_2 > q_1$, discontinuous condensed films are obtained, rather than true Van der Waals adsorption. If this situation

exists then the isotherm obtained are convex towards the horizontal axis (pressure axis). In the case of the more usual types of isotherms the part of the curve at low pressure is concave towards the horizontal pressure axis. In this case $q_1 > q_2$. As the pressure increases the surface is progressively covered with a monomolecular layer of adsorbate. In chemisorption q_1 is very large compared to q_2 and therefore the formation of second adsorbed layer does not result. In Van der waäl's adsorption q_1 is slightly greater than q_2 and therefore the formation of a second layer commenses before the completion of the first layer occurs. The quantities α, μ and ν are functions of p, T and s. Instead of using the surface concentration, the fraction of the surface covered with molecules can be used. Let s denote the number of molecules per square centimeter, then

$$\theta = s_1/s \tag{2.7}$$

where s_1 denotes the number of molecules which cover the fractional area θ. Langmuir has introduced two assumptions in his derivation. The first assumption states that the probability of evaporation of the adsorbed molecule is the same regardless of whether the space on the surface adjacent to adsorbed molecule is occupied by another molecule or not. In other words, the mutual force exerted by adjacent molecules resting on the surface is neglected. This assumption is expressed mathematically (Brunauer, 1943) as,

$$\nu = \nu_1\theta \tag{2.8}$$

where ν_1 denotes the rate of evaporation from a completely saturated surface. The above equation also assumes that uniform heat of

adsorption is taking place over the entire surface. Langmuir's second assumption states that molecules from the gas phase that strike the already adsorbed molecules on the surface rebound elastically and returns to a gas phase where those molecules from the gas phase that strike the bare surface condense on the surface. This assumption is expressed mathematically (Brunauer, 1943) as,

$$\alpha\mu = \alpha_o(1-\theta)\mu \tag{2.9}$$

where $(1-\theta)$ is portion of the surface unoccupied by the adsorbate molecules and α_o is the ratio of the number of molecules that condense on the surface to the number of molecules that strike the surface. Because elastic collisions are infrequent on the bare surface the numerical value of α_o is close to unity. Substituting $\nu = \nu_1\theta$ and $\alpha\mu = \alpha_o(1-\theta)\mu$ in $\alpha\mu = \nu$ gives

$$\nu_1\theta = \alpha_o(1-\theta)\mu \tag{2.10}$$

$$\nu_1\theta + \alpha_o\theta\mu = \alpha_o\mu \tag{2.11}$$

$$\theta = \frac{\alpha_o\mu}{\nu_1 + \alpha_o\mu} = \frac{\frac{\alpha_o}{\nu_1}\mu}{1 + \frac{\alpha_o}{\nu_1}\mu} \tag{2.12}$$

This is the Langmuir isotherm equation (Brunauer, 1943). This equation is usually written in the form

$$\theta = \frac{bp}{1 + bp} \tag{2.13}$$

where b denotes the absorption coefficient and is calculated from the relationship (Brunauer, 1943),

$$b = \frac{\alpha_o e^{q/kT}}{k_o (2\pi mkT)^{\frac{1}{2}}} \qquad (2.14)$$

If v denotes the volume adsorbed at pressure p and v_m denotes the total volume adsorbed when the surface is covered with a complete monomolecular layer, then

$$\theta = v/v_m \qquad (2.15)$$

substituting $\theta = \frac{bp}{1 + bp}$ for θ (2.16)

gives $v = \frac{v_m bp}{1 + bp}$.

The two assumptions in the Langmuir derivation of the isotherm equation restricts the application of this equation yet this equation has found its use in a large number of instances (Brunauer, 1943).

2.3.4 The B.E.T. Equation

When molecules strike a layer of molecules that are already adsorbed on the surface and if the force of attraction between the striking molecules and the adsorbed molecules is sufficiently great, then their time of adsorption may not be small enough to be neglected. If this happens then conditions for multimolecular adsorption are met. Attempts have been made for the derivation of an isotherm equation for multimolecular adsorption. The most successful attempt was made by the combined effort of Brunauer, Emmet and Teller (1938). They also assumed in their derivation that the molecules of one layer do not mutually influence each other while the building up of the layer progresses. They have also made the assumption that the adsorption energy

of the first layer is constant and the heat of adsorption in each of the following layers is also constant.

They let θ_1 represent the fraction of the surface area that is covered by a single layer of molecules and θ_2 represent the fraction covered by two layers of molecules such that one layer is resting on top of the other. Similarly, θ_3 represents the fraction of surface area covered by a layer which is three molecules thick, hence θ_i will represent part of the surface area covered by a layer the thickness of which is equal to i molecules. If the unit area is taken to be one square centimeter then the total number of molecules adsorbed on one square centimeter area is (deBoer, 1953),

$$\eta = \eta_o\theta_1 + 2\eta_o\theta_2 + 3\eta_o\theta_3 + ,. . .,i\eta_o\theta_i + ,. . . \qquad (2.17)$$

where η_o is the number of molecules that would cover a unit area of one square centimeter with a complete unimolecular layer.

$$\eta = \eta_o \sum_{i=1}^{i=\infty} i\theta_i \qquad (2.18)$$

When equilibrium is reached the fractions θ_1, θ_2,. . .,θ_i remain constant. This also means that the bare part of the area is also constant. If we denote the bare fraction of the area by θ_o then

$$\theta_o = 1 - \theta_1 - \theta_2,. . .,\theta_i \qquad (2.19a)$$

or

$$\theta_o = 1 - \sum_{i=1}^{i=\infty} \theta_i \qquad (2.19b)$$

Since the fraction θ_o remains constant at equilibrium, this means that the number of molecules adsorbed on the bare area (reduces θ_o) should be equal to the number of molecules that evaporate (increases

θ_o) from a layer one molecule thick. If the number of molecules adsorbed is $n\theta_o$ and the number of molecules evaporating from fraction θ_1 is $\nu\eta_o\theta_1$, then

$$n\theta_o = \nu\eta_o\theta_1 \tag{2.20}$$

where n is the number of molecules striking one square centimeter area per second and ν is the rate of evaporation. Similarly the fraction θ_1 is maintained by molecules adsorbed on the bare surface ($n\theta_o$) and by moleclues evaporating from the top layer of the fraction $\theta_2(\nu_1\eta_o\theta_2)$. Both of these phenomenon will increase the fraction θ_1 and in order to maintain θ_1 constant there must be molecules evaporating from θ_1 and other molecules being adsorbed on top of θ_1 (deBoer, 1953). For example,

Adsorption on bare surface = $n\theta_o$.

Evaporation from $\theta_2 = \nu_1\eta_o\theta_2$

Increase in $\theta_1 = n\theta_o + \nu_1\eta_o\theta_2$

Evaporation from $\theta_1 = \nu\eta_o\theta_1$

Adsorption on $\theta_1 = n\theta_1$

Decrease in $\theta_1 = n\theta_1 + \nu\eta_o\theta_1$

Since θ_1 should remain constant, $n\theta_o + \nu_1\eta_o\theta_2 = n\theta_1 + \nu\eta_o\theta_1$. Since $n\theta_o = \nu\eta_o\theta_1$, then $n\theta_1 = \nu_1\eta_o\theta_2$.

Continuing the argument in a similar fashion, $n\theta_{i-1} = \nu_{i-1}\ \eta_o\ \theta_i$. Since ν_i denotes the rate of evaporation from a unit surface the reciprocal of this rate of evaporation will give the time of adsorption, therefore, $t_i = \frac{1}{\nu_i}$.

Substitution gives the following set of equations (deBoer, 1953)

$$\begin{aligned} n_o\theta_1 &= t\, n\, \theta_o \\ n_o\theta_2 &= t_1\, n\, \theta_1 \\ &\cdots \\ n_o\theta_i &= t_{i-1}\, n\, \theta_{i-1} \end{aligned} \tag{2.21}$$

where t denotes the time of adsorption of those molecules which are directly resting on the surface, t_1 denotes the time of adsorption of the molecules adsorbed on the first layer and so on. Since the mutual attracting forces between the molecules of the same kind is approximately the same the time of adsorption of a molecule bound on top of another molecule of the same type will be the same regardless of the number of layers (deBoer, 1953). Therefore,

$$t_1 = t_2 = ,\ldots, = t_{i-1} \tag{2.22}$$

From the above equations,

$$n_o\theta_2 = t_1 n\theta_1 \text{ or } \theta_2 = \frac{t_1 n}{n_o}\theta_1 = x\theta_1$$

where

$$x = \frac{t_1 n}{n_o}$$

Similarly, $n_o\theta_3 = t_2 n\theta_2$

and $n_o\theta_3 = t_1 n\theta_2$ since $t_1 = t_2$

or $\theta_3 = \frac{t_1 n}{n_o}\theta_2 = x\theta_2 = x^2\theta_1$

$$\cdots$$

$$\theta_i = x^{i-1}\theta_1 \tag{2.23}$$

Now, $n_o\theta_1 = tn\theta_o$, or $\theta_1 = \frac{tn\theta_o}{n_o} = \frac{tt_1 n\theta_o}{n_o t_1} = x\,\frac{t\theta_o}{t_1}$

Therefore, $\theta_i = \frac{x^i t\theta_o}{t_1}$, and $\eta = n_o \sum_{i=1}^{i=\infty} i\theta_i$

Substituting for θ_i

$$\eta = n_o \frac{t\theta_o}{t_1} \sum_{i=1}^{i=\infty} ix^i$$

and $$\theta_o = 1 - \sum_{i=1}^{i=\infty} \theta_i = 1 - \frac{t\theta_o}{t_1} \sum_{i=1}^{i=\infty} x^i$$

Therefore $$\theta_o = \frac{1}{1 + \frac{t}{t_1} \sum_{i=1}^{i=\infty} x^i}$$

Let $\frac{t}{t_1} = \omega$, and substituting for θ_o in the equation $\eta = n_o \frac{t\theta_o}{t_1} \sum_{i=1}^{i=\infty} ix^i$

gives $$\eta = \frac{n_o\omega \sum_{i=1}^{i=\infty} ix^i}{1+\omega \sum_{i=1}^{i=\infty} x^i} \quad . \qquad (2.24)$$

The summation in the numerator can be written as

$$\sum_{i=1}^{i=\infty} ix^i = \frac{x}{(1-x)^2} \qquad (2.25)$$

and the summation in the denominator can be written as

$$\sum_{i=1}^{i=\infty} x^i = \frac{x}{1-x} \qquad (2.26)$$

Substituting into equation 2.24 gives

$$\eta = \frac{\eta_o\omega \dfrac{x}{(1-x)^2}}{1 + \dfrac{\omega x}{1-x}} = \frac{\dfrac{\eta_o\omega x}{(1-x)^2}}{\dfrac{1 - x + \omega x}{(1-x)}}$$

or

$$\eta = \frac{\eta_o\omega}{(1 - x)(1 - x + \omega)} \qquad (2.27)$$

where x is a dimensionless quantity and is equal to nt_1/η_o. As n is proportional to the pressure, p, then n is given by the relationship (deBoer, 1953),

$$n = \frac{Np}{\sqrt{(2\pi MRT)}} = \beta_o p \qquad (2.28)$$

where:

N = Avogadro's number = 6.023×10^{23}, R = Molar Gas constant,

T = Absolute temperature and M = Molecular weight.

Let,

$$x = \frac{\beta_o p t_1}{\eta_o}$$

where $\frac{\eta_o}{\beta_o p}$ has the dimensions of pressure and will be denoted by q, hence $x = p/q$.

Now if the magnitude of pressure, p, is increased until p equals q, then the value of x becomes equal to unity. This would mean that n_q, the value of n corresponding to the pressure q, is such that

$$n_q t_1 = \eta_o$$

Physically, this equation means that, if the adsorption takes place on a free surface, then the second, third, etc, layers are filled to capacity, i.e., η_o molecules are adsorbed on one square centimeter

surface area (deBoer, 1953). Substituting $x = 1$ in to equation 2.27, the value of η becomes infinity. Substituting $x = p/q$ in to equation 2.27 gives

$$\eta = \frac{\eta_o \omega \frac{p}{q}}{(1 - \frac{p}{q})(1 - \frac{p}{q} + \omega\frac{p}{q})} = \frac{\frac{\eta_o \omega p}{q}}{(\frac{q-p}{q})(1 + \frac{\omega p}{q} - \frac{p}{q})} = \frac{\eta_o \omega p}{(q-p)[1 + (\omega-1)p/q]}$$

where ω, q and η_o are constants. Instead of expressing this equation in terms of number of molecules it can also be expressed in terms of the volume of gas which has been adsorbed. Let the volume of n molecules be equal to v and let the volume of η_o molecules be v_m (deBoer, 1953). Then substituting for η and η_o in the above equation gives

$$v = \frac{\omega p v_m}{(q-p)[1 + (\omega-1)\frac{p}{q}]} \qquad (2.29)$$

If the three constants ω, q and v_m are determined from experimental results, then the value of v_m gives a direct measure for the surface area of the adsorbent. Brunauer, Emmet and Teller (1938) further simplified this equation by taking q as the pressure at which the saturation value of the adsorbate is obtained at the temperature of the experiment. Replacing q by p_o gives

$$v = \frac{\omega p v_m}{(p_o-p)[1 + (\omega-1)\frac{p}{q}]} \qquad (2.30)$$

Now if v is plotted as a function of p/p_o, the value of v will approach infinity as p/p_o approaches unity. Note that at the point where $p/p_o = 1$ the curve approaches a vertical line asymptotically.

Equation 2.30 can be rearranged (deBoer, 1953) as

$$\frac{p}{v(p_o-p)} = \frac{1}{\omega v_m} + \frac{\omega-1}{\omega v_m}\frac{p}{p_o} \qquad (2.31)$$

By plotting $\frac{p}{v(p_o-p)}$ against p/p_o the intercept on the vertical axis equals $\frac{1}{\omega v_m}$ and the slope of the straight line portion equals $\frac{\omega-1}{\omega v_m}$ from which the two unknown constants v_m and ω and therefore the surface area can be calculated.

2.4 Compressibility of Organic Soils

Organic soils have a reputation for being very compressible. This volume change occurs due to decrease in volume of gas bubbles, drainage of water from the sample, and compression of the solid material. Consolidation behavior of the soil and compressibility of the solids are reviewed in this section.

2.4.1 Consolidation Behavior

Organic soils consist of mineral solids and organic material in various states of decomposition. Some peat soils are fibrous, others show little or no fibrous texture. Pulp and papermill sludges are similar to organic soils. These organic soils may be considered to be a skeleton of solid particles or fibers enclosing macrovoids and microvoids which may be filled with air, liquid or a combination of the two. If a sample is subjected to an external load, compression of the sample will take place due to 1) compression of the solid matter, 2) compression of water and gas, and 3) escape of water from the sample. Under the usual loads encountered in engineering problems, compression of solid

and water is negligible. Compression of air trapped in macrovoids and the change in volume due to escape of water can be finite. The problem of determining the change in volume can be complex since compression of air may take place without allowing water to escape. Compressibility and the rate of consolidation for organic soils will be influenced by soil composition, water content and permeability. Composition of the organic soil will vary with time depending upon the extent of decomposition that has taken place. For example, the solid content of papermill sludge can vary from 5 to 65 percent depending upon the method of dewatering. The result is that the physical properties of sludge can show a wide variation. Various micro-organisms are responsible for decomposition of the organic matter. Waksman (1960) showed that cellulose decomposition is dependent upon a favorable carbon to nitrogen ratio. Imshenetsky (1968) indicated that cellulose decomposition ceases when the available nitrogen content of a soil is below 1.2 percent. Other factors influencing decomposition include temperature, aeration moisture content, pH value and the relative proportion of lignin.

Compressibility of soil is a function of the extent to which particles can shift with respect to each other to attain more stable positions. The rigidity of the soil skeleton depends upon the rigidity of the solids, shape of solids and the binding forces between solids. A coarse fibrous structure may exhibit a different compressibility from a fine-fibrous structure. The compressibility may also vary with the amount of amorphous material and crystalline material present in the cellulose. Compressibility is a function of the water content

of the soil. Water found in cellulose exists in three different phases (Gehm, 1959) 1) free water, 2) interstitial water, and 3) water of imbibition. Free water will drain readily. Interstitial water is held by adsorption on the fiber surface and is difficult to remove. Water of imbibition is a part of the structure of cellulose fiber and it cannot be removed by mechanical means. Water content in organic soils depends to a large extent upon the proportion of organic matter in the sample. For example, water content in peat soils may vary from 50 percent to 1000 percent.

The rate of compression is dependent on the permeability of soil. The presence of cellulose fibers increases the permeability and therefore the rate of compression. The physical structure and the arrangement of constituent particles in organic soils greatly effect the size and continuity of pores and/or capillaries. These differences plus incomplete saturation result in a wide range of permeabilities in organic soils. The effects of undissolved gas in peat show up particularly in consolidation tests (MacFarlane, 1969). In laboratory consolidation tests, a large initial compression and an indistinct completion of primary consolidation in time-compression curves reflect the presence of gas.

The basic assumptions made in applying conventional consolidation theory to inorganic soils include 1) homogeneous material 2) complete saturation, 3) negligible compressibility of the solid matter, 4) validity of Darcy's law, and 5) constant properties during each stage of consolidation. Application of consolidation theory to peat soils includes major deviations from assumptions three and five,

compressibility of gas within a solid particle and change of permeability under applied load. MacFarlane (1969) indicates that these two anomalies account for the significant differences in consolidation behavior between organic and mineral soils.

A porous material subjected to an all around compression under drained conditions will experience a decrease in volume. If, for example, the pressure is increased by a small amount from p' to p' + $\Delta p'$ the corresponding change in volume will be from V to V + ΔV. Where ΔV denotes the decrease in volume and therefore is negative. The volume compressibility of a material is defined as the change in volume per unit volume per unit pressure, therefore the compressibility of the material for the particular pressure increment is given by the relationship,

$$- \frac{\Delta V/V}{\Delta p'} = C \qquad (2.33a)$$

or

$$- \frac{\Delta V}{V} = C.\Delta p' \qquad (2.33b)$$

where C is the compressibility of the material. Compressibility is not a constant but decreases gradually with increasing pressure and at sufficiently high magnitudes of pressures when the voids in the material are eliminated the value of C becomes equal to the value of C_s where C_s is the compressibility of the solid substance. Figure 2.6 shows Vermont marble (Zismann, 1933; Bridgman, 1928). Note that at 600 kg/cm^2 the compressibilities have decreased to a magnitude only about 15 percent higher than the compressibilities of quartz and calcite.

In actual laboratory tests and in the field a saturated porous

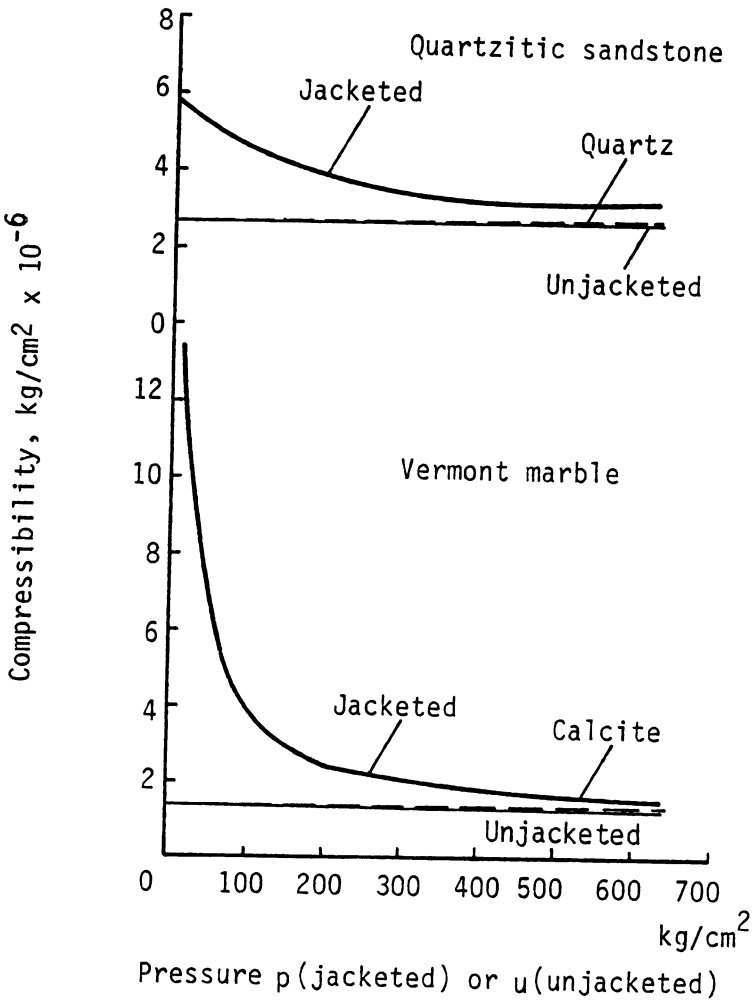

Figure 2.3 Compressibility tests on Quartzitic sandstone and Vermont marble (after Zismann, 1933; Bridgman, 1928).

material is subjected to a pore pressure change Δu as well as a change in the applied pressure Δp. In this type of problem the structural compressibility of the solid particle C_s is considered as follows. If a porous material is subjected to an equal all around hydrostatic pressure of Δu (pore pressure) as in undrained tests the solid particles will undergo cubical compression and the relationship between the volume change and the compressibility can be written as,

$$-\left(\frac{\Delta V}{V}\right)_{solid} = C_s \Delta u \qquad (2.34)$$

Assuming that the inclination of the intrinsic line (Section 2.5.3) is negligible, then a net applied pressure increment $(\Delta p - \Delta u)$ will cause a structural volume change of the material and therefore the total change of the porous material must be

$$-(\Delta V/V) = C(\Delta p - \Delta u) + C_s \Delta u \qquad (2.35)$$

A more complete expression will involve the inclination of the intrinsic line. Skempton (1961) considered it sufficiently accurate to write

$$-\left(\frac{\Delta V}{V}\right) = C[\Delta p - (1 - \frac{C_s}{C})\ \Delta u] \qquad (2.36)$$

where $\Delta p' = \Delta p - (1 - \frac{C_s}{C})\ \Delta u$ (2.33b).

Some representative values of Cs/C are given in Table 2.3 for rocks and some soils. It can be seen that for inorganic soils the value of Cs/C is negligible and therefore Terzagni's concept of effective stress is acceptable (Skempton, 1961) to a high degree of approximation. The value of C_s/C for rocks and concrete is significant,

therefore a considerable error could be involved in using the equation

$$\Delta p' = \Delta p - \Delta u \qquad (2.37)$$

in such materials.

TABLE 2.2. COMPRESSIBILITY CONSTANTS (After Skempton, 1961)

Material	Compressibility per kg/cm^2 x 10^{-6}		$\frac{C_s}{C}$
	C	C_s	
Quartzitic sandstone	5.8	2.7	0.46
Quincy granite (100 ft deep)	7.5	1.9	0.25
Vermont marble	17.5	1.4	0.08
Concrete (approx. values)	20	2.5	0.12
Dense sand	1,800	2.7	0.0015
Loose sand	9,000	2.7	0.0003
London Clay (over-cons.)	7,500	2.0	0.00025
Gosport Clay (normally-cons.)	60,000	2.0	0.00003

Compressibilities at p = 1 kg/cm^2
Water $C_w = 48 \times 10^{-6}$ per kg/cm^2

2.4.2 Compressibility of Solids

When the pore water pressure in a volume of soil changes the soil solids experience a change in total stress and also a change in effective stress at the contact points. Change in stress means a change in strain and may include change in volume and unit weight. The effects of these changes can be significant depending upon the magnitude of stress changes. The volume compressibility of soil grains under hydrostatic stress (Scott, 1963) can be written as

$$\gamma_s = \gamma_{s_o}[1 + \beta_s(u + \gamma_w h_p)] \qquad (2.37)$$

where γ_s is the unit weight of the soil solids, u is the pore water pressure, γ_w is the unit weight of water, γ_{s_o} is the unit weight of the soil solids at atmospheric pressure, β_s is the compressibility of solids, and h_p is the hydrostatic pressure head. Table 2.3 presents the compressibility coefficients for different inorganic soil grains. The value for solids (0.1×10^{-8} psf^{-1}) is very small and therefore it will influence the value of γ_s only at very high pressures. Because of its low value it can be neglected for most geotechnical engineering problems.

TABLE 2.3 COMPRESSIBILITY CONSTANTS
(After Scott, 1963)

Soil	Compressibility terms in 10^{-8} $(psf)^{-1}$				
		(1) Gas	(2) Structural	(3) Water	(4) Solids
	So%*		Dense:		
Sand	100	0	10 to 100	2.5	0.1
	95	1000	Loose:		
	90	2000	1000		
	100	0			
Silt	95	1000	2000	2.5	0.1
	90	2000			
	100	0	2000		
Clay	95	500	to	2.5	0.1
	90	1000	100,000		

*Initial degree of saturation.

In the case of organic solids the coefficient of compressibility for the solids are approximately of the same magnitude (small compared to the compressibility of the soil structure), however the solid may experience a significant change in volume due to the compression of the air trapped in the minute voids. If that is the case then the degree of saturation will be less than 100 percent and

as a consequence the value of the pore pressure parameter B will be less than unity. In such cases the magnitude of β_s may effect the results significantly and should be taken into account.

2.5 Shear Strength of Organic Soils

The Mohr-Coulomb failure theory, which has been found to be very successful in defining failure in inorganic soils, appears also to apply to organic soils. The material reviewed here is presented under three sections: stress-strain behavior, failure condition, and strength of porous materials.

2.5.1 Stress-Strain Behavior

Deformation in soils includes elastic behavior (shape change), decrease in volume (consolidation), and slippage between soil particles (plastic flow). When deformation occurs in a restricted zone or along some localized surface in the soil element, it is common to call this a failure plane. Deformation may occur simultaneously on many surfaces so that no localized failure zone is apparent. The triaxial test (Bishop and Henkel, 1962) permits measurement of axial deformation of a cylindrical soil sample under all-around confining pressures with increase in the axial stress. The observed stress-strain behavior will vary depending on soil composition, water content, and past stress history. Terzaghi and Peck (1967) illustrate the differences in stress-strain behavior for drained and undrained conditions on both normally loaded and overconsolidated clay soils. Typical stress-strain curves for fibrous papermill sludges under undrained conditions have been reported by Charlie (1975).

The stress-strain characteristics of soils depend greatly upon whether the water content can adjust itself to the state of stress. Two extreme conditions used for triaxial tests include drained conditions and undrained conditions. For drained conditions changes in stress are applied so slowly that no excess pore pressures develop. With undrained tests no dissipation of pore pressures are permitted and their magnitude is recorded along with other test data. Undrained triaxial tests conducted on fibrous papermill sludges (Charlie, 1975) showed that excess pore pressures approached values equal to the all-around confining pressure at about 20% axial strain. This behavior raised questions as to the suitability of using consolidated-undrained tests for measurement of the angle of internal friction for the fibrous papermill sludge.

The ratio between the observed excess pore pressure and the axial stress difference is the pore pressure parameter $\bar{A}$ (Bishop and Henkel, 1962) and equals BA. For saturated soil samples and B equal to unity, $\bar{A}$ equals the pore pressure parameter A. Data reported by Charlie (1975) on fibrous papermill sludges and $\overline{CIU}$ tests show values for A_f ranging from 0.45 up to 1.08 with an average value close to 0.76. These low A values for the normally consolidated samples and excess pore pressures close to cell pressures at failure strains appear related to the high organic (fiber) content of the papermil sludges. Most inorganic soils show A values at failure close to unity and smaller excess pore pressures under similar stress history conditions.

2.5.2 Failure Conditions

The strength of organic soils includes both the concept of rupture and that of excessive deformation. There is some question as to what stage in the shear process represents failure. Normal procedure (Leonards, 1962) is to use the peak stress difference, $(\sigma_1 - \sigma_3)_{max}$, for soils which show a brittle type failure. When the stress difference continues to increase up to 20 or more percent axial strain, it is convenient to specify failure at some strain level, usually 20 percent. Whitman (1960) illustrates several field problems where the stage of a shear process which represents failure must be defined to fit each problem.

The Mohr-Coulomb failure theory has been found to be the most successful in defining failure in inorganic soils. According to this theory, shear failure commences at a point in a soil mass when on some plane passing through the point the ratio of shear stress to normal stress attains a critical limiting value. The equation that expresses this in terms of stresses for cohesionless soil is

$$\tau_{ff} = \sigma'_{ff} \tan\phi' \qquad (2.38)$$

where τ_{ff} and σ'_{ff} are the shear stress and the normal stress, respectively on the failure plane at failure and ϕ' is the angle of internal friction of the cohesionless material. The shear stress, τ_{ff}, is also called the shear strength, therefore failure is said to occur when the shear stress becomes equal to shear strength on the potential failure surface. It should be emphasized at this point that the shear strength is not necessarily the maximum shear stress that can occur in a specimen.

The above equation is linear and when plotted (Figure 2.4a) yields a straight line called the Mohr failure envelope. The strength of the soil is given by line AB under the Mohr envelope for a given normal effective stress represented by point B. Any point below the Mohr envelope OC represents a stable (at rest) condition in a mass of soil.

From strength of materials, Mohr's circle represents the stress condition at a point in a body acted upon by a system of external forces. The co-ordinates of any point on the circumference of the Mohr's circle (Figure 2.4b) represents the magnitude of normal stress and shear stress at that point on a certain plane passing through the same point. If the stress condition at a point is such that the normal stress and shear stress values are small, then Mohr's circle corresponding to this condition is represented by the small circles (Figure 2.4b) labeled as stable (at rest) condition. Increasing the shear stress will increase the diameter of Mohr's circle and if it is increased sufficiently Mohr's stress circle will touch the Mohr failure envelope. The state of stress given by the coordinates of point F, the point of tangency (Figure 2.4b), represents the limiting condition. The slope of the Mohr envelope at failure is a maximum and the shear stress on the failure plane is less than the maximum shear stress given by the radius of Mohr's stress circle. The slope of the line OF also represents the maximum ratio of shear stress to normal stress for the circle shown. This ratio is termed the obliquity (Taylor, 1948). The obliquity of the tangents to the two circles representing the stable condition is less than the obliquity of the Mohr envelope,

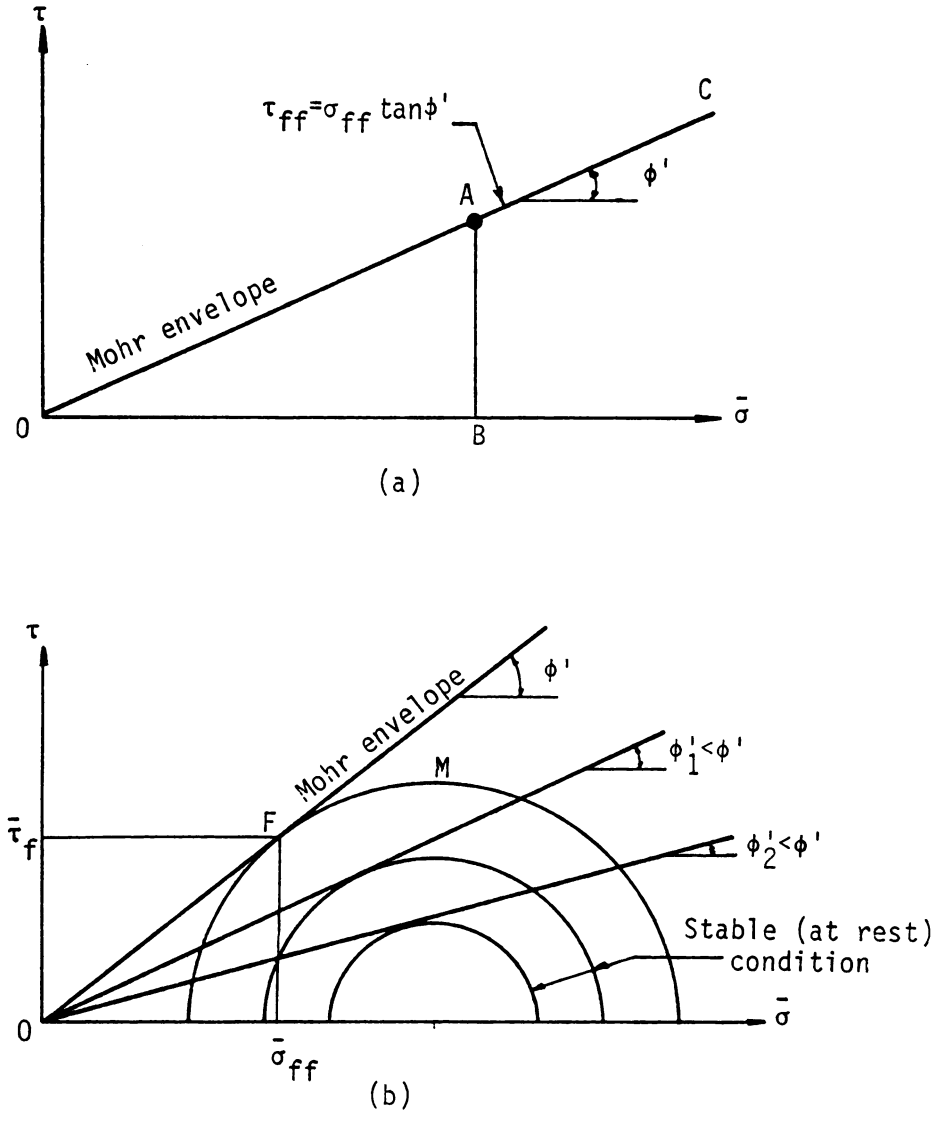

Figure 2.4 (a) Mohr envelope (b) Relation between Mohr stress circles and Mohr-Coulomb failure criterion.

therefore, we conclude that failure in granular soils occur at maximum obliquity and not at maximum shear stress. Because the Mohr-Coulomb failure line is a limiting envelope to all the possible failure circles, it is often called the Mohr-Coulomb failure envelope.

It is not always necessary for the Mohr envelope to emerge from the origin of the coordinate axis. In the case of overconsolidated clays the Mohr envelope will have an intercept on the vertical axis whereas in the case of normally consolidated clays no intercept is obtained. The shear strength equation is modified to take into account the strength contribution due to the vertical intercept as follows:

$$\tau'_{ff} = c' + \sigma'_{ff}\tan\phi' \qquad (2.39)$$

where c' represents the value of the intercept and in conventional terms is called cohesion. The point representing σ'_{ff} on the Mohr circle in this case is the point of tangency of the Mohr envelope to the Mohr circle.

In the case of clays, four possible stresses representing failure are shown in Figure 2.5. The differences between σ_{tf}, σ_{ff} and $\sigma_{\beta f}$ are usually small and these points commonly fall within the range of uncertainty in the data. According to Whitman (1960)

> "The choice among σ_{tf},σ_{ff}, $\sigma_{\beta f}$ and σ_{mf} in research work is essentially a matter of which theory of failure is believed to be correct for the soil in question. Thus, in the research at M.I.T., the author and his colleagues are likely to plot the data in whatever way seems to give the clearest picture of shear strength behavior in the particular problem at hand."

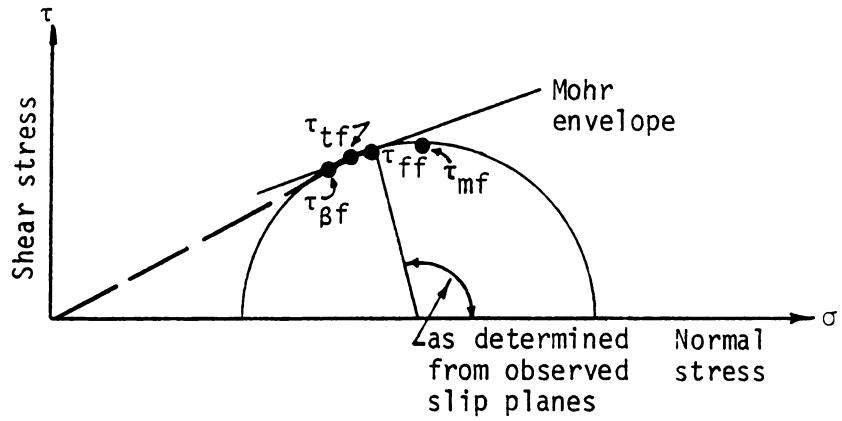

τ_{tf} - shear stress on the plane of tangency of the Mohr envelope at failure,

τ_{ff} - shear stress on the failure plane at failure,

$\tau_{\beta f}$ - shear stress on the plane of maximum obliquity at failure,

τ_{mf} - maximum shear stress at failure.

Figure 2.5 Stress circle at failure and four possible shear strengths (after Whitman, 1960).

2.5.3 Strength of Porous Materials

Before examining the strength behavior of organic soils in terms of the experimental data, it is useful to review one aspect of the strength behavior for porous materials which is generally of little importance at stress levels common to most soil mechanics problems. According to Skempton (1961), "The failure envelope for concrete and rocks, and to some extent for sands, becomes progressively flatter with increasing pressure." This failure envelope gradually approaches the intrinsic line of the solid substance for the triaxial test results on marble, shown in Figure 2.6. At sufficiently high stress levels the particles yield resulting in the elimination of voids, with the failure envelope becoming coincidental with the intrinsic line and the contact area, a, becoming equal to unity. This phenomenon may occur at much lower stress levels in organic solids.

The geometry of the Mohr envelope is a function of the extent to which changes occur in the contact area. The slope of the failure envelope changes according to the change taking place in the porosity of the soil. When the porosity is relatively high a given pressure increment $\Delta\sigma$ causes a high increase in contact area Δa. The porosity gradually reduces and therefore $\Delta a/\Delta\sigma$ becomes smaller and at a sufficiently high stress level (σ^*) the porosity becomes zero and the contact area, a, becomes equal to unity. For example, in Figure 2.6 σ^* equals 6000 kg/cm^2 and the corresponding a value equals unity. At the intrinsic stress level $\Delta a/\Delta\sigma$ becomes zero and the slope of the failure envelope decreases to the value of ψ. In Figure 2.6 τ_i represents the intrinsic line and τ_d gives the failure envelope. One

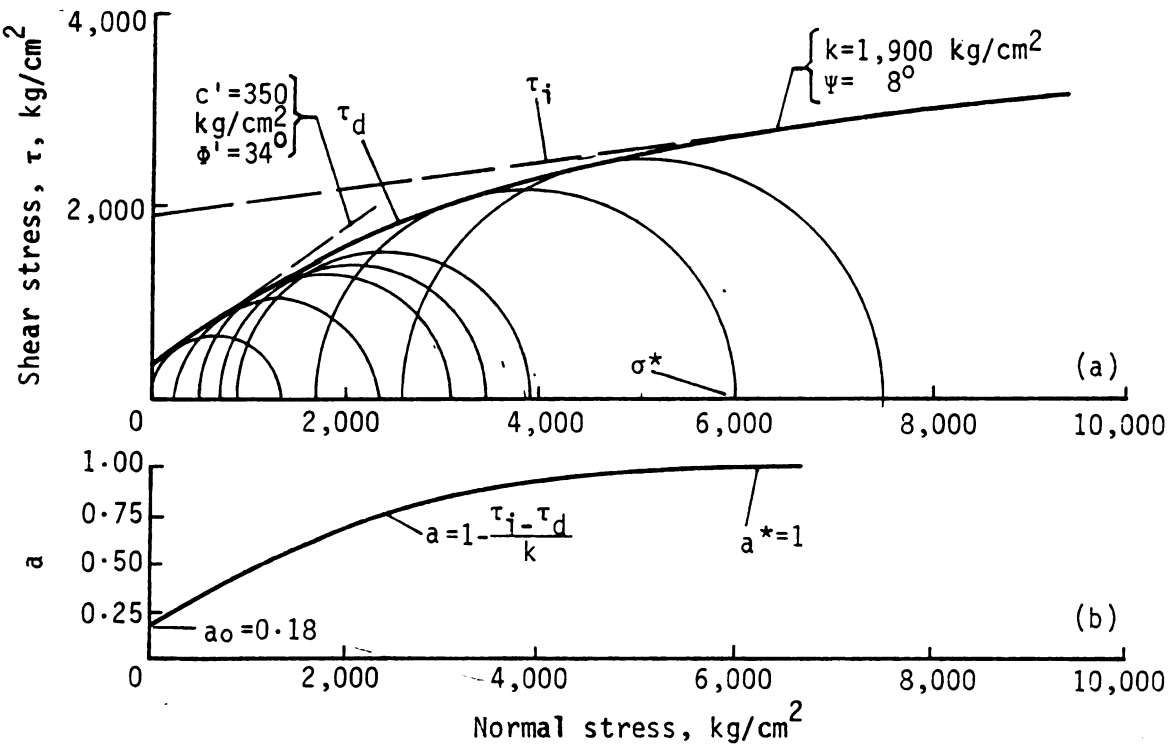

Figure 2.6 Triaxial test on Marble (after Von Karman, 1911)

of the reasons why the failure envelope is assumed linear is that in most laboratory tests the magnitude of the applied stress σ is small compared to σ^*. The shear strength equation 2.39 is linear when $\frac{\sigma}{\sigma^*}$ is small.

CHAPTER III

LABORATORY EQUIPMENT AND TEST PROCEDURES

The physical properties and stress-deformation behavior of the model organic soil were studied using standard equipment where possible. This section includes a description of the equipment, procedures followed, and sample preparation. The initial part of this chapter is related to the physical properties of the fibers and the later part is concerned with measurement of the compressibility and shear strength of the organic soil.

3.1 Physical Properties of Pulp Fibers

Physical properties of pulp fibers important to their mechanical behavior include fiber length expressed in terms of a weighted average, specific gravity described in terms of the ratio of the weight in air of a given volume of fiber solids to the weight in air of an equal volume of distilled water at 4 deg. C, and fiber particle surface area per gram of dry material.

3.1.1 Weighted Average Fiber Length

The weighted average fiber length may be determined by a procedure used by the pulp and paper industry (Tappi, 1974). If a fiber 1 mm in length weighs w micrograms, then for a given sample, the weighted average length L equals the sum of the products of the weight times the length of each fiber divided by the total weight of the fibers in the sample, thus

$$L = \frac{\Sigma wl}{\Sigma w} \qquad (3.1)$$

The Tappi (1974) testing procedure for fiber length of pulp by classification gives satisfactory results using the weights and lengths of five graduated fractions which are provided by a four screen classifier. The apparatus, a Clark Fiber Classifier, consisted of a tub having a shape of a half cylinder. Four screens--1.41 mm (no. 14), 0.595 mm (no. 30), 0.297 mm (no. 50), and 0.149 mm (no. 100)--were selected so as to hold about one-fourth of the sample on the largest screen and to provide for close separation of the long fibered fraction. The screens were mounted on a common shaft rotated by a motor. The tub consisted of four compartments. The partitions between the compartments were provided with split tubes of soft composition material. The rim of the rotating screen travelled in the split tube, thus providing a seal between adjacent compartments. An adjustable water supply outlet from a constant level tank allowed water to travel through a weir and baffle arrangement into the bottom of the tub at a rate of about 10 liters per minute. The motion of the water kept the fibers afloat and presented them repeatedly to the rotating screens through which the fibers having a length less than the screen opening passed. The classification time used was five minutes. Drain plugs provided at the bottom of the tub allowed the contents of each compartment to flow into drainage cups.

Preparation of the suspension for classification involved soaking the fibers in a dessicator long enough to convert the suspension into a slurry. The approximate consistency of the slurry was determined by measuring a volume of 230 ml in a graduated cylinder with dry weight of solids equal to 8.80 grams. The relative proportions of the slurry was (8.80 x 100) ÷ 230 = 3.86 gms/100 ml.

To obtain a recommended consistency of 0.15 percent of a suspension having a volume of 12 liters, the weight of fibers required was

$$\frac{x}{12000} = .0015 \quad \text{or} \quad x = 18 \text{ gms.}$$

The slurry volume from the dessicator required to yield approximately 18 gms of fibers was 18 (100)/3.86 = 466 ml. Additional water was added to the 466 ml of slurry to make the total volume equal to 12 liters. This suspension was subjected to dispersion at 3000 rpm utilizing a cowles dissolver. Since 5 gms of material was required for each classification experiment, the required volume was 100(5)/0.15 = 3333 ml. This volume, 3333 ml of suspension, was carefully measured for each run and used in the Clark classifier.

Before use of the equipment the screens were cleaned thoroughly. The procedure required that the water supply to the tub be controlled at a rate of 10 liters per minute. The motor to drive the screens was started after the drain plugs were in place and the tub was full of water. The 3333 ml specimen with 5 gms of fibers was poured into the first compartment simultaneously with starting the stop watch when steady flow conditions were established. This operation was completed in about 20 seconds. The screens were allowed to rotate for five minutes after pouring of the specimen was complete. In the meantime clean moist filter paper was added to each of four drainage cups previously placed in position. At the end of five minutes the water supply to the tub was shut off, screens were stopped, and drain plugs were opened as soon as the overflow from the last compartment ceased. Screens were rinsed and the contents from each compartment

were collected in the corresponding drainage cup on filter paper. Filter paper was removed gently from each cup, squeezed to remove the excess water, dried in an oven at 105°C and the weight of dried fibers determined after 24 hours. This procedure was repeated three times to obtain three readings. The fibers collected from running the test the fourth time were used to prepare the glass slides for measuring the length of the fibers after projecting their image on a screen.

3.1.2 Specific Gravity

Apparatus for the specific gravity test consisted of a pycnometer, hot plate, and a thermometer. The bouyancy medium employed was boiled cooled distilled water.

The procedure consisted of determining the weight of a clean dry pycnometer in air followed by adding 10 gms of freeze dried fibers to the pycnometer and weighing the container with its contents. Distilled water was added until the pycnometer was half full. Trapped air was expelled from the fibers by gentle boiling. Weight of the pycnometer with stopper and its contents was determined again after the water was allowed to cool to room temperature and additional distilled water was added to fill the pycnometer. The contents of the pycnometer were removed, refilled with distilled water, the stopper was seated properly and its weight determined after the temperature measurement. The particle density was determined using the following relationship (Blake, 1965)

$$Dp = \frac{dw(Ws-Wa)}{(Ws-Wa) - (Wsw-Ww)} \qquad (3.2)$$

where,

dw = density of water in grams per cubic centimeter at the observed temperature,

Ws = weight of pycnometer plus cellulose fibers,

Wa = weight of pycnometer filled with air,

Wsw = weight of pycnometer filled with water and cellulose fibers,

Ww = weight of pycnometer filled with water at the observed temperature.

3.1.3 Fiber Particle Surface Area

The Perkin-Elmer Shell Model 212 Sorptometer was used for the determination of the surface area of the fibers through measurement of nitrogen adsorbed by the fibers. The instrument is composed of a sample tube, detector, gas flow lines and various gas controls. A potentiometric recorder was connected to the detector.

Surface area measurements by the sorptometer is termed the continuous flow method. In this method a cooled solid sample is subjected to a stream of gas and the surface area of the sample is determined by measuring the amount of adsorbed gas. The mobile gas phase is a known mixture of a suitable adsorbate and an inert gas carrier. Generally nitrogen is employed as the adsorbate and helium as the inert carrier gas.

The principle of the method used was as follows. A known mixture of nitrogen and helium was passed through the U-shaped cellulose fiber container which was cooled with liquid nitrogen. The effluent was closely observed by a thermal conductivity detector. The cooled sample adsorbed a certain amount of nitrogen from the gas stream. This was indicated on the recorder chart as a peak whose area was in proportion

to the volume of adsorbed nitrogen. The adsorption recorder pen returned to its original position when equilibrium was established. The liquid nitrogen bath was removed from the sample tube. The adsorbed gas was released from the sample producing a desorption peak as the sample warmed. A known volume of nitrogen was added to the nitrogen-helium stream after the desorption was complete at a position located downstream of the sample tube and the resulting peak was recorded. By comparing the areas of the desorption and caliberation peaks the volume of nitrogen adsorbed by the sample was calculated.

The second method used to determine the surface area consisted of water vapor adsorption. Six desiccators with 69.44% H_2So_4, 55.01% H_2SO_4, 45.41% H_2SO_4, saturated $NaNO_2$, saturated NaCl, and saturated $NH_4H_2PO_4$ were used to provide variable vapor pressure environments for the dry cellulose fiber samples placed in these desiccators at room temperature. The weight of the moisture adsorbed by each sample was determined. Using the B.E.T. equation the monolayer capacity was determined followed by determining the number of water molecules in the single layer. Using the cross-sectional area of one water molecule as 10.56 $\mathring{A}^2$ the surface area per gram of dry cellulose fibers was determined.

3.2 Compression Tests

Compression tests involved measurement of the compressibility of the fibrous soil mixture using a ram and test cylinder. The compression test cylinder, sample preparation, and test procedures are described.

3.2.1 Compression Test Cylinder

A detailed sectional view of the compression test cylinder is shown in Figure 3.1. It consists of a cylinder C_1 firmly screwed to flange f1. The Flange f_1 rests directly on the load cell 1 which is supported by a base plate p1. The base plate, load cell and flange are held together firmly by eight bolts b. A porous stone supporting unit s1 was designed to screw in and seat directly on the load cell. The supporting unit s1 was provided with an O-ring r and a drainage line, the former to prevent leakage and the latter to allow the water to escape from the bottom of the sample resting on the porous stone. The centerline of the drainage pipe was displaced by 1.587 mm (1/16 in) from the centerline of the port, provided in the flange to accomodate the drainage pipe, in order to maintain enough clearance so as not to interfere with the free deflection of the diaphram of the load cell. The test sample is shown positioned between porous stones at the top and bottom of the sample. A loading ram, with an O-ring r_1, a vertical drain line and a nozzle for connecting the flexible tubing was used to transfer load P to the sample.

3.2.2 Sample Preparation

Using dry pulp material which had been separated to a very loose condition, dry kaolinite was added until a uniform combination was obtained in the specified weight proportions. Water was added until the water content was greater than the liquid limit. A small portion of this material was dropped into the test cylinder C_1 (Figure 3.1) and gently leveled so as to avoid formation of separate layers. This process was continued until sufficient material had been added to give

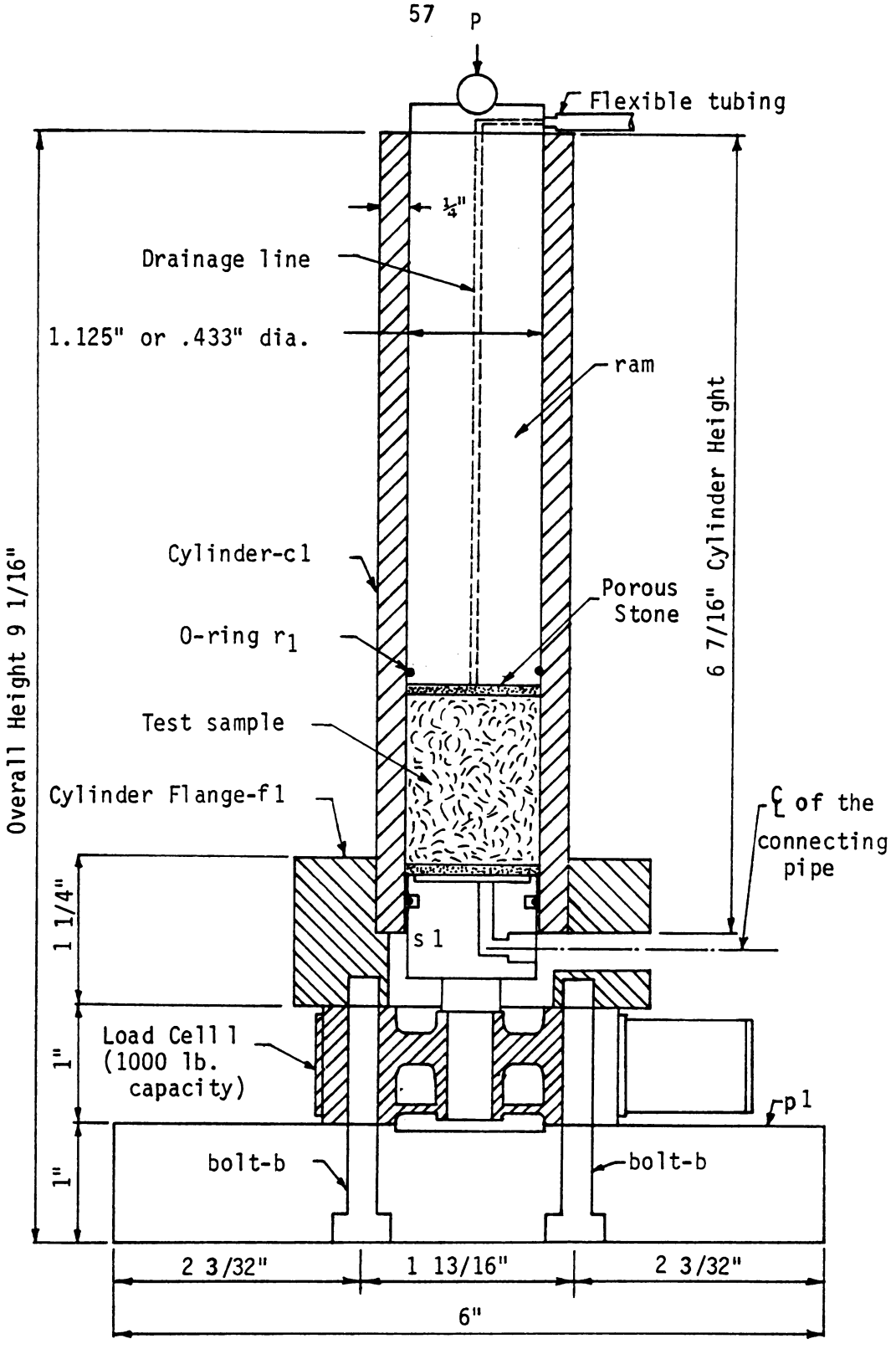

Figure 3.1 Sectional view of the Compression Test Cylinder

an acceptable test sample size (1 cm dia. x 4.5 cm height). A porous stone was gently seated on top of the sample. Cylinder cross-sectional areas were 645 mm^2 (1 in^2) and 100 mm^2 depending on the desired load range for the test. Next the ram was inserted into the cylinder with the drain hole open so that no air would be trapped below the ram. The ram was gently lowered until it was seated against the porous stone resting on the top of the sample. The ram was now loaded with the desired load and with both drainage lines open the sample was allowed to normally consolidate for 24 hours with respect to the applied load.

3.2.3 Test Procedure

The normally consolidated sample was subjected to an increment of load. The magnitude of the load increment, the vertical displacement of the sample and the burette reading were recorded after the sample reached equilibrium condition. Due to the high permeability of the fibers the time required to reach equilibrium was smaller for pure fibers as compared to the time required for equilibrium for a mixture of fibers and kaolinite. For samples with a cross-sectional area of 100 mm^2 the maximum stress to which the sample was subjected was over 350 kg/cm^2.

3.3 Direct Shear Tests

Direct shear tests involve sample failure by moving one part of the sample container relative to another. It involves the use of a special shear box, sample preparation, and test procedure.

3.3.1 Shear Box

The sample container consisted of a shear box (Model WF 2500, constant strain rate, Wykeham Farrance engr Ltd., England) with separate top and bottom halves and a 25.4 mm square sample area. Additional height for the top half permitted use of high initial water content fiber-kaolinite samples. This gave sufficient sample height after one dimensional consolidation for the shear test. The shear box was supported by a carriage which ran on ball bearing tracks guided by hardened vee grooves. The lower half of the shear box was fixed to the carriage which transmitted the shear force to a load cell. The normal force from a loading frame and dead weights was applied to the sample through a loading block. Horizontal and vertical displacements were measured by dial gages placed at the appropriate locations.

3.3.2 Sample Preparation

Sample specimens consisting of saturated fiber and dry fibers were subjected to direct shear tests. Homogeneous test samples were prepared from saturated dispersed fibers by transferring a small quantity of slurry at a time, under drained conditions into the shear box. Gentle tapping helped to avoid formation of any layers. This process was continued until sufficient height of sample was obtained. A square metal ram with 25 mm side dimensions seated on top of the specimen permitted application of a one dimensional consolidation load by means of a hanger with dead weights. The loaded hanger was supported on a ball bearing resting on the recessed top surface of the metal ram thus transmitting the load to the sample. The consolidation load was maintained for 24 hours, resulting in one dimensional

compression of the sample and the consequent penetration of the metal ram into the square slot with 25.4 mm sides provided in the shear box. The ram penetration was recorded and the sample height determined after equlibrium was established. The sample preparation procedure for dry specimens was essentially the same except that well dispersed freeze dried fibers were used instead of saturated fibers.

3.3.3 Test Procedure

The strain box was connected to the load cell to record the diaphram deflection, hence the applied load. A vertical displacement dial guage was mounted against the top of the loading frame and a horizontal displacement dial guage was placed against the carriage. A hypodermic needle, connected at one end to a sensitive manometer, was inserted through a narrow aperture provided in the loading ram far enough into the sample to provide a means for measuring any pore pressure developed during the process of shear displacement.

The shearing force was applied to the test specimen through a spindle resting against the carriage and operated by a controlled speed motor, after recording the initial readings of the strain box, vertical displacement gauge and horizontal displacement gauge. Readings for the applied stress, vertical and horizontal displacements were recorded simultaneously until 20 percent displacement was reached. No excess pore pressures were observed during the test. This was perhaps due to the combined effect of a low rate of strain and the high permeability of the fibers. Several samples were subjected to a slow cyclic loading and unloading during which vertical and horizontal displacements were observed. The failure in this case was also assumed

at 20 percent strain since the material did not exhibit a brittle failure mechanism.

3.4 Triaxial Compression Tests

A triaxial compression test on a cylindical soil specimen requires special equipment for controlling cell pressures, axial pressures, pore pressures and drainage conditions. Procedures followed for the consolidated undrained ($\overline{CIU}$) and consolidated (CID) drained tests are outlined.

3.4.1 Triaxial Equipment

The triaxial equipment (Figure 3.2) consists of three major parts: 1) a self-compensating mercury pressure control system, 2) triaxial cell, and 3) pore pressure measuring device. The self-compensating mercury pressure control system (Bishop and Henkel, 1962) consists of an adjustable mercury cup suspended from a spring designed to maintain the desired pressure. A column of mercury provides the pressure. Any gradual loss of elevation head of mercury due to leakage during the process of experimentation is compensated by the simultaneous gradual upward deflection of the spring. This process continues and results in keeping the mercury level constant and hence a constant pressure. The mercury cup is connected to the pressure gauge by a flexible plastic tube, the screw control, and the cell.

The cylindrical compression test requires use of a triaxial cell (Bishop and Henkel, 1962) consisting of three principal components--the base, which forms the pedestal on which the sample rests and which incorporates the various pressure connections, the removable cylinder and top cap which enclose the sample and enable fluid

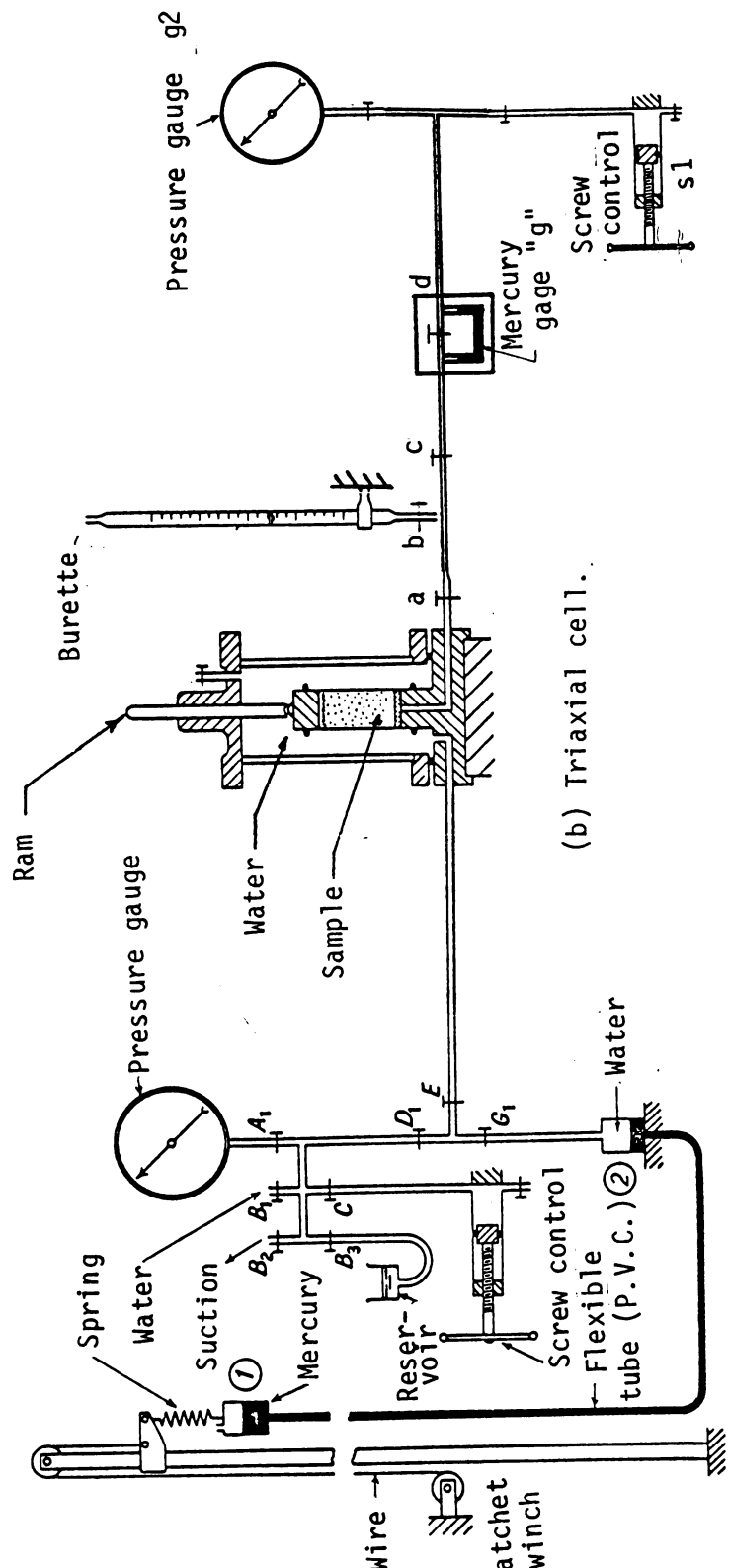

(a) Self-compensating mercury pressure control.

(b) Triaxial cell.

(c) Null method for pore pressure measurement.

Figure 3.2 Triaxial equipment.

pressure to be applied; and the loading ram which applies the deviator stress to the sample. This cell was connected to a burette, to the self-compensating mercury pressure control, and through a mercury U-tube "g" (Figure 3.2) to a pressure gauge and a pressure control cylinder.

The pore pressure measuring device consists of a pressure gauge, a pressure control cylinder, and the mercury U-tube. This device, which connects to the bottom of the test sample through a line connected to mercury U-tube passing through the pedestal, permits measurement of pore pressures developing in the specimen during the process of testing.

3.4.2 Sample Preparation

Samples prepared and tested were divided into the following four groups depending upon their composition:

1) all fiber,
2) 54 percent fiber and 46 percent kaolinite by volume,
3) 25 percent fiber and 75 percent kaolinite by volume, and
4) all kaolinite.

Uniform combinations in the specified weight (or volume) proportions were obtained by mixing dry kaolinite with freeze dried loose cellulose fibers. Water was added until the water content was greater than the liquid limit. Samples representing groups (2), (3) and (4) were trimmed from a larger normally consolidated cylindrical sample to give the desired 2:1 length-diameter ratio. A rotary-type of cutting tool permitted trimming of the fibrous material. For easier preparation, samples consisting of all fibers

(group 1), were molded in a split cylinder to give a specimen with the desired dimensions.

3.4.3 Consolidated-Undrained Tests

This test consisted of mounting the specimen, provided with side drains, on the pedestal inside the cell (Figure 3.2b). The sample was jacketed in two rubber membranes and consolidated by keeping valves "a" and "b" open, with respect to a desired three dimensional pressure applied through the fluid in the cell by the self-compensating pressure control system.

For convenience the consolidation process was continued for 24 hours then valve "b" was closed. To increase the degree of saturation, a specified back pressure was applied to the sample in small increments simultaneously with increasing the cell pressure. The pore pressure parameter, B, was determined by temporarily isolating system (a) in Figure 3.1 by turning off valve G1, and with the screw control increasing the cell pressure by a small increment. The increase in cell pressure increases the pore pressure upsetting the balance in the mercury U-tube "g." Using screw control "s1" the mercury columns were balanced and the increment of pore pressure Δu was read on the dial gauge g2. The pore pressure coefficient B was calculated using the relationship,

$$B = \frac{\Delta u}{\Delta \sigma_3} \tag{3.3}$$

After the cell pressure and the pore pressure were returned to their previous values, valve G1 was opened. After the sample pore pressures were allowed to come to equilibrium, the deviator stress was applied,

through a mechanically operated ram. During application of the deviator stress the mercury U-tube "g" was kept balanced by turning the screw control "s1" permitting excess pore pressure to be read on the dial gauge. Pore pressures, deviator stress, and axial strain were recorded at selected intervals until sample failure was observed.

3.4.4 Consolidated Drained Test

The procedure followed for the drained tests was essentially the same as for the undrained tests up to application of the deviator stress. To ensure no excess pore pressure development and to permit measurement of the volume of water leaving the sample, valves "a" and "b" were opened and valve "c" was closed (Figure 3.2). The volume of water leaving the sample and entering the burette was recorded at the respective axial strain. Time to failure (20% axial strain) for the drained tests was calculated on the basis of c_v from the consolidation portion of the test and the theory provided by Bishop and Henkel (1962). For all fiber sample CD-F2, c_v = 11.27 x 10^{-3} cm^2/min for a sample height = 7.306 cm, sample radius = 1.729 cm, and t_{100} - 32.5 min. The estimated time to failure equals about 9.7 hours. A sample deformation rate was selected to give an axial strain of 20 percent for this time to failure.

CHAPTER IV

EXPERIMENTAL RESULTS

The experimental results are presented under four headings: physical properties of the test materials, compression tests, direct shear tests, and triaxial compression tests.

4.1 Physical Properties of the Test Materials

Test materials used in this study were limited to kaolinite and an organic pulp fiber, both raw materials used in the paper making process. The fiber description required for this study included the weighted average fiber length, specific gravity and surface area of the pulp fiber. For kaolinite, the study included the Atterberg limits and the particle size distribution based on the hydrometer analysis.

Atterberg limits were not determined for pure fiber or the fiber-clay mixture. The interference due to the fiber length during cutting the standard groove would lead to misleading liquid limit values. The determination of a plastic limit for fibers is not possible using the standard method of rolling threads of 1/8 in. diameter at a water content at which the threads begin to crumble.

4.1.1 Atterberg Limits and Particle Size for Kaolinite

The liquid limit (ASTM D423-66) and plastic limit (ASTM D424-59) were determined using a standard liquid limit device and the method of rolling kaolinite threads down to 1/8 in diameter at a water content at which it just crumbled.

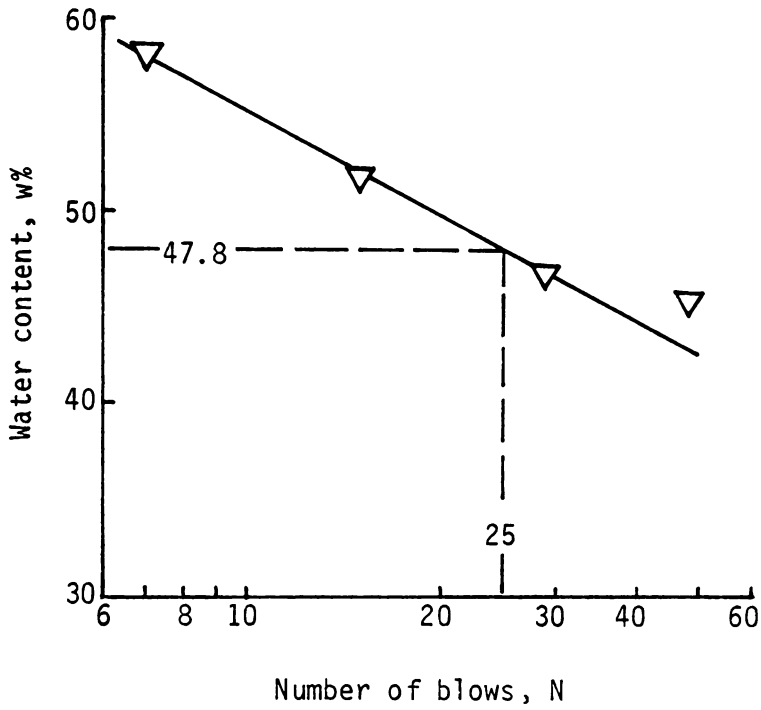

Liquid limit = 47.80%
Plastic limit = 27.50%
Plasticity index = 20.30

Figure 4.1 Water content vs. number of blows for Kaolinite.

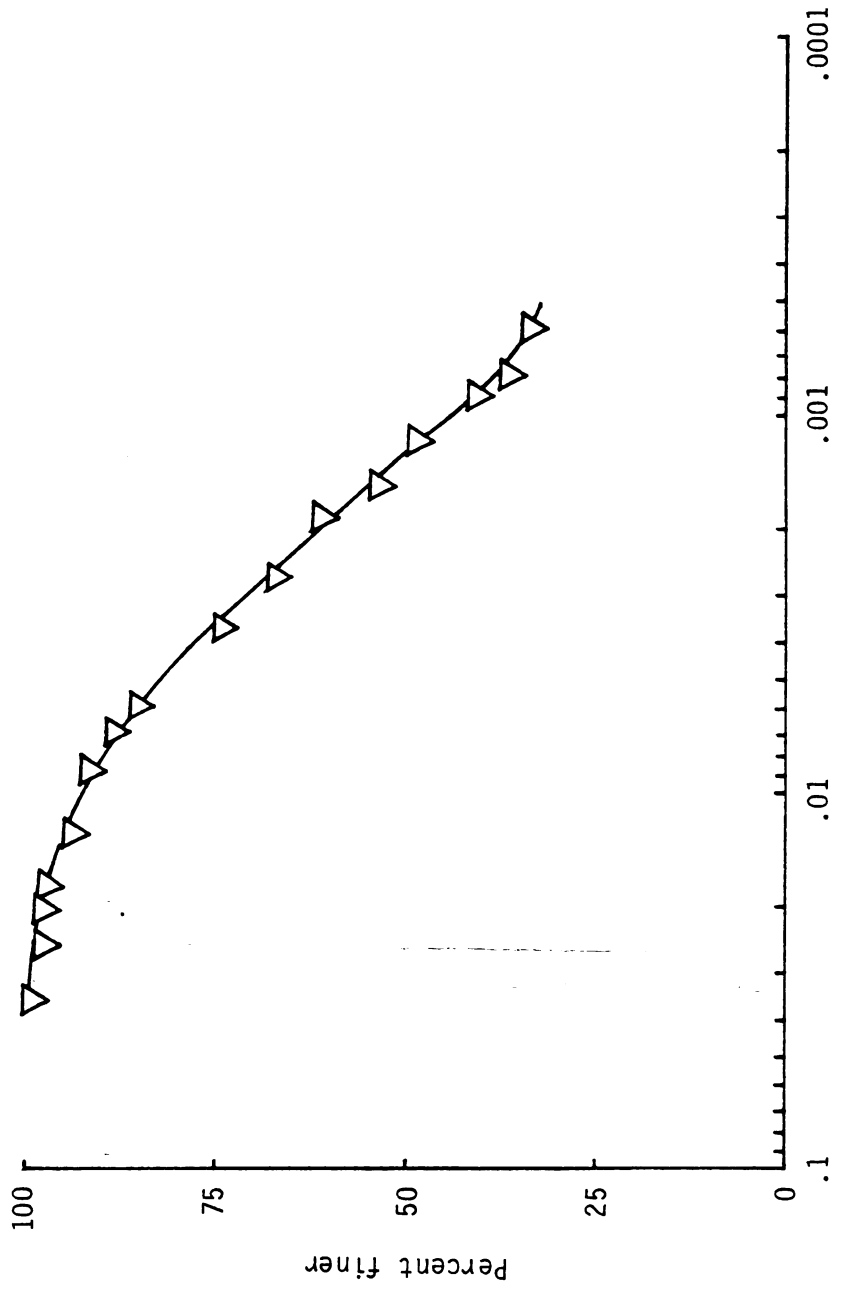

Figure 4.2 Grain size distribution curve for Kaolinite.

Table A.1 and A.2 in the Appendix show the required data for determination of the liquid and plastic limits, respectively. Figure 4.1 shows the number of blows plotted against water content. The liquid limit, determined from the plot corresponding to 25 blows, is equal to 47.8 percent. The plastic limit, determined from averaging the data obtained from three determinations, is 27.50 percent. The plasticity index equals 20.30 percent.

The hydrometer analysis (ASTM D422-63) was performed using the model 152H hydrometer in a kaolinite suspension with sodium hexametaphosphate ($NaPO_3$) as the dispersing agent. Table A.3 represents the data recorded for the grain size distribution. Figure 4.2 shows the size distribution of the clay particles. All sample particles passed through a 0.074 mm opening (U.S. Standard Sieve #200).

4.1.2 Weighted Average Fiber Length

The weighted average fiber length was determined by a procedure used by the pulp and paper industry and described in Section 3.1.1. The measured lengths of projected fiber shadows are tabulated below the U.S. standard sieve sizes in Table 4.1. The summations give the total length and the total number of fibers measured on the screen.

The screens used were U.S. standard sieve No. 14 (1.41 mm), No. 30 (.595 mm), No. 50 (.297 mm) and No. 100 (.149 mm). Projected shadow lengths of the fibers on the screen from different slides are shown in Figures 4.3a, 4.3b, 4.3c, and 4.3d. Simple calculations for the determination of the average weighted length are derived from these projected shadows. It can also be observed from Figure 4.3 that the lengths of the fibers are decreasing with decreasing sieve opening.

TABLE 4.1 FIBER LENGTH CLASSIFICATION

U.S. Standard Sieve Sizes												
No. 14 1.41 mm			No. 30 0.595 mm			No. 50 0.297 mm			No. 100 0.149 mm			
Projected Lengths, in.												
2.75	1.50	2.10	2.55	1	1.40	1.60	1		.23	.50	1.40	
3	1.50	2	2.50	1.60	2.50	1.60	2.50		.50	.70	1.35	
2	1.40	1	2.30	2.40	2.30	2	1.20		.50	1.13	1	
1.75	2.90	2.20	3.10	2.40	1.30	1.40	1.40		1.50	.65	.70	
4.75	1.40	2	4	2.10	1.40	1.50	1.50		1	1	.90	
1.60	1.50	3.50	3.60	2.70	2.50	1.60	2.50		.50	1	1	
2.50	2.60	0.75	2.60	2.90	1.60	1.50	2.50		1.30	1.13	1.35	
2.50	3.20	1	1.40	3.60	2.30	2.10	1.60		1.75	.65	.40	
3.80	4.10	2.25	3.50	1.60	1.50	2	1.50		.85	.65	.50	
2.80	1.60	2.25	4.50	2.60	1.80	1.40	1.50		.95	.50	.70	
4.00	1.50	2.25	2.25	2.40	2.40	1.60	1.50		.50	2.1	1.30	
3.00	1.20	3	1.90	1.60	1.50	2.10	2		.35	.65	1	
2.50	1.60	2	2.50	2.00	1.80	1.30	1.60		.90	1	2	
3.00	1.80	4.4	1.45	3.20	1.30	1.50	1.80		2.12	.75	.50	
2.00	1.50	2.60	2.20	3.20	1.50	1.40	1.20		.90	1	.70	
1.90	2.50	1.80	2.80	5.70	2	1.70	2.40		.50	2	1.40	
2.80	1.00	4	2.80	1.80	1.4	1.20	2.75		1	.70	.55	
4.20	2.20	2.10	1.50	2.30		1.50	2.30		2.4	.90	1	
3	3.50	3	1.90	2.40		1.60	1.50		1	.70	1.75	
1.60	1.80	1.50	2.20	1.70		1.50	1.50		.35	.70	.50	
2.80	1	3	4	2		2.50	3.50		1.30	1.80	1.35	
3.50	1.80	1.5	1	1.50		2.30	3.00		.50	1		
2.50	2	3.1	1.60	2.50		1.45			1	1		
2.40	3.3	2.4	1.50	2.30		2.50			1.45	1.50		
3.10	1.6		2.40	1.30		1.50			.70	1		
Total Length, in.												
170.20			126.35			107.60			70.11			
Number of Fibers												
73			54			60			71			
Scaled Average Length,* in.												
2.3315			2.3398			1.7933			.9875			
Actual Length,+ mm.												
2.6645			2.6740			2.0495			1.1285			

TABLE 4.1 Continued.

*Scaled average length = $\frac{\text{Total Length}}{\text{Number of Fibers}}$

+Actual length = $\frac{\text{Scaled Average Length}}{0.875}$

Where .875 is derived from the scale used.

Simple calculations for determination of the weighted average fiber length are given in Table 4.2. The weight of fibers used in each test run, W = 5 gms.

TABLE 4.2 WEIGHT OF FIBERS RETAINED ON FOUR U.S. STANDARD SIEVES

Screen Used	Weight of Fibers Retained on Screen (gms.)
#14(1.41mm.)	w_1 = .3841
#30(.595 mm.)	w_2 = 1.0663
#50(.297 mm.)	w_3 = 1.5486
#100(.149 mm.)	w_4 = .6016
<#100	w_5 = 5-(.3841 + 1.0663 + 1.5486 + .6016)
	= 1.3994

Loss = 1.3994 ÷ 5 = 27.99
≈ 28%

Weighted average fiber length, $L = \frac{\Sigma wl}{w}$

$$= \frac{(.3841x2.6645)+2.674x1.0663)+(2.0495x1.5486)+(1.1285x.6016)+(1.3994x.1)}{5}$$

= 1.5734 mm

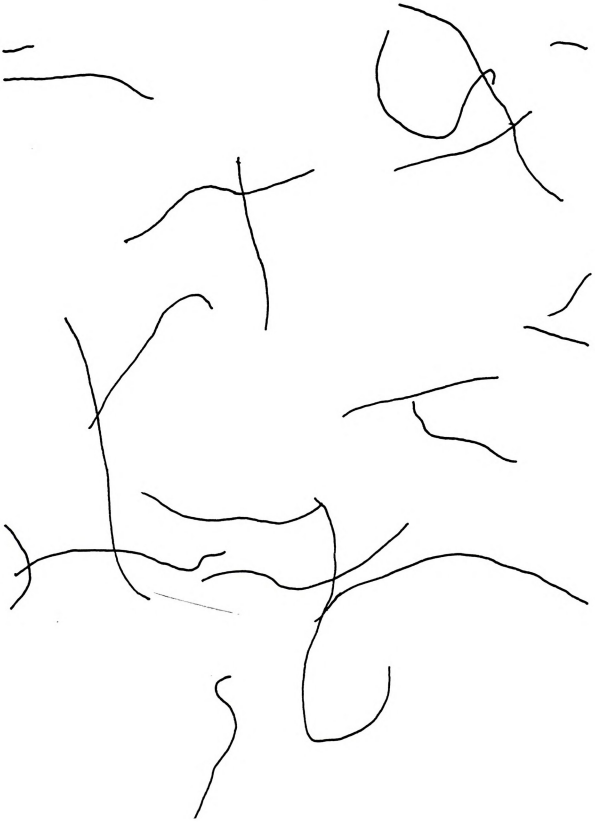

Figure 4.3a Projected fiber lengths, No. 14 sieve size.
Scale: 1 mm = 0.875 in.

Figure 4.3b Projected fiber lengths, No. 30 sieve size.
Scale: 1 mm = .875 in.

Figure 4.3d Projected fiber lengths, No. 100 sieve size.
Scale: 1 mm = .875 in.

4.1.3 Specific Gravity of Pulp Fiber

Specific gravity or density of the pulp fibers was determined by the pycnometer method using water as the displacement medium for measuring the volume. Data for six determinations are included in Table A.4 giving an average density of 1.5976 g/cm^3. This value of density is high because water used as the displacement medium is a polar swelling liquid and has a high capability to penetrate the cellulose fiber. A value for the density equal to 1.54 (Hermans, 1949) is obtained when the displacement medium is an organic liquid such as benzene. The larger organic molecules are unable to penetrate the fiber. The value of 1.54 g/cm^3 has been used in subsequent calculations for this project.

4.1.4 Surface Area of Pulp Fiber

Two methods were employed to determine the surface area of the cellulose fibers. One method consisted of using nitrogen adsorption and the second method employed the use of water vapor adsorption. The results obtained using these two methods were different, 1.5 m^2/g for nitrogen absorption versus 133 m^2/g for water vapor absorption. Grim (1968) states that the surface area value for montmorillonite determined using water vapor adsorption are much higher than those obtained by nitrogen adsorption, owing to the penetration of water between the basal planes of the montmorillonite units. A comparison of the surface areas for the same clay mineral determined by the two methods is given by Grim (1968).

The chemical agents used to give rise to different vapor pressures are listed in Table 4.3. Dry pulp fiber samples with known weights were placed in air tight desiccators and subjected to

TABLE 4.3 CHEMICAL AGENTS USED FOR DIFFERENT WATER VAPOR PRESSURES

p/p_o	Agent Used
0.05	69.44% H_2SO_4
0.25	55.01% H_2SO_4
0.45	45.41% H_2SO_4
0.66	Saturated $NaNO_2$
0.757	Saturated NaCl
0.930	Saturated $NH_4H_2PO_4$

Room temperature = 20°C

Barometer pressure, p_o = 17.535 mm of Hg

Density of Hg = 13.5462

Density of H_2O = .99823

environments of different vapor pressures. The room temperature saturation pressure and the related data necessary to calculate the monomolecular capacity after plotting the B.E.T. adsorption isotherm are given in Table 4.4. Table 4.5 lists the magnitudes of the different terms in the B.E.T. equation with respect to different vapor pressures. Figure 4.4 shows p/p_o on a horizontal scale plotted against water content with respect to the dry weight of the solids on a vertical scale. The curve obtained is similar to the one expected for cotton, since cotton is at least 90 percent pure cellulose (West and Todd, 1955). Figure 4.5 provides the basis for determination of the unknown parameter v_m, i.e., the monomolecular capacity where k is a constant. In this plot of p/p_o versus $p/\frac{x}{m}(p_o-p)$, the intercept $1/kv_m$ and the slope of the initial portion of the curve, which should be a straight line due to single layer adsorption, was determined. Using the calculated cross-sectional area of a water molecule equal to 10.56Å^2 gives the specific surface area of $133m^2$ based on the number of water molecules adsorbed by cellulose fibers in a single layer.

The following formula (Perkin-Elmer Corp., 1961) was used to determine the cross-sectional area of a molecule of water,

$$a_1 = 4 \times .866 \left(\frac{M}{4N_a \cdot d\sqrt{2}} \right)^{2/3} \qquad (4.1)$$

where a_1 = cross-sectional area of a molecule of water, cm^2,

M = molecular weight of absorbate, gm,

N_a = Avogadro's no. 6.02×10^{23},

d = density of water, gm/cm^3.

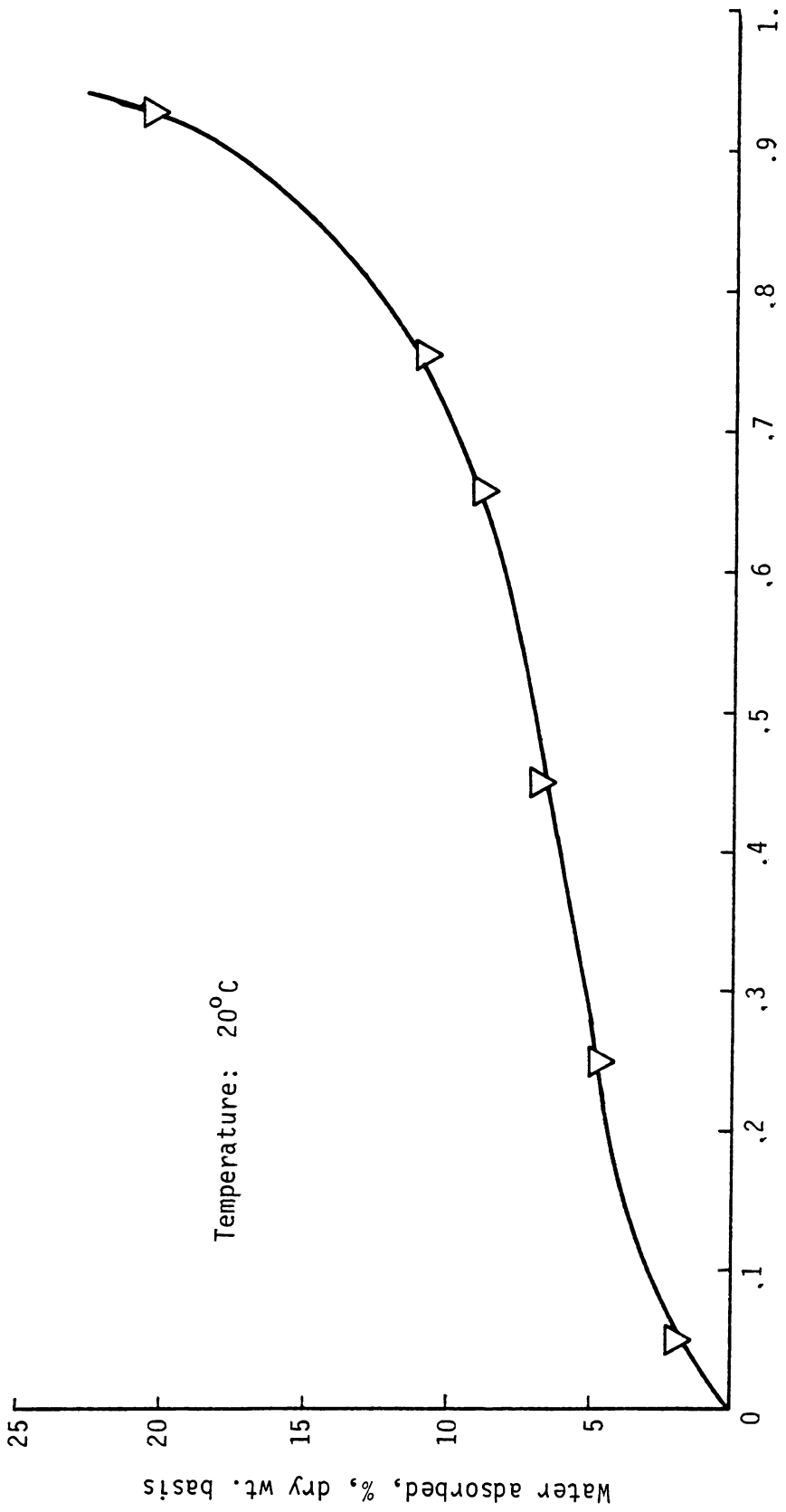

Figure 4.4 Adsorption isotherm of water on pulp fiber (cellulose).

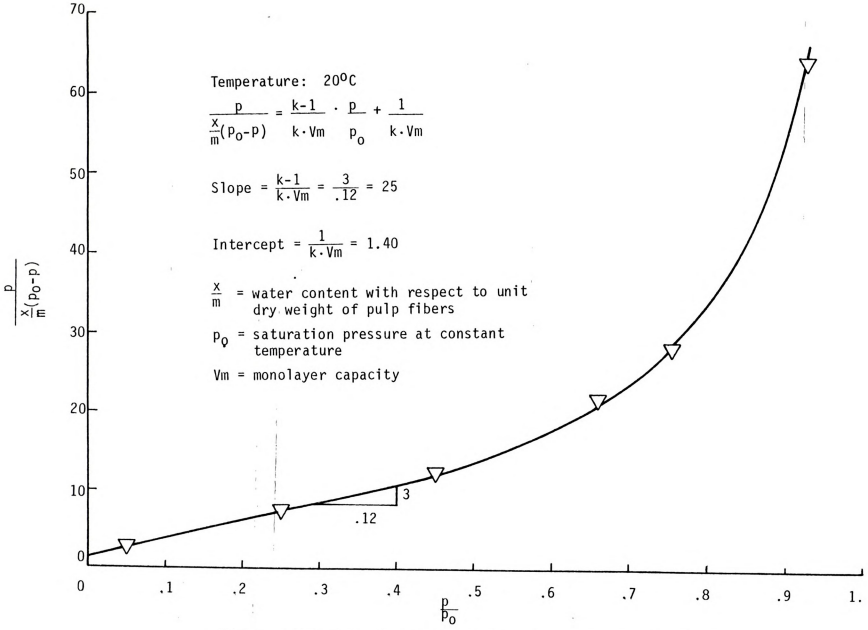

Figure 4.5 B.E.T. Adsorption isotherm of water on pulp fiber.

TABLE 4.4 TABULATED VALUES FOR THE B.E.T. EQUATION

No. of Samples	p	p/p_o	m Dry wt. of sample (gms.)	x Wt. of Moisture (gms.)	$\frac{x}{m}$	$\frac{x}{m}$ (Average)
a	.8767	0.05	0.37455	.00738	.01970	
b	.8767	0.05	0.38811	.00772	.01989	.01953
c	.8767	0.05	0.33081	.00629	.01901	
a	4.3837	0.25	0.23297	.01057	.04537	
b	4.3837	0.25	0.32689	.01531	.04683	.04624
c	4.3837	0.25	0.21077	.00981	.04654	
a	7.8907	0.45	0.32684	.02193	.06709	.06759
b	7.8907	0.45	0.36054	.02455	.06809	
a	11.5731	0.66	0.29015	.02606	.08981	.08925
b	11.5731	0.66	0.27341	.02425	.08869	
a	13.2739	0.757	0.25087	.02759	.10997	.10974
b	13.2739	0.757	0.33080	.03623	.10952	
a	16.3075	0.93	0.25571	.05433	.21246	.20599
b	16.3075	0.93	0.26176	.05223	.19953	

Room temperature = 20°C

Saturation pressure, p_o = 17.535 mm of Hg.

Density of Hg. = 13.546

Density of H_2O = 0.9982

TABLE 4.5 B.E.T. ADSORPTION ISOTHERM DATA

No.	p	$\frac{p}{\frac{x}{m}(p_o-p)}$	$\frac{p}{p_o}$
1	0.88	2.69	0.05
2	4.38	7.21	0.25
3	7.89	12.10	0.45
4	11.57	21.75	0.66
5	13.27	28.39	0.757
6	16.31	64.49	0.93

Temperature = 20°C

Saturation pressure, p_o = 17.535 mm of Hg.

$$\frac{p}{\frac{x}{m}(p_o-p)} = \frac{1}{kv_m} + \frac{k-1}{kv_m} \cdot \frac{p}{p_o}$$

$$\text{Slope} = \frac{11-8}{.40-.28} = 25, \qquad \frac{k-1}{kv_m} = 25$$

$$\text{Intercept} = 1.4 \qquad \frac{1}{kv_m} = 1.4$$

$v_m = .03787$

and $k = 18.8571$

The molecular weight of water is 18 grams per mole and there are 6.02×10^{23} water molecules in one mole, hence

$$a = 4 \times .866 \left(\frac{18}{4 \times 6.02 \times 10^{23} \times .99823 \sqrt{2}} \right)^{2/3}$$

$$= 10.56 \times 10^{-16} \text{ cm}^2 = 10.56 \text{ Å}^2$$

From the slope of the B.E.T. curve, Figure 4.5, the monomolecular capacity v_m equals 0.0378 and the number of water molecules in this monolayer capacity therefore equals,

$$\frac{6.02 \times 10^{23}}{18} \times .0378 = 1.26 \times 10^{21} \text{ molecules}$$

and the specific surface area = $(1.26 \times 10^{21})(10.56 \times 10^{-16})/100^2$

$= 133 \text{ m}^2/\text{dry gram of cellulose.}$

4.2 Compression Tests

Compression tests on fiber/kaolinite samples of varying composition were conducted in one dimension, the load approaching 360 kg/cm^2. Samples tested included those made from fibers, 25 percent fibers/75 percent kaolinite by volume, 54 percent fibers/46 percent kaolinite by volume, and kaolinite.

4.2.1 Kaolinite

Compressibility characteristics of kaolinite samples were studied by confining the soil sample in directions at right angles to the axis of controlled stress application. This is similar to the conditions in natural soil strata, one dimensional deformation in the direction of the principal applied stress. This compressive deformation

is expressed in terms of the soil void ratio, hence the results are referenced to a scale which is independent of the size of the specimen tested (Scott, 1963). The void ratios corresponds to equilibrium conditions with respect to the applied stresses, that is the stable condition achieved by interparticle contact for a given load. The effective normal stresses are plotted on a horizontal scale against the equilibrium void ratios on a vertical scale in Figure 4.6a. The initial larger deformations occur as a result of grain movements or adjustments between particles. As the stress increases these movements decrease as the grains settle into more stable positions. With increase in vertical stress a large proportion of the movement appears to be due to elastic compression (Scott, 1963) of the grains. Figure 4.6a shows that the initial part of the diagram is curvilinear whereas the part corresponding to high stress levels is approximately a straight line. At a stress level of 2.40 kg/cm^2, which is the consolidation load of the sample, the void ratio was 1.189. This void ratio for pure kaolinite is relatively high suggesting that the particles of clay are randomly oriented. At a stress of 330 kg/cm^2 the void ratio decreases to a value of 0.50 suggesting a denser structure in which the clay particles have perhaps achieved a more orderly arrangement. The straight line portion has a gentle slope indicating a small change in void ratio corresponding to a relatively large change in the applied normal stress.

The normal effective stress on a logarithmic scale is plotted against void ratio on a natural scale in Figure 4.6b with a straight

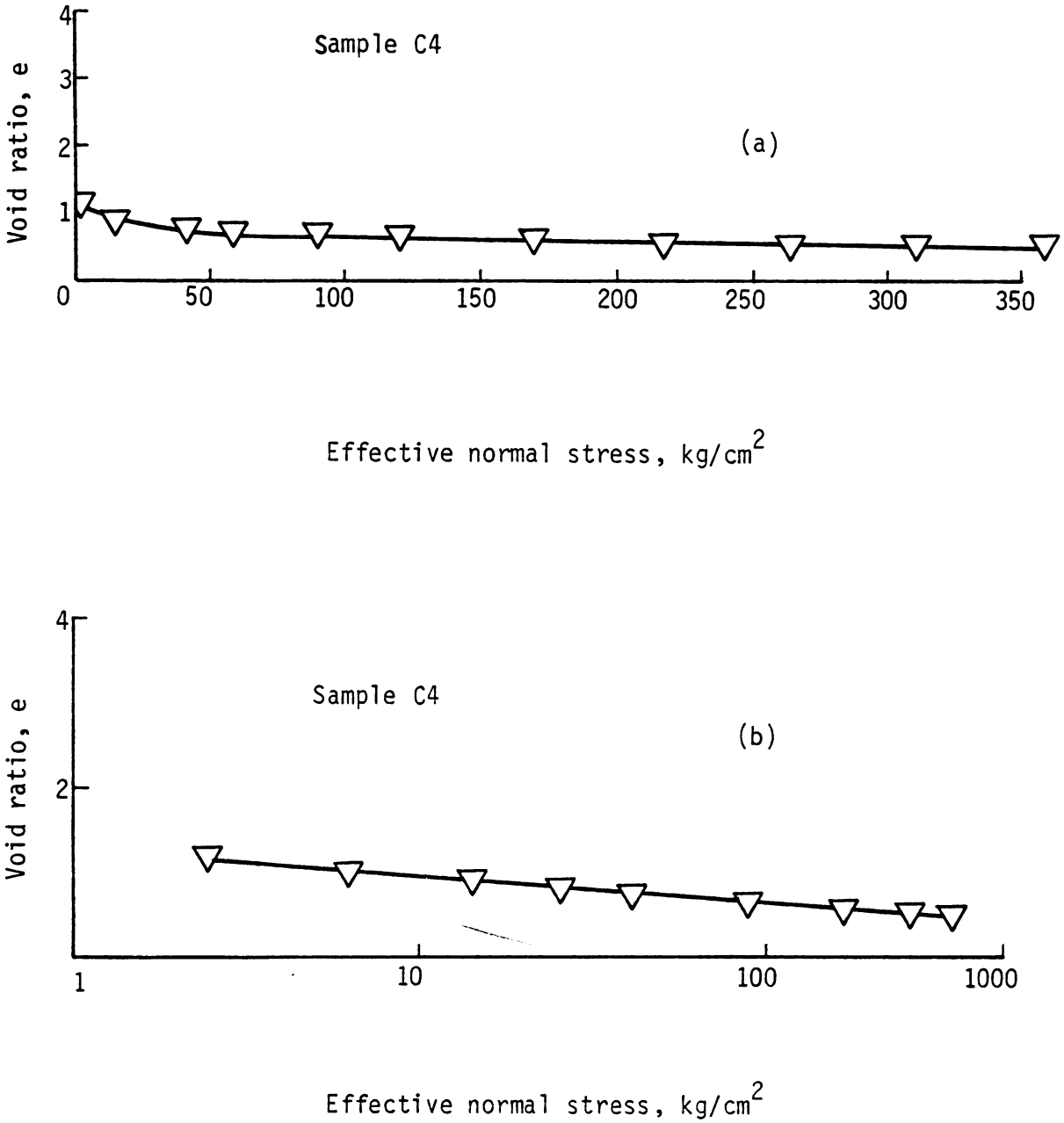

Figure 4.6 Effective normal stress (Natural and logarithmic scale) vs. void ratio curves for Kaolinite samples.

line drawn through the data points. This straight line relationship is common for dispersed clays.

4.2.2 Kaolinite-Fiber Mixtures

Samples subjected to compressibility tests were prepared from 1) a mixture of 54 percent fibers and 46 percent kaolinite by volume and 2) a mixture of 25 percent fibers and 75 percent kaolinite by volume.

Effective normal stress is plotted against the corresponding equilibrium void ratio in Figures 4.7a and 4.8a. The initial part of the curves corresponding to relatively low normal effective stresses are curvilinear whereas at higher normal effective stresses they display approximately a linear relationship between the normal effective stresses and the corresponding void ratios at equilibrium.

The normal effective stresses are plotted on a logarithmic scale against the corresponding void ratios at equilibrium on a natural scale in Figures 4.7b and 4.8b. The behavior indicated by the curvilinear nature of these plots is similar to the behavior expected from a flocculated clay (Scott, 1963) subjected to the same type of compression test. The radius of curvature of these curves appear to decrease with increasing fiber content in the test sample.

4.2.3 Fiber Samples

All fiber samples were subjected to compression tests in a manner similar to those for kaolinite and mixed samples. The void ratio-stress curves for all fiber samples are shown in Figure 4.9. The shape of the curve in Figure 4.9a is similar to the curve shown

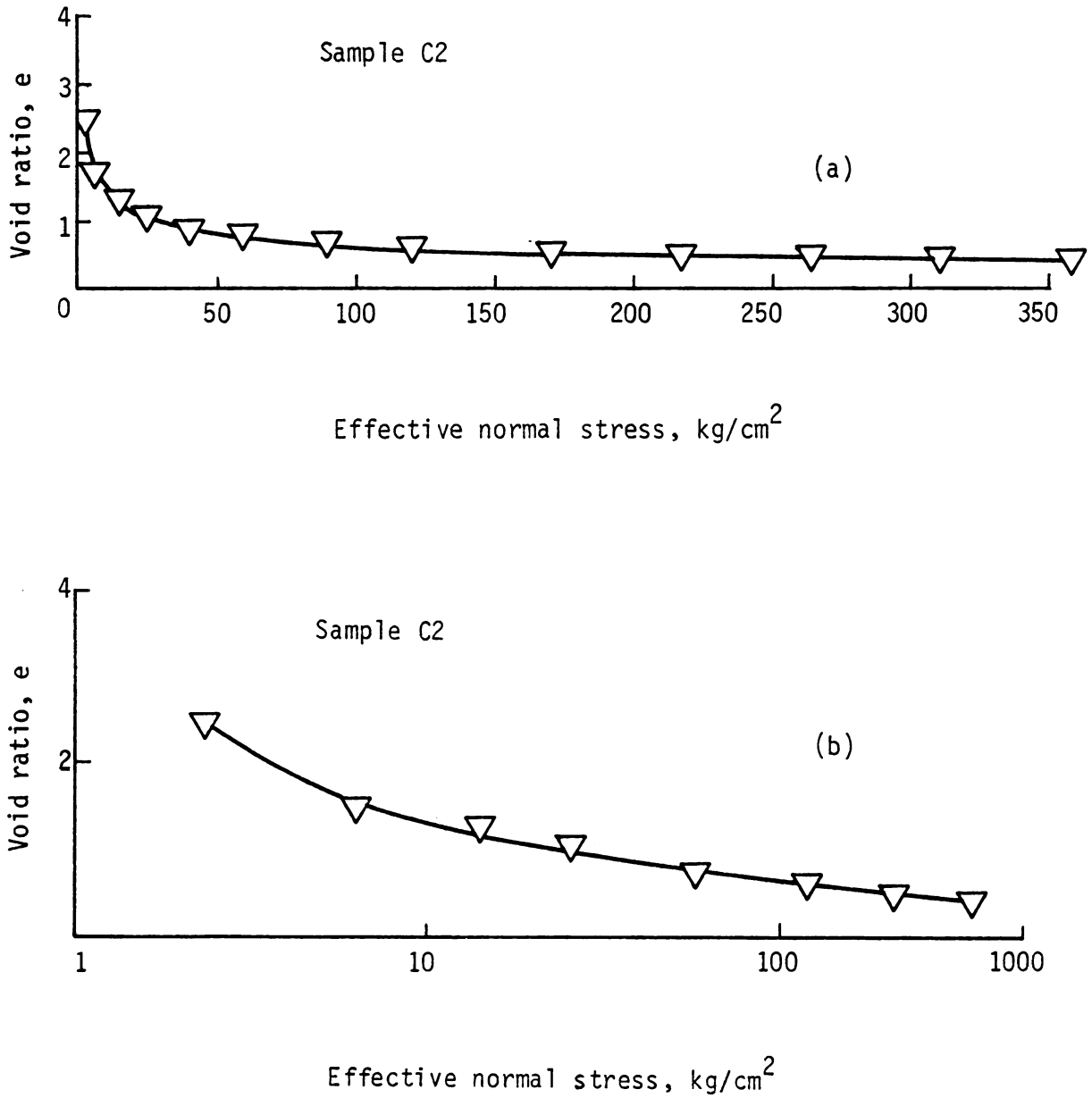

Figure 4.7 Effective normal stress (Natural and logarithmic scale) vs. void ratio curves for 54% fibers/46% Kaolinite samples (by volume).

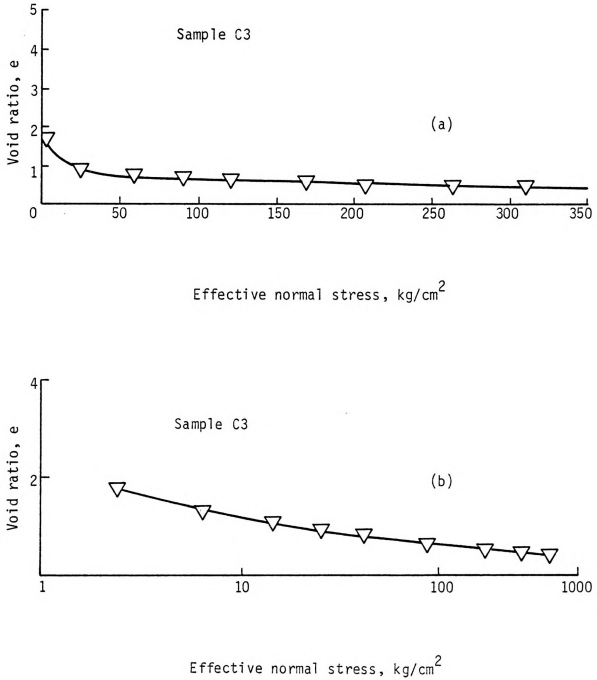

Figure 4.8 Effective normal stress (Natural and logarithmic scale) vs. void ratio curves for 25% fibers/75% Kaolinite samples (by volume).

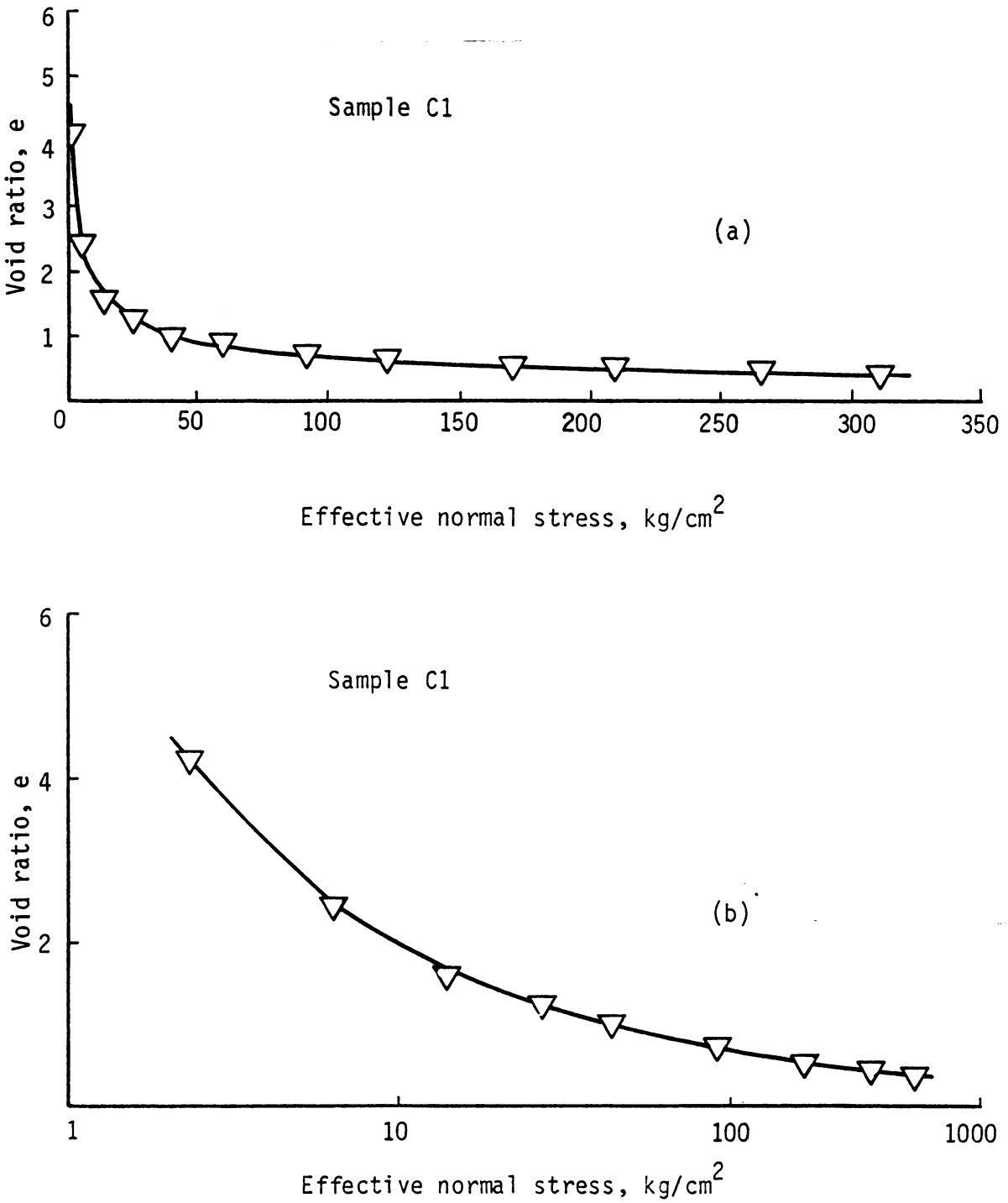

Figure 4.9 Effective normal stress (Natural and logarithmic scale) vs. void ratio curves for all fiber samples.

TABLE 4.6 SUMMARY OF COMPRESSION TEST DATA

Test No.	Sample Composition (% by Vol.)	Compression Load (kg/cm^2)	Final Void Ratio	Coefficient of Vol. Compresibility (cm^2/kg)
C_1	100%F*	6.3974	2.4383	980×10^{-4}
		43.8087	0.9916	156.42×10^{-4}
		171.6723	0.5285	43.10×10^{-4}
		360.2678	0.3588	21.22×10^{-4}
C_2	54%F + 46%C	6.3975	1.6886	558.04×10^{-4}
		42.4974	0.8948	112.82×10^{-4}
		170.3610	0.5449	32.95×10^{-4}
		358.9199	0.4127	16.59×10^{-4}
C_3	25%F + 75%C	6.4315	1.3344	384.65×10^{-4}
		42.0928	0.8159	86.33×10^{-4}
		169.9563	0.5527	26.13×10^{-4}
		358.5245	0.4344	13.49×10^{-4}
C_4	100%C*	6.3975	1.0123	202.41×10^{-4}
		42.0338	0.7403	51.75×10^{-4}
		169.8974	0.5720	16.83 c 10^{-4}
		358.4202	0.4791	9.11×10^{-4}

*F = Fibers
C = kaolinite

in Figure 4.7a for the fiber/kaolinite mixture. At a consolidation pressure of 2.40 kg/cm^2 the void ratio of 4.65 (Figure 4.9a) was the highest compared to the void ratios obtained for previous fiber/kaolinite samples at the same level of normal effective stress, however, the void ratio decreased more rapidly with increasing stress. Note that all fiber samples display consistently higher void ratios compared to all other test samples as long as the normal effective stress level was less than approximately 118 kg/cm^2. A summary of compression tests is presented in Table 4.6.

4.3 Direct Shear Tests

Samples subjected to direct shear tests were prepared from full length fibers and powdered fibers. Tests were carried out on saturated and dry fiber samples.

4.3.1 Saturated Fiber

Typical curves for direct shear tests on a saturated fiber sample are shown in Figure 4.10. Shear displacement is plotted against shear stress and vertical displacement. Failure was arbitrarily assumed at 20 percent strain since the material exhibits a continuous increase in shear strength with increasing displacement.

The behavior of a saturated fiber sample subjected to two cycles of loading and unloading is presented in Figure 4.11a with shear displacement plotted against shear stress and vertical displacement. Each cycle of load produces permanent strain as shown by the two intercepts on the horizontal axis. Figure 4.11b shows the change in the vertical displacement caused by the cyclic load. The variation of water content with consolidation pressure for saturated fiber samples is summarized in Figure 4.12.

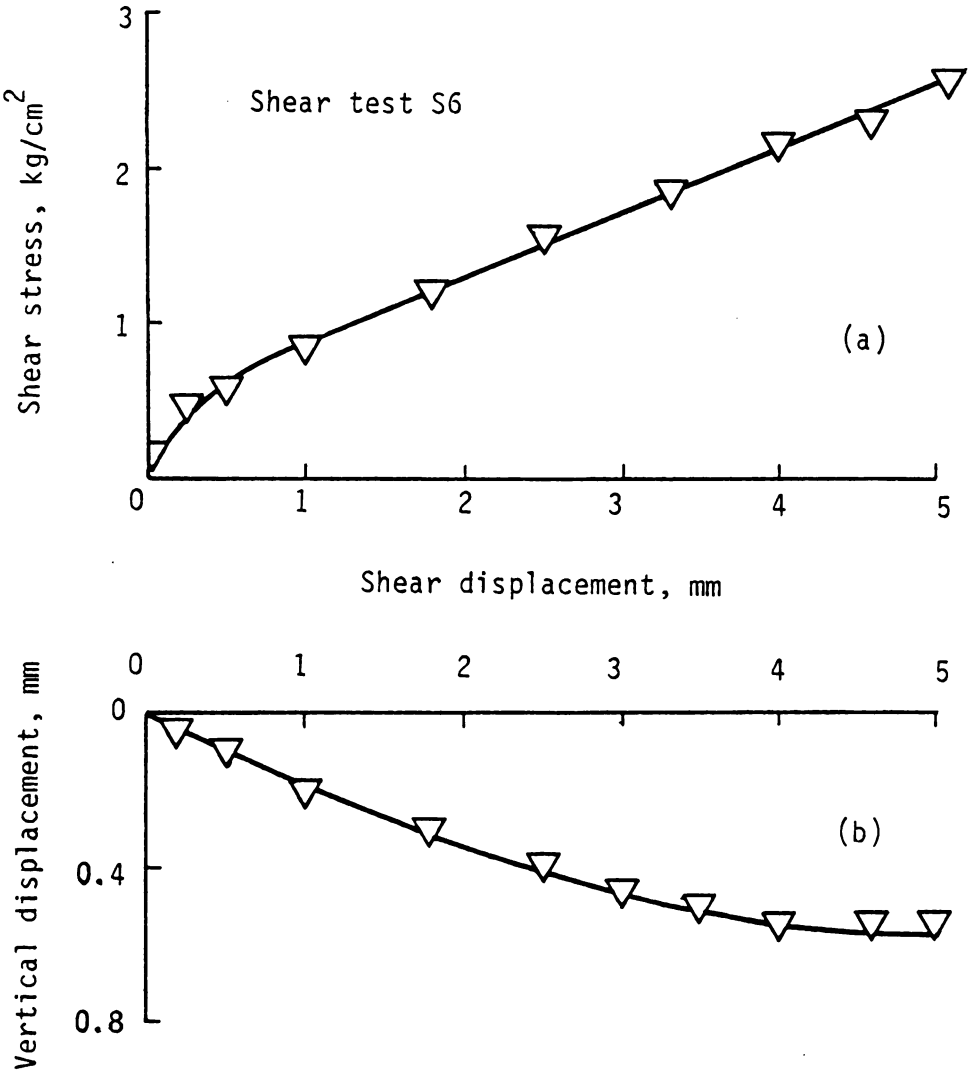

Figure 4.10 Typical Shear displacement vs. Shear stress and Vertical displacement curves for saturated fiber samples.

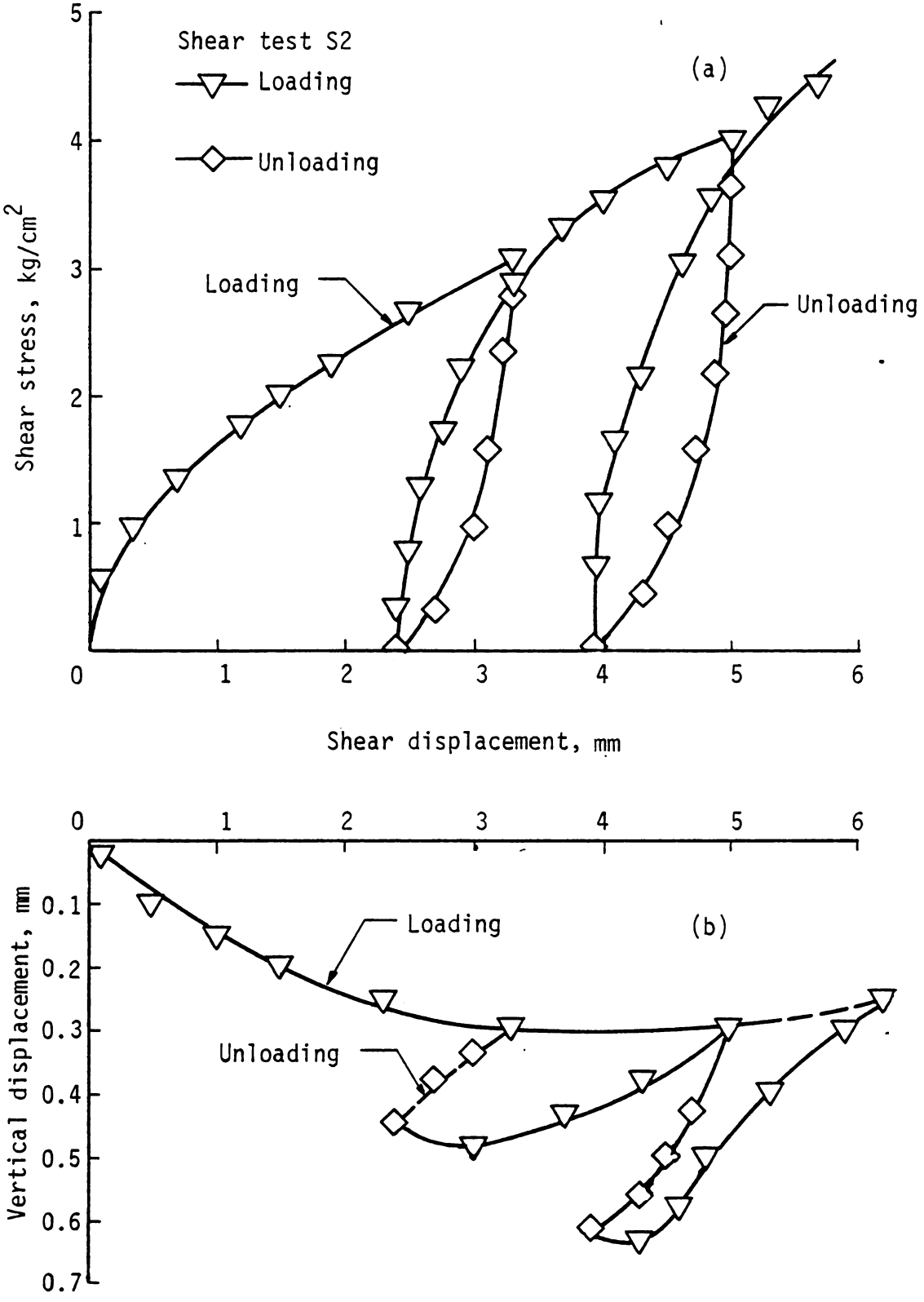

Figure 4.11 Shear displacement vs. Shear stress and Vertical displacement curves caused by two cycles of loading and unloading a fiber sample.

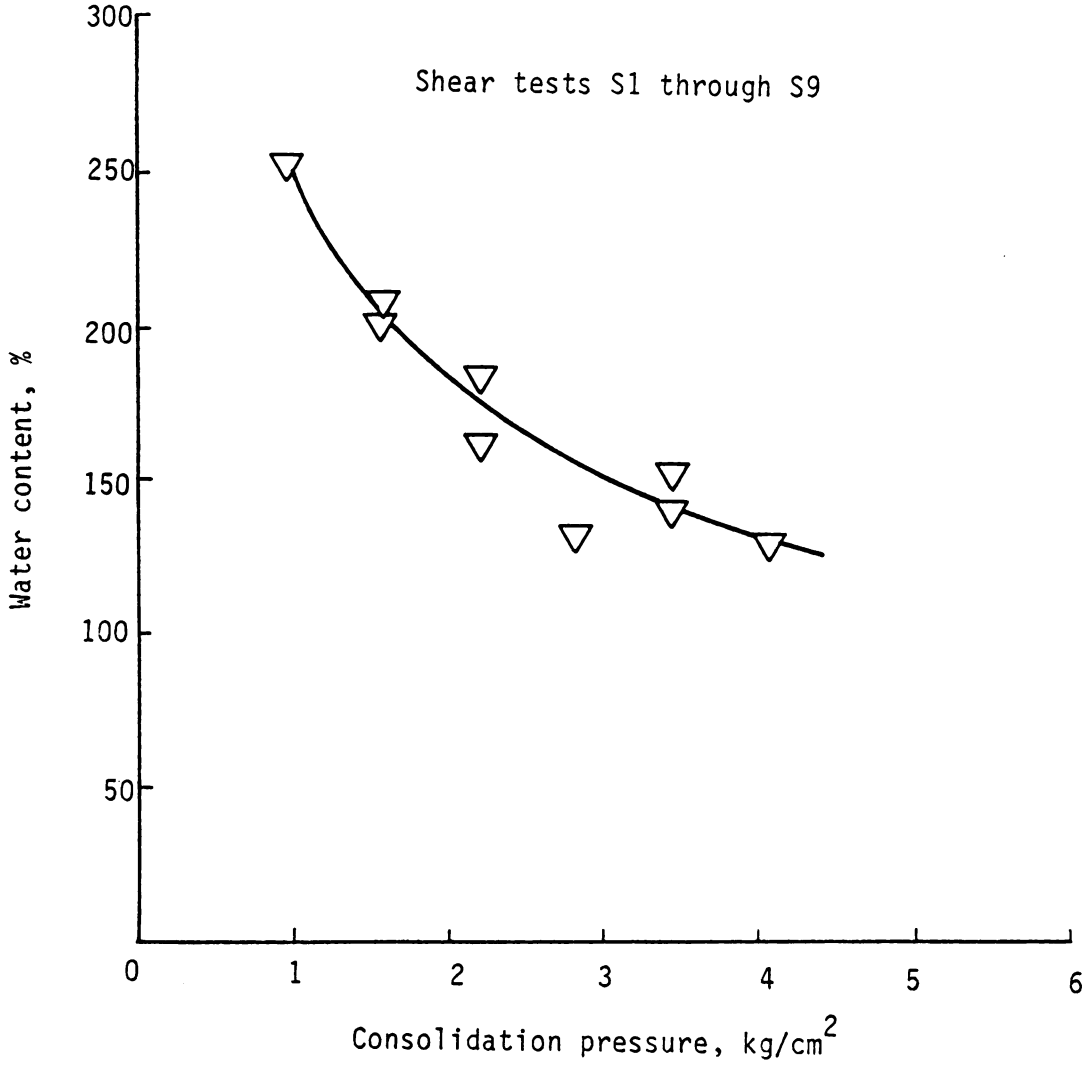

Figure 4.12 Consolidation pressure vs. final water contents for saturated fiber samples.

4.3.2 Dry Fiber

Two types of dry fiber samples, one oven dried (hard cake) and the second prepared from freeze dried fibers, were subjected to direct shear tests. The results obtained for the two sample types were expected to be different due to the difference between their physical characteristics caused by the methods used to dry the fibers.

Consolidation pressure is plotted against void ratio for dry and saturated fiber samples in Figure 4.13. The dry fiber samples consistently maintained a higher void ratio than the saturated fiber samples for the same consolidation pressure.

Horizontal displacement is plotted against shear stress and vertical displacement for a sample composed of dry powdered fibers in Figure 4.14. The continuous increase of shear strength with increasing lateral strain is shown in Figure 4.14a. The decrease in sample volume with increasing lateral strain is shown in Figure 4.14b.

Shear displacement is plotted against shear stress and vertical displacement for an oven dried sample composed of all fibers in Figure 4.15. The behavior of this sample was quite different from that observed for the dry powdered fiber sample. The shear strength of the sample increased rapidly with a small increment of strain and the sample failed suddenly at approximately 12 percent strain (Figure 4.15a). Sudden rupture was perhaps due to the fracture of the bond between the fibers in the case of the oven dried sample. The sample exhibited an increase in volume with increasing lateral strain (Figure 4.15b). A summary of the direct shear tests conducted on dry and saturated fiber samples is presented in Table 4.7.

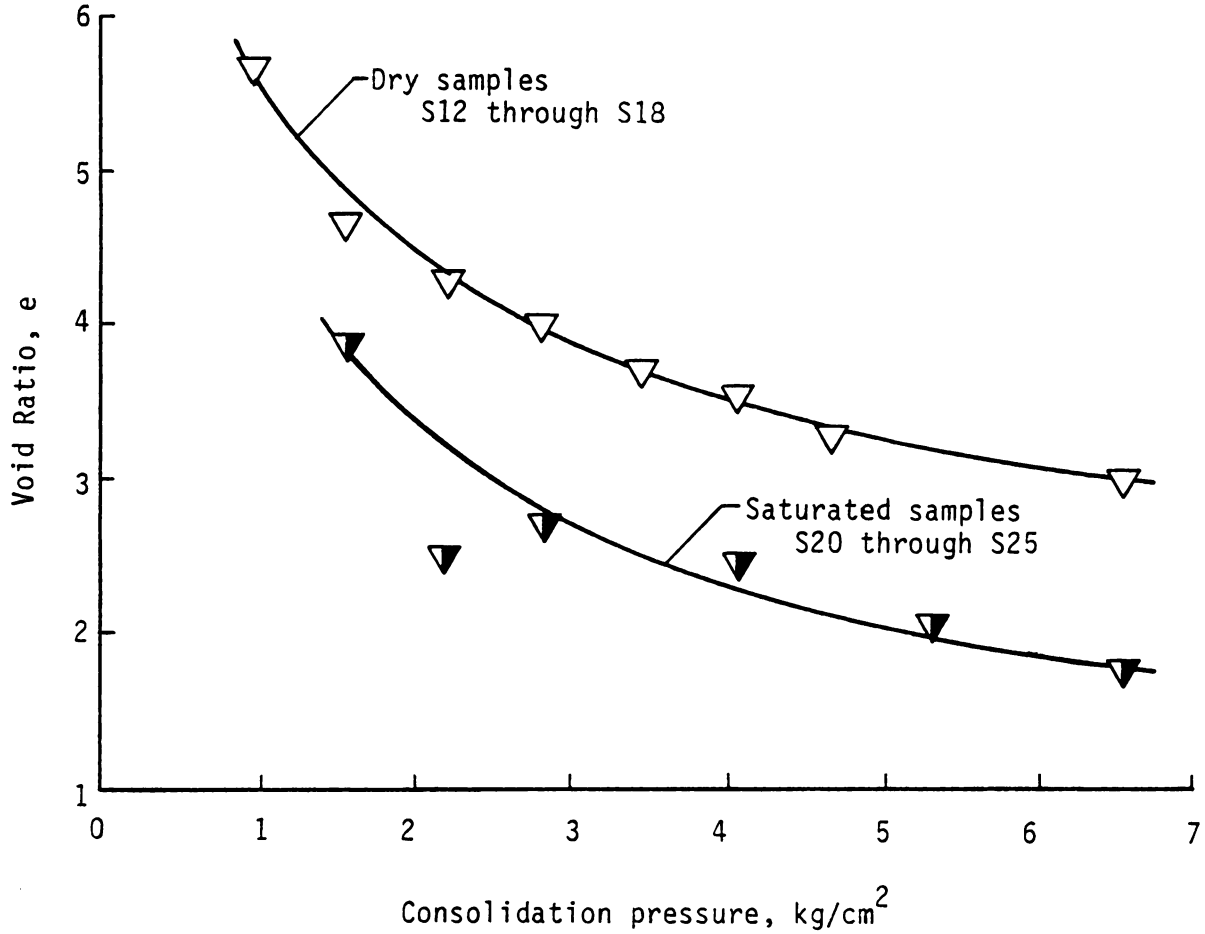

Figure 4.13 Consolidation pressure vs. Void ratio curves for saturated and dry powdered fiber samples.

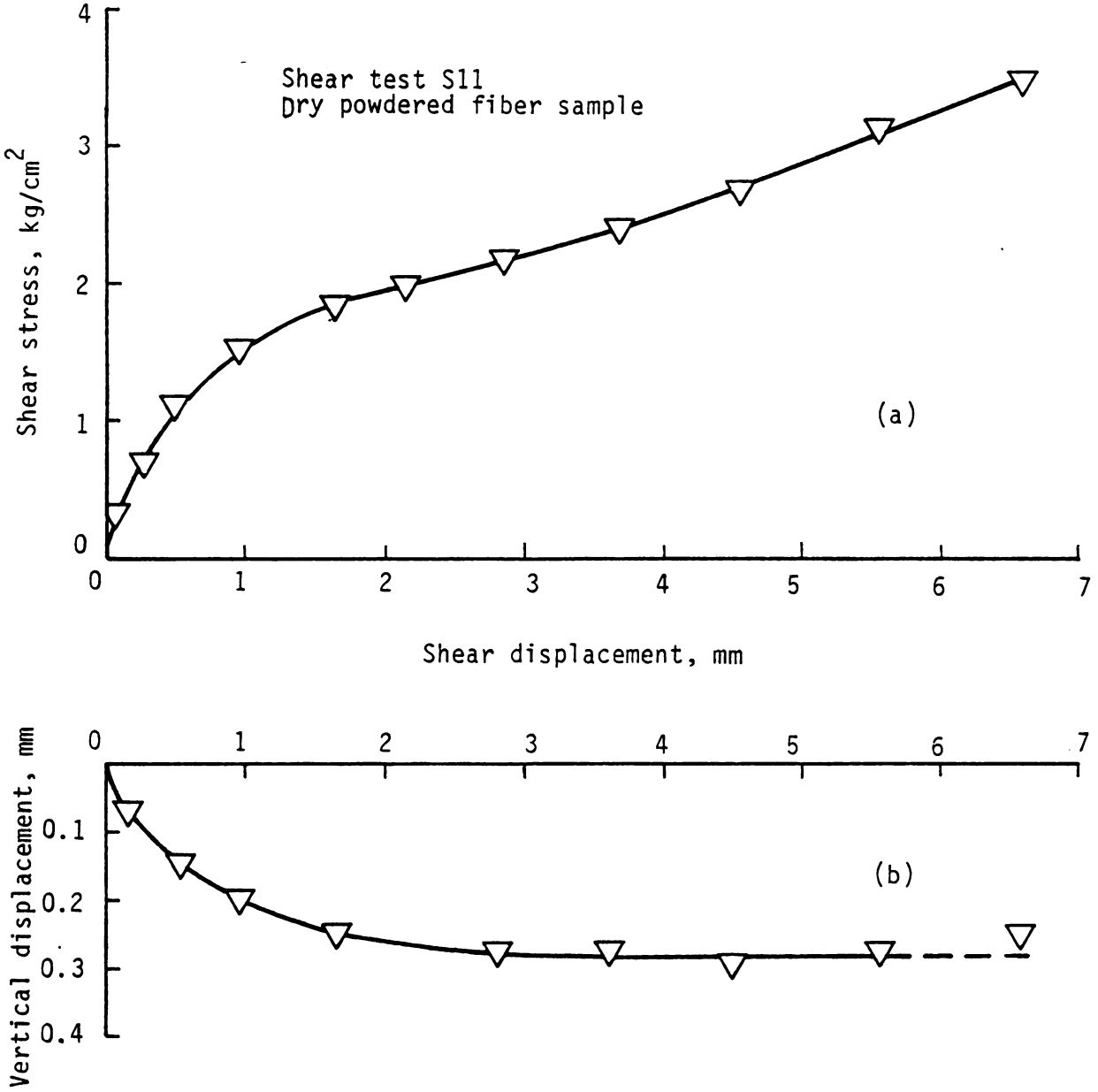

Figure 4.14 Typical Shear displacement vs. Shear stress and Vertical displacement curves for dry powdered fiber samples.

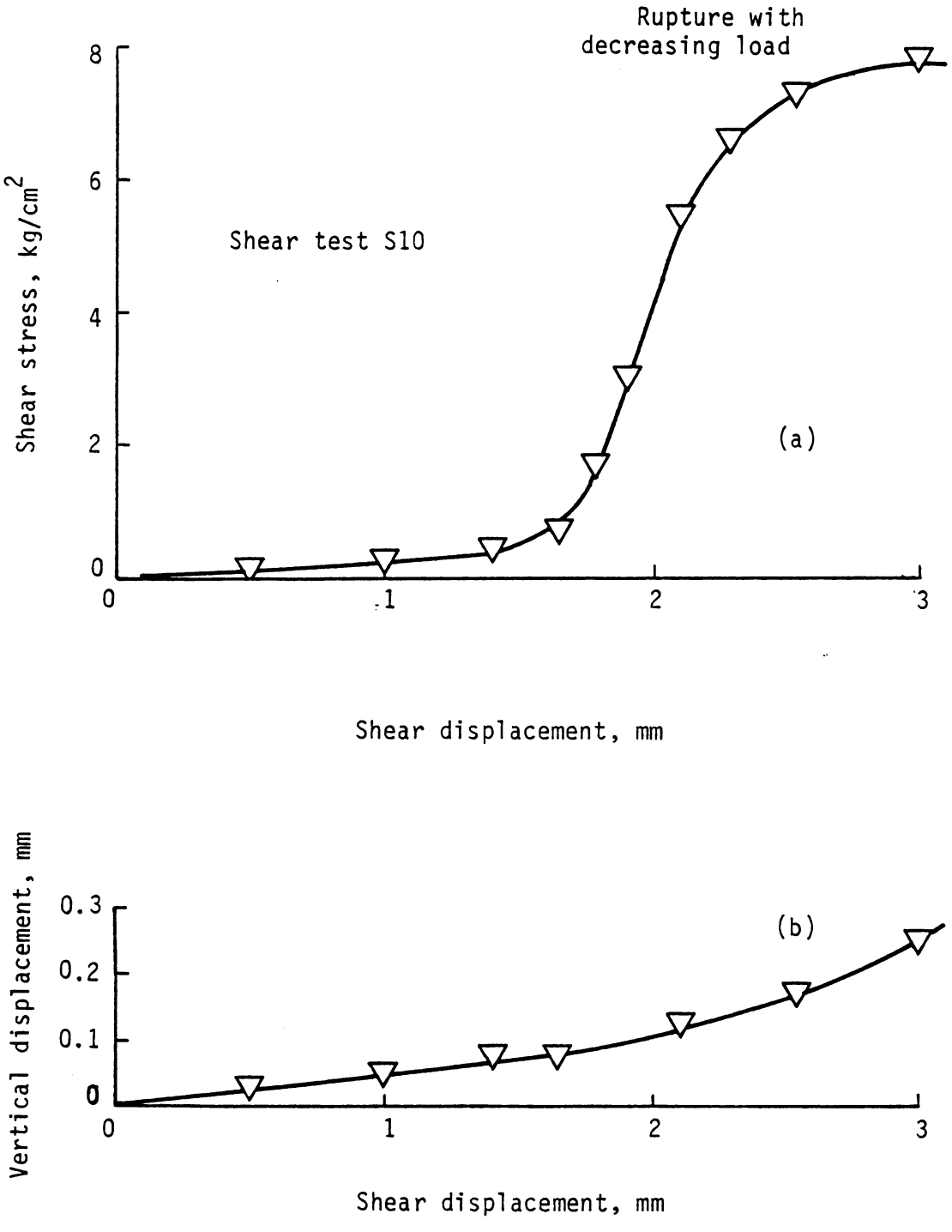

Figure 4.15 Shear displacement vs. Shear stress and Vertical displacement curves for an oven-dried fiber sample.

TABLE 4.7 SUMMARY OF DIRECT SHEAR TEST RESULTS

Test Sample	Consolidation Pressure (Kg/cm^2)	Water* Content (%)	Dry* Density (pcf)	Normal Stress $\bar{\sigma}_v$ (kg/cm^2)	Shear Stress $\bar{\tau}$ at Failure (kg/cm^2)	Failure Displacement (%)	$\phi=\tan^{-1}\frac{\bar{\tau}}{\bar{\sigma}_v}$ (Degrees)	Remarks
S1	2.83	131.50	31.77	2.83	3.4682	20	50.78	Saturated Sample
S2	3.45	140.00	30.45	3.45	4.0220	20	49.38	Saturated Sample
S3	4.06	129.00	32.18	4.06	5.1644	20	51.83	"
S4	1.58	201.00	23.47	1.58	1.9487	20.50	50.96	"
S5	.96	253.00	19.63	.96	1.1422	20	49.95	"
S6	2.21	174.00	26.12	2.21	2.5160	20	48.70	"
S7	3.45	153.00	28.63	3.45	3.6415	20	46.55	"
S8	1.58	207.00	22.95	1.58	1.7050	20	47.18	"
S9	2.21	161.00	27.62	2.21	2.6650	20	50.33	"
S10	1.27	250.00	19.81	2.21	7.8252	12	74.23	Oven dried Sample
S11	2.20	---	n.a.	2.21	2.8640	20	52.34	Dry Fiber Sample
S12	.962	---	14.50	.962	1.2911	20	53.31	"
S13	1.584	---	17.06	1.584	2.003	20	51.66	"
S14	2.21	---	18.17	2.21	3.0150	20.50	53.76	"
S15	2.83	---	18.97	2.83	3.2118	20	48.62	"
S16	3.452	---	20.51	3.452	3.8732	20	48.29	"
S17	4.075	---	21.23	4.075	4.0722	20	44.98	"
S18	4.686	---	22.43	4.686	5.3465	20	48.77	"
S19	6.550	---	24.14	6.550	7.1846	20	47.65	"
S20	1.584	185	24.89	1.584	2.1524	20	53.65	Saturated

TABLE 4.7 (Continued)

Test Sample	Consolidation Pressure (Kg/cm^2)	Water* Content (%)	Dry* Density (pcf)	Normal Stress $\bar{\sigma}_v$ (kg/cm^2)	Shear Stress τ at Failure (kg/cm^2)	Failure Displacement (%)	$\phi=\tan^{-1}\frac{\tau}{\bar{\sigma}'_v}$ (Degrees)	Remarks
S21	2.206	159	27.83	2.206	2.7309	20	51.07	Saturated
S22	2.830	175	26.04	2.830	3.3104	20	49.47	"
S23	4.075	157	28.12	4.075	4.1057	20	45.22	"
S24	6.550	112	35.07	6.550	7.1846	20	47.65	"
S25	5.304	132	31.71	5.304	5.6610	20	46.86	"

*Water content and dry density after consolidation.

n.a. = Not available

4.4 Triaxial Compression Tests

Triaxial tests involved measurement of the shear strength of fibrous organic soil samples subjected to both consolidated undrained and drained conditions. Test results are shown under three sections: kaolinite, kaolinite/fiber mixtures, and fiber samples.

4.4.1 Kaolinite

Kaolinite samples approximately 3 inches high by 1 1/2 inches in diameter were cut from a normally consolidated kaolinite cylinder approximately 8 inches in height and 4 inches in diameter. Before running the undrained triaxial test the sample was again consolidated for 24 hours inside the triaxial cell to a slightly higher consolidation pressure to ensure a normally consolidated condition. The consolidation pressure ranged from a minimum of 1.50 kg/cm^2 to a maximum of 6.50 kg/cm^2. A back pressure was utilized to ascertain saturation. Nine normally consolidated kaolinite samples were subjected to undrained triaxial shear tests with pore pressure measurements. Brittle failure occurred in all samples at a maximum effective deviator stress $(\bar{\sigma}_1 - \bar{\sigma}_3)_{max}$ with strain at failure ranging from a minimum of 6.6 percent to a maximum of 12.7 percent.

There was a tendency of the failure strain to diminish with increasing consolidation pressure. Figure 4.16 shows percent strain at failure plotted against the consolidation pressure. Higher consolidation pressures resulted in lower water contents and therefore a higher degree of brittleness. Samples with lower consolidation pressures also exhibited a brittle type of failure at a relatively higher strain. The variation of water contents with consolidation pressure

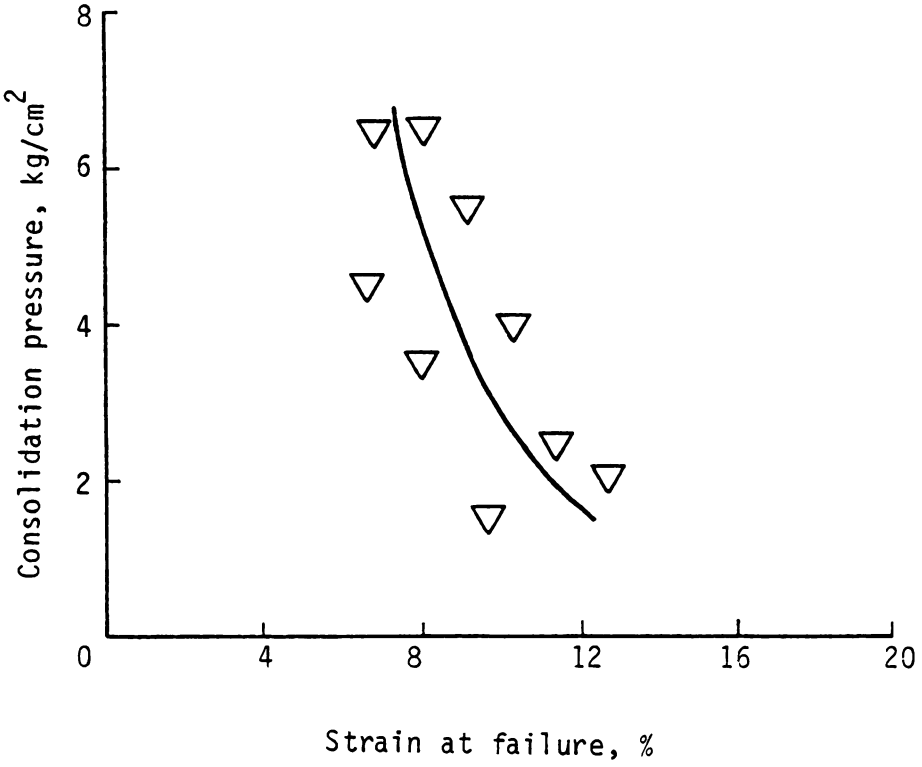

Figure 4.16 Strain at failure vs. Consolidation pressure for Kaolinite samples.

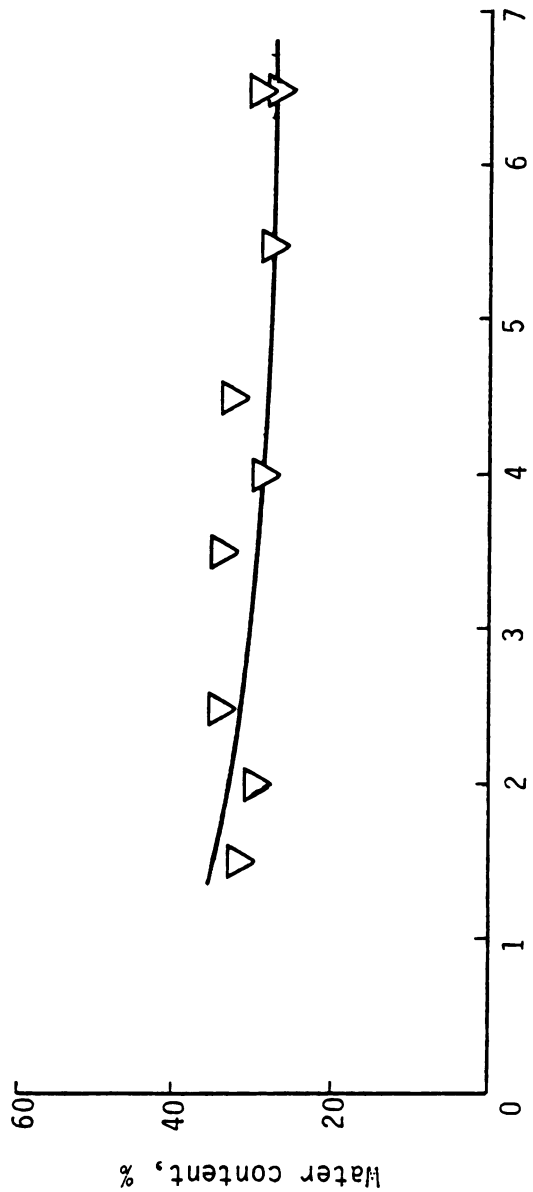

Figure 4.17 Consolidation pressure vs. final water contents for Kaolinite samples.

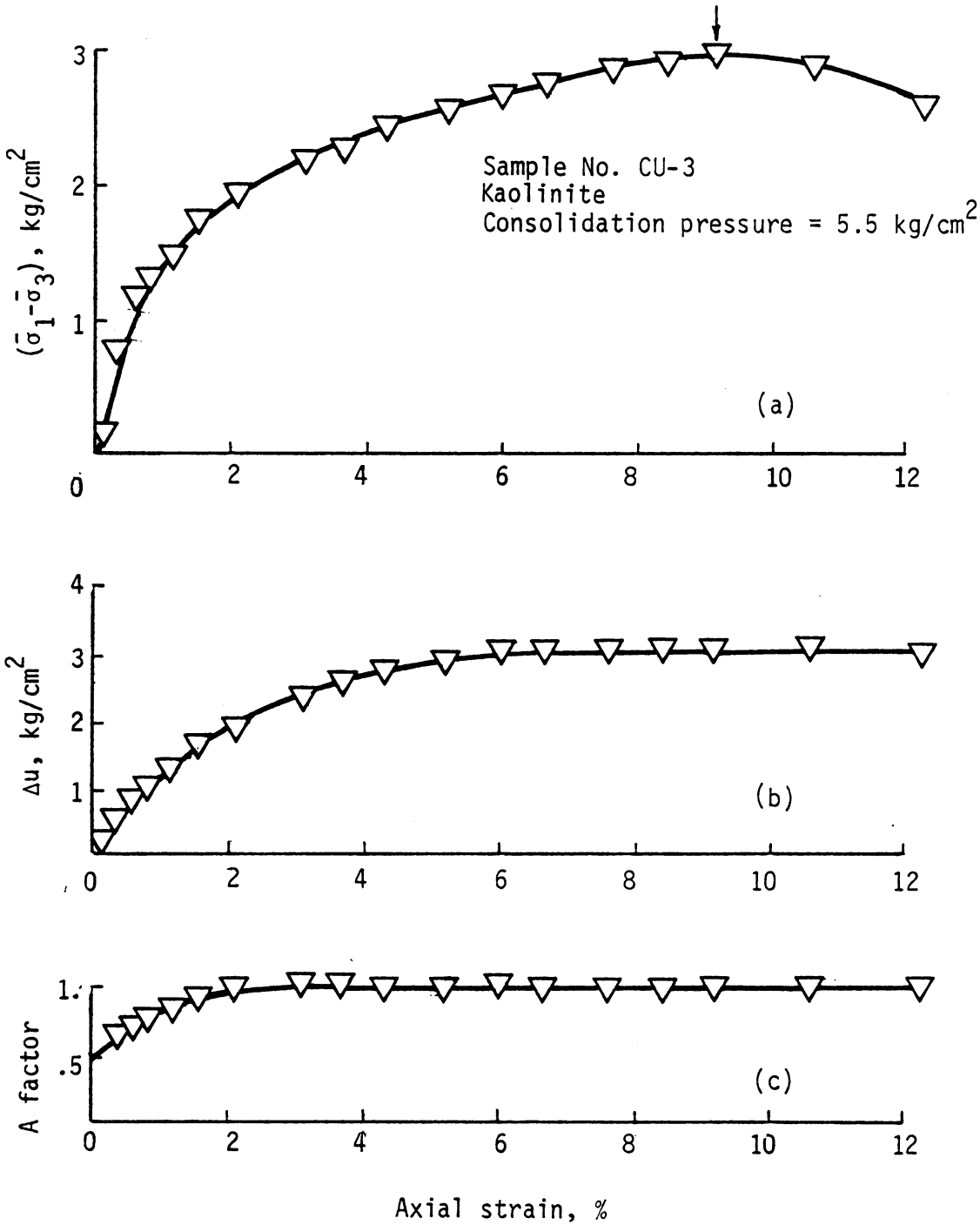

Figure 4.18 Axial strain vs. effective deviator stress, pore pressure and pore pressure coefficient, A, curves for Kaolinite sample CU-3.

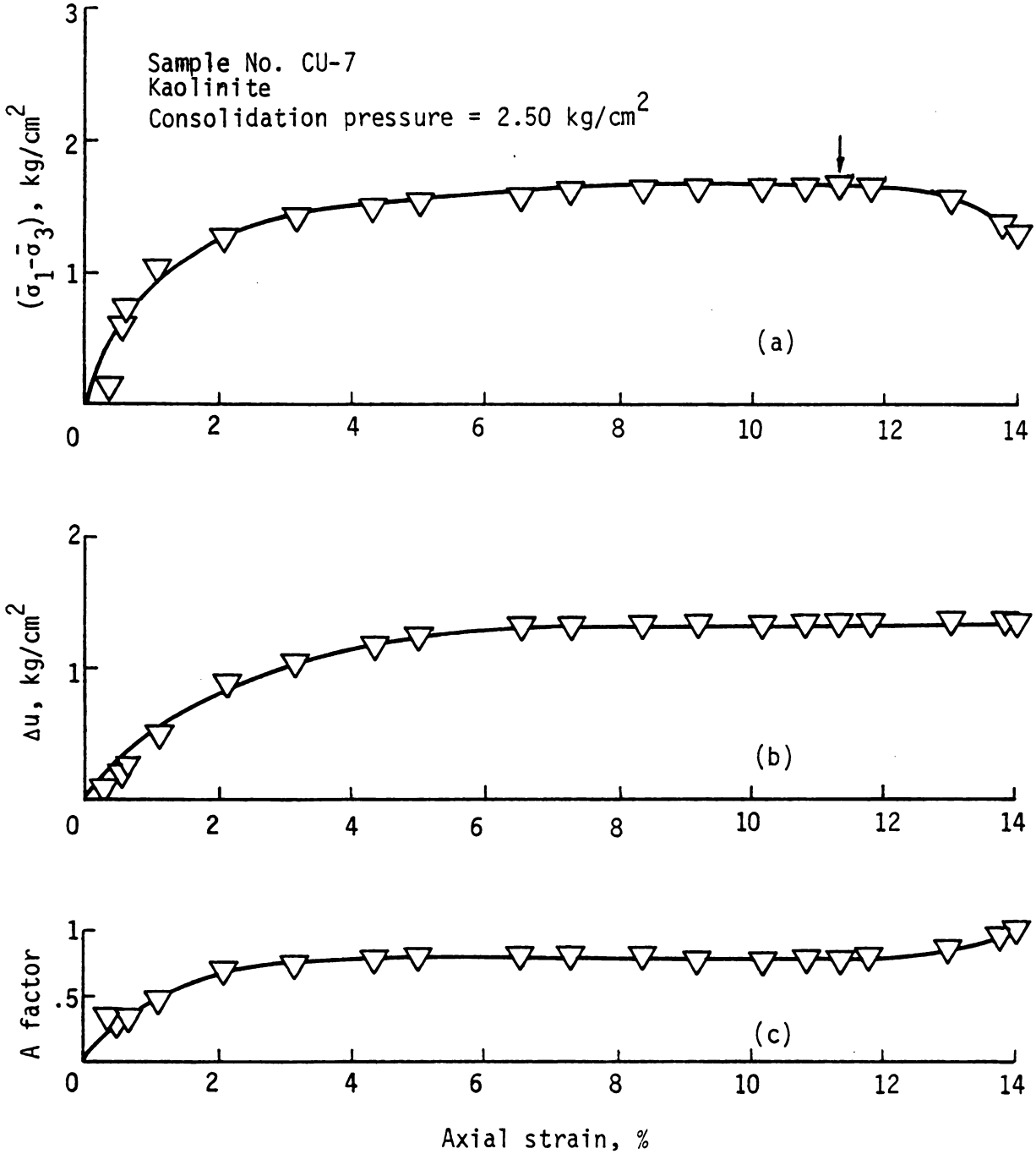

Figure 4.19 Axial strain vs. effective deviator stress pore pressure and pore pressure coefficient, A, curves for Kaolinite sample CU-7.

is shown in two typical plots with percent axial strain plotted against deviator stress ($\bar{\sigma}_1 - \bar{\sigma}_3$), pore pressure Δu, and the pore pressure coefficient A are shown in Figures 4.17, 4.18 and 4.19. These figures represent kaolinite samples normally consolidated to pressures of 5.50 kg/cm^2 and 2.50 kg/cm^2 with failure at 9.2 percent and 11.3 percent axial strain, respectively. The pore pressures in both cases increased rapidly during the early part of the test and leveled off as failure was approached. Pore pressure values at failure were 3.06 kg/cm^2 (Figure 4.18b) and 1.33 kg/cm^2 (Figure 4.19b). The pore pressure coefficient A increased rapidly at low strain values, then leveled off with final values of 1.03 and 0.79, respectively, for the two tests.

4.4.2 Kaolinite/Fiber Mixtures

The kaolinite/fiber mixtures included two combinations, 54% fiber/46% kaolinite and 25% fiber/75% kaolinite by volume. Triaxial tests first involved preparation of a mixture of kaolinite and fiber into a high water content slurry which was consolidated into 200 mm high by 100 mm diameter cylinders. Using a high speed 19 mm diameter circular saw, test specimens 76 mm high by 38 mm in diameter were cut from the larger sample. After placement in the triaxial cell samples were consolidated to a slightly higher pressure. Next a back pressure was applied to the sample in order to achieve a high degree of saturation. Consolidation pressures ranged from 1.5 to 6 kg/cm^2 for the triaxial samples. Six complete triaxial tests were conducted, three consolidated drained and three consolidated undrained, on the 54% fiber/46% kaolinite mixtures. Water contents following consolidation

are summarized in Figure 4.20 for all the tests. Typical curves showing deviator stress, pore water pressure, and the pore pressure coefficient A, all plotted against axial strain for an undrained triaxial test are shown in Figure 4.21. Axial strain was extended to 20 percent so as to permit definition of failure at this value of strain or by the maximum ratio of shear stress to effective normal stress described in a later section. The continuous increase of the deviator stress with increasing strain is shown in Figure 4.21a. The pore pressure value corresponding to 20 percent axial strain equals 2.86 kg/cm^2 in Figure 4.21b and the pore pressure coefficient A equals 0.63 in Figure 4.21c. Typical curves for the consolidated drained triaxial tests, are shown in Figure 4.22 where percent axial strain is plotted against the deviator stress $(\bar{\sigma}_1 - \bar{\sigma}_3)$ and the volumetric strain $\frac{\Delta V}{Vo}$. The change in volume is ΔV with the initial volume equal to Vo. Figure 4.22a shows a continuous increase of strength with increasing strain, hence failure was assumed at 20 percent axial strain. The relationship between the axial strain and the volume change of the sample is shown in Figure 4.22b.

Kaolinite-fiber samples with 25 percent fibers and 75 percent kaolinite by volume were prepared in the same manner as described for fiber-clay mixtures in section 4.4.1. Seven triaxial samples were tested, four consolidated undrained and three consolidated drained. The consolidation pressures used, ranged from a minimum of 2 kg/cm^2 to a maximum of 6 kg/cm^2. Prior to application of the deviator stress, back pressures were used in an attempt to insure saturation and to deair the space between the rubber membrane and the sample.

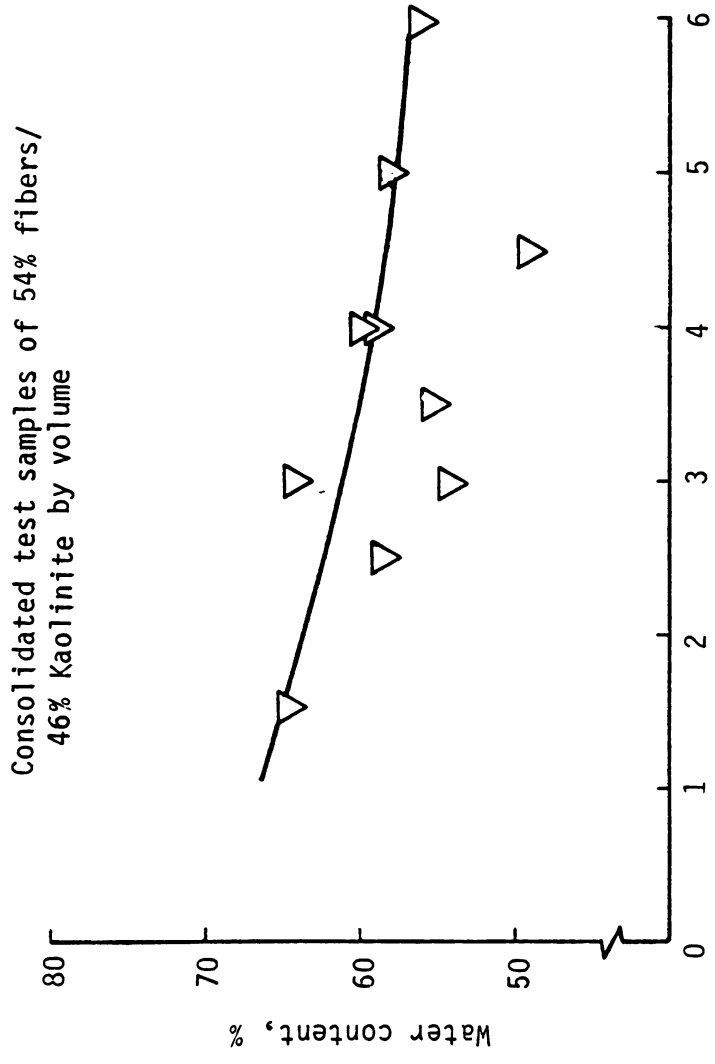

Figure 4.20 Consolidation pressure vs. Water content curve for 54% fibers/46% Kaolinite samples (by volume).

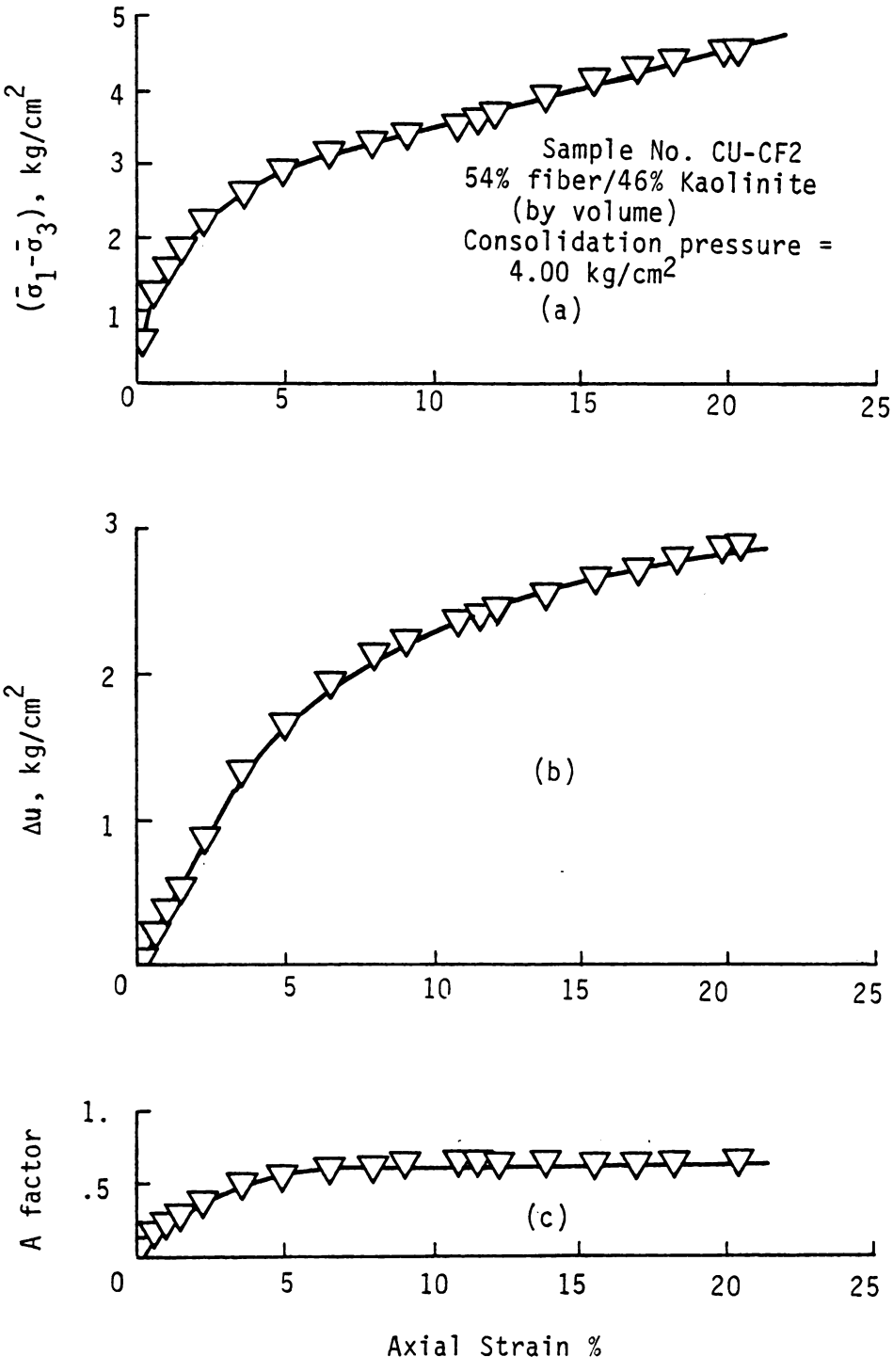

Figure 4.21 Typical results from a normally consolidated undrained triaxial test on 54% fiber/46% Kaolinite (by volume). (a) Deviator stress (b) Pore pressure change (c) Change in parameter A.

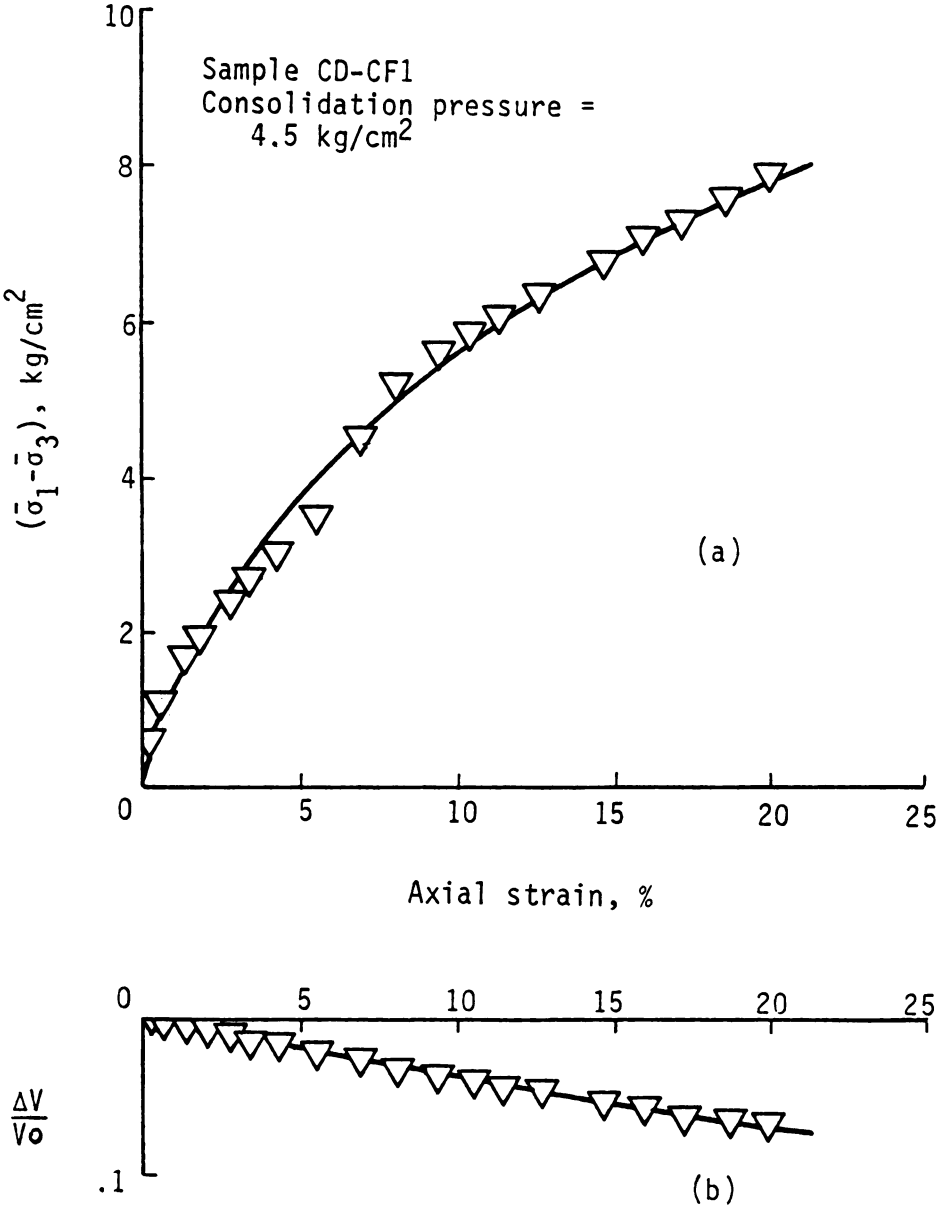

Figure 4.22 Typical results from a drained triaxial test on 54% fiber/ 46% Kaolinite (by volume). (a) Deviator stress (b) Volume change.

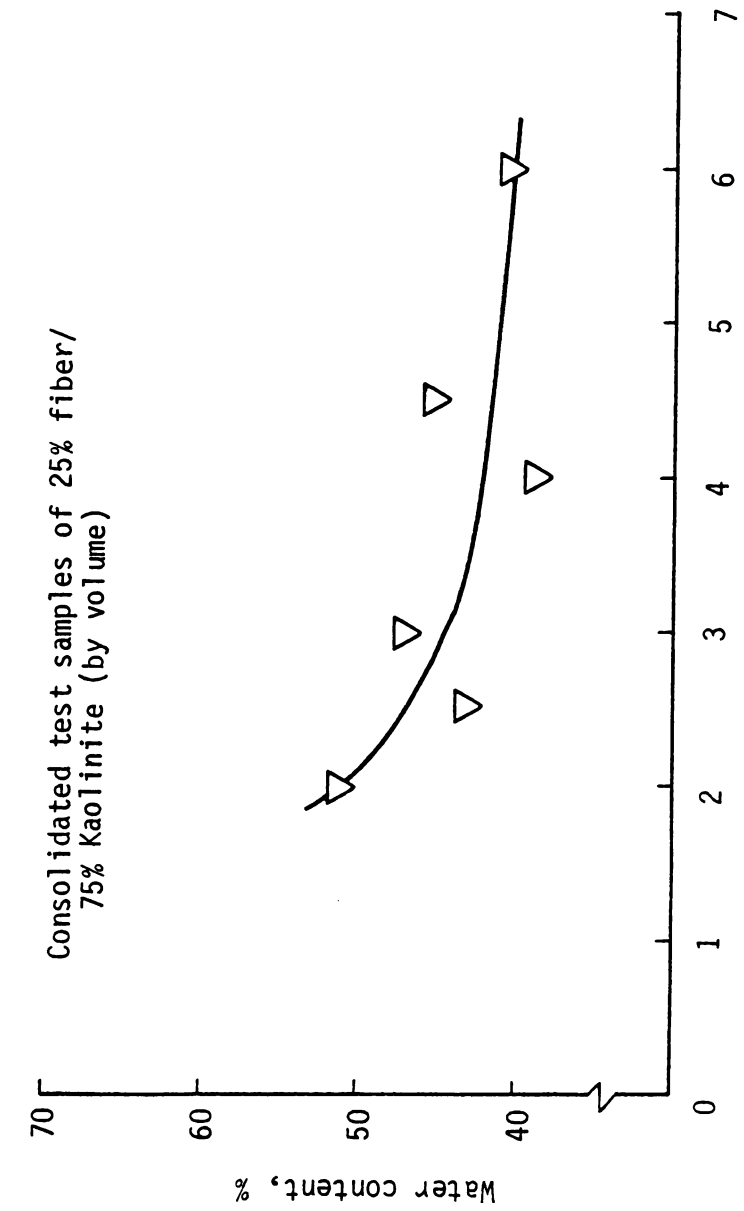

Figure 4.23 Consolidation pressure vs. Water content for 25% fibers and 75% Kaolinite samples (by volume).

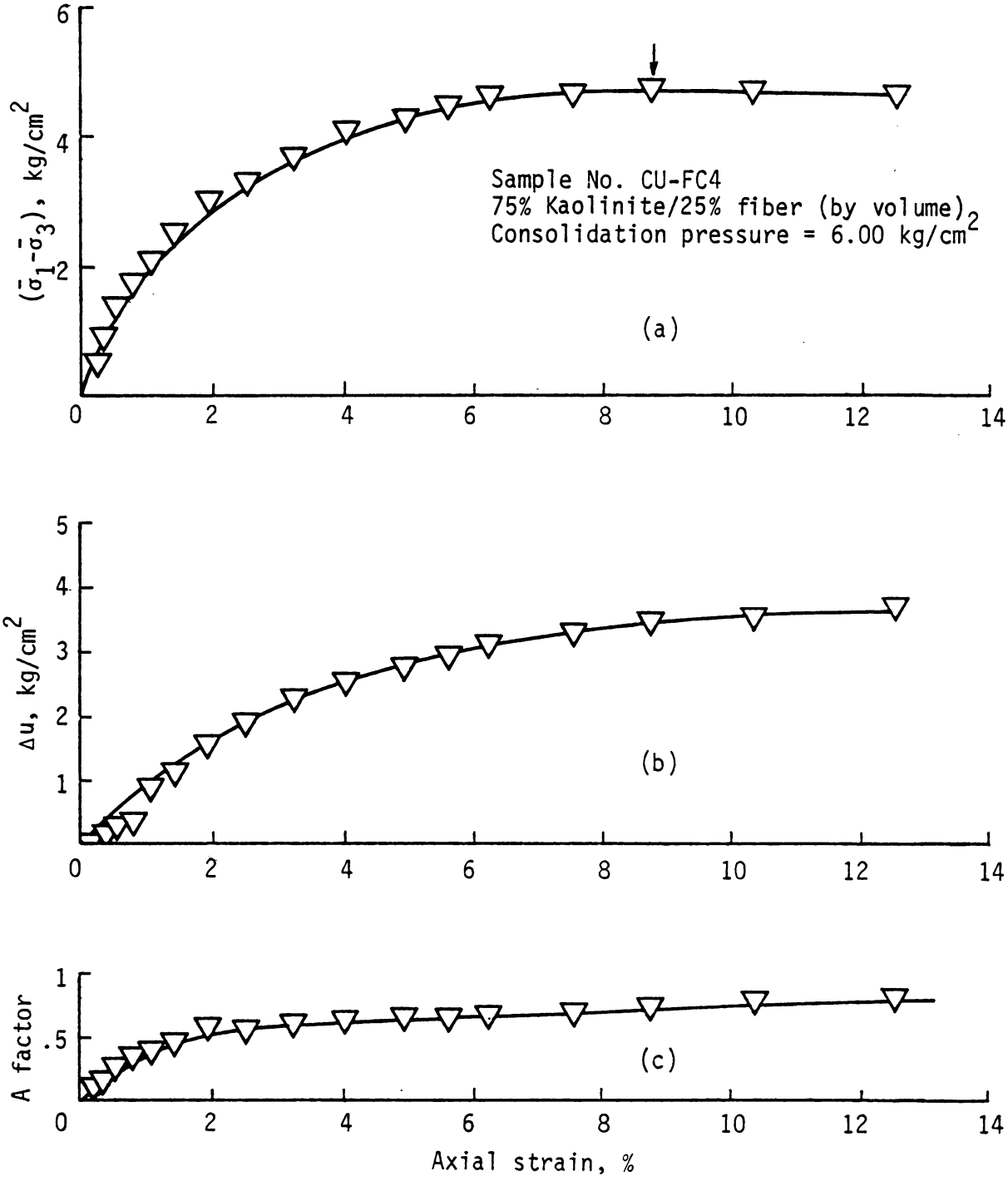

Figure 4.24 Typical results from a normally consolidated undrained triaxial test on 25% fiber/75% Kaolinite (by volume) (a) Deviator stress (b) Pore pressure change (c) Change in parameter A.

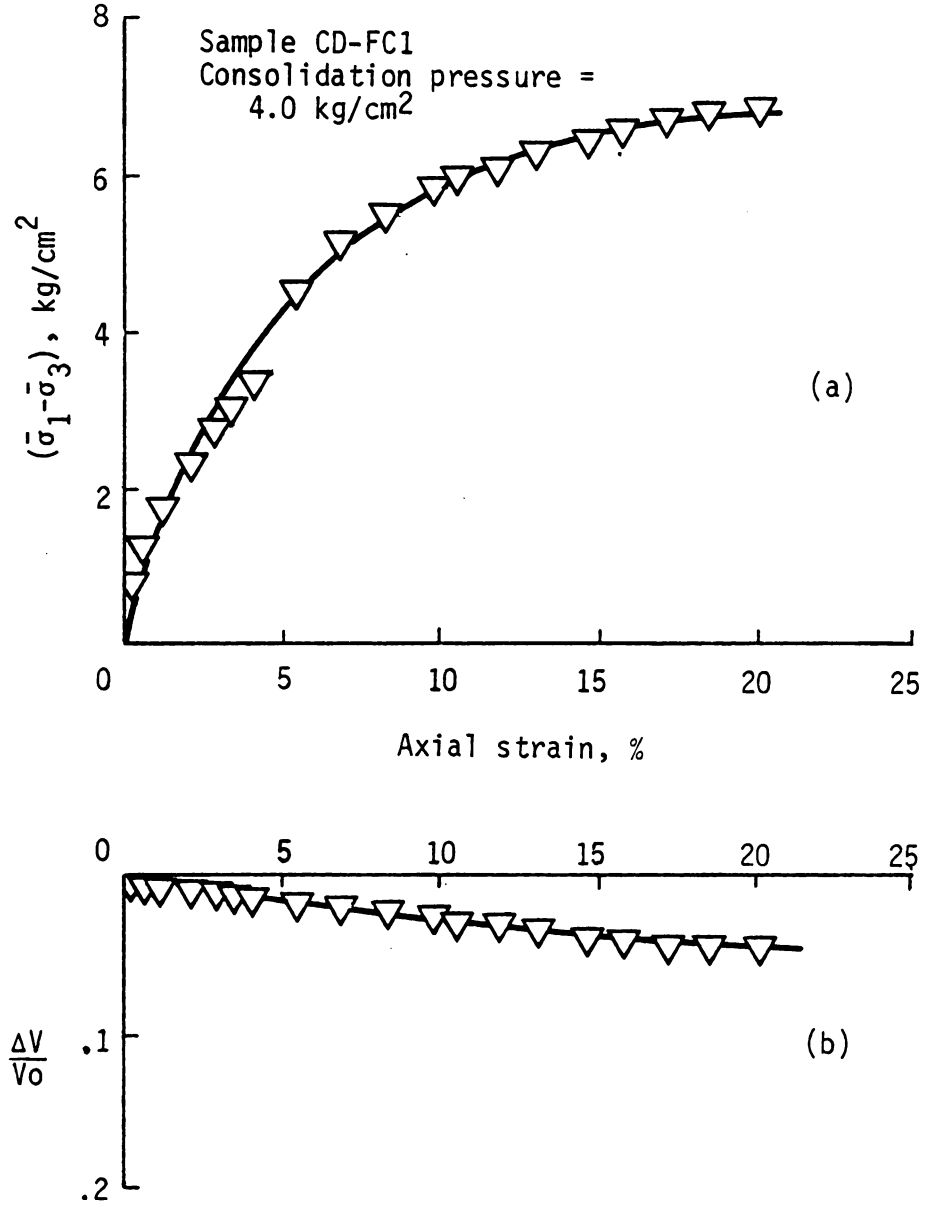

Figure 4.25 Typical results from a drained triaxial test on 25% fiber/75% Kaolinite (by volume). (a) Deviator stress (b) Volume change.

The variation of water content with consolidation pressure is shown in Figure 4.23. Water contents ranged from a minimum of 40.51 percent to a maximum of 51.05 percent corresponding to consolidation pressure of 2 kg/cm^2 and 6 kg/cm^2, respectively. Typical curves for the consolidated undrained condition with axial strain plotted against the deviator stress ($\bar{\sigma}_1 - \bar{\sigma}_3$), pore pressure Δu, and the pore pressure coefficient A are shown in Figure 4.24. Failure occurred at a deviator stress of 4.759 kg/cm^2 corresponding to a strain of 8.807 percent (Figure 4.24a). The sample, even though a mixture of fiber and kaolinite, exhibited a brittle type of failure. This behavior may be due to the presence of a high percentage of kaolinite. Figures 4.24b and 4.24c show the pore pressure and the pore pressure coefficient A at failure as 3.48 kg/cm^2 and 0.73, respectively.

Typical data for consolidated drained triaxial tests on the 75% kaolinite/25% fiber samples are shown in Figure 4.25, where percent axial strain is plotted against the deviator stress ($\bar{\sigma}_1 - \bar{\sigma}_3$) and the volumetric strain given by the ratio $\frac{\Delta V}{Vo}$. The initial sample volume after normal consolidation is designated by Vo where ΔV denotes the change in volume of the sample during the time when the deviator stress was operative. The sample showed a continuous increase of strength with increasing axial strain (Figure 4.25a), hence failure was assumed at 20 percent axial strain. The relationship between axial strain and volume change is shown by Figure 4.25b.

4.4.3 Fiber Samples

Fiber samples were prepared in a mold approximately 76 mm high by 38 mm in diameter by pouring a cellulose/water slurry directly into

the mold in small quantities. Excess water was allowed to drain and more slurry was added. Small quantities of slurry were used for each increment so as to minimize any layering effect. This method for preparation of fiber samples was adopted due to the difficulty involved in cutting the soft fiber test specimens to the desired dimensions from a larger cylinder.

After placement in the triaxial cell, samples were normally consolidated to the desired pressures. Next a back pressure was applied to the sample in order to achieve a high degree of saturation. The measured pore pressure coefficient B was consistently below unity due to trapped air in the voids of the fiber structure with the B parameter ranging from .80 to .90. The computed pore pressure coefficient A values at failure had a range from .20 to .72 with an average of .57.

The water content ranged from about 100 to 150 percent for consolidation loads ranging from 1.5 kg/cm^2 to 4.5 kg/cm^2 as shown in Figure 4.26. Typical data for a sample subjected to consolidated undrained triaxial test conditions with pore pressure measurements are shown in Figure 4.27 where axial strain is plotted against the deviator stress $(\bar{\sigma}_1 - \bar{\sigma}_3)$, pore pressure Δu, and the pore pressure coefficient A. Since the material displays a continuous increase of strength with increasing strain (Figure 4.27a) failure was assumed at an arbitrary value of 20 percent axial strain. In the case of undrained tests on all fiber samples, the calculated stresses corresponding to 20 percent strain are questionable since the pore pressure increases to the cell pressure (Figure 4.27b) at an axial strain less than 20 percent. The pore pressure value measured at 18.66 percent axial strain was 2.51

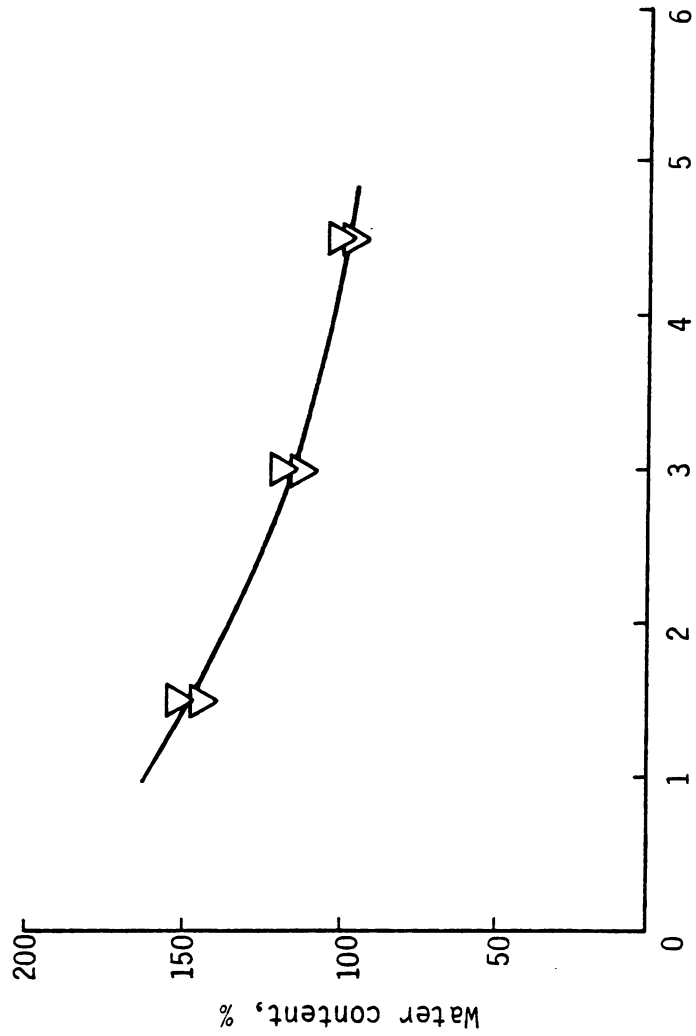

Figure 4.26 Consolidation pressure vs. Water content for fiber samples.

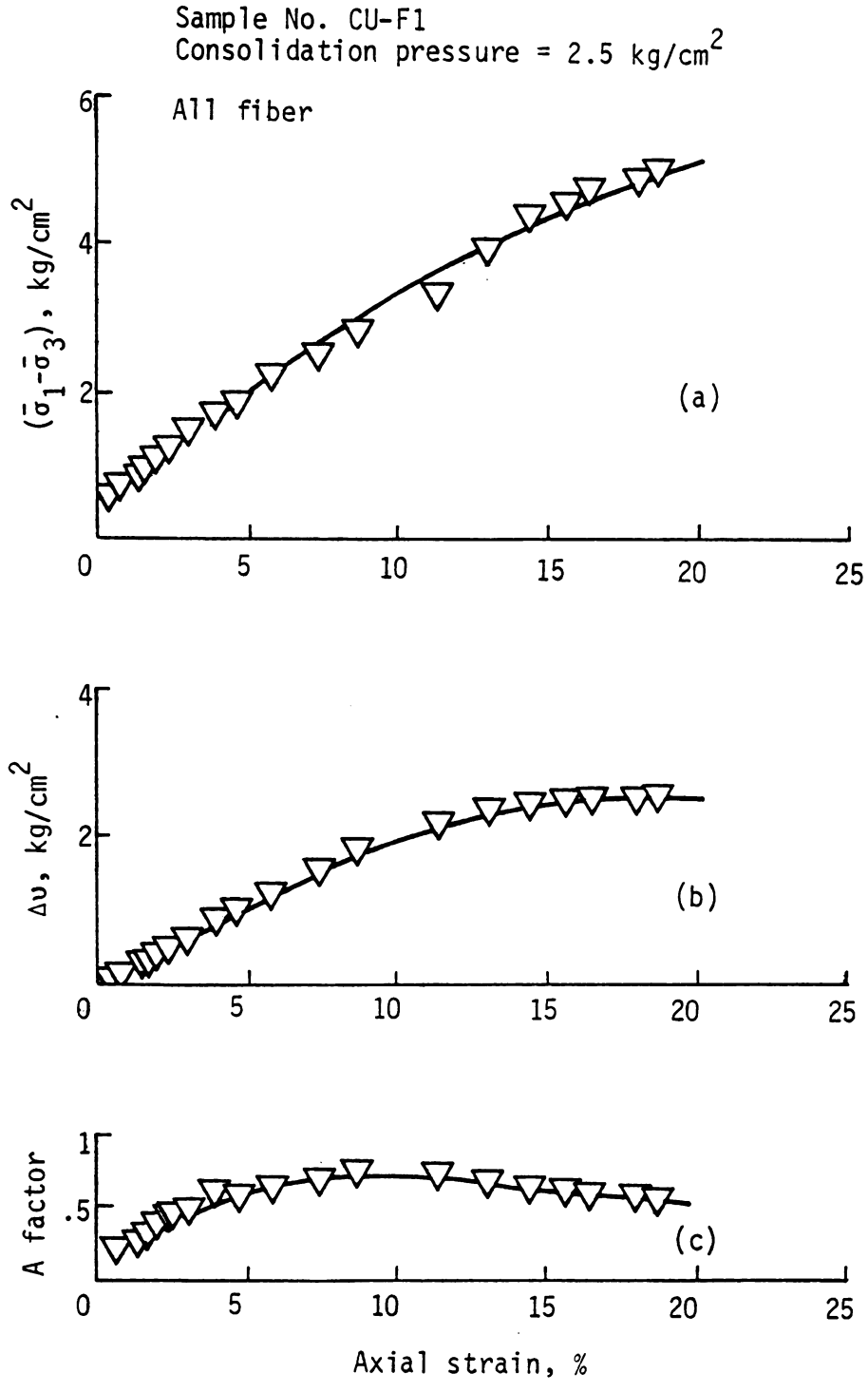

Figure 4.27 Typical results from a normally consolidated undrained triaxial test on a fiber sample. (a) Deviator stress (b) Pore pressure change (c) Change in parameter A.

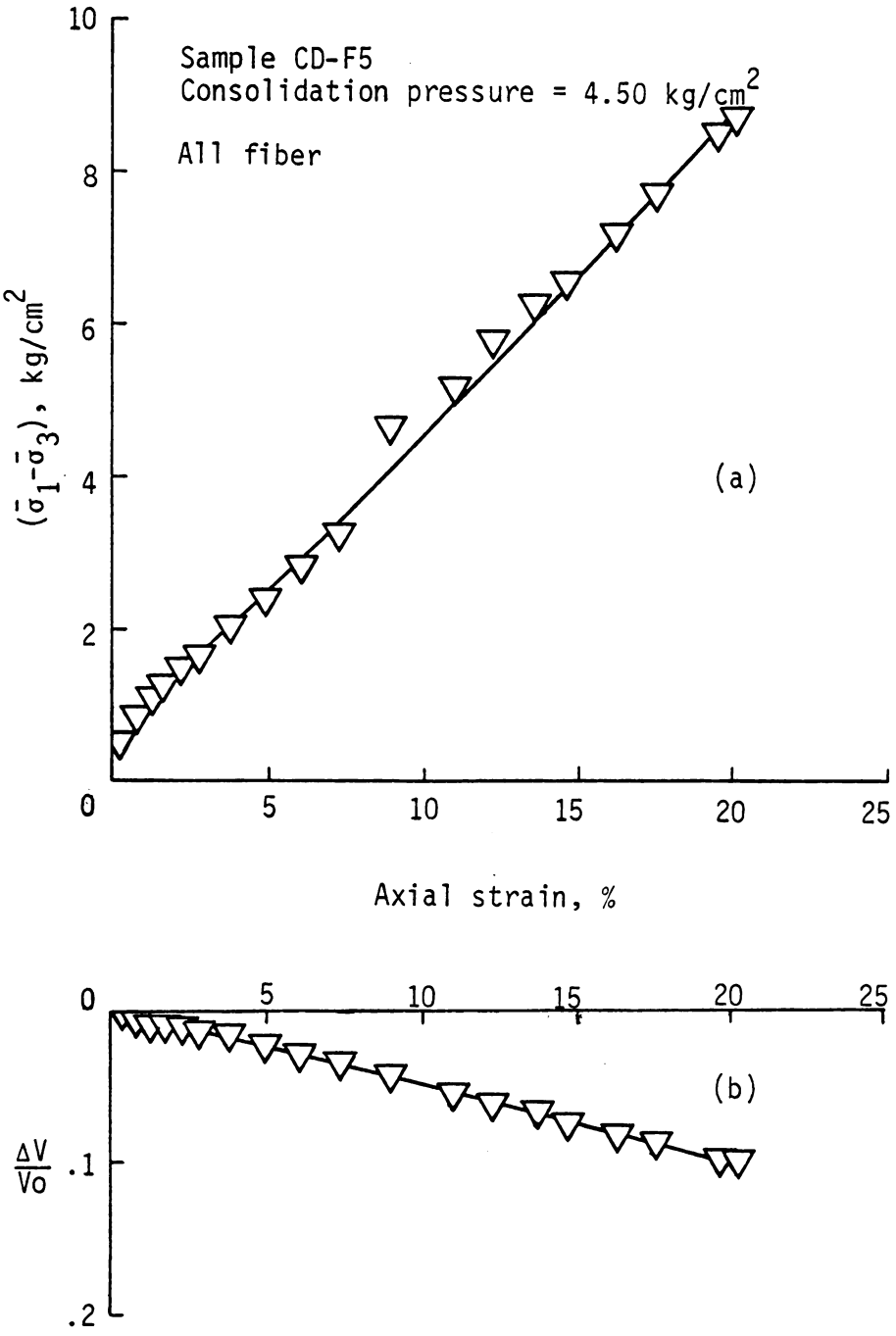

Figure 4.28 Typical results from a drained triaxial test on a fiber sample. (a) Deviator stress (b) Volume change.

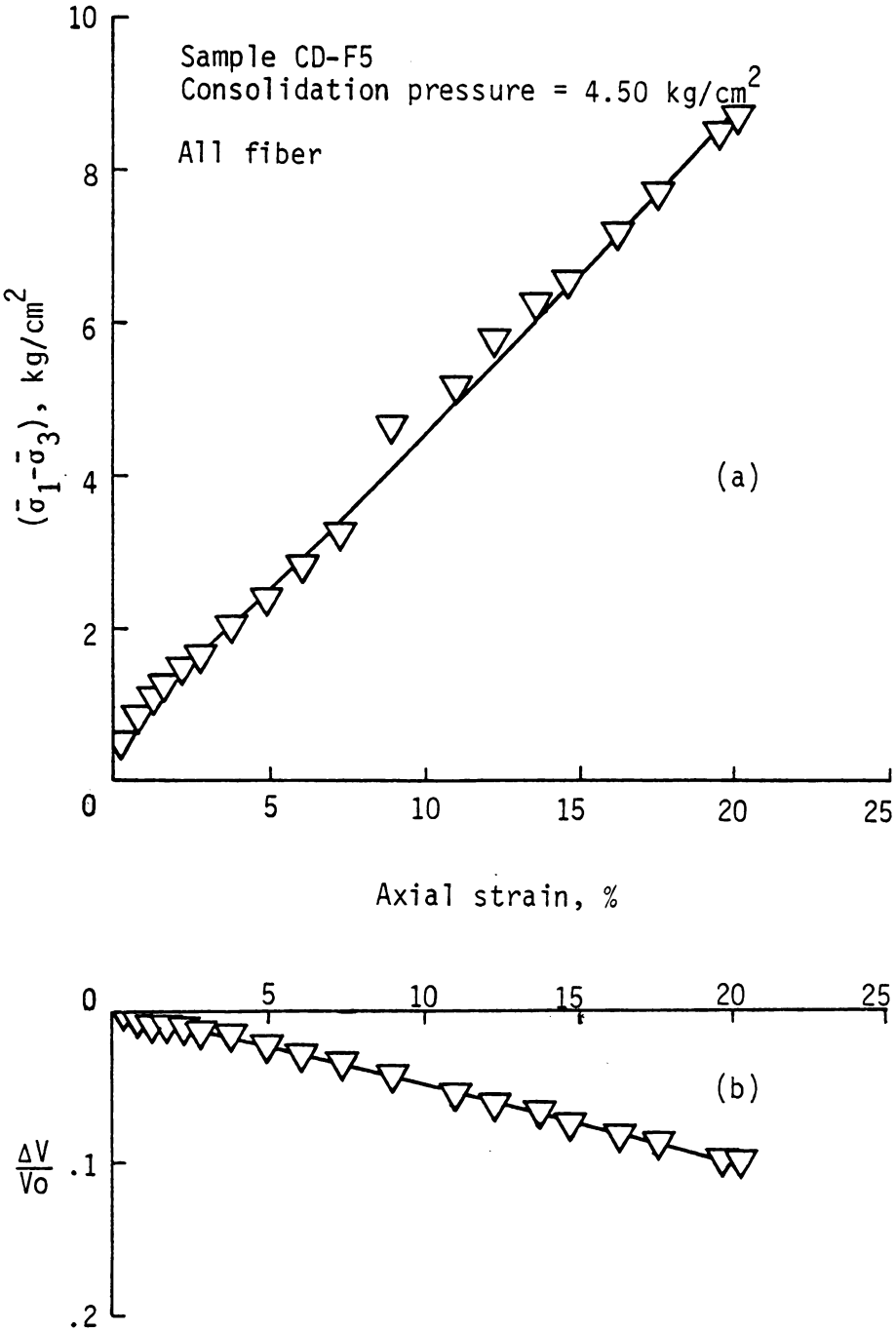

Figure 4.28 Typical results from a drained triaxial test on a fiber sample. (a) Deviator stress (b) Volume change.

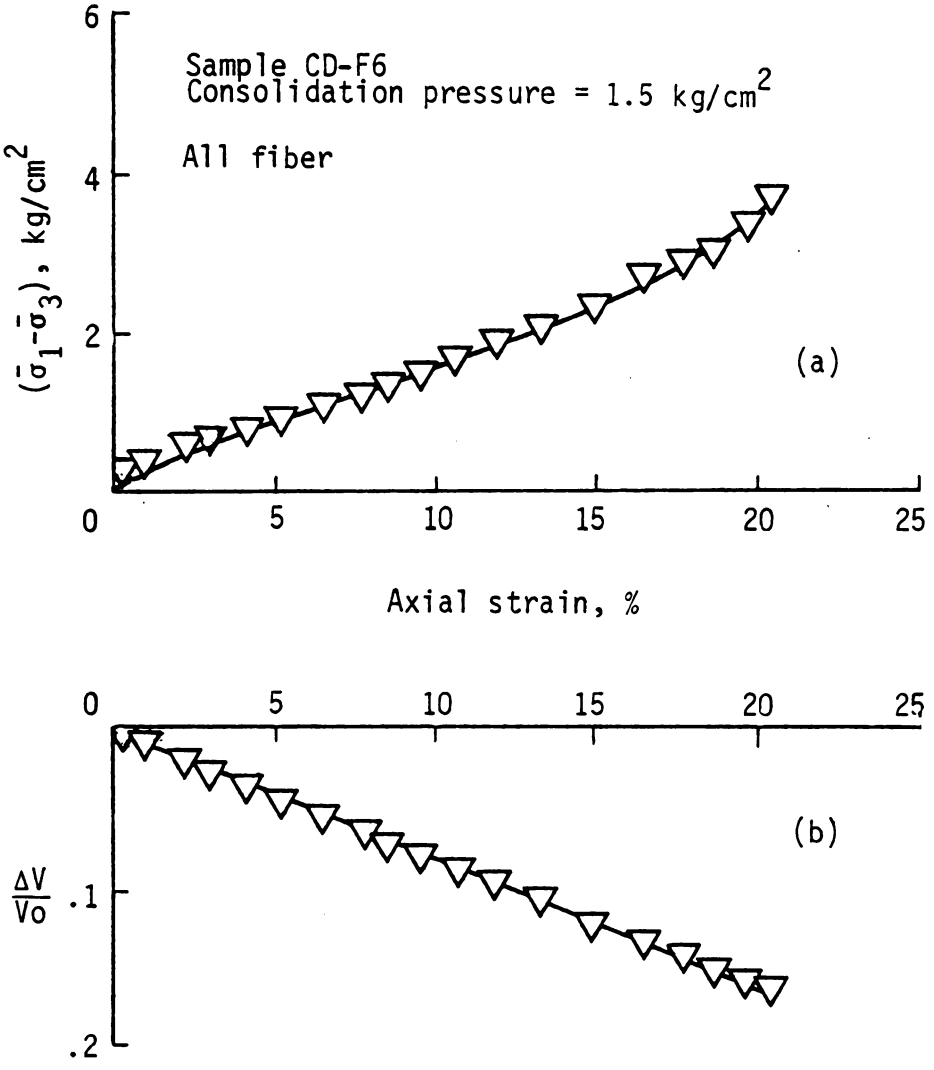

Figure 4.29 Typical results from a drained triaxial test on a fiber sample consolidated to a low pressure. (a) Deviator stress (b) Volume change.

kg/cm^2 (Figure 4.27b) giving a pore pressure parameter A equal to 0.55 (Figure 4.27c).

Typical curves for all fiber samples subjected to consolidated drained test conditions are shown in Figure 4.28. Drained tests were included so as to avoid problems with the minor principal effective stress going to zero at high strain levels. The increase in strength with increasing axial strain is shown in Figure 4.28a with failure assumed at 20 percent axial strain. The percent axial strain plotted against the ratio $\frac{\Delta V}{Vo}$, is shown in Figure 4.28b, can be approximated by a straight line.

Typical curves for a fiber sample consolidated to a low pressure of 1.5 kg/cm^2 and tested under drained conditions is shown in Figure 4.29. Comparing Figures 4.28 and 4.29 it is observed that increased density due to consolidation strongly influences the strength development in fiber samples. The volume change in Figure 4.28 is smaller than the volume change in Figure 4.29 at the same strain value due to the higher consolidation pressure.

Tables A.7 and A.8 in the appendix represent recorded values of $\sqrt{\text{Time}}$ and volume change ΔV for a kaolinite sample and a fiber sample subjected to an all around consolidation pressure of 3.50 and 3 $kg.cm^2$, respectively. The $\sqrt{\text{Time}}$ is plotted on a horizontal axis against volume change ΔV, on a vertical axis in Figure 4.30. The times for 100 percent primary consolidation for clay and fibers determined from Figure 4.30 are 219 and 32.5 minutes, respectively. The summary of consolidated undrained and drained triaxial tests conducted on kaolinite samples, fiber/kaolinite samples, and fiber samples is given in Table 4.8.

kg/cm^2 (Figure 4.27b) giving a pore pressure parameter A equal to 0.55 (Figure 4.27c).

Typical curves for all fiber samples subjected to consolidated drained test conditions are shown in Figure 4.28. Drained tests were included so as to avoid problems with the minor principal effective stress going to zero at high strain levels. The increase in strength with increasing axial strain is shown in Figure 4.28a with failure assumed at 20 percent axial strain. The percent axial strain plotted against the ratio $\frac{\Delta V}{Vo}$, is shown in Figure 4.28b, can be approximated by a straight line.

Typical curves for a fiber sample consolidated to a low pressure of 1.5 kg/cm^2 and tested under drained conditions is shown in Figure 4.29. Comparing Figures 4.28 and 4.29 it is observed that increased density due to consolidation strongly influences the strength development in fiber samples. The volume change in Figure 4.28 is smaller than the volume change in Figure 4.29 at the same strain value due to the higher consolidation pressure.

Tables A.7 and A.8 in the appendix represent recorded values of $\sqrt{\text{Time}}$ and volume change ΔV for a kaolinite sample and a fiber sample subjected to an all around consolidation pressure of 3.50 and 3 $kg.cm^2$, respectively. The $\sqrt{\text{Time}}$ is plotted on a horizontal axis against volume change ΔV, on a vertical axis in Figure 4.30. The times for 100 percent primary consolidation for clay and fibers determined from Figure 4.30 are 219 and 32.5 minutes, respectively. The summary of consolidated undrained and drained triaxial tests conducted on kaolinite samples, fiber/kaolinite samples, and fiber samples is given in Table 4.8.

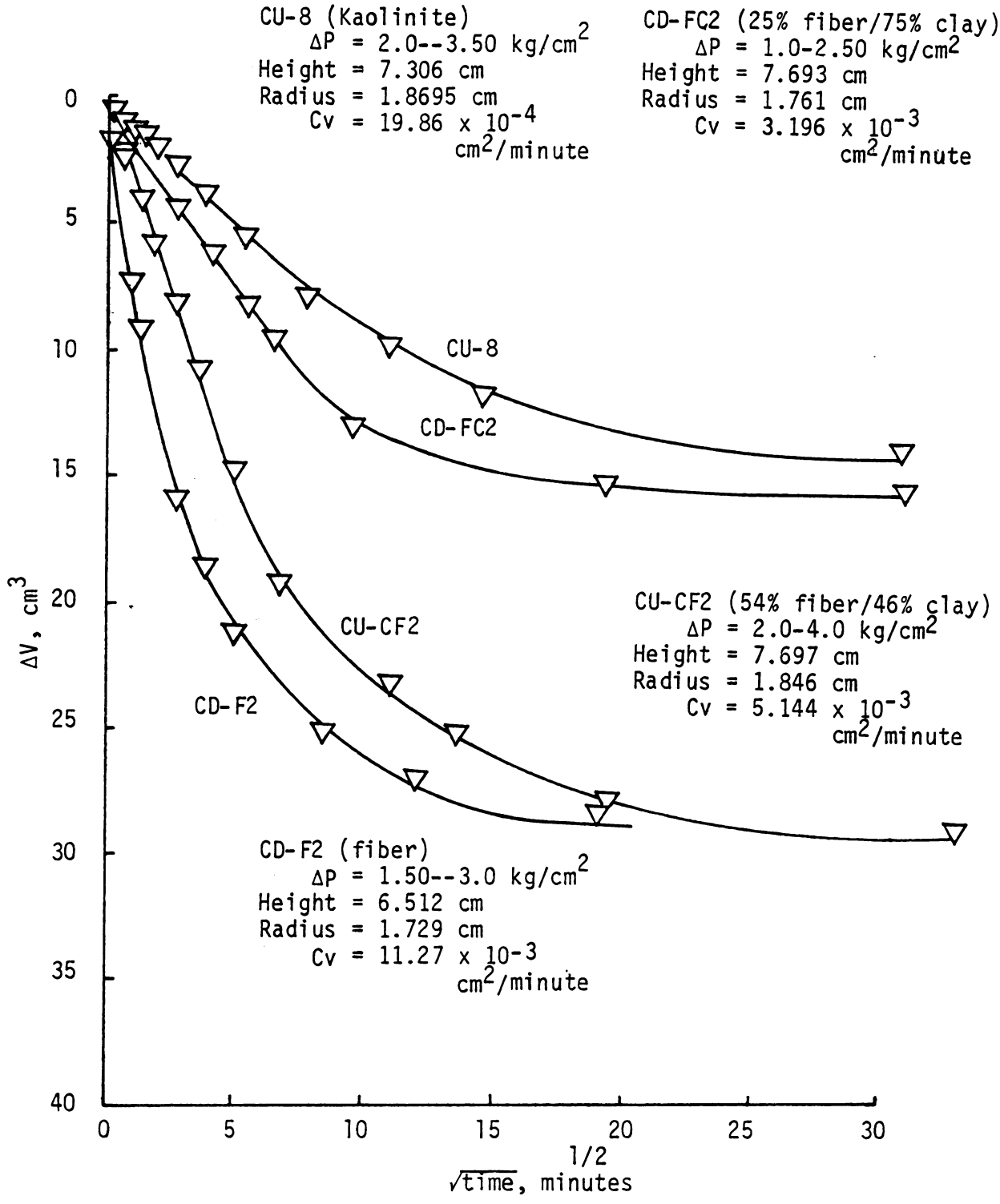

Figure 4.30 Relationship between Volume change and $\sqrt{\text{Time}}$ for a Kaolinite, 54%fiber/46% clay, 25% fiber/75% clay and fiber sample under all around pressure (radial and end drainage).

TABLE 4.8 SUMMARY OF TRIAXIAL TEST RESULTS

Test Sample	Sample Composition by Volume	Consolidation Pressure (kg/cm^2)	Water Content (%)	Dry Density (pcf)	Undrained Strength (kg/cm^2)	$\bar{\sigma}_{1_f}$ (kg/cm^2)	$\bar{\sigma}_{3_f}$ (kg/cm^2)	$A_f^{\neq}$
CU-1	100%C*	2.00	29.21	93.21	1.057	3.634	1.52	0.23
CU-2	100%C	4.00	28.28	94.65	1.349	5.219	2.52	0.55
CU-3	100%C	5.50	27.85	95.20	1.485	5.409	2.44	1.03
CU-4	100%C	1.50	31.05	90.71	0.761	2.561	1.04	0.30
CU-5	100%C	6.50	26.45	97.21	2.072	8.184	4.04	0.59
CU-6	100%C	6.50	29.40	92.95	2.193	8.176	3.79	0.62
CU-7	100%C	2.50	33.78	87.26	0.839	2.848	1.17	0.79
CU-8	100%C	3.50	33.58	87.49	0.964	3.627	1.70	0.93
CU-9	100%C	4.50	32.33	88.91	2.290	4.500	2.21	1.00
CU-FC1	75%C+25%F*	3.00	46.71	70.16	1.379	3.958	1.20	0.65
CU-FC2	75%C+25%F	4.50	45.29	70.50	1.969	5.898	1.96	0.64
CU-FC3	74%C+25%F	2.00	51.05	66.90	1.056	2.882	0.77	0.58
CU-FC4	75%C+25%F	6.00	40.51	75.44	2.379	7.279	2.52	0.73
CU-CF1	46%C+54%F	3.00	54.28	60.36	1.631	4.202	0.94	0.63
CU-CF2	46%C+54%F	4.00	59.85	57.35	2.264	5.668	o.14	0.63
CU-CF3	46%C+54%F	6.00	56.06	64.92	3.445	8.659	1.77	0.61
CU-CF4	46%C+54%F	1.50	64.82	41.18	---	---	---	---
CU-CF5	46%C+54%F	3.00	64.42	41.33	---	---	---	---
CU-CF6	46%C+54%F	4.00	58.56	43.59	---	---	---	---
CU-CF7	46%C+54%F	5.00	58.11	43.78	---	---	---	---
CD-FC1	75%C+25%F	4.00	38.73	75.69	3.403	10.806	4.00	---
CD-FC2	75%C+25%F	2.50	42.44	73.47	2.641	7.782	2.50	---
CD-FC3	75%C+25%F	1.50	51.84	66.39	1.186	3.873	1.50	---
CD-CF1	46%C+54%F	4.50	48.96	63.06	3.936	12.372	4.50	---
CD-CF2	46%C+54%F	3.50	54.85	59.05	3.280	10.060	3.50	---

TABLE 4.8 (Continued)

Test Sample	Sample Composition by Volume	Consolidation Pressure (kg/cm^2)	Water Content (%)	Dry Density (pcf)	Undrained Strength (kg/cm^2)	$\bar{\sigma}_{1_f}$ (kg/cm^2)	$\bar{\sigma}_{3_f}$ (kg/cm^2)	$A_f \neq$
CD-CF3	46%C+54%F	2.50	56.77	59.24	2.813	8.126	2.50	---
CD-F1	100%F	1.50	144.57	29.09	1.766	5.032	1.50	---
CD-F2	100%F	3.00	113.22	35.02	3.929	10.858	3.00	---
CD-F3	100%F	4.50	100.17	35.23	4.620	13.740	4.50	---
CD-F4	100%F	3.00	118.81	31.36	3.062	9.123	3.00	---
CD-F5	100%F	4.50	96.65	33.99	4.326	13.152	4.50	---
CD-F6	100%F	1.50	150.22	27.69	1.746	4.991	1.50	---
CU-F1	100%F	2.50	143.29	28.88	2.268	4.536	0.0	0.55
CU-F2	100%F	0.50	246.88	19.10	0.393	1.126	0.34	0.20
CU-F3	100%F	0.50	299.61	16.90	0.387	0.773	0.00	0.65
CU-F4	100%F	3.50	158.53	30.15	2.174	4.738	0.39	0.72
CU-F5	100%F	1.00	234.40	20.86	0.858	1.715	0.0	0.58
CU-F6	100%F	1.00	n.a.	n.a.	0.67	1.340	0.0	0.75
CU-F7	100%F	2.03	169.81	29.70	2.006	4.032	0.02	0.50

* C = Kaolinite
F = Fiber
CU = Consolidated undrained
CD = consolidated drained
n.a. = not available
$\neq$ A_f values computed using B = 1

The values of the pore pressure coefficient A depends upon whether the soil is normally consolidated or overconsolidated and also upon the proportion of the failure stress applied (Bishop and Henkel, 1962). Pore pressure coefficient A_f at failure seems to decrease with increasing organic content as shown in Figure 4.31 where average values of A_f versus percent fiber are plotted. A summary of the pore pressure coefficients A and B is given in Table 4.9 for kaolinite, 75% kaolinite/25% fiber, 46% kaolinite/54% fiber and fibers.

TABLE 4.9 SUMMARY OF PORE PRESSURE COEFFICIENTS A AND B

Sample	Composition	Pore Pressure Coeff. B	Pore Pressure U_f*	Pore Pressure Coeff. A_f*	Average A_f
CU-2	Kaolinite	0.67	1.48	0.82	
CU-3	Kaolinite	1.00	3.06	1.03	
CU-5	Kaolinite	0.80	2.46	0.74	
CU-6	Kaolinite	0.66	2.71	0.92	0.89
CU-7	Kaolinite	1.00	1.33	0.79	
CU-8	Kaolinite	1.00	1.88	0.93	
CU-9	Kaolinite	1.00	2.29	1.00	
CU-FC1	75%C/25%F	0.90	1.80	0.73	
CU-FC2	75%C/25%F	0.80	2.54	0.80	
CU-FC3	75%C/25%F	0.80	1.23	0.73	0.75
CU-FC4	75%C/25%F	1.00	3.48	0.73	
CU-CF1	46%C/54%F	0.90	2.06	0.70	
CU-CF2	46%C/54%F	0.90	2.86	0.70	0.71
CU-CF3	46%C/54%F	0.85	4.23	0.72	
CU-FL	FIber	0.90	2.50	0.61	
CU-F2	Fiber	1.00	0.16	0.20	
CU-F3	Fiber	1.00	0.50	0.65	
CU-F4	Fiber	1.00	3.11	0.72	0.57
CU-F5	Fiber	1.00	1.00	0.58	
CU-F6	Fiber	1.00	1.00	0.75	
CU-F7	Fiber	1.00	2.01	0.50	

*At failure

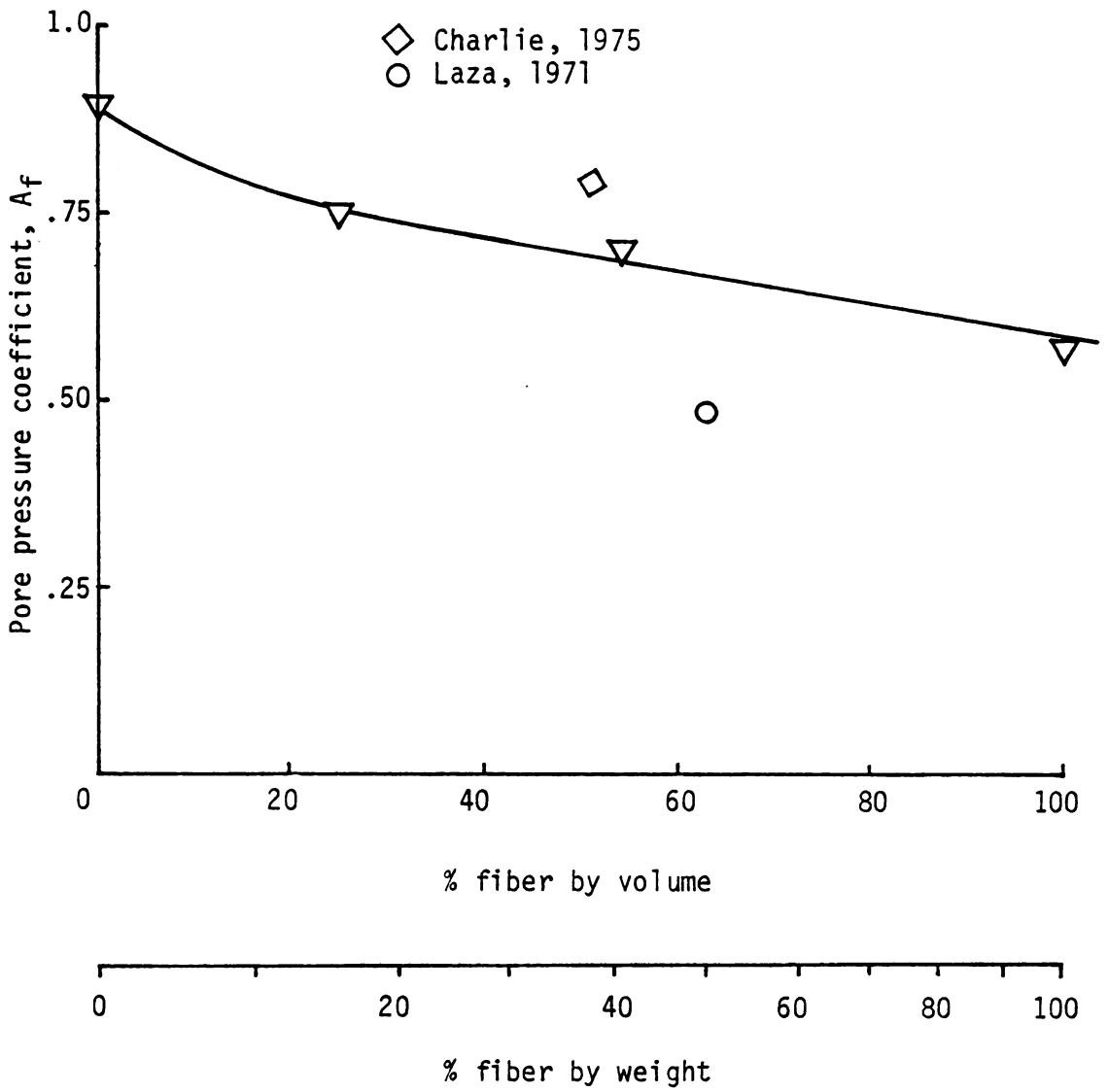

Figure 4.31 Influence of organic (fiber) content on the pore pressure parameter A at failure in triaxial tests.

CHAPTER V

DISCUSSION AND INTERPRETATION OF RESULTS

This discussion and interpretation of project data is presented in four sections: physical properties, compressibility of the kaolinite/fiber mixtures, shear strength of kaolinite/fiber mixtures, and implications for stability problems.

5.1 Physical Properties

The initial part of this section describes the fiber structure and shape as seen through a scanning electron microscope. The latter part of the section appears under a heading of kaolinite/fiber mixtures.

5.1.1 Fiber Size, Shape, and Structure

Fiber size, shape, and structure is not readily apparent to the unaided eye. To obtain a better understanding of the fiber material, photographs shown in Figures 5.1, 5.2, 5.3 and 5.4 were taken using a scanning electron microscope. The fiber sample must be dried before exposing it to the scanning electron microscope. Cellulose fibers shown at 120 magnification in Figure 5.1b resembles grass blades. The cross-section of a single cellulose fiber is magnified 2000 times in Figure 5.1a. An elongated hole appears to extend through the body of the fiber. A single fiber magnified 2000 times in Figure 5.2a has an average dimension on the photograph equal to 53 mm. One micron magnified 1000 times will equal one mm on the photograph, therefore,

$$.053 \div 2000 \approx .00002 \text{ meter} = .00002 \times 10^{10}\text{Å} = 200{,}000\text{ Å} = 20 \text{ micron.}$$

(a)

(b)

Figure 5.1 (a) 2000 magnification of the cross section of a single pulp fiber (b) 120 magnification of several pulp fibers.

(a)

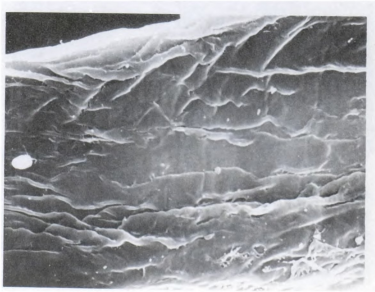

(b)

Figure 5.2 Surface characteristics of cellulose pulp fibers, 2000 magnification.

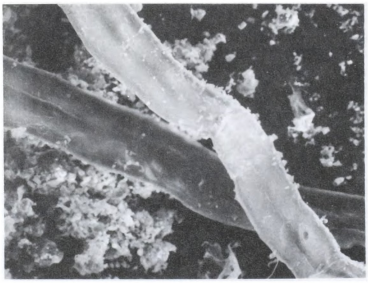

(a)

(b)

Figure 5.3 Fiber-clay particle size comparisons, 1000 magnification

(a)

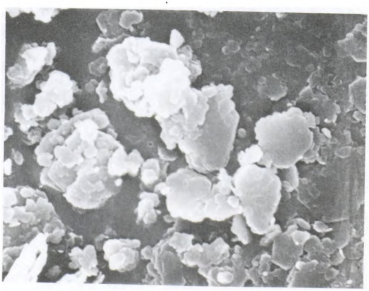

(b)

Figure 5.4 Scanning electron microscope photographs, 10000 magnification. (a) Cellulose pulp fiber. (b) Kaolinite particles.

In a cotton fiber there are approximately 1500 fibrils and each fibril has an approximate area of $0.16\mu^2$ (Denlin, 1966). Therefore the approximate cross-sectional area of a cotton fiber equals $1500 \times 0.16\mu^2 = 240\mu^2$. Assuming a circular cross-section, $\frac{\pi}{4} d^2 = 240\mu^2$, or $d = 17.48\mu \approx 18\mu$. The 18μ is in approximate agreement with the calculated value of 20μ. Assuming that the average lateral dimension of a single fiber is about 20μ, the larger dimension of the hole in Figure 5.2a is about 15μ and the smaller dimension is about 2μ. The size of the hole in Figure 5.1a is approximately $4\mu \times 12\mu$.

A sample composed of all fiber would be resilient, especially if the fibers are dry since the addition of water significantly enhances their compressibility. A saturated sample would be expected to be resilient at very high stress levels.

The size comparison of kaolinite and fiber particles is shown in Figures 5.3a and 5.3b. A small portion of pulp fiber and kaolinite particles magnified 10,000 times are shown in Figure 5.4. Particle "m" and "n" with dimensions 15 mm and 19 mm, respectively, on the photographs give particle sizes of

$$\frac{.015}{10{,}000} = 15 \times 10^{-7}\text{m} \times 10^6 = 1.5\mu$$

$$\frac{.019}{10{,}000} = 19 \times 10^{-7}\text{m} \times 10^6 = 1.9\mu$$

The calculated dimensions for the two particles satisfy the soil mechanics definition for clay particles with a maximum size of 2μ.

5.1.2 Kaolinite/Fiber Mixtures

The physical properties of kaolinite/fiber mixtures change in proportion to the amount of each component present. The specific

gravity of kaolinite particles was 2.65 compared to 1.54 for the much lighter cellulose fibers. A simple proportion in terms of the ratio kaolinite by volume, X_k, can be used to calculate the specific gravity, G, of the mixture, thus

$$G = (1 - X_k)\ 1.54 + 2.65\ X_k \qquad (5.1)$$

The weight-volume relationships from soil mechanics can now be used to calculate unit weights, void ratios, water contents, and degree of saturation.

The influence which organic (fiber) content has on the mechanical properties is not simple. The surface area per gram of fiber solids was measured at 133 m^2 when both external and internal surfaces are considered. Compare this to an approximate value of 12 m^2/g for kaolinite. One gram of cellulose occupies a larger volume due to the lower specific gravity and the presence of internal cavities. Also, cellulose is hydrophyllic, that is it has a high water holding capacity as compared to kaolinite. This hydrophyllic property of cellulose gives it a high swelling potential. MacFarlane (1969) reports that water contents for fibrous peats vary between 750 to 1500 percent by weight. A small percentage of inorganic material in the peat sharply lowers this natural water content. In the same manner, the mixture of kaolinite with fiber alters the water content for a given load.

For the saturated condition, change in water content also changes the void ratio. The water holding capacity, or void ratio, will take on increasing values for higher organic contents at the same load. This

phenomenon has been shown by Laza (1971) and in Figure 4.13. An increase in organic content requires that a larger load be placed on the sample in order to maintain the same void ratio. This becomes a significant factor relative to compressibility of the kaolinite/fiber mixtures and is discussed in a later section.

The compressible structure of the fibrous material means that large strains are needed to mobilize shearing resistance. The peak stress difference continued to increase up to and above 20 percent axial strain for the 60% kaolinite/40% fiber mixtures by weight (Figure 4.21) and all fiber samples (Figure 4.27). Fibers 1.6 mm in length go into tension along the failure surface as shown by a photograph presented by Charlie (1975). The mechanical reinforcement of soil by plant roots has been described by Gray (1974). The shear strength was increased by an apparent increase in cohesion with little effect on the friction angle.

Decomposition of the organic (fiber) material has not been considered as a variable in this study. Natural organic soils including peat, muskeg, or fibrous papermill sludge would be in some state of decomposition. Gray (1974) reports that gradual decay in root systems leads to a decrease in strength. This effect may possibly be simulated by kaolinite/fiber mixtures with lower fiber contents. A concurrent study presently in progress is studying the decomposition effects on engineering properties of kaolinite/fiber mixtures.

5.2 Compressibility of Kaolinite/Fiber Mixtures

One dimensional compression and triaxial compression of samples with various organic (fiber) contents is discussed. The coefficient

of compressibility for the soil structure and the solids are considered in a review of the application of Terzaghi's effective stress concept to organic soils.

5.2.1 One-Dimensional Compression

Consider a saturated soil element whose sides are subjected to constant external total stresses. A change in the magnitude of pore pressure will cause a change in the effective stresses at a point on a given plane. For one-dimensional compression the total stress on the top and bottom faces of the element will be different from the stress on the other faces. The increase or decrease in pore pressures will cause changes in the effective stress components to which the soil skeleton is subjected. The stress at a point will also change with orientation of the plane passing through the point, hence the description of the change in void ratio in such a system is very complex and only a simplified discussion of the problem is given here.

The variation of water content with variation in sample composition is shown in Figure 5.5 for the same final compressive load of about 358 kg/cm^2. The greater water holding capacity due to higher organic contents is apparent. Consider the all fiber sample. When each of the OH groups in cellulose ($C_6H_{10}O_5$) is hydrogen bonded to one molecule of water, that is when cellulose is fully hydrated there are three water molecules for each cellulose unit and the hydrated formula becomes $(C_6H_{10}O_5) \cdot 3H_2O$. One mole of dry cellulose weighs 162 gm and three moles of water weighs (3 x 18) = 54 gm., therefore, the water content of fully hydrated cellulose would be (54/162)100 = 33.33 percent (Skaar, 1972). The water content of the all fiber sample

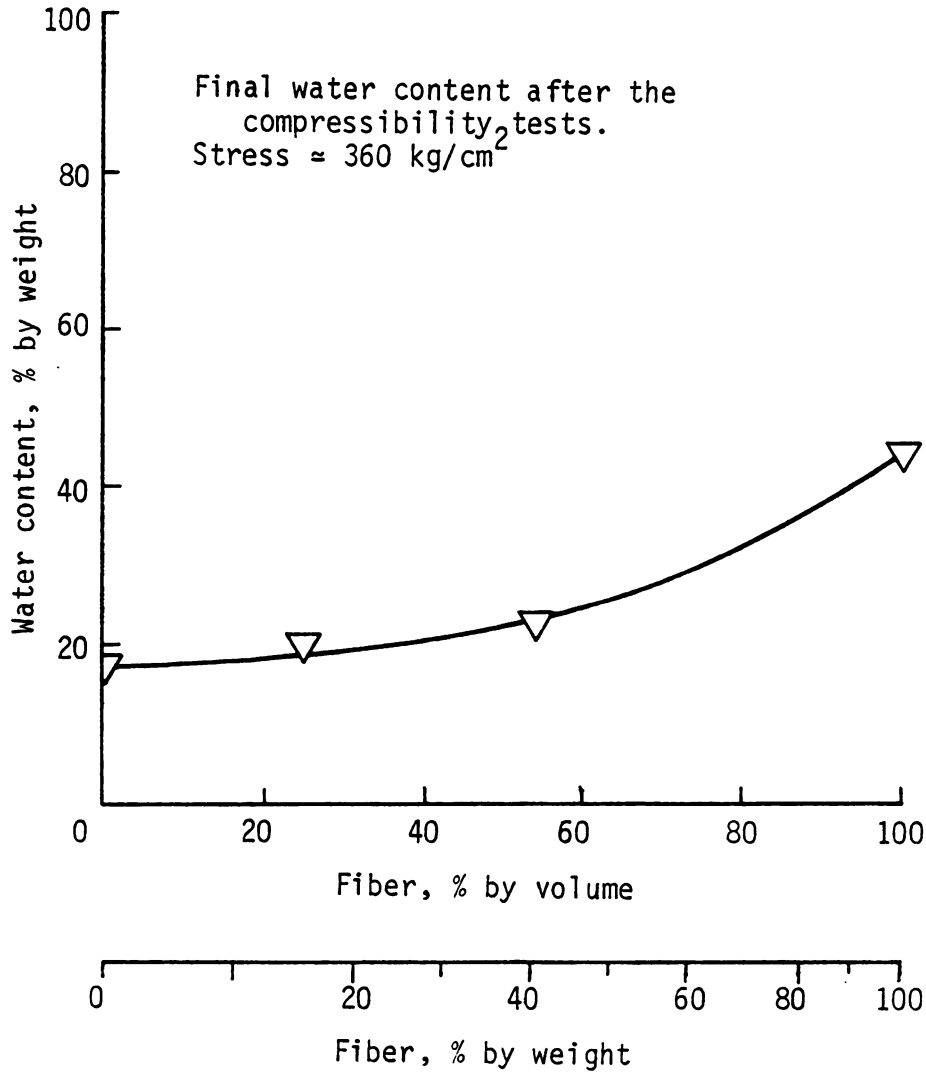

Figure 5.5 Final water contents after one-dimensional loading to about 360 kg/cm^2 for kaolinite, two kaolinite/fiber mixtures, and fiber samples.

after being loaded to a compressive stress of 360.26 kg/cm^2 in Figure 5.5 was 42.13 percent. This is higher than the fully hydrated moisture content, hence the number of molecules of water attached to the fibers is greater than three. The number of water molecules present in the all fiber samples may be estimated. For example, $x/162 = 0.4213$ and $x = 68.25$. The number of molecules equals $68.25/18 = 3.79$ or approximately 4. The data show that it is extremely difficult to remove the first layer of water molecules from the cellulose fibers by mechanical means.

Effective normal stresses are plotted against the equilibrium void ratio on a natural scale in Figure 5.6 for kaolinite, kaolinite/fiber mixtures, and all fiber samples. Note that all curves have a common point of intersection. The immediate region surrounding the intersection point is shown to an exaggerated scale in Figure 5.7. The normal effective stress is plotted on a logarithmic scale against the equilibrium void ratio on a natural scale in Figure 5.8. The plot for kaolinite shows a straight line whereas the radius of curvature of plots for other samples decrease with an increase in fiber content. Note that all fiber samples continued to show the larger change in void ratio at stress levels above the common point of intersection (Figure 5.7).

The behavior of the fiber and kaolinite/fiber samples resemble to some degree the behavior of floculated clays (Scott, 1963) where the void ratio-logarithm of pressure curve is concave upwards. The change in void ratio is most probably due to two phenomena:

1) Squeezing of water from between fibers resulting in a

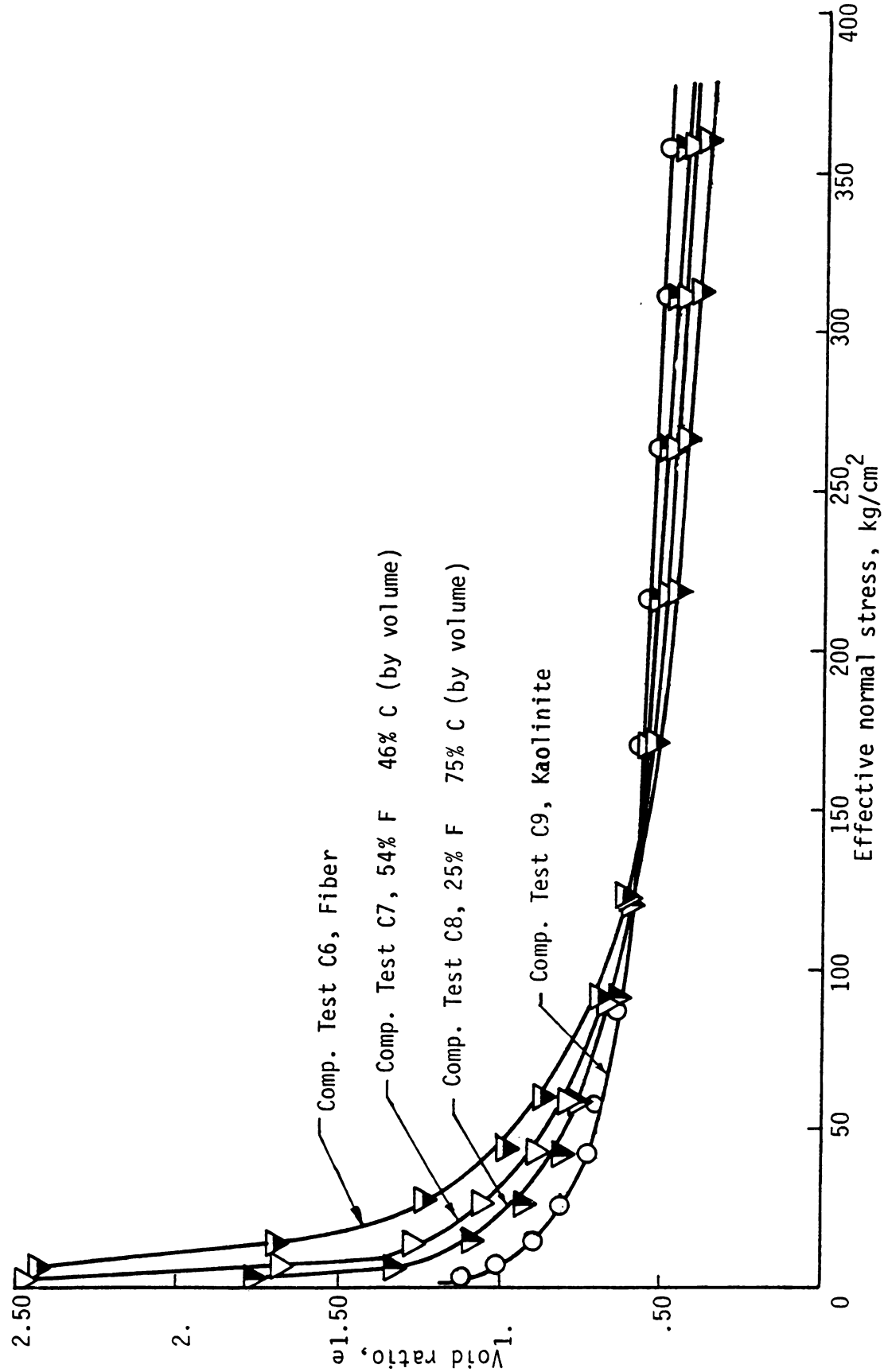

Figure 5.6 Effective normal stress vs. Void ratio curves for all fiber, 25% fiber/75% Kaolinite, 54% fibers/46% Kaolinite, and all Kaolinite samples.

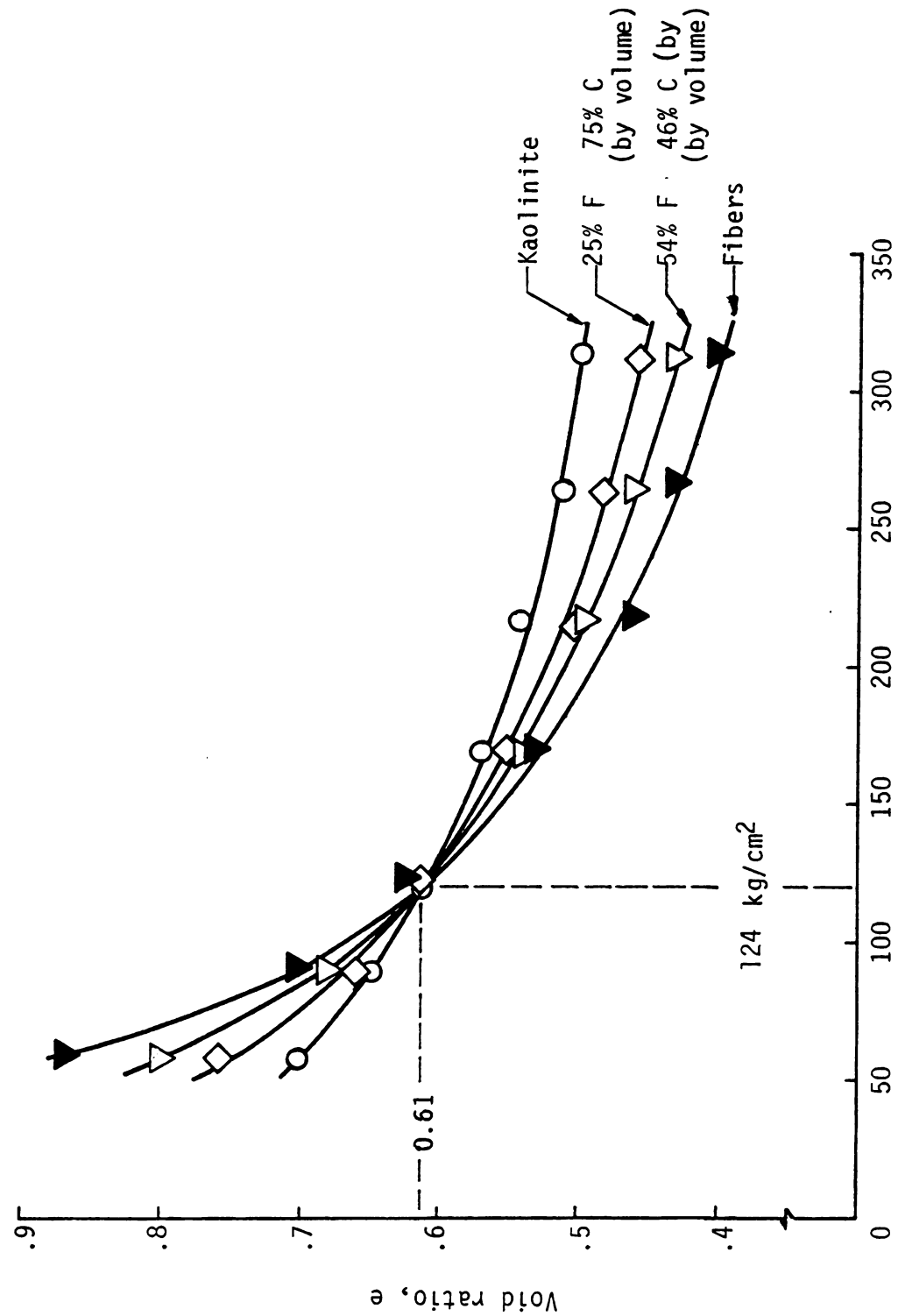

Figure 5.7 Effective normal stress vs. Void ratio plot for the Kaolinite/fiber samples near the common point of intersection of all curves.

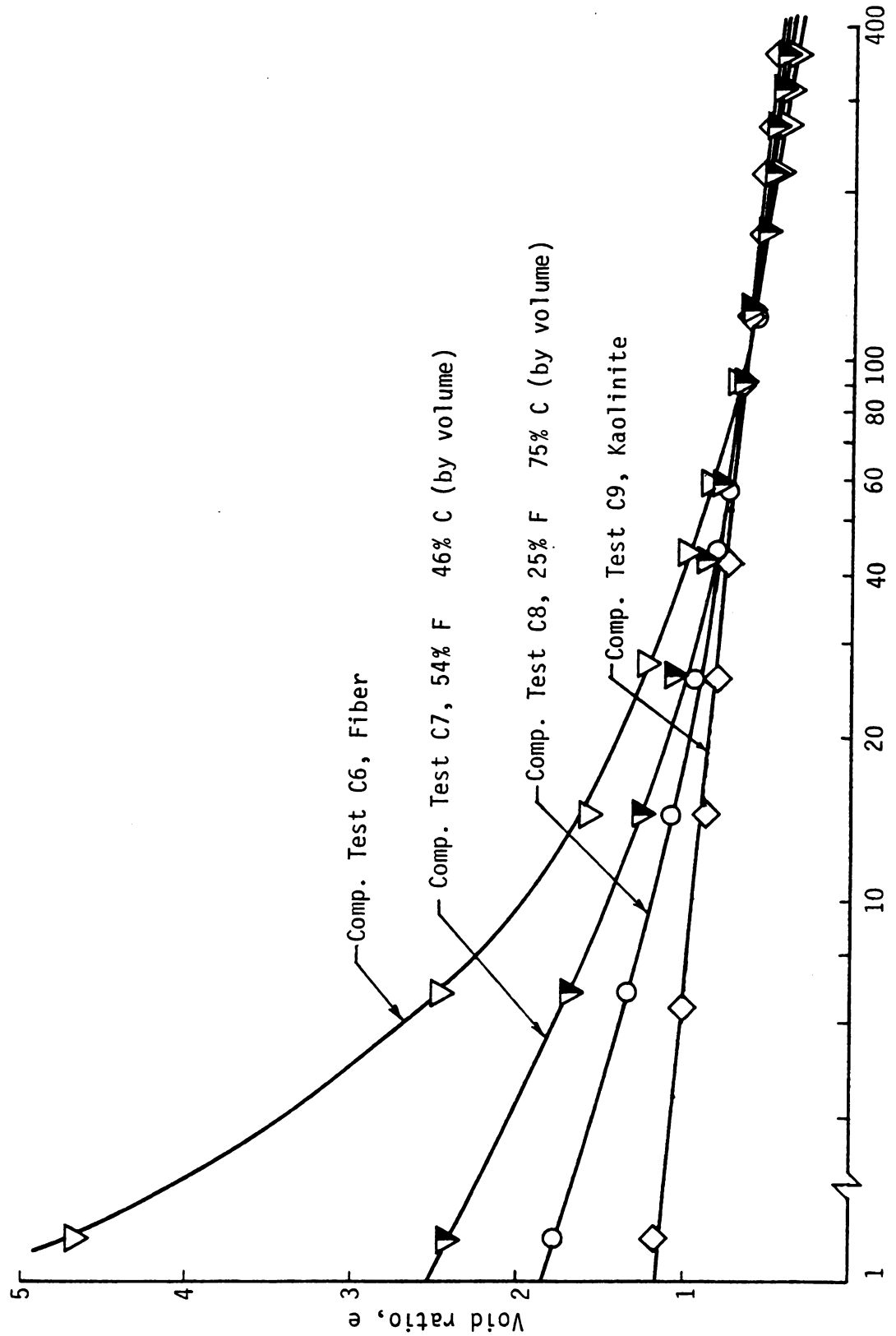

Figure 5.8 Effective normal stress vs. Void ratio curves for the Kaolinite/fiber samples on a semi logarithm scale.

reduced spacing of particles.

2) Removal of water from the inner fiber structure resulting in a reduced cross-section of the total fiber.

Assuming that, somehow, one can separate process (1) from process (2), assign to each a different compression coefficient, C_1 and C_2, such that the cumulative effect yields a curve instead of a straight line as shown in Figure 5.8. The question arises as to which of the two phenomena is responsible for the nonlinear relationship between the normal effective stress and void ratio. Process one is identical to that in dispersed clays (Scott, 1963) which yields a straight line relationships between the logarithm of effective stress and void ratio. Therefore, removal of water from the inner fiber structure must be responsible for the nonlinearity. The processes active in the samples may not be limited to only two as explained in the simplified picture. Some of the fibers are folded, others are bent, and some perhaps are in tension, but the dominant variable effecting the shape of the curves appears to be the proportion of fibers.

In the case of kaolinite/fiber mixtures the process is perhaps more complex due to bending of clay particles, decreasing distance between clay particles, or a clay particle and a fiber or a combination of both. Regardless of how many or how complex the processes are the overall behavior resembles the behavior of a dispersed or flocculated clay depending upon the proportion of constituents in the test samples. There is one difference which will not support the above conclusions for all samples containing fibers. In the case of flocculated structures failure is generally of a brittle type yielding a

maximum strength. Samples containing fibers in excess of a certain proportion did not show a brittle failure mode. They showed a plastic type of behavior similar to that of remolded clay. Samples with 54 percent fiber and 46 percent kaolinite by volume and all fibers showed a plastic behavior. Samples with 25 percent fiber and 75 percent kaolinite by volume show a brittle failure, hence their behavior is similar to that of flocculated clays.

When only a small pressure increment is applied to naturally existing clay, the change in void ratio is small and the approximation can be made that compression takes place as a linear function of pressure. Such an assumption would be far in error if applied to a large change in void ratio such as that occurring between the time of its first deposition and its subsequent burial under deep layers of later sediments. One can therefore assume that the variation of normal stress and void ratio is linear for the range of loads which are commonly encountered in engineering problems. Pressure on a horizontal scale is plotted against the coefficient of volume compressibility in Figure 5.9 for the kaolinite/fiber samples. The compressibility in each case is sharply decreasing at low magnitudes of pressure indicating the movement of individual particles closer to one another. At high pressures the compressibility change is practically negligible for all samples, an indication of the close contact of particles. The compressibility of all fiber samples was consistently higher whereas for kaolinite it was consistently lower with kaolinite/fiber samples falling between these two limits (Figure 5.9). These data show that higher organic (fiber) contents

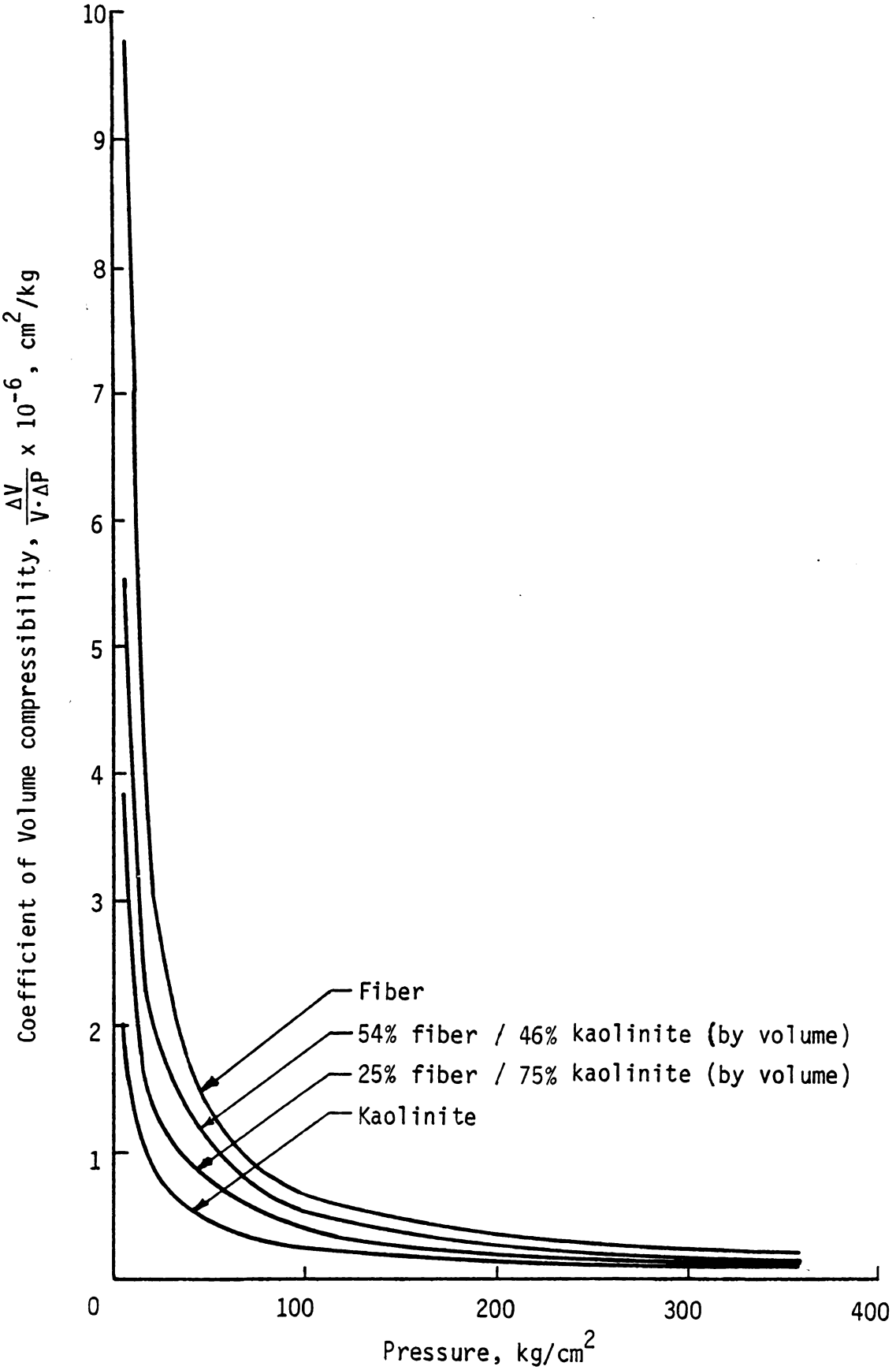

Figure 5.9 Pressure vs. Coefficient of Volume compressibility kaolinite, two kaolinite/fiber mixtures, and fiber samples.

increases the coefficient of volume compressibility.

Compressibility test sample C1, all fiber, one square cm area and initial volume of 4.99 cm^3 at an effective stress of 3.99 kg/cm^2 gave a change in volume of 1.96 cm^3. Using the relationship, $-\left(\frac{\Delta V}{V}\right) = C\Delta p$, gives the sample compressibility

$$C = \frac{1.96}{4.99 \times 3.99} = 98 \times 10^{-3} = 98{,}000 \times 10^{-6} cm^2/kg.$$

From Table 2.3 note that values of C_s for clay are close to $2 \times 10^{-6} cm^2/kg$. If it is assumed that C_s varies directly with the specific gravity of the material, then a reasonable value of C_s can be obtained for freeze dried solid fiber material as follows,

$$C_s = \frac{2.65}{1.54} \times 2 \times 10^{-6} = 3.44 \times 10^{-6}$$

Therefore,

$$\left(\frac{C_s}{C}\right)_{fiber} = \frac{3.44 \times 10^{-6}}{98{,}000 \times 10^{-6}} = .000035$$

For comparison consider pure kaolinite. From compressibility test sample C4, a sample of one sq. cm. area at an effective stress of 3.99 kg/cm^2 gave a volume change equal to .4597 cm^3. For an initial volume of 5.684 cm^3 compute

$$C_{clay} = \frac{.4597}{5.684 \times 3.99} = 20.27 \times 10^{-3} = 20270 \times 10^{-6} \ cm^2/kg$$

and

$$\left(\frac{C_s}{C}\right)_{clay} = \frac{2 \times 10^{-6}}{20270 \times 10^{-6}} = .000099$$

The numerical value of $\left(\frac{C_s}{C}\right) = .000035$ for a pressure of 3.99 kg/cm^2

and all fibers is too small to have any significant effect in the equation,

$$-\left(\frac{\Delta V}{V}\right) = C[\Delta p - (1 - \frac{Cs}{C})\Delta] \qquad (5.2)$$

Therefore the $\frac{Cs}{C}$ factor for organic soils can be neglected and it can be concluded that Terzaghi's effective stress concept is valid to a high degree of approximation for kaolinite/fiber mixtures and all fiber samples.

5.2.2 Triaxial Consolidation

In the triaxial test a sample was subjected to three dimensional isotropic consolidation before application of the deviator stress. To accelerate the consolidation process side drains were provided in addition to the rigid porous stones at the top and at the bottom of the sample. Use of side drains reduced the time required for 95 percent consolidation to about one-tenth of the time for only double end drainage (Bishop and Henkel, 1962). Since both vertical and radial flow were permitted, separate solutions to vertical and radial flow may be combined. In the triaxial specimen the applied stress will initially cause a uniformly distributed excess pore pressure throughout the medium which will begin to dissipate first near the drainage boundary Thus in the early stages of consolidation the material near the periphery of the specimen will have consolidated to a greater degree than the material along the axis of the sample. As a result the vertical settlement near the periphery will be larger than the vertical settlement near the axis. If the porous stones were flexible, then, due to this nonuniform settlement from the axis of the sample to the periphery, the stones would attain a shape

that is concave downward during the consolidation process before becoming plane again when it was completed. Since the porous stones used were rigid, the material was strained equally in a vertical direction at all points on the radius near the sample ends and the soil near the surface away from the ends was compressed radially during consolidation, a condition that does not correspond to the field situation. The $\overline{CIU}$ test was employed to insure that the soil sample had experienced a specified stress history before shear strength testing and was considered acceptable for the project objectives. Anisotropic consolidation can be used to similate field conditions.

Consolidation pressure is plotted against water content at equilibrium for all fiber, kaolinite/fiber mixtures, kaolinite samples in Figure 5.10. These results are similar to those shown in Figure 5.6 for one dimensional compression except that the horizontal scale has been greatly exaggerated.

5.3 Shear Strength of Kaolinite/Fiber Mixtures

The shear strength of kaolinite/fiber mixtures is presented in three sections: direct shear study, triaxial compression, and shear strength parameters ϕ' and c'.

5.3.1 Direct Shear Study

Direct shear tests on samples prepared from pulp fibers included:

1) Saturated full length fiber samples;

2) Saturated powdered fiber samples; and

3) Oven dry fiber samples.

Shear displacement versus shear stress for several saturated

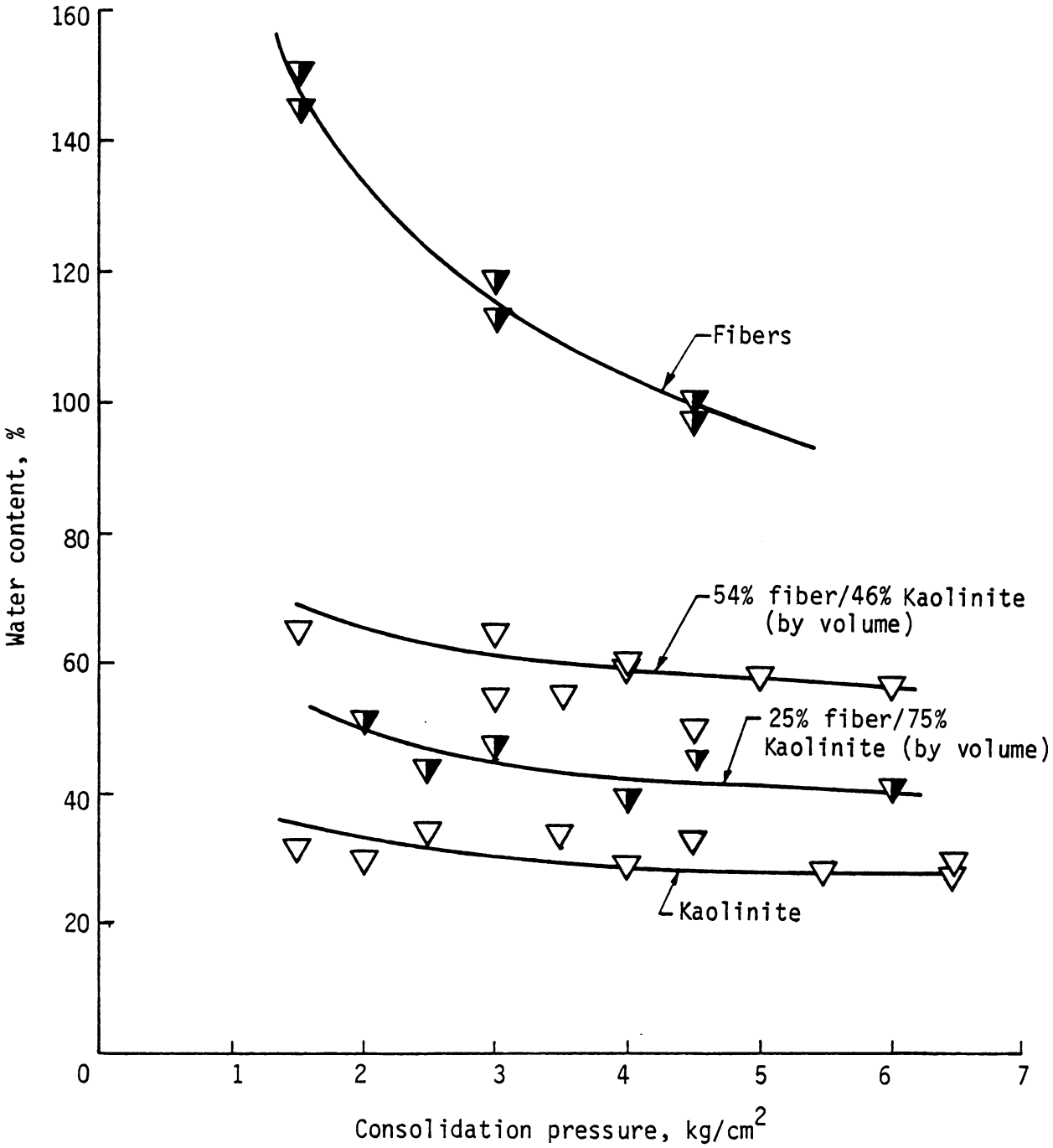

Figure 5.10 Consolidation pressure vs. % Water content for kaolinite/fiber samples.

fiber test specimens and subjected to varying consolidation pressures are summarized in Figure 5.11. Note that the shear strength of the specimens continued to increase with increasing strain and no peak shear point values were obtained. The shear strength also increases with increasing consolidation pressure or normal stress for a given shear displacement. For example, sample S6 shows that the shear strength corresponding to a displacement of 0.25 cm is about 1.50 kg/cm^2 and for a displacement of 0.50 cm the shear strength has increased to 2.50 kg/cm^2. Sample S5 loaded with a normal stress of 0.962 kg/cm^2 shows a shear strength of about 1.12 kg/cm^2 corresponding to a shear displacement of 0.50 cm, whereas Sample S3 with a normal stress of 4.06 kg/cm^2 shows a strength of about 4.6 kg/cm^2 at the same shear displacement. This increase of shear strength with increasing normal stress implies that the shear strength was predominantly due to friction. A linear relationship between shear displacement and shear stress is shown in Figure 5.11 for displacements larger than 0.15 cm which corresponds to a strain of about 6 percent. Shear strength also increased with increasing strain for the same normal stress, indicating a continuous mobilization of the coefficient of friction, $\tan\phi'$. The factor which has the maximum effect on the friction angle ϕ' appears to be the density of the material. It is apparent that increased density changes the friction angle ϕ' which leads to improved shear strength at a constant normal stress with increasing strain. It was observed during the test that the sample appeared to be more dense in the vicinity of the shear plane, as shown in Figure 5.12. The zone of higher compression is outlined schematically in Figure 5.13.

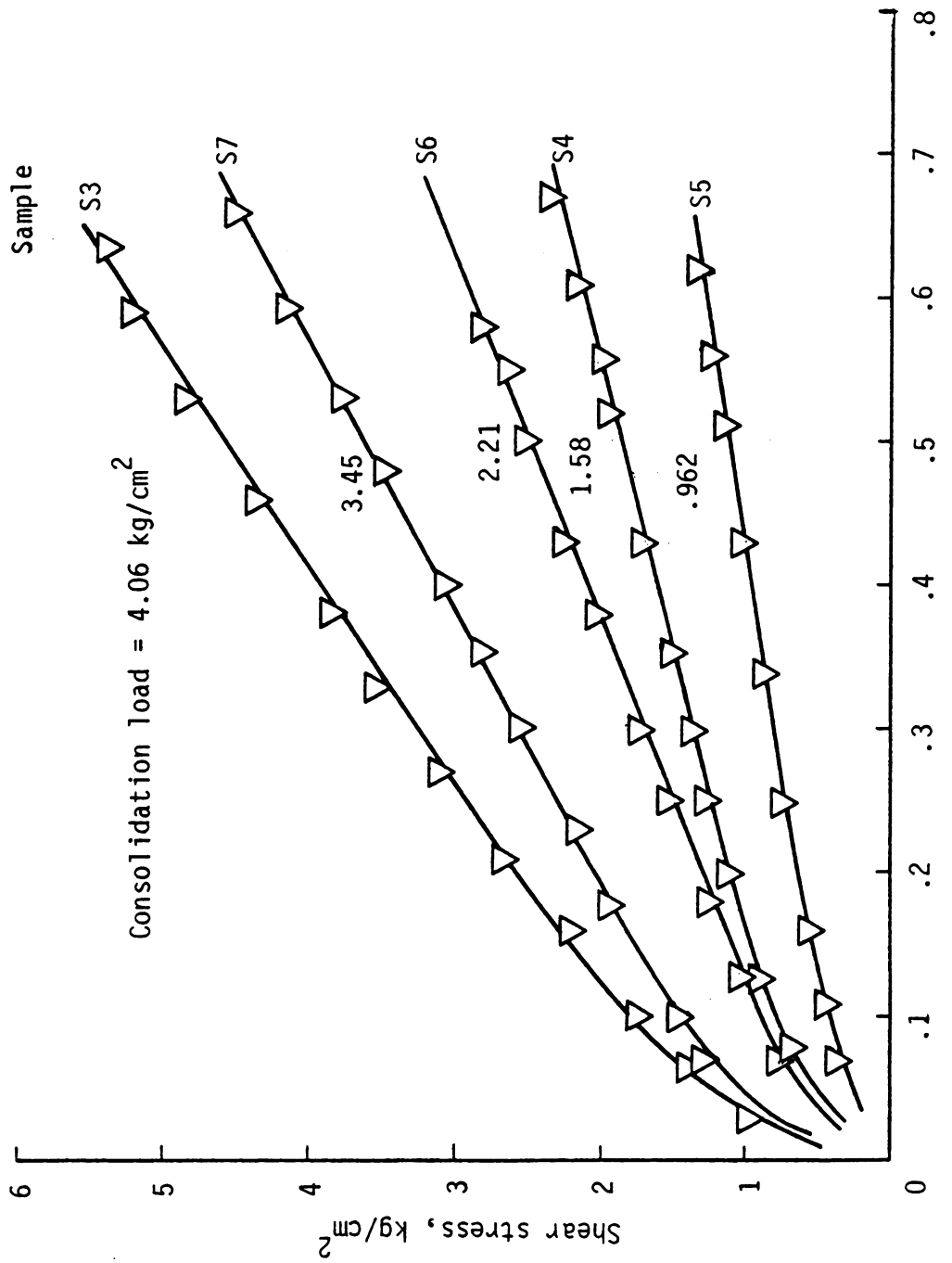

Figure 5.11 Direct shear stress displacement curves for consolidated saturated fiber samples.

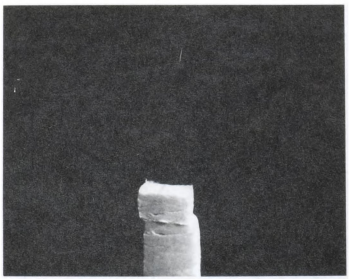

(a)

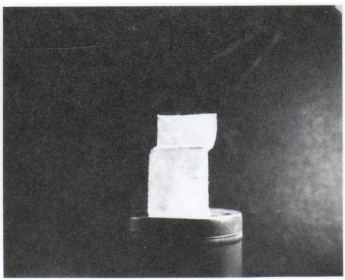

(b)

Figure 5.12 Direct shear test samples after completion of the tests.

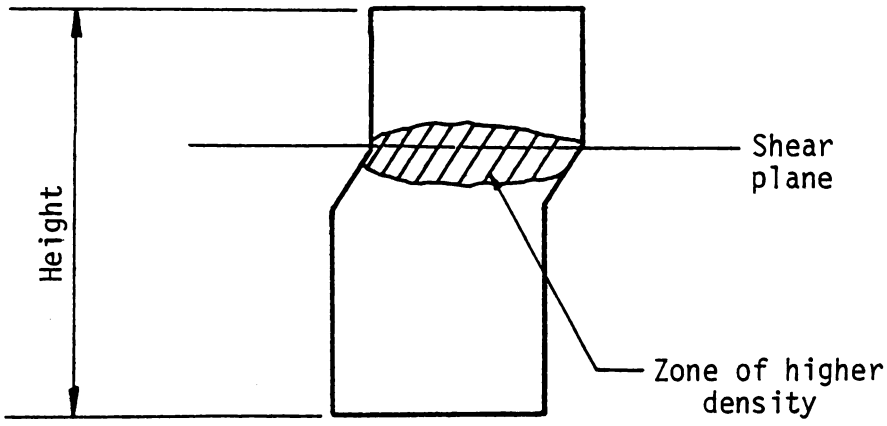

Figure 5.13 Schematic of the failure zone in a fiber sample after being subjected to a direct shear test.

Shear displacement plotted against shear stress and vertical displacement is shown in Figure 5.14 for Samples S6 and S9. Water absorption during conduct of the test has lowered the strength and increased the vertical displacement for Sample S6 as compared to Sample S9 for the same consolidation pressure and lateral displacement.

Shear displacement plotted against shear stress for samples composed of dry powdered fibers are summarized in Figure 5.15. The shear strength for dry powdered fiber samples also increases with increasing normal stress and increasing shear displacement.

The behavior of dry fiber versus saturated fiber samples is shown in Figure 5.16, where shear displacement has been plotted against shear stress and vertical displacement. The dry fiber samples in Figure 5.16a consistently show a higher shear strength than the saturated fiber samples for the same magnitude of consolidation pressure and shear displacement. The slope of the curves for dry samples are flatter than the slope of the curves for saturated samples indicating a smaller rate of change in the density of the material which is further evidenced from the lower vertical displacements shown in Figure 5.16b.

Figure 5.17 presents normal stress plotted on a horizontal scale against shear stress on a vertical scale for saturated samples corresponding to an assumed failure strain of 20 percent. The resulting angle of internal friction ϕ', equals 49.60 degrees with no intercept on the vertical axis. Figure 5.18 shows normal stress plotted against shear stress for dry powdered fiber samples to yield an angle of internal friction ϕ', of 47.50 degrees and an intercept on the vertical axis equal to 0.26 kg/cm^2.

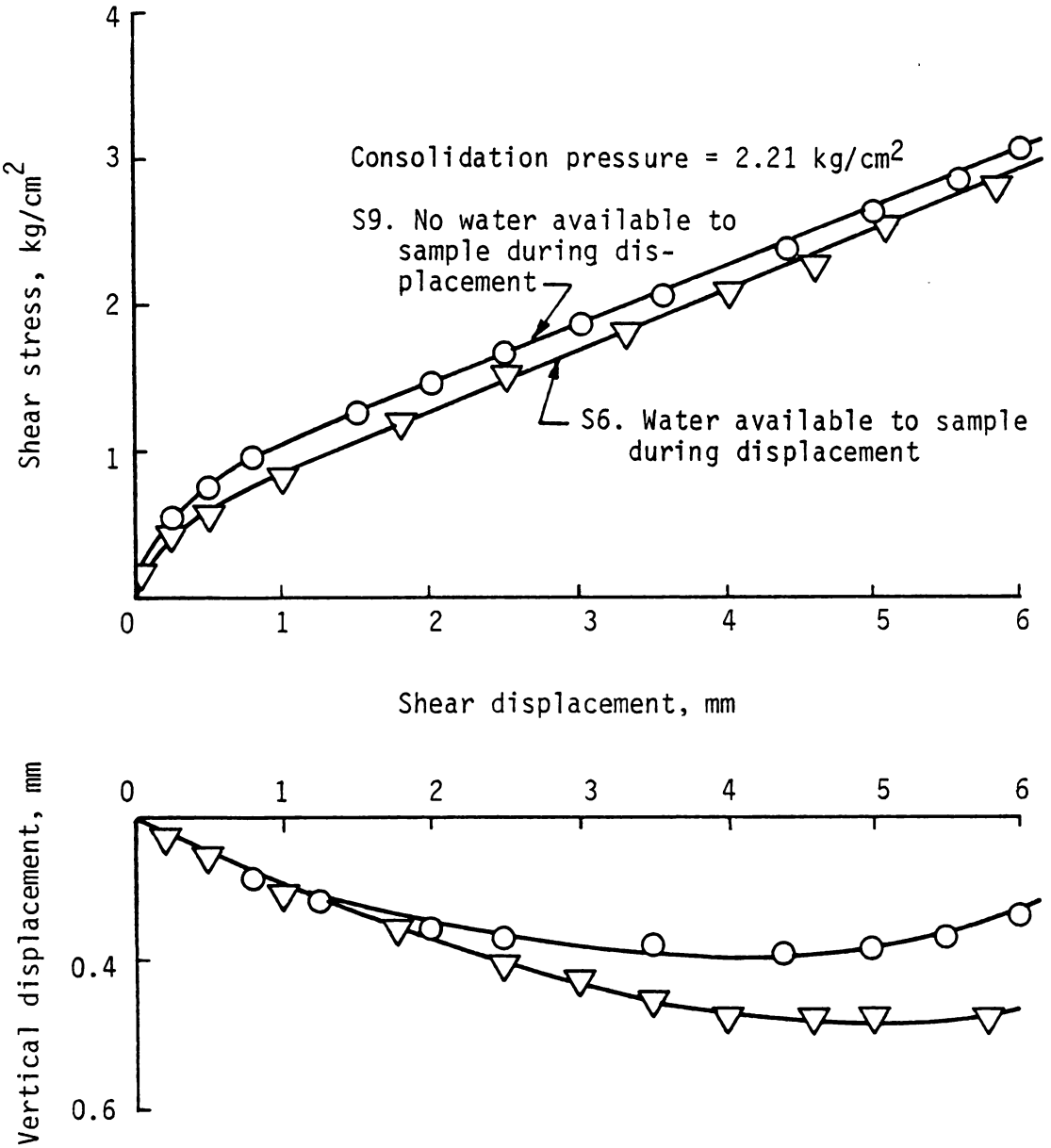

Figure 5.14 Shear displacement vs. Shear stress and Vertical displacement curves showing the effect of water absorption during the test by saturated fiber samples.

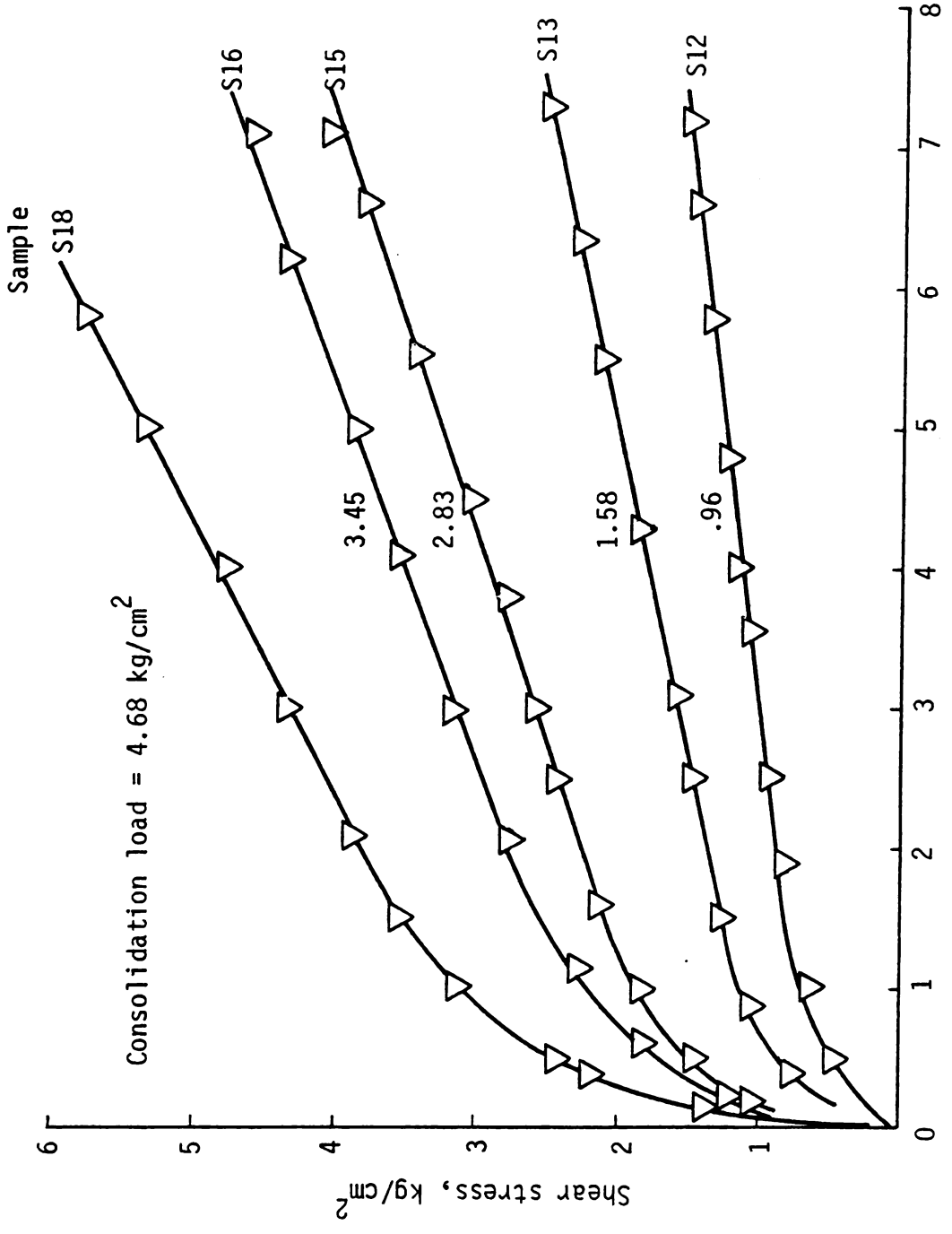

Figure 5.15 Direct shear stress displacement curves for consolidated dry powdered fiber samples.

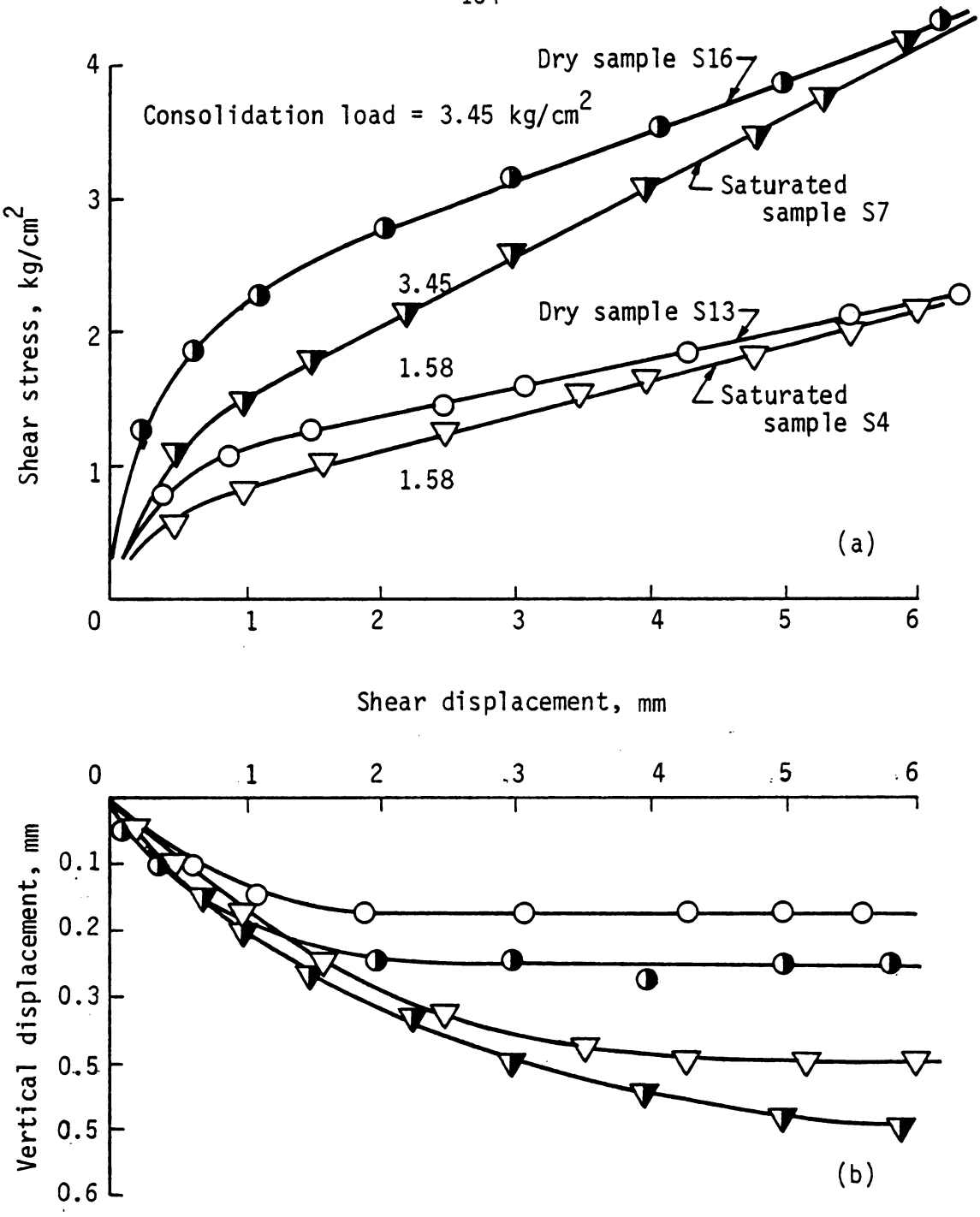

Figure 5.16 Shear displacement vs. Shear stress and Vertical displacement curves for dry and saturated fiber samples showing the effect of water.

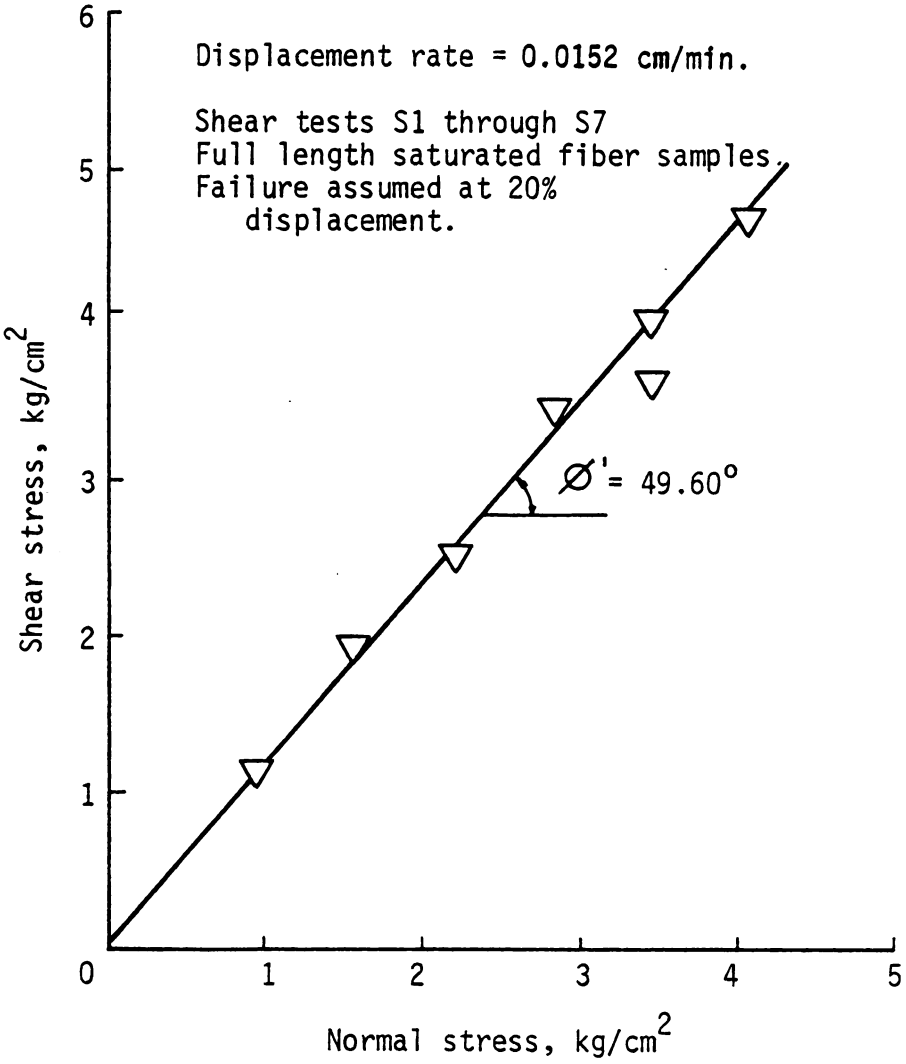

Figure 5.17 Summary of direct shear data for fully saturated full-length fiber samples.

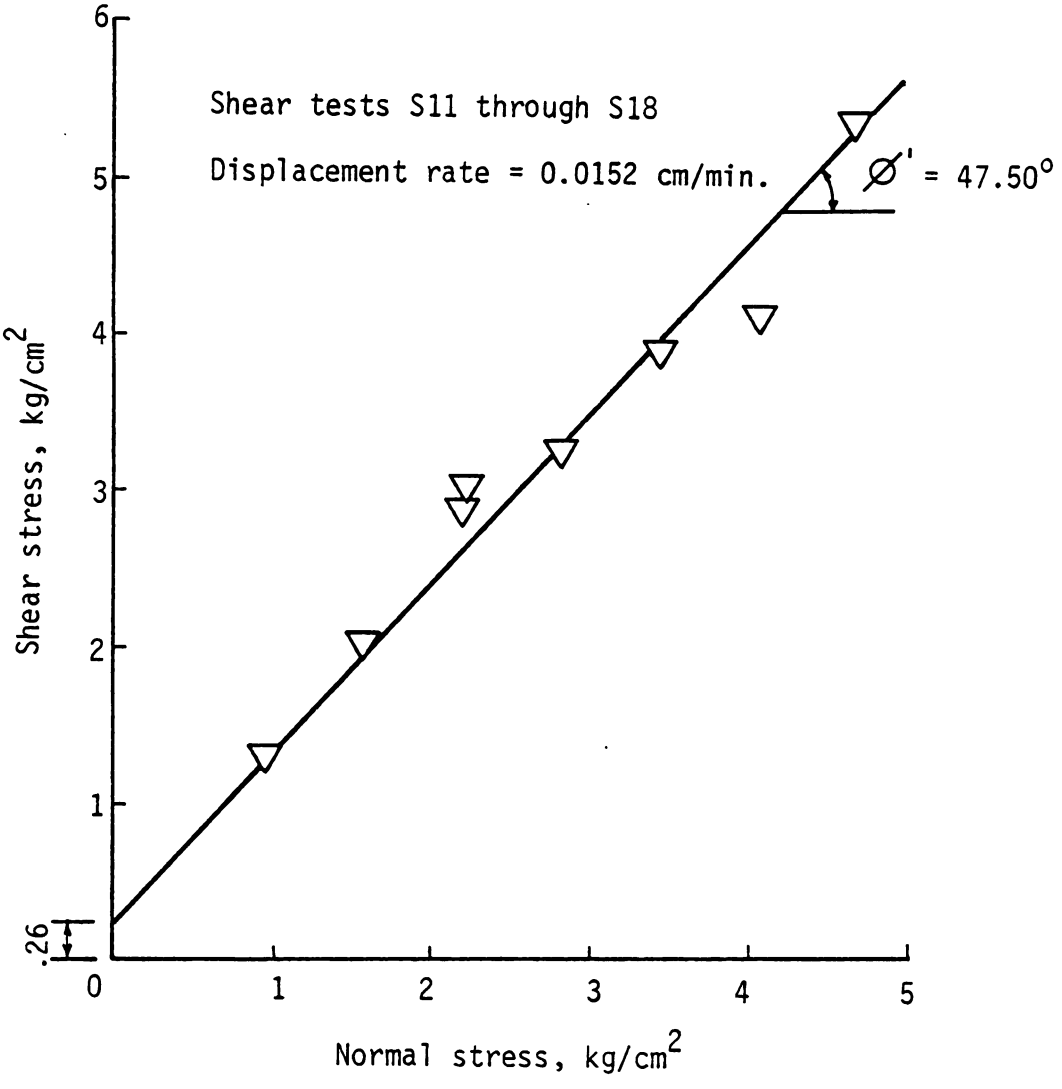

Figure 5.18 Summary of direct shear data for dry powdered fiber samples.

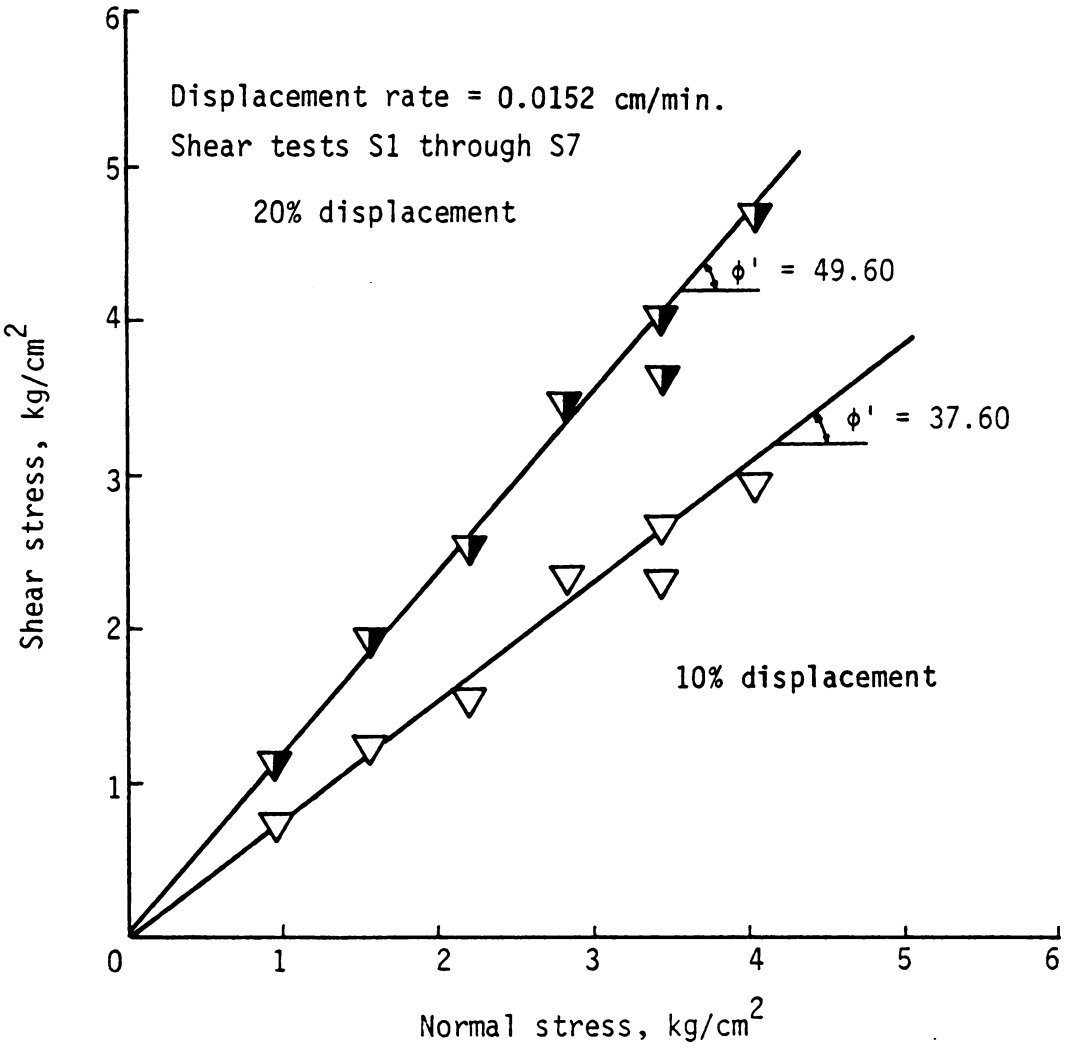

Figure 5.19 Comparison of direct shear data for fully saturated fiber samples at 10 and 20 percent displacement strain.

Figure 5.19 shows normal stress plotted against shear stress at assumed values of failure strains of 20 percent and 10 percent. The test samples show an angle of internal friction ϕ', of 49.60 degrees corresponding to a strain of 20 percent, and a much smaller angle of internal friction of 37.60 degrees with respect to a strain of 10 percent. There are perhaps two possibilities to explain the significant difference between the frictional angles. The material is either densifying during the conduct of the test with increasing strain or the fiber tension is contributing to the strength of the material which appears in the form of improved frictional angle.

5.3.2 Triaxial Compression

A discussion of organic versus inorganic soils illustrates the differences in response of the two soils under triaxial compression. This is followed by a discussion of consolidated undrained tests and consolidated drained tests.

5.3.2.1 Organic Versus Inorganic Soils

Consider the cross-section of an idealized organic soil, i.e., cross-section of fibers and an inorganic soil as shown in Figure 5.20. In inorganic soils, for example sand, the solid grains are very stiff and the imposed load is carried by the solid particles structure under drained conditions. The external load is transmitted through the contact points of the solid grains. For all practical purposes the deformation of the solid particle is very small and can be neglected. The change in void ratio during application of a load occurs due to small movements of the particles, i.e., the particles move closer together resulting in the reduction of the volume

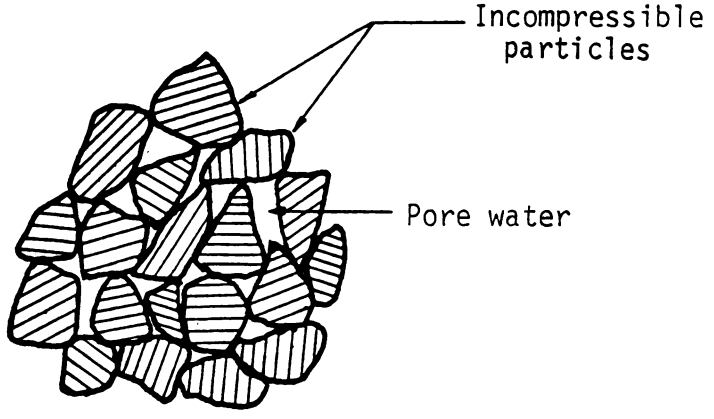

(a)

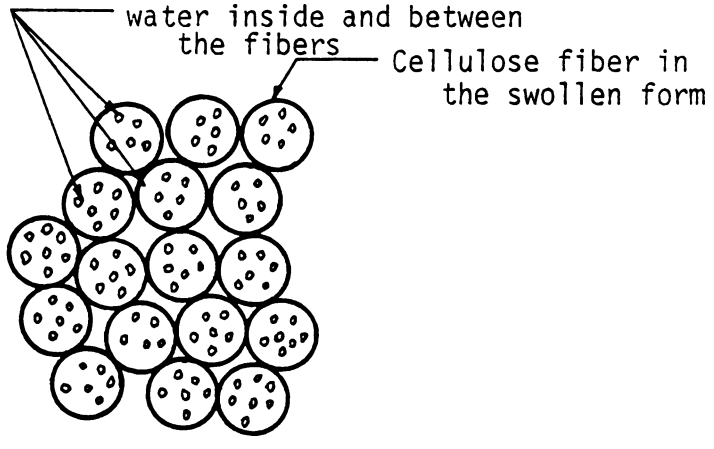

(b)

Figure 5.20 (a) Saturated inorganic soil fabric (b) Idealized saturated organic soil.

of voids. The change in void ratio is due entirely to the change in the volume of the space existing between the solid particles. The same reasoning can also be applied to compressible inorganic soils such as clay.

In organic soils the phenomenon includes the hydrophyllic nature of the fibers. The total amount of water in a saturated organic soil sample is the sum of the amount retained between the individual (solid) fibers and the amount stored within the porous structure of the fibers. When this sample is subjected to an external load under drained conditions the water from between the fibers and from within the structure of the fibers is squeezed out giving rise to a large change in void ratio and a reduction in the initial swollen volume of the fibers resulting in a smaller cross-section. Hence the total change in the void ratio is due to the cumulative effect of a reduction in internal pore volume and a closer packing of the individual particles. This would mean that at higher consolidation pressures the amount of water contained within the fiber structure will be reduced resulting in smaller cross-sectional areas. It is this hydrophyllic nature and structure of the fibers that is responsible for the high compressibility of organic soils. A dry fiber structure should not be nearly as compressible as the saturated fiber structure as has been observed in the direct shear tests.

Consider a saturated sample composed of a fiber-clay mixture. At low consolidation pressures and at equilibrium, water retained by the fibers will maintain flexible swollen structure and larger distances between fiber particles. Fiber and clay particles will be separated by

several layers of water molecules. Due to the hydrophyllic nature of the fibers the water distribution within the sample will be nonuniform, larger masses of water being held by the organic fibers. At higher consolidation pressures clay and fiber particles will be forced closer together. The expulsion of water results in a denser fiber-clay structure. If the fiber quantity is controlled with respect to the clay, a matrix of these materials may behave like a reinforced material at low water contents. It would appear that the strength of the fiber-clay sample depends upon the ratio of the two materials present and the magnitude of the applied consolidation pressure.

5.3.2.2 Consolidated Undrained Tests

Both brittle and plastic failure (Whitman, 1960) can be observed in inorganic cohesive soils. Brittle failure is characterized by the development of a peak stress and the formation of failure planes. Plastic failure involves a continuous increase in deviator stress past 20 percent axial strain and sample bulging. The pure clay samples and the samples with 25 percent fiber/75 percent clay exhibited peak strength, $(\bar{\sigma}_1 - \bar{\sigma}_3)_{max}$. Failure in soils is usually a progressive type of process and the $(\bar{\sigma}_1 - \bar{\sigma}_3)_{max}$ value corresponds approximately to the point at which structural collapse of relatively stiff material takes place. Soils lacking structural stiffness or rigidity show a more viscous type behavior. For such soils it becomes difficult to define the stage in the shear process which represents failure.

Consolidated undrained triaxial tests with pore pressure measurements were performed on kaolinite, kaolinite/fiber mixtures, and fiber samples. The results from nine undrained triaxial tests on kaolinite

samples is summarized in Figure 5.21. The values of $\frac{\bar{\sigma}_1 + \bar{\sigma}_3}{2}$ on a horizontal scale are plotted against $\frac{\bar{\sigma}_1 - \bar{\sigma}_3}{2}$ on a vertical scale resulting in a k_f-line inclined at an angle α of 19°, hence a ϕ' of 20.14°. All samples exhibited a brittle type failure with a well-defined failure plane. The data points corresponding to consolidation pressures higher than 2.5 kg/cm^2 align well on the k_f-line (Figure 5.21) indicating reasonably good agreement. The first two points corresponding to lower consolidation pressure fell above the k_f-line. This deviation indicates some overconsolidation related to the method of sample preparation.

The result of four consolidated undrained triaxial tests on samples with 25 percent fiber/75 percent kaolinite, by volume, are summarized in Figure 5.22. All samples exhibited a brittle failure with no clearly developed failure plane. The failure strains for three of the samples varied from 8.45 percent to 8.81 percent, whereas the fourth sample failed at about 15 percent. For consolidation pressures of 2 kg/cm^2 to 6 kg/cm^2 good agreement between data points was observed. The k_f-line in Figure 5.22 gives an angle α of 23° with an intercept of 0.26 kg/cm^2 on the vertical axis. The shear strength parameters ϕ' and c' are therefore 25.12° and 0.29 kg/cm^2. The vertical intercept may be caused by development of tension in fibers extending across the failure plane.

As the fiber content in the fiber kaolinite mixtures was increased a decrease in stiffness with a more plastic behavior was observed. In such cases an arbitrary 20 percent axial strain was defined as failure. This criterion has been extensively used as a definition of failure,

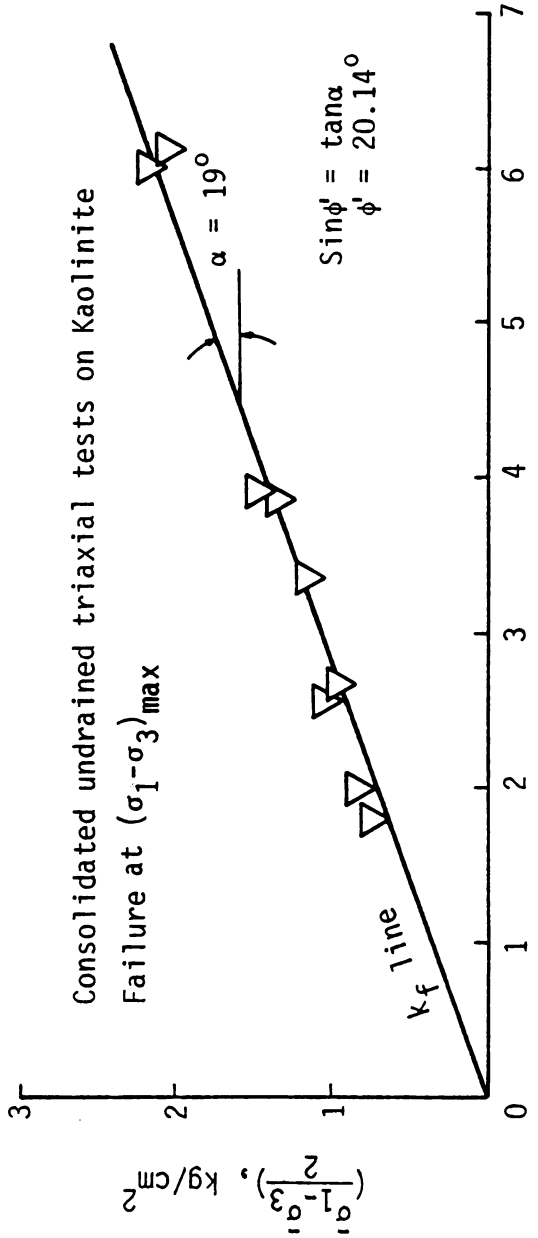

Figure 5.21 Summary of consolidated undrained triaxial test data for Kaolinite.

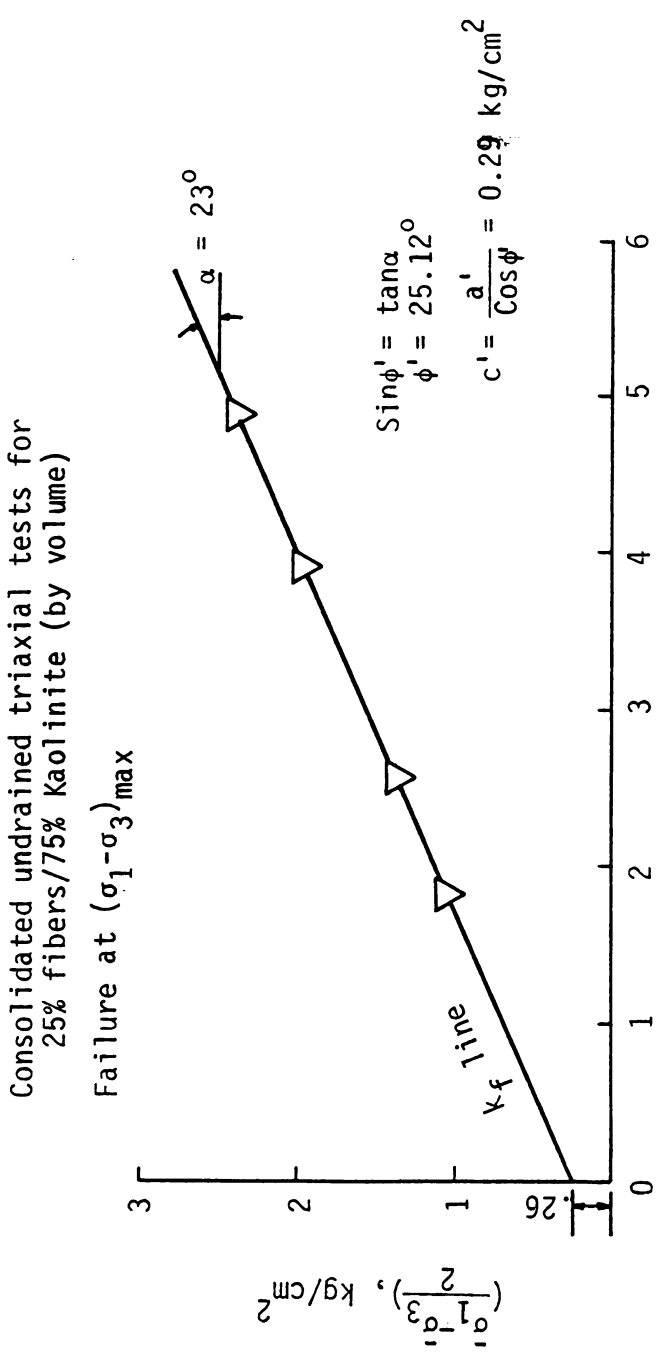

Figure 5.22 Summary of consolidated undrained triaxial data for 25% fiber/75% Kaolinite samples (by volume).

especially in the case of inorganic soils like clays. This failure criterion appears to have shortcomings, some obvious and some not so obvious, particularly in the case of soils with high organic and water contents. An alternate technique for defining strength at failure is suggested for organic soils in the following paragraphs.

Data from three consolidated undrained triaxial tests on samples with 54 percent fiber/46 percent kaolinite by volume are shown in Figure 5.23. The test samples did not exhibit brittle failure, therefore the Mohr envelope shown was based on an arbitrarily assumed axial failure strain of 20 percent. Consolidation pressures ranged from 3 kg/cm^2 to 6 kg/cm^2. The k_f-line passes through the origin with an inclination α of 33°, hence a shear strength parameter ϕ' of 40.49°. The strength envelope does not show any intercept on the vertical axis indicating a lack of any cohesion.

Using a $\bar{p}$-$\bar{q}$ plot for the determination of the shear strength parameter ϕ', is a standard procedure in geotechnical engineering, however, in certain cases as will be seen later in this section, it can lead to unrealistic conclusions if the limitations on the method are overlooked. The limitation of the method becomes obvious when applied to compressible organic soils in which excess pore pressures reach values equal to the cell pressure, i.e., the effective minor principal stress goes to zero.

The $\bar{p}$-$\bar{q}$ plot shown in Figure 5.24 was based on the results of triaxial tests performed on pure fiber samples subjected to consolidated undrained conditions with pore pressure measurements. Pulp fibers are hyrophyllic in nature giving rise to high water contents. All fiber

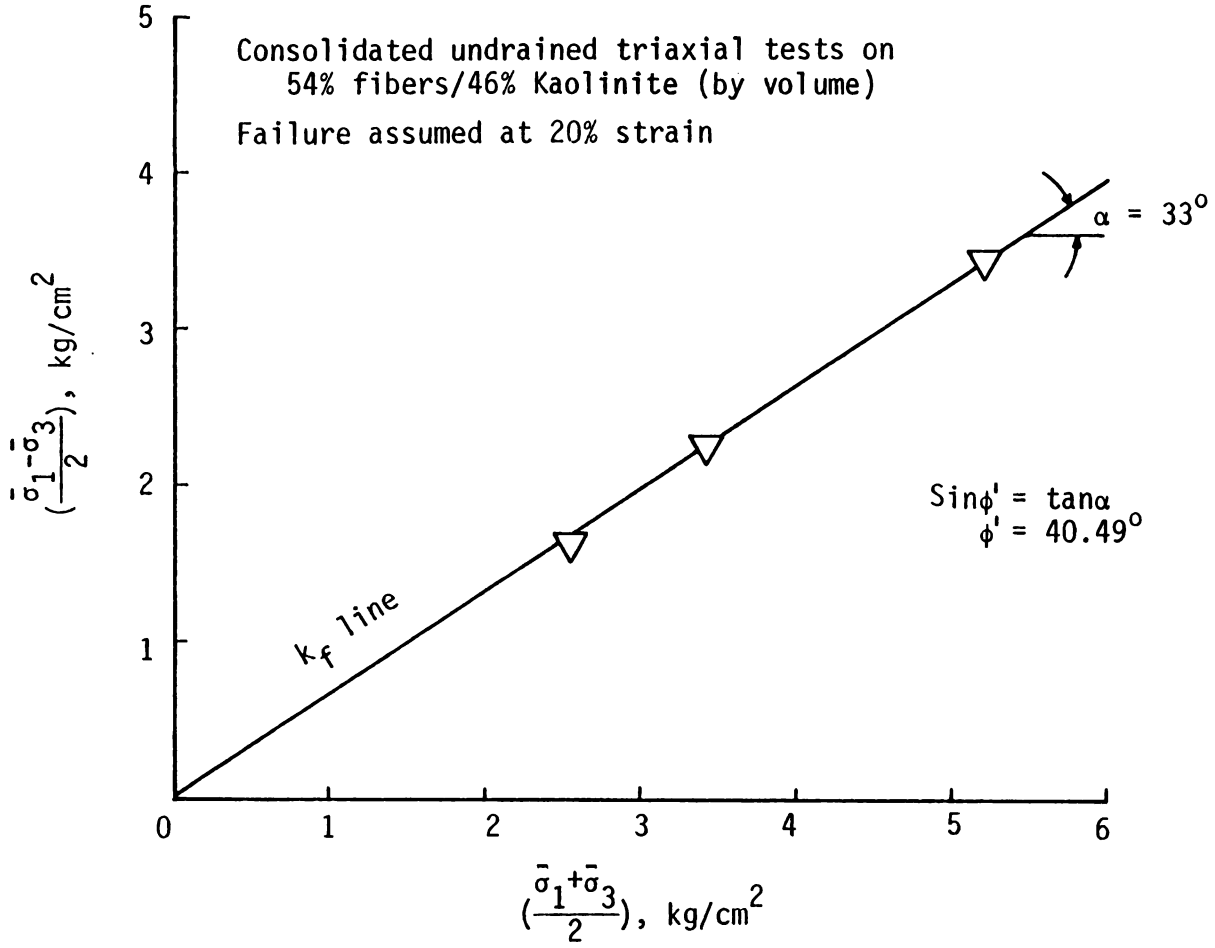

Figure 5.23 Summary of consolidated undrained triaxial data for 54% fiber/46% clay (by volume) mixtures.

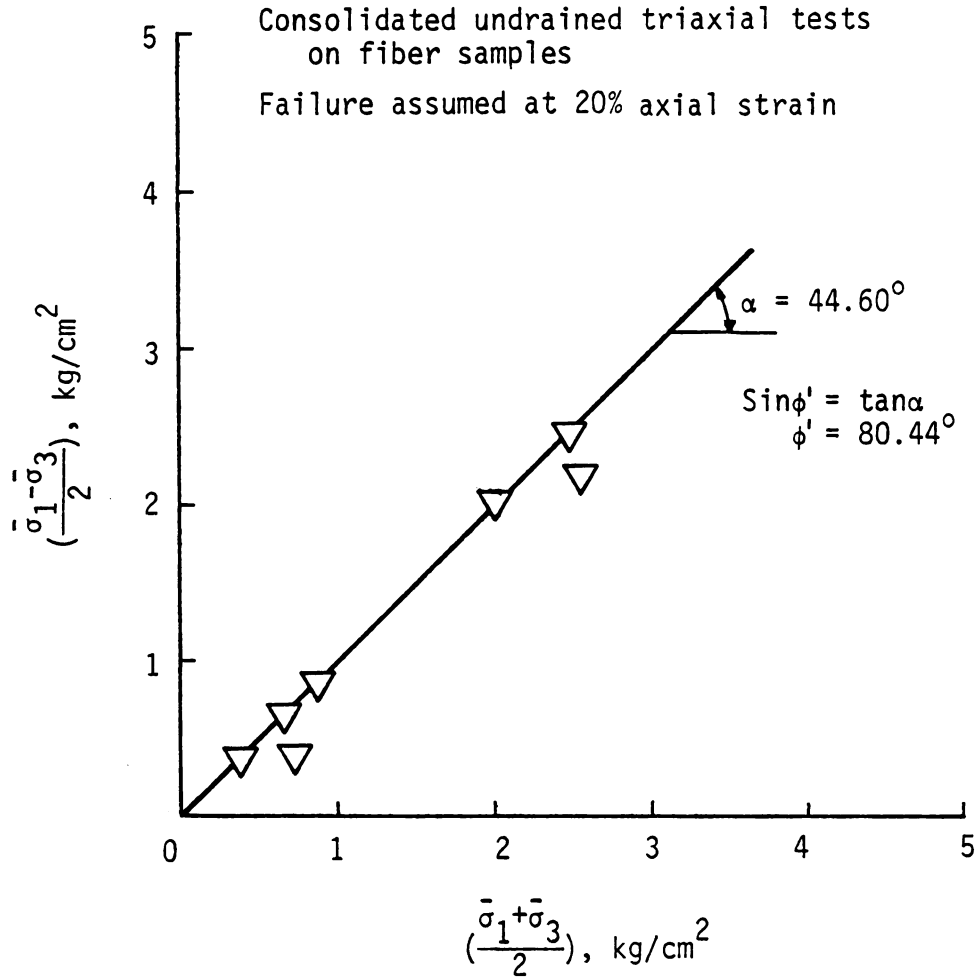

Figure 5.24 Summary of consolidated undrained triaxial data for all fiber samples.

samples, when subjected to triaxial shear, exhibited plastic failure. In such cases failure is usually based on an arbitrarily assumed axial strain. The value often selected varies from 10 to 20 percent depending upon the project type under consideration. One phenomenon, perhaps a unique characteristic of organic soils, is the tendency of the pore pressure to become equal to the minor principal stress σ_3 (cell pressure) at strains anywhere between 15-20 percent. In some extreme cases, which have been observed (Hanrahan, 1954; Andersland and Charlie, 1975) during triaxial tests, the effective minor principal stress $\bar{\sigma}_3$ becomes equal to zero resulting in a $\bar{p}$-$\bar{q}$ plot with k_f-line inclined at an angle α close to 45°, hence a shear strength parameter ϕ' close to 90°. As long as the pore pressure becomes equal to the cell pressure a ϕ' value of 90° will be consistently obtained from a $\bar{p}$-$\bar{q}$ plot regardless of the material tested. In Figure 5.24 $(\bar{\sigma}_1 + \bar{\sigma}_3)/2$ on a horizontal scale is plotted against $(\bar{\sigma}_1 - \bar{\sigma}_3)/2$ on a vertical scale for 100 percent fiber samples subjected to consolidated undrained triaxial tests, where $\bar{\sigma}_1$ and $\bar{\sigma}_3$ values are based on an assumed failure strain of 20 percent. Excess pore pressures were equal to the cell pressure at 20 percent strain for samples normally consolidated to low pressures. In the case of samples normally consolidated to relatively higher pressures, $\bar{\sigma}_3$ values were not zero but their magnitudes were small compared to $\bar{\sigma}_1$ values at 20 percent strain. The average k_f-line shown is inclined at an angle α of 44.60°, hence a shear strength parameter ϕ' of 80.44°. Note that the pore pressure indirectly controls the inclination of the k_f-line. This observation is obscure for inorganic soils since brittle failure takes place long before the

pore pressure has a chance to rise and become equal to the cell pressure.

An alternate method is suggested, the application of which is limited to those normally consolidated materials demonstrating plastic failure. Two assumptions are made, namely that the cohesion is zero for normally consolidated samples and that the failure is defined at a maximum $\frac{\tau}{\sigma'_n}$ ratio where τ is the shear stress and σ'_n is the effective normal stress at any strain value during the test process. A stress path or the locus of $(\frac{\tau}{\sigma'_n})_{max}$ is plotted and the peak point on the curve is assumed to be the shear strength. A straight line passing through the origin and the peak point is assumed to represent the strength envelope inclined at an angle equal to $\tan^{-1}(\frac{\tau}{\sigma'_n})_{max}$. Experimental data for an all fiber sample and a sample with 54 percent fiber/46 percent kaolinite by volume is shown in Figure 5.25a and 5.25b using this criteria. Note that the shear strength corresponding to a $\tan^{-1}(\frac{\tau}{\sigma'_n})$ of 90° is zero. For samples with pure fibers $\tan^{-1}(\frac{\tau}{\sigma'_n})$ equals 39° and for samples with 54 percent fiber/46 percent kaolinte by volume, $\tan^{-1}(\frac{\tau}{\sigma'_n})$ equals 34.8°. For pure kaolinite and samples with 25 percent fiber/75 percent kaolinite by volume this criteria was not used since a brittle failure, i.e., $(\bar{\sigma}_1 - \bar{\sigma}_3)_{max}$ was observed. This approach appears to define a useful strength criteria for those materials in which the pore pressure tends to approach the confining pressure. This definition is limited to normally consolidated materials. At this stage of the development, overconsolidated fibrous organic soils have not been investigated.

Mohrs failure envelope was assumed to be a straight line in Figure 5.22, 5.23 and 5.24. In reality this envelope may not be a straight line depending to a significant extent upon the magnitude of

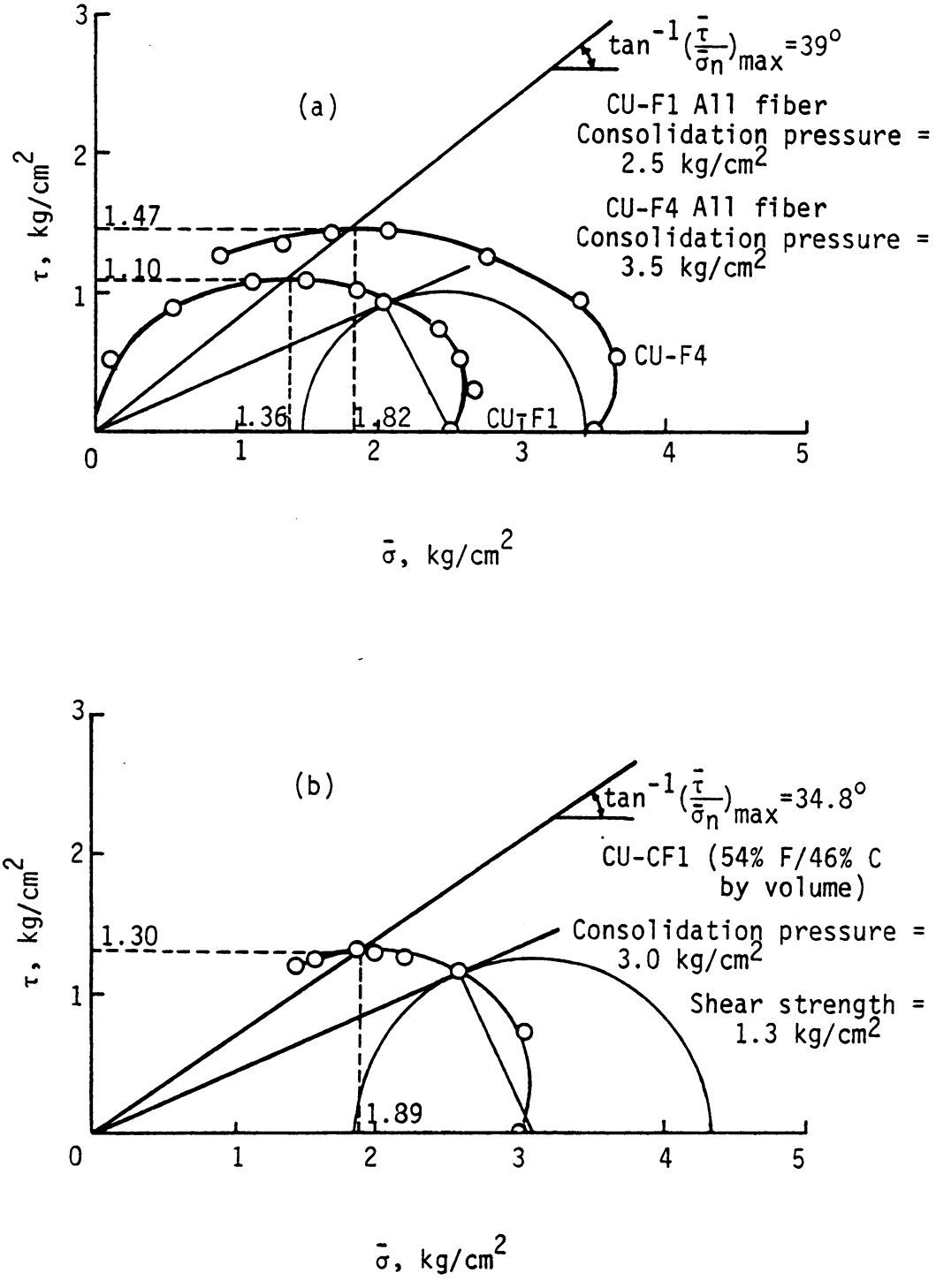

Figure 5.25 Stress paths for samples with (a) all fibers and (b) 54% fibers/46% Kaolinite (by volume).

the applied loads. The loads in turn cause a change in porosity giving rise to a curvilinear failure envelope. A brief discussion related to the geometry of the failure envelope for soils follows.

If a change in porosity causes the failure envelope to change its shape from approximately a straight line to a curved line, (Section 2.5.3) then one should expect a curved failure envelope for normally consolidated clays since with increasing consolidation pressures the porosity will decrease. But normally the failure envelope for normally consolidated clays is approximated by a straight line for the stress levels encountered in most geotechnical problems. The porosity change causing a nonlinear failure envelope is associated with the increase in contact area of the solids and this change in contact area can only occur if there is 1) yielding of the solid material at the points of contact or 2) the increase in the number of contact areas. In normally consolidated clays the contact area does not change significantly. Consider Figure 5.26a where the clay particles are shown a certain distance apart by layers of water with respect to a certain consolidation pressure. When the consolidation pressure is increased clay particles are forced to move closer, (Figure 5.26b) but the contact area between the solids remains practically unchanged, and consequently the Mohr envelope will exhibit a straight line geometry.

Consider now Figure 5.26c where an idealized diagram of two adjacent saturated fibers is shown. At a low deviator stress and therefore at low strains the near saturated fibers maintain approximately a cylindrical cross-section and the contact area between the solids is relatively small. As the deviator stress increases, strain will increase with more and more of water being expelled from the

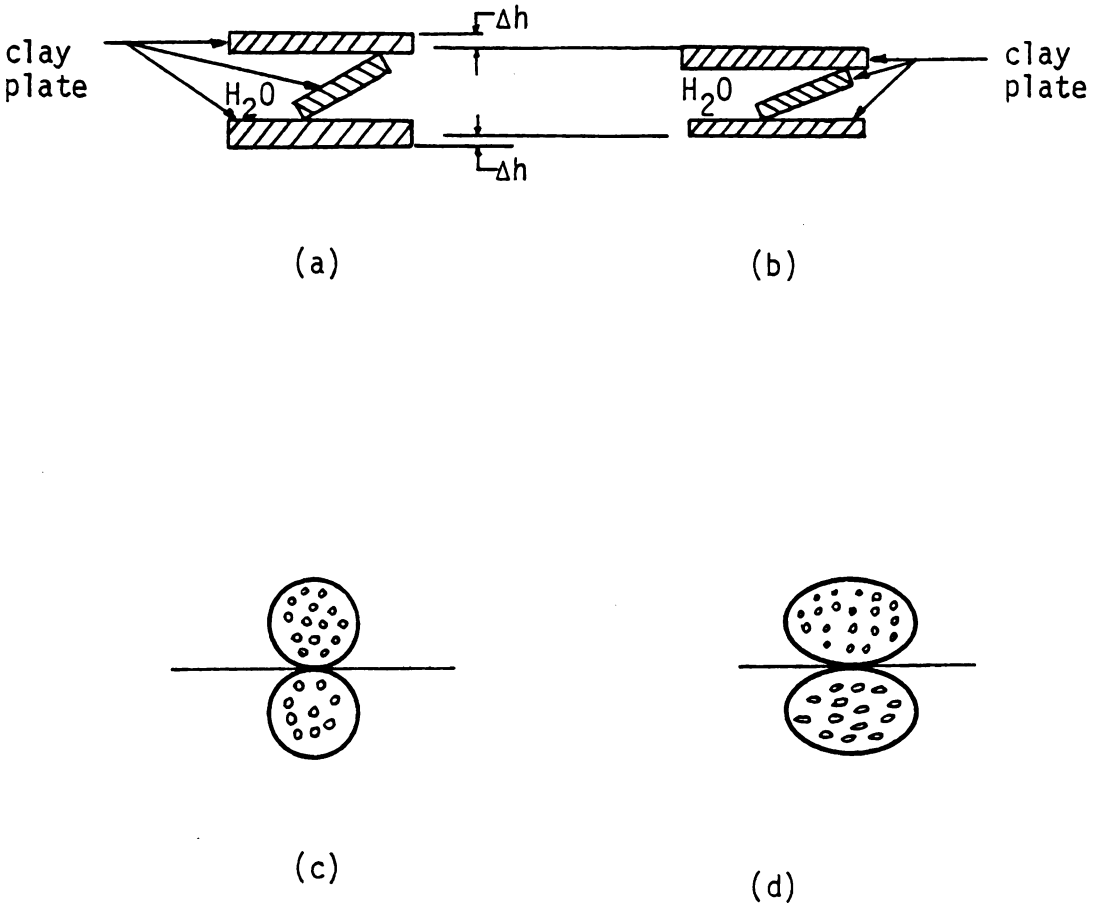

Figure 5.26 (a) Clay plates at low consolidation pressure (b) Clay plates at relatively higher consolidation pressure (c) Cross section of fibers at low strain and (d) at higher strain.

fibers resulting in a change of geometry as shown in Figure 5.26d. This change in geometry will result in an increase in contact area and therefore a change in the porosity as well. Assuming the above explanation is reasonable, the failure envelope for samples having a composition of all fibers or fiber-kaolinite mixtures subjected to a drained triaxial test, will probably in the strictest sense be curvilinear, where the curvature of the envelope would be a function of the proportion of fibers in the sample and the consolidation pressures. Pressures used in these triaxial tests were comparatively small, hence no curvature is observed and the straight line with an intercept on the vertical axis gives an acceptable approximation of the failure envelope.

5.3.2.3 Consolidated Drained Tests

For inorganic soils experimental work (Bishop and Henkel, 1962) has shown that the strength parameters ϕ' and c' are almost identical for consolidated undrained and drained triaxial tests. Test data presented in Section 4 show that this is not the case for a model organic soil. The previous section outlined the problems involved in identification of the stage in the shear process at which a soil is said to be failed for undrained tests. Questions arose when the pore pressure increase reached values equal to the confining pressure. This problem was avoided for drained tests in that drainage is permitted and excess pore pressures are permitted to dissipate. Measured total stresses are therefore equal to effective stresses.

Triaxial test results on samples made of 25 percent fiber/75 percent clay by volume subjected to consolidated drained conditions are shown in Figure 5.27 with $(\bar{\sigma}_1 + \bar{\sigma}_3)/2$ plotted on a horizontal axis

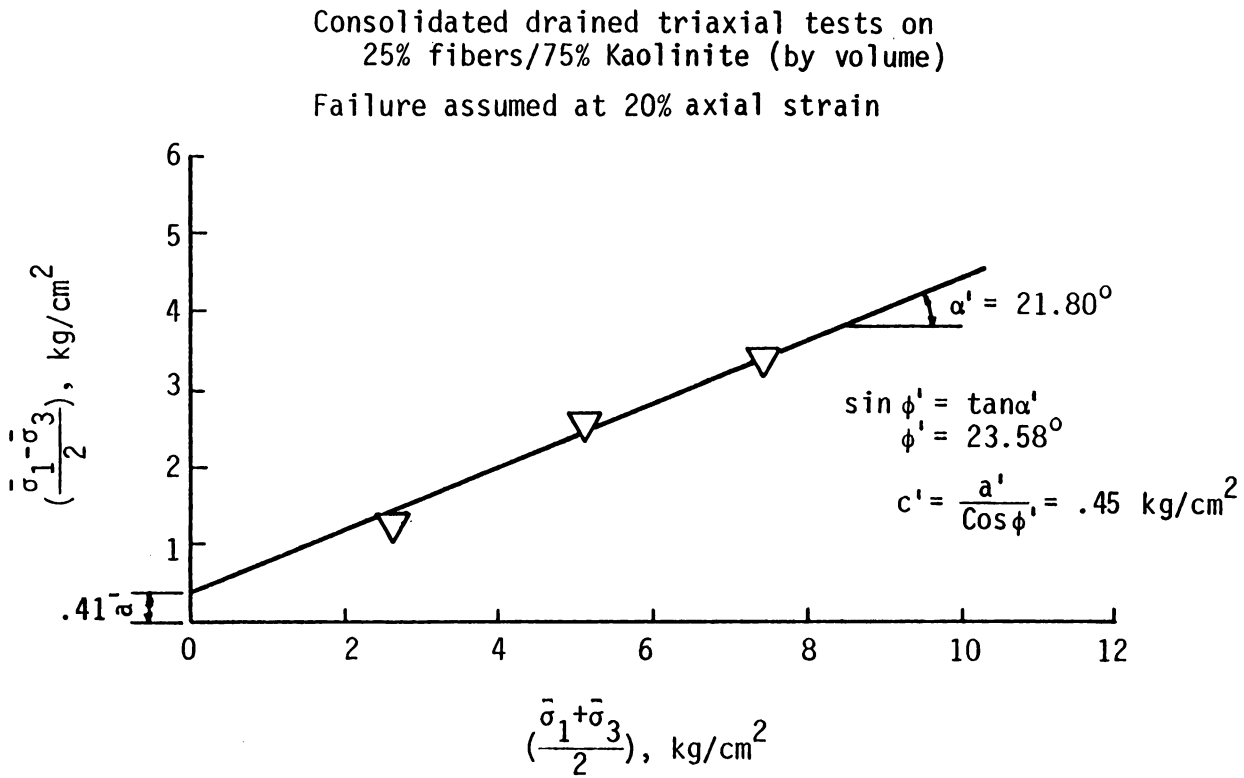

Figure 5.27 Summary of consolidated drained triaxial data for 25% fiber/75% Kaolinite (by volume) mixtures.

against $(\bar{\sigma}_1 - \bar{\sigma}_3)/2$ on a vertical axis. The data approximate a k_f-line inclined at an angle α of 21.80°, hence a ϕ' of 23.58°. The k_f-line also gives a cohesion c' of 0.45 kg/cm^2 on the vertical axis. This intercept may be the result of fibers extending across the shear plane going into tension.

Triaxial test results on samples made of 54 percent fiber/46 percent kaolinite by volume subjected to consolidated drained conditions are shown in Figure 5.28 with $(\bar{\sigma}_1 + \bar{\sigma}_3)/2$ plotted on a horizontal axis against $(\bar{\sigma}_1 - \bar{\sigma}_3)/2$ on a vertical axis. The k_f-line is inclined at an angle α of 22.50°, hence a ϕ' of 24.74°. The cohesion c' given by the k_f-line on the vertical axis equals 0.53 kg/cm^2. The shear strength parameter ϕ' of 24.47° for this case is larger than the ϕ' of 23.58° given by samples with 25 percent fiber/75 percent clay by volume, showing perhaps the additional friction contribution by the fiber in the sample.

A plot of k_f-line for fiber samples subjected to triaxial drained tests is shown in Figure 5.29 with $(\bar{\sigma}_1 + \bar{\sigma}_3)/2$ plotted on a horizontal axis against $(\bar{\sigma}_1 - \bar{\sigma}_3)/2$ on a vertical axis. The k_f-line is inclined at an angle α of 27.25° making ϕ' equal to 31°, an angle larger than those obtained for mixtures containing kaolinite. This behavior shows a frictional contribution of the fibers. The data points plotted in Figures 5.27, 5.28 and 5.29 are all based on an assumed 20 percent axial strain since in the case of drained tests essentially all samples showed a plastic type failure.

A comparison of the stress-strain curves for samples made of kaolinite, 25 percent fiber/75 percent kaolinite by volume, 54 percent fiber/46 percent kaolinite by volume, and all fiber is shown in

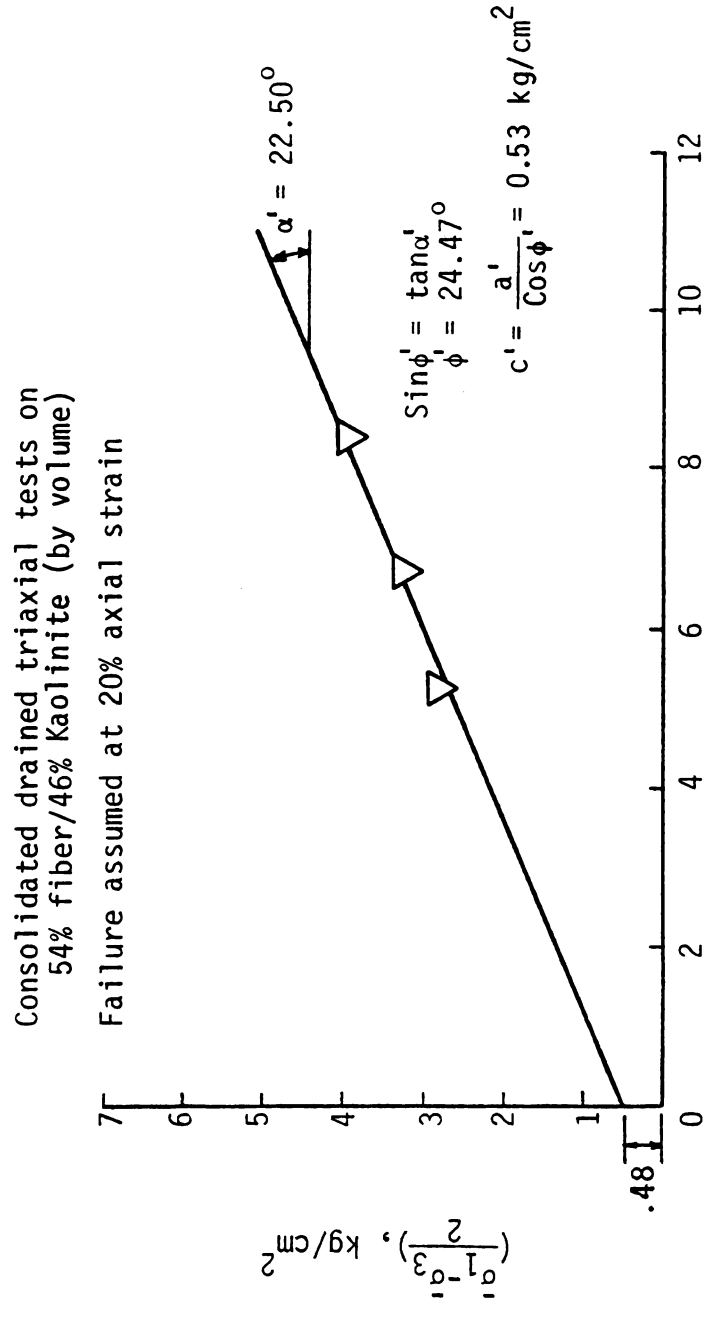

Figure 5.28 Summary of consolidated drained triaxial data for 54% fiber/46% Kaolinite (by volume) mixtures.

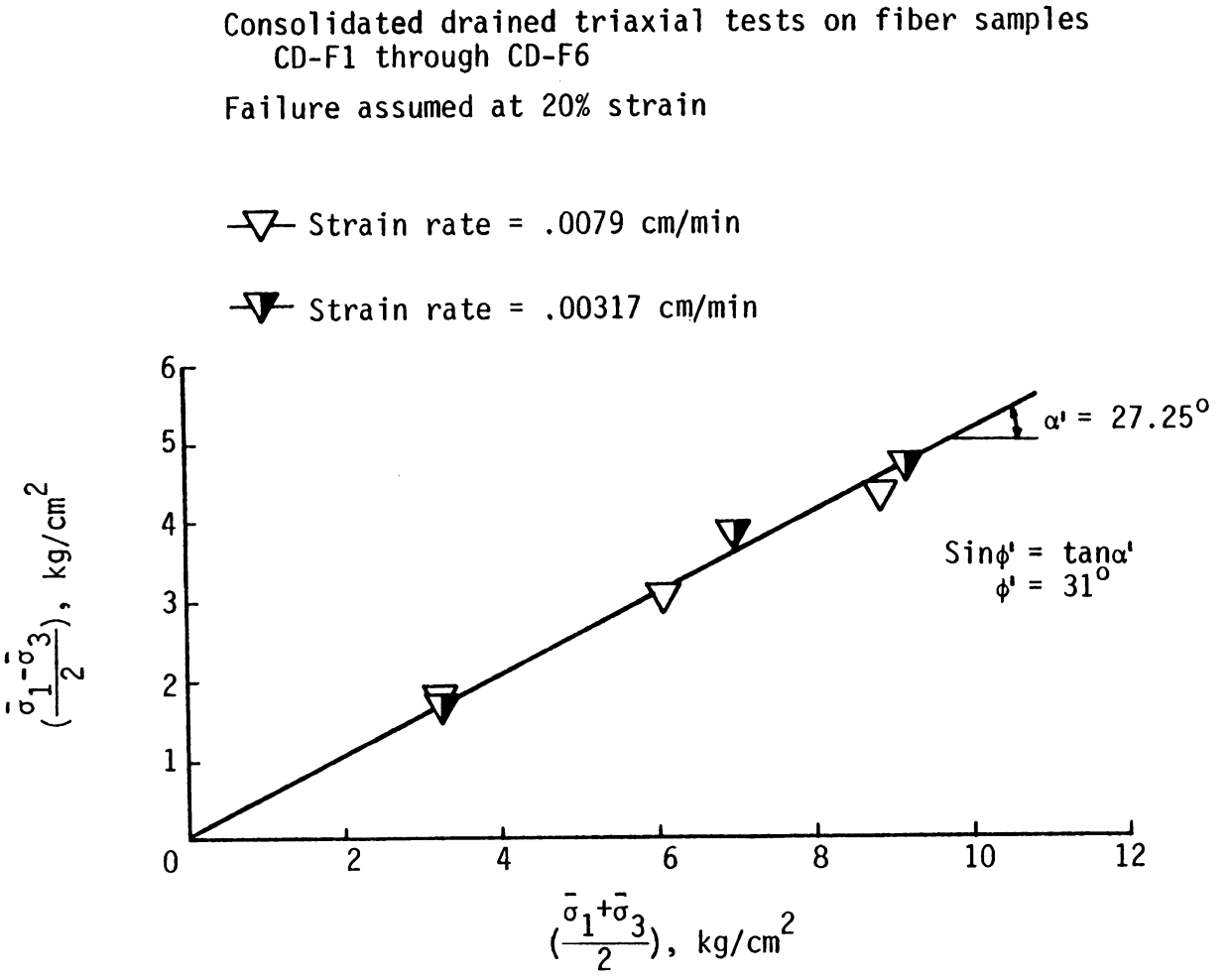

Figure 5.29 Summary of consolidated drained triaxial data for all fiber samples.

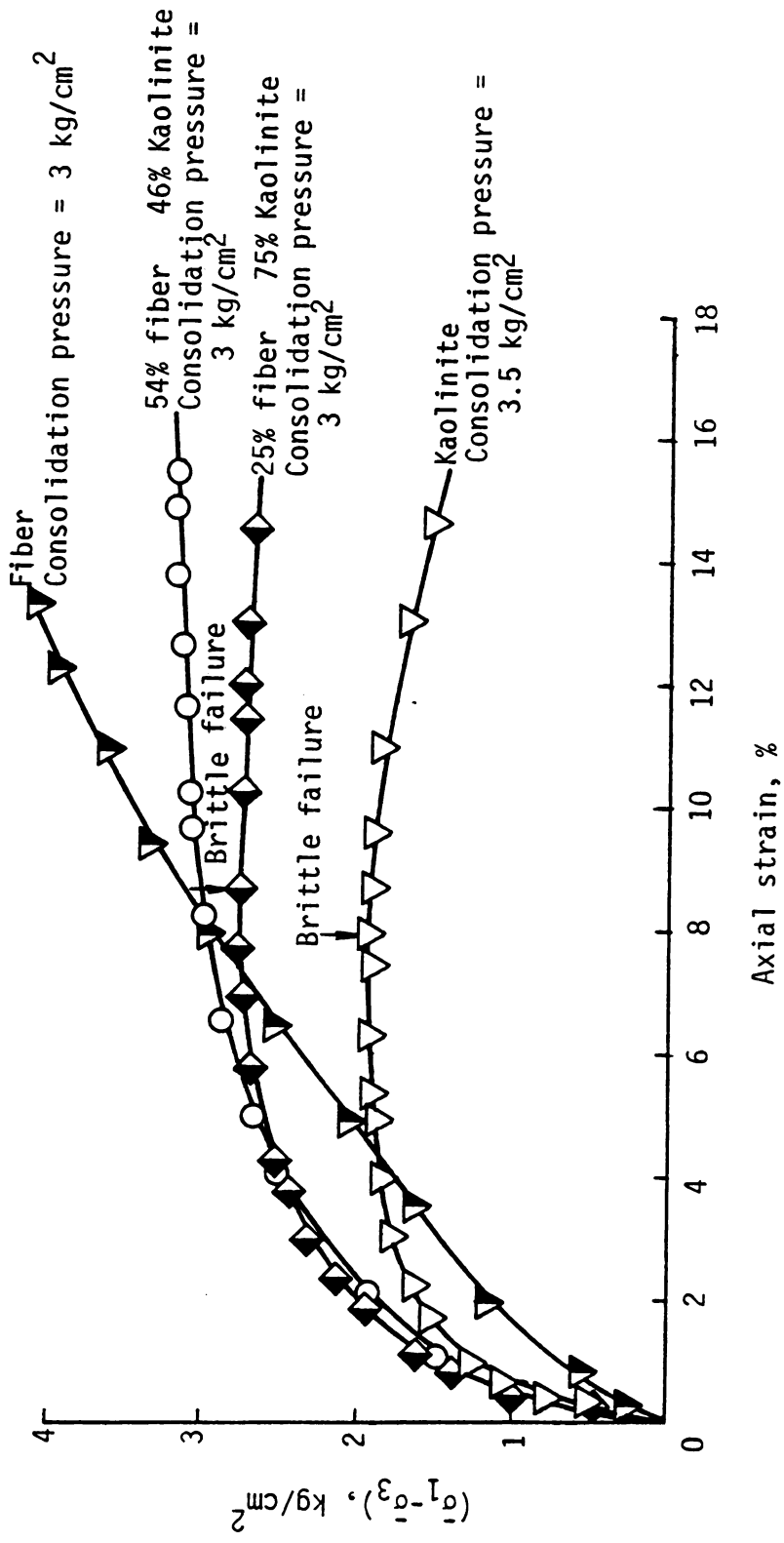

Figure 5.30 Stress-strain curves for samples with varying Kaolinite/fiber compositions showing the change in failure mechanisms for undrained conditions.

Figure 5.30. The curves demonstrate the change in the failure mechanism as the proportion of the constituents in the sample is altered. Kaolinite samples and samples with 25 percent fiber/75 percent kaolinite by volume exhibited peak strength values marked by an arrow on the figure. Samples with 54 percent fiber/46 percent kaolinite by volume showed a behavior similar to that of dispersed clay where shear strength gradually rises with increasing strain. Samples with all fibers exhibited a behavior typical of remolded clays.

5.3.3 Shear Strength Parameters ϕ' and c'

When effective normal stresses and shear stresses acting on the failure plane at failure are plotted on a horizontal and vertical axis, respectively, the resulting line is defined as the Mohr failure envelope. The inclination of this line and the intercept of the shear strength envelope are defined here as the shear strength parameters ϕ' and c', respectively.

A summary of triaxial data for consolidated undrained tests on samples with 54 percent fiber/46 percent kaolinite by volume, is shown in Figure 5.31 in terms of the maximum ratio of shear stress to effective normal stress. The plot includes results from tests CU-CF1 through CU-CF3 and the data reported by Charlie (1975) for papermill sludge samples with about the same organic content. Samples prepared from the fiber kaolinite mixture and the papermill sludge both show good agreement. Each point on the straight line inclined at an angle ϕ' of 35° is based on the peak point of the stress path as shown for samples U-1-13 and CU-CF3.

A summary of the shear strength parameters ϕ', for all the

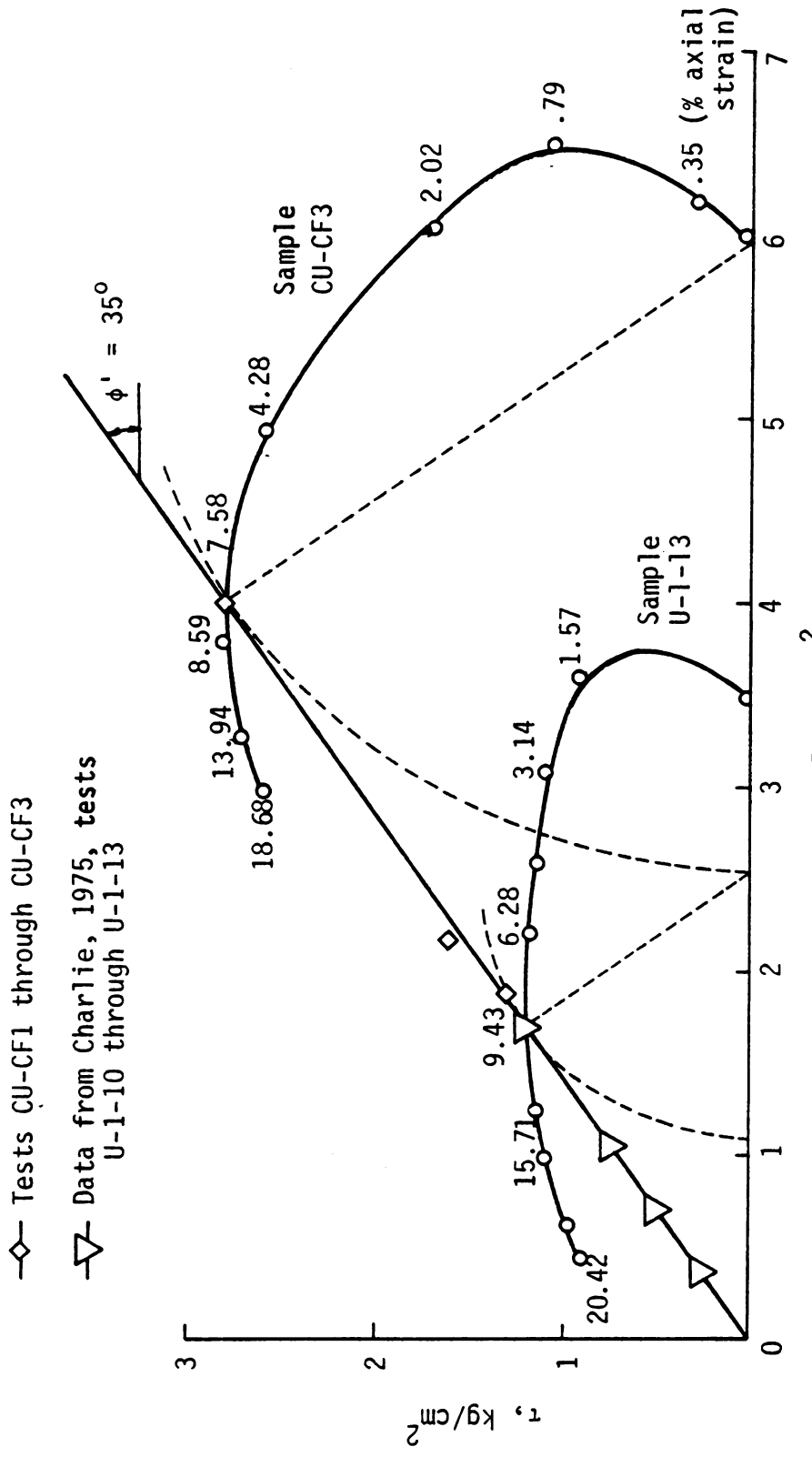

Figure 5.31 Triaxial data for consolidated undrained tests on samples with 54% fiber/46% clay by volume, failure based on the maximum shear stress to effective normal stress.

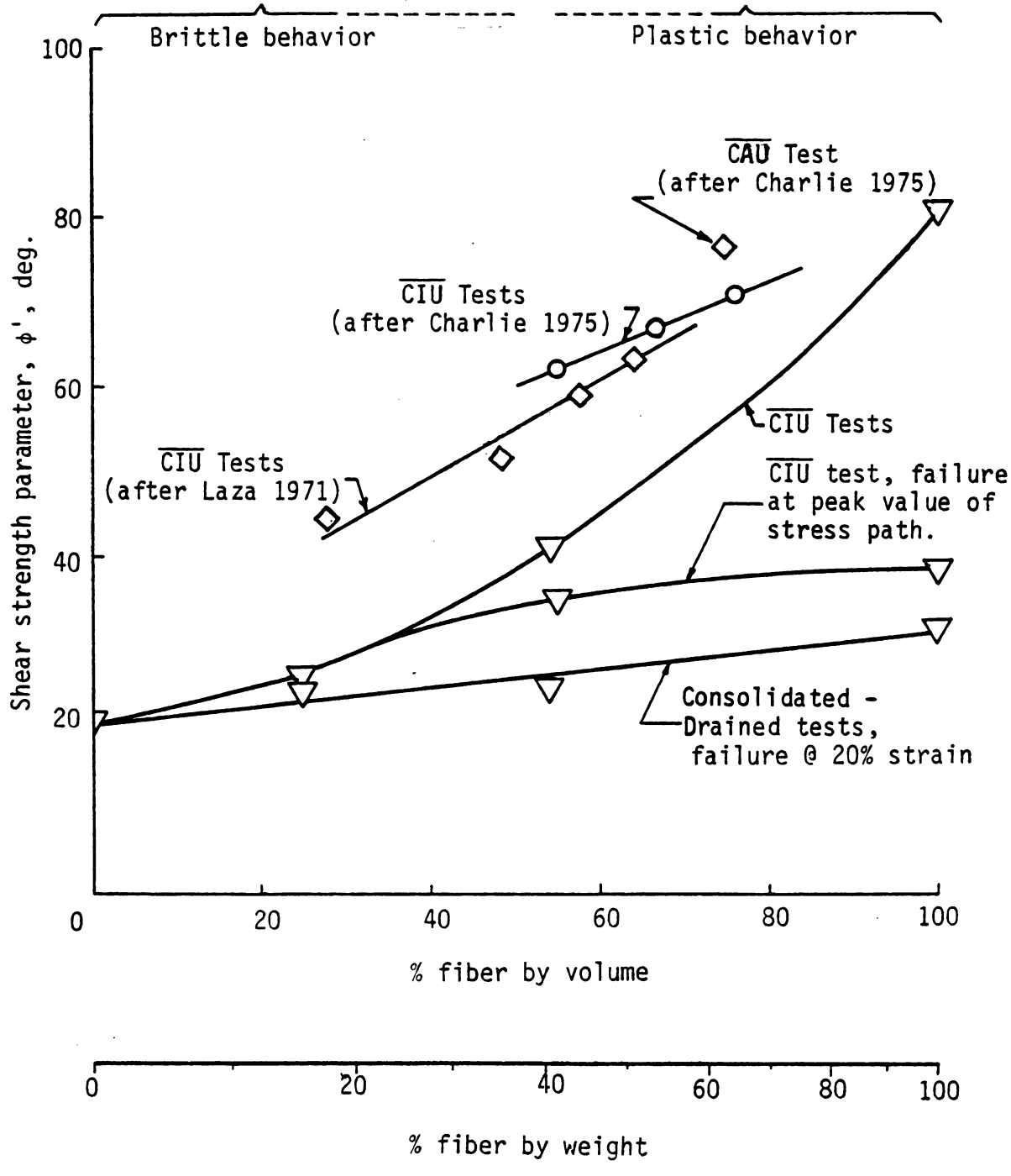

Figure 5.32 Fiber (organic) content vs. shear strength parameter ϕ', consolidated undrained and consolidated drained triaxial tests.

samples subjected to consolidated undrained and drained triaxial tests is shown in Figure 5.32. Kaolinite samples and samples made of 25 percent fibers/75 percent kaolinite exhibited typical brittle failure. All fiber samples and samples made of 54 percent fiber/46 percent kaolinite showed a departure from brittle failure. In these cases an arbitrarily assumed value of 20 percent axial strain was used as the failure criteria giving upper and lower curves shown in Figure 5.32. For the intermediate case the shear strength parameter ϕ' was determined on the basis of $(\frac{\tau}{\sigma'})_{max}$ stress paths for undrained triaxial tests. Peak values on the stress paths were defined as failure since they represent the maximum shear strength as shown in Figure 5.25. Note that this method was used only for fiber samples and samples with 54 percent fiber/ 46 percent kaolinite by volume, since they did not show brittle failure.

The values for the shear strength parameter ϕ', for organic soils depend upon the test method used. Note that the disagreement between ϕ' values, based on different test methods used, increases with increasing organic content. A summary of shear strength parameters determined from different test methods and based on different failure criteria are given in Table 5.1.

5.4 Implications for Stability Problems

This section reviews the compressibility and stability of organic soil deposits in terms of experimental results for the model kaolinite/fiber soil. The material is presented under two headings: settlement and stability.

TABLE 5.1 A SUMMARY OF SHEAR STRENGTH PARAMETERS

Sample Composition	Type of Test	Assumed Failure Criteria	Shear Strength Parameters	
			ϕ'(deg.)	c'(kg/cm^2)
Fiber (Full Length)	Direct Shear Test	20% Displacement	49.6	0
Fiber (Powdered)	Direct Shear Test	20% Displacement	47.5	0.26
Kaolinite	$\overline{CIU}$ +	Peak strength $(\bar{\sigma}_1-\bar{\sigma}_3)_{max}$	20.1	0
25%F*/75%C (by volume) 16%F/84%C (by weight)	$\overline{CIU}$	Peak strength $(\bar{\sigma}_1-\bar{\sigma}_3)_{max}$	25.1	0.29
54%F/46%C (by volume) 40%F/60%C (by weight)	$\overline{CIU}$	20% axial strain	40.5	0
		Peak value, $(\tau/\bar{\sigma})_{max}$ stress path	35	0
Fiber (Full length)	CID ≠	20% axial strain	80.4	0
		Peak value $(\tau/\bar{\sigma})_{max}$ stress path	39	0
25%F/75%C (by volume) 16%F/84%C (by weight)	CID	20% axial strain	23.6	0.45
54%F/46%C (by volume) 40%F/60%C (by weight)	CID	20% axial strain	24.5	0.53
Fiber (Full Length)	CID	20% axial strain	31	0

+$\overline{CIU}$ = Consolidated isotropically undrained triaxial test, effective stress basis
*F = full length fiber C = clay
≠CID = Consolidated isotropically drained triaxial test

5.4.1 Settlement

The compressibility tests show that samples prepared with fibers are the most compressible. This is due to the porous structure and the swelling nature of the material. As the clay content was increased in the fiber samples, the compression index, i.e. slope of the e-log p curve, decreased at lower levels of applied stress as shown in Figure 5.8. At stress levels much higher than those encountered in most civil engineering problems the rate of change of the compression index becomes negligible. In view of the previous discussion where the behavior of a kaolinite/fiber mixture was compared to the behavior of a flocculated and a dispersed clay it is apparent that settlement theory used for clays can also be used to predict settlements in a clay-fiber matrix. Since the compression index, C_c, changes with organic content and stress level it is essential that C_c be determined for the range of effective stresses expected in the design problems.

The value of $(C_s/C)_{fiber}$ determined for fibers was compared with $(C_s/C)_{clay}$ for clay in Section 5.2.1. These experimental results show that Terzaghi's concept of effective stress, as used with the coefficient of volume compressibility, can be applied with a high degree of approximation to the kaolinite/fiber mixtures. The change in void ratio with effective stress over a wide range is not a simple function in the case of clays but over the small range of void ratios, say from 6 to 2 for a montmorillonite or from 3 to 1 for an illite, the relationship is approximately exponential. The void ratios shown in Figure 5.8 are comparable with the range in

void ratios mentioned for montmorillonite and illite and therefore for the expected stress range we may write

$$e = e_o - C_c \log \frac{\bar{\sigma}}{\bar{\sigma}_o} \tag{5.3}$$

where e_o is the reference void ratio corresponding to $\bar{\sigma}_o$.

5.4.2 Stability

The stability of organic soils including peat, muskeg, etc., involves bearing strength for road embankments, dikes, pipelines, and building foundations. Slope stability becomes important for excavations in landfills or ship channels through soft organic sediments. These engineering problems require an understanding of the shear strength of the organic soils if they are to be rationally analyzed. Section 2.5 has reviewed the shear strength of organic soils and questions relative to the stage of a shear process which represents failure. Experimental data on the fiber/kaolinite mixtures has been discussed in Section 5.3. The range of ϕ' values obtained for the consolidated undrained and drained triaxial tests are given in Figure 5.32. The question remains as to which test procedure and which definition of failure gives the ϕ' which is most suitable for application to field problems.

Published information regarding the stability analysis for bearing strength or slope stability in organic soils is very limited. Data for an excavated slope in consolidated fibrous papermill sludge (Andersland and Charlie, 1975) is available with sludge properties similar to the kaolinite/fiber mixtures used in this study. The excavated 1 to 8 slope, shown in Figure 5.33, consisted of two

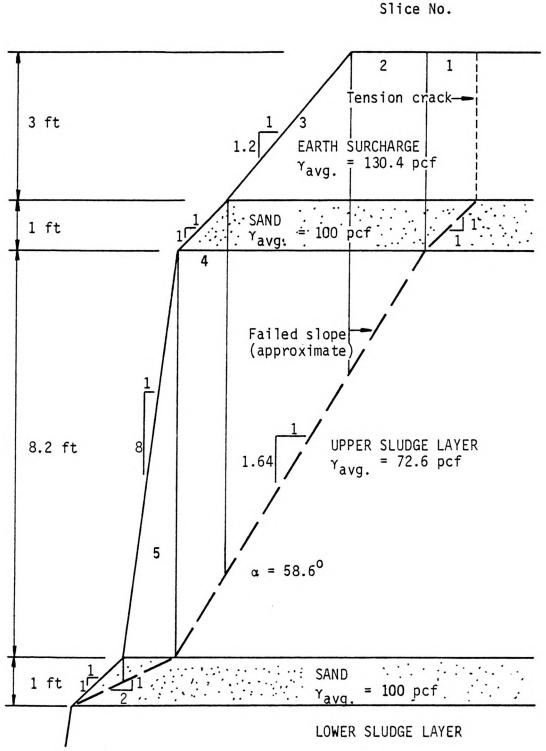

Figure 5.33 Cross section of the 1:8 slope, before and after failure, with slice locations shown for the stability analysis (after Charlie, 1975).

consolidated sludge layers with sand drainage blankets at the bottom, middle, and top. A three foot earth surcharge, used as a consolidation load, served to help produce the planned slope failure. Instrumentation (Charlie, 1975) behind the excavated slope included pneumatic type piezometers, slope indicator casings,and settlement plates. Data from the piezometers are shown in Figure 5.34 including the distance behind the toe of the slope failure. Data at the slope failure surface was not available.

Use of ϕ' in a stability analysis requires effective stresses and that pore pressures be extrapolated to the failure surface. Water retention characteristics for the fibrous papermill sludge (Laza, 1971) indicates that pore pressures at the excavation surface would be in tension, i.e. water would be absorbed. This fact was used in estimating the pore pressure variations shown in Figure 5.34. Organic contents of the embankment sludge varied with production changes at the papermill. Using ash content data reported by Charlie (1975), average value of 43 percent for the upper layer, gives an organic content close to 57 percent by weight. For this organic content Figure 5.32 gives three possible ϕ' values for the kaolinite/fiber mixtures. The higher value of 52 degrees appears to more closely represent field conditions in recomputation of the factor of safety of the excavated experimental slope (Charlie, 1975).

The composite failure surface shown in Figure 5.33 has been analyzed using Janbu's (1954, 1957) method (Table 5.2) with the same slices selected by Charlie (1975). Values for $\tan\alpha$, Δx, and p remain the same with a new value for ϕ' equal to 52 degrees used

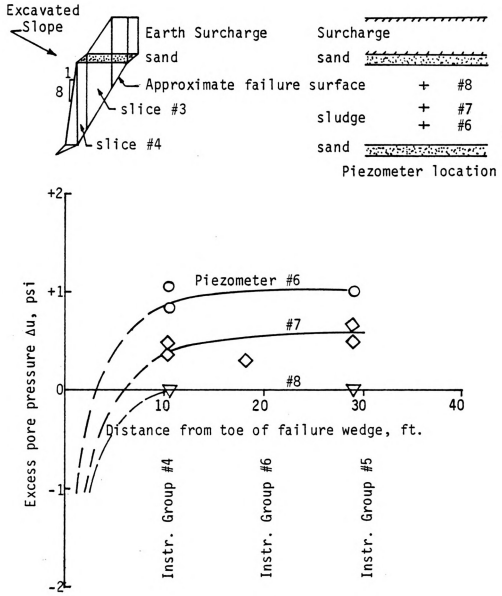

Figure 5.34 Estimated pore pressures near the exposed sludge surface based on field (Charlie, 1975) and laboratory (Laza, 1971) data.

for the fiberous papermill sludge. Extrapolated pore pressures (Figure 5.34) appear to be negative in slices 2, 3, and 4. The computed factor of safety is close to unity suggesting that ϕ' from the consolidated undrained triaxial test is best suited for fibrous organic soils. Lower values of ϕ' will give a much lower factor of safety thus eliminating the drained test and the $\overline{CIU}$ test with failure based on the peak value of the stress path from consideration. Values of ϕ' from Laza (1971) and Charlie (1975), shown in Figure 5.32, require excess pore pressures greater than measured values in order to give a factor of safety equal to unity. In either case, the consolidated-undrained triaxial test gives ϕ' values in best agreement with field behavior of the excavated slope.

Some doubt still exists regarding the selection of ϕ' when the failure slope of 58.6 degrees is taken into consideration. If the active Rankine state (Terzaghi, 1943) exists in the slope at the time of failure, the slope angle α (Figure 5.33) should equal $(45 + 1/2\phi')$. Measured lateral movements (Charlie, 1975) close to two inches greater at the top of the upper sludge layer as compared to the bottom would satisfy the usual requirements for the active Rankine state. Computation of ϕ' in this manner gives a ϕ' value close to 27 degrees, the same value observed for the drained test at an organic content of 52 percent by weight. It is apparent that more field data are required before this anomaly can be fully explained.

TABLE 5.2 TABULATED VALUES FOR THE SLOPE STABILITY ANALYSIS USING JANBU'S METHOD (1954,1957)

Slice No.	Tanα	Δx (ft.)	p (psf)	[1](Δu) (psi)	[2](ϕ') (deg)	$\bar{p}$ (psf)	B_o	A'_o	n_α	A_o
1	1.00	1.00	441.20	0	39	441.20	441.20	357.277	0.978	365.314
2	1.64	1.50	580.50	-0.35	52	630.90	1428.03	1211.27	0.943	1284.488
3	1.64	2.50	623.0	-0.35	52	623.0	2554.30	2154.782	0.943	2285.029
4	1.64	1.00	585.80	-.25	52	571.40	960.71	795.868	0.943	843.975
5	0.50	1.00	322.70	0	39	322.70	161.35	261.317	1.182	221.080
6	0.50	1.00	25.0	0	39	25.0	12.50	20.245	1.182	17.128
							Σ=5558.09	Σ=4800.759		Σ=5017.014

Notes: [1]Pore pressures from Figure 5.36

[2]Angle of internal friction from Figure 5.33 for an average organic content ≈ 57% by weight.

[3]Tanα, Δx, and p for all slices and ϕ' for slices 1, 5 and 6 remain the same as given by Charlie (1975)

$B_o = p\tan\alpha \cdot \Delta x$, $A'_o = p\tan\phi' \cdot \Delta x$, $A_o = A'_o/n_\alpha$, $n_\alpha = \cos^2\alpha \left(1 + \frac{\tan\alpha \tan\phi'}{F}\right)$

Table complete only for $F_o = \frac{\Sigma A_o}{\Sigma B_o} = \frac{5017.014}{5558.09} = 0.903$

Additional calculations give $F_2 = \frac{\Sigma A_1}{\Sigma B_1} = .964 \approx 1$ for a line of thrust for side forces on each slice through the lower 1/3 points.

CHAPTER VI

SUMMARY AND CONCLUSIONS

This summary and conclusions present a brief review followed by conclusions pertinent to the observed behavior for each part of the study. The material is presented under three headings: physical properties, compressibility of the kaolinite/fiber samples, and shear strength of the kaolinite/fiber mixtures.

6.1 Physical Properties

Physical properties observed for the fibers included average weighted fiber length, physical appearance of the cellulose fibers, specific surface area, and specific gravity.

1) The weighted average fiber length, defined as the sum of the products of their weight and length divided by their total weight, served as a convenient means for describing the organic material. When particles less than 0.1 mm in length were excluded, this definition gave a weighted average fiber length equal to 1.5734 mm for the material used in this study.

2) Pictures taken of the dry cellulose fibers, using a scanning electron microscope, revealed a shape resembling grass blades with noncircular cross-sections. This cross-section may become circular when allowed to adsorb water.

3) The average fiber width, measured on the enlarged photographs was approximately 20μ. This value agrees with reported values

for cotton fiber, which are 90 percent pure cellulose and have an average diameter of about 18μ. The surface of the pulp fibers was uneven with perforations. The size of the largest observed hole was about 4μ by 12μ. The cross-section of a single fiber shows an aperture perhaps extending full length of the fiber.

4) The shape of the adsorption isotherm for cellulose fibers was similar to that expected for cotton fibers. The specific surface area, based on nitrogen and water vapor adsorption, was 1.508 m^2/gm solids and 133m^2/gm solids, respectively. The determination of the specific surface area was a function of the method employed. The lower value of surface area, using nitrogen adsorption, is a measure of the external surface area only. The higher value, 133m^2/gm solids, is a measure of external as well as internal surface areas due to the ability of water molecules to penetrate the fiber structure.

6.2 Compressibility of Kaolinite/Fiber Mixtures

The compressibility of kaolinite, kaolinite/fiber mixtures, and all fiber samples was determined using a special compression test cylinder. Compression loads ranged from about 2 to over 350 kg/cm^2. The experimental results have been summarized in terms of void ratio versus effective normal stress.

1) The void ratio-logarithm of pressure relationship for all fiber and kaolinite/fiber samples show nonlinear relationships which are dependent on both organic content and stress level. This is in sharp contrast to the linear relationship typical for the pure kaolinite.

2) The compression index, the slope of the void ratio-logarithm of pressure curves, is dependent on fiber content and stress level with

all fiber samples giving the larger values at all stress levels. The data suggest that settlement behavior for field deposits will vary significantly for different organic contents.

3) The void ratio-logarithm of pressure curves for all combinations of kaolinite and fiber have a common point of intersection at close to 124 kg/cm^2. For higher stress levels the equilibrium void ratio is smallest for all fiber samples. The intermediate fiber/clay combinations increase in void ratio up to the pure kaolinite for a given high stress level.

4) The ratio of solid compressibility to sample compressibility (C_s/C) for cellulose fibers was close to 0.000035. This small value will not significantly influence calculations using the equation

$$-\left(\frac{\Delta V}{V}\right) = C[\Delta p - (1 - \frac{C_s}{C})\ \Delta u],$$

hence the Terzaghi equation

$$-\frac{\Delta V}{V} = C[\Delta p - \Delta u]$$

can be used with a high degree of approximation for kaolinite/fiber soil mixtures. This conclusion may also apply to most organic soils.

6.3 Shear Strength of Kaolinite/Fiber Mixtures

Shear strength of the model kaolinite/fiber soil was studied using both consolidated-undrained ($\overline{CIU}$) and consolidated-drained (CID) triaxial tests. Direct shear tests were conducted only on all fiber samples. Criteria considered in evaluating the stage at which failure occurs in the triaxial test included the peak stress difference for a brittle behavior, 20 percent axial strain, and the peak value of the

stress path defined by the maximum ratio of shear stress to effective normal stress.

1) Shear strength of the kaolinite/fiber mixtures increased with normal stress suggesting a frictional type behavior in accordance with the principal of effective stress. The angle of internal friction (ϕ') is dependent on both the organic (fiber) content of the model soil and the test procedure. Small observed values of cohesion (c') may be due to fibers extending across the shear plane going into tension.

2) Consolidated-drained tests with failure based on 20 percent axial strain gave shear strength parameters (ϕ') which increased from 20 degrees for kaolinite to 31 degrees for all fiber samples. Consolidated-undrained tests with failure based on the peak stress difference and/or 20 percent axial strain gave ϕ' values ranging from 20 degrees for kaolinite to over 80 degrees for all fiber samples.

3) A new failure criterion for the $\overline{CIU}$ tests based on the peak value of the stress path defined by the maximum ratio of shear stress to effective normal stress gave intermediate values of ϕ' ranging from 20 degrees for the kaolinite to 39 degrees for all fiber samples. This criteria recognized the effect which the minor principal stress going to zero has on ϕ' and avoid values approaching 90 degrees.

4) Direct shear tests on all fiber samples gave shear strength parameters (ϕ') ranging from 47.5 degrees for powdered fibers to 49.6 degrees for full length (average 1.57 mm) fibers. Dry samples gave a more resilient stress-strain response as compared to saturated fibers.

5) Recomputation of the factor of safety for an experimental

slope failure (Charlie, 1975) in an excavated fibrous papermill sludge with properties similar to the kaolinite/fiber mixtures strongly supports use of ϕ' values based on the $\overline{CIU}$ test with failure defined at the peak stress difference and/or 20 percent axial strain. The angle of slope failure and use of the active Rankine theory agrees with ϕ' from the consolidated-drained test. Additional field research is needed to clarify this anomally relative to the ϕ' values.

BIBLIOGRAPHY

BIBLIOGRAPHY

Bacon, V. W. "Sludge Disposal," Industrial Water Eng. 4, 27, 1967.

Bishop, A. W. and Henkel, D. J. The Measurement of Soil Properties in the Triaxial Test. Edward Arnold, Ltd., London, 1962.

Brunauer, S. The Adsorption of Gases and Vapors, Vol. I, Physical Adsorption. Princeton University Press, 1943.

Brunauer, S., Emmett, P. H. and Teller, E. "Adsorption of Gases in Multimolecular Layers," J. Am. Chem. Soc. 69, 309. 1938.

Bridgman, P. W. "The Compressibility of Thirteen Natural Crystals," Amer. J. Sci., 15:287-296. 1928.

Blake, G. R. Methods of Soil Analysis: Part I. American Society of Agronomy, Inc. Publisher, Madison, Wis. 1965.

Charlie, W. A. "Two Cut Slopes in Fibrous Organic Soils Behavior and Analysis" Ph.D. Dissertation, Michigan State University, East Lansing, Michigan. 1975.

Cude, H. E. and Hullet, G. A. "Some Properties of Charcoals," J. Amer. Chem. Soc., 42:391. 1920.

Denlin, R. M. Plant Physiology. Reinhold Publishing Corp., New York. 1969.

deBoer, J. H. The Dynamical Character of Adsorption. At the Clarendon Press, Oxford. 1953.

Eirich, F. R. Rheology, Theory and Application, Vol. II. Academic Press Inc., Publishers, New York. 1958.

Gehm, H. W. "Current Developments in the Dewatering of Papermill Sludges," National Council of Stream Improvements, Tech. Bull. No. 113. March, 1959.

Gillespie, W. J. "Summary Report - Questionnaire Survey - Sludge Cake Disposal on Land." National Council of the Paper Industry for Air and Stream Improvement, Inc., unpublished. September 1969.

Gillespie, W. J., Mazzola, C. A. and Gellman, I. "Landfill Disposal of Papermill Waste Solids," Presented at the 7th Technical Association of the Pulp and Paper Industry Air and Water Conference, Minneapolis, Minn. June 7-10, 1970.

Gray, Donald H. "Reinforcement and Stabilization of Soil by Vegetation," Journal of the Geotechnical Engineering Division, ASCE, Vol. 100, No. GT6, pp. 695-699, June 1974.

Grim, R. E. Clay Minerology. McGraw-Hill Book Company, New York. 1968.

Hanrahan, E. T. "An Investigation of Some Physical Properties of Peat," Geotechnique IV: 108-123. 1954.

Hertjex, P. M. "Dichtheidsmetingen aan vezels en enkele toepassingen hiervan." (Density Determination of Fibers and Some of Their Uses) Diss., Delft, 1938; Rec. trav. Chim. 60, 689. 1941.

Hermans, P. H. Physics and Chemistry of Cellulose Fibers with Particular Reference to Rayon. Elsevier Publishing Company, Inc., New York. 1949.

Imshenetsky, A. A. The Ecology of Soil Bacteria. University of Toronto Press, Canada. 1968.

Janbu, N. Discussion on "Application of Composite Slip Surfaces for Stability Analyses." European Conference on Stability of Slopes, Stockholm, III:43-49. 1954.

Janbu, N. "Earth Pressure and Bearing Capacity Calculations by Generalized Procedure of Slices," Proc. 4th Internat. Conf. on Soil Mech. and Found. Engr., II:207-212. 1957.

Karman, Th. Von. "Festigkeitsversuche unter allseitigem Druck. Ziet. Vereines Deutsch Ing., 55, 1749-1757. 1911.

Laza, R. W. "Permeability and Shear Strength of Dewatered, High Ash Content Pulp and Papermill Sludges," Ph.D. dissertation, Michigan State University, East Lansing, Michigan. 1971.

Langmuir, I. "The Adsorption of Gases on Plane Surfaces of Glass, Mica and Platinum," J. Am. Chem. Soc., 40, 1361. 1918.

Langmuir, I. "Vapour Pressures, Evaporation, Condensation and Adsorption," J. Am. Chem. Soc., 54, 2798. 1932 Nobel Lecture, 1932.

Leonards, G. A. Chapter 2 "Engineering Properties of Soils," in Foundation Engineering. McGraw-Hill Book Co., New York, 1962.

Perkin-Elmer Corporation, Instrument Division, Norwalk, Connecticut, Instruction Manual of Perkin-Elmer Shell Model 212B Sorptometer, December 1961.

Radforth, N. W., "Classification of Muskeg." Chapter 2 in Muskeg Engineering Handbook edited by Ivan C. MacFarlane, University of Toronto Press, 1969.

Scott, R. F. Principles of Soil Mechanics. Addison-Wesley Publishing Company, Inc., Massachusetts. 1963.

Skaar, C. Water in Wood. Syracuse University Press, 1972.

Skempton, A. W. "Effective Stress in Soils, Concrete and Rocks," in Pore Pressure and Suction in Soils. Butterworth & Co., Publishers, Ltd., London. 1961.

Tappi Testing Procedures, Fiber Length of Pulp by Classification, T233 SU-64. 1974.

Taylor, D. W. Fundamentals of Soil Mechanics. Asia Publishing House Bombay, India. 1948.

Taylor, D. W. "A Comparison of Results of Direct Shear and Cylindrical Compression Tests," Proc. ASTM. 1939.

Terzaghi, Karl. Theoretical Soil Mechanics. John Wiley and Sons, Inc., New York, 1943.

Terzaghi, K. and Peck, R. B. Soil Mechanics in Engineering Practice. John Wiley and Sons, Inc., New York. 1967.

Waksman, Selman A. "Cellulose and Sludge Decomposition in Soil." National Council for Air and Stream Improvement, Inc., Tech. Bulle. No. 120. 1960.

West, E. S. and Todd, W. R. Textbook of Biochemistry. The Macmillan Company, New York. 1955.

White, A., Handler, P. and Smith, E. L. Principles of Biochemistry, McGraw-Hill, Inc., New York. 1964.

Whitman, R. V. "Some Consideration and Data Regarding the Shear Strengths of Clays," ASCE Research Conference on Shear Strength of Cohesive Soils, Boulder, Colorado, 1960.

Winterkorn, H. F. and Fang, H. Y. "Soil Technology and Engineering Properties of Soil." Chapter 2 in Foundation Engineering Handbook edited by Hans F. Winterkorn and Hsai-Yang Fang, Van Nostrand Reinhold Co., New York, 1975.

Zisman, W. A. "Compressibility and Anisotropy of Rocks at and Near the Earth's Surface," Proc. Nat. Acad. Sci., 19:666-679. 1933.

APPENDICES

TABLE A.1 LIQUID LIMIT DETERMINATION, KAOLINITE

Can no.	L1	L2	L3	L4
Wt. of wet soil + can	33.22	35.66	34.44	33.87
Wt. of dry soil + can	28.84	30.75	29.33	28.51
Wt. of can	19.16	20.29	19.46	19.27
Wt. of dry soil	9.68	10.46	9.87	9.24
Wt. of moisture	4.38	4.91	5.11	5.36
Water content, w%	45.24	46.94	51.77	58.01
No. of blows, N	48	29	15	7

TABLE A.2 PLASTIC LIMIT DETERMINATION, KAOLINITE

Can no.	P1	P2	P3
Wt. of wet soil + can	24.63	24.24	24.98
Wt. of dry soil + can	23.53	23.26	23.72
Wt. of can	19.59	19.73	19.03
Wt. of dry soil	3.94	3.53	4.69
Wt. of moisture	1.10	0.98	1.26
Water content, w% = w_p	27.92	27.76	26.87

TABLE A.3 HYDROMETER ANALYSIS FOR KAOLINITE

Hydrometer no.: 152 H G_s of solids = 2.65 a = 1.0

Dispersing agent: Sodium Hexametaphosphate ($NaPO_3$) Wt. of soil, W_s: 50 grams

Zero correction: 7.00 Meniscus correction: 1

Elapsed time, min.	Temp., °C	Actual Hyd Reading R_a	Corr. Hyd. Reading R_c	% Finer	Hyd. Corr. only for Meniscus R	L from Table 6-5*	$\frac{L}{t}$	K from Table 6-4*	D. mm
1	19.50	57	49.85	99.70	58	6.80	6.800	.01375	.0359
2	19.50	56.00	48.85	97.70	57	7.00	3.500	.01375	.0257
3	19.50	56	48.85	97.70	57	7.00	2.333	.01375	.0210
4	19.50	55.50	48.35	96.70	56.50	7.05	1.763	.01375	.0182
8	19.50	54.00	46.85	93.70	55	7.30	.913	.01375	.0131
16	20.00	53.00	46	92	54	7.40	.463	.01370	.0093
30	20.00	51.00	44	88	52	7.80	.260	.01370	.0069
43	20.00	49.50	42.50	85	50.50	8.00	.186	.01370	.0059
123	20.00	44.00	37	74	45	8.90	.072	.01370	.0037
243	20.00	40.50	33.50	67	41.50	9.50	.039	.01370	.0027
491	19.00	37.50	30.70	61.40	38.50	10.00	.020	.01380	.0019
806	18.50	34.50	27.10	54.20	35.50	10.45	.013	.01390	.0016
1446	18.00	32.00	24.50	49	33	10.90	.007	.01400	.0012
2826	18.00	28.00	20.5	41	29	11.50	.004	.01400	.0009
4326	20.00	25.50	18.50	37	26.50	11.95	.003	.01370	.0008
5691	21.00	23.50	16.70	33.40	24.50	12.30	.002	.01350	.0006

correction + C_r

*See "Engineering Properties of Soils and Their Measurements," by Joseph E. Bowles.

% finer = $R_c(a)/W_s$

$D = K\sqrt{L/t}$

TABLE A.4 SPECIFIC GRAVITY OF PULP FIBER USING WATER AS THE DISPLACEMENT MEDIUM

No.	1^{+}	2^{+}	3^{+}
dw	0.9953	0.9953	0.9953
Ws	23.91725	23.80467	20.92912
Wa	23.56530	23.47375	20.64487
Wsw	48.48987	48.40584	45.54709
Ww	48.37042	48.31686	45.43205
Dp*	1.507	1.361	1.672
No.	$1^{\neq}$	$2^{\neq}$	$3^{\neq}$
dw	0.9965	0.9965	0.9965
Ws	25.01132	25.30079	21.85130
Wa	24.43553	24.26795	20.77728
Wsw	49.48072	49.52106	46.02078
Ww	49.30200	49.07488	45.61839
Dp*	1.4450	1.7543	1.5935

For Temp of 27°C, Average density,

$$D_{p_{avg.}} = \frac{D_p}{\text{Total No.}} = 1.5976$$

+Test temperature = 31°C $\neq$Test temperature = 27°C

*Fiber density, $D_p = \frac{dw(Ws-Wa)}{(W_s-Wa) - (Wsw-Ww)}$

dw = water density,
Ws = wt. (Pycnometer + solids)
Wa = wt. pycnometer in air
Wsw = wt. (Pycnometer + water + solids)
W_w = wt. (pycnometer + water)

TABLE A.5 DATA FOR DETERMINATION OF SPECIFIC SURFACE AREA, PULP FIBER

Symbol	Measurement or Calculation	Dimension		Result
w_2	Weight of Sample: 610.54 mg.	Tube + sample:	20.53485 grams	
w_1		Tube:	19.92431 grams	
w		Sample:	.61054 grams	
P_T	Barometric pressure at T°K temperature	mmHg	72.85	728.50
T_R	Room temperature	°K	273.16 + 20 =	293.16
f	Correction factor for STP conditions: $f=\frac{P_T \cdot 273.16}{760 \cdot T_R} = 0.3595\frac{P_T}{T_R}$		$0.3595\frac{728.50}{293.16}$	.8933
	Inlet pressure of carrier gas (Helium)	in.		
t_c	Soap film transit time for	sec.		52.20
v_{meter}	Volume of bubble flow meter between two calibration marks	ml.		20.01
Fc	Flow rate of the carrier gas (Helium) $Fc = \frac{60}{t_c} v_{meter}$	ml/min	$\frac{60}{52.20}$ x 20.01	23
Po	Saturation pressure of N_2 at the temperature of the liquid N_2 used	mmHg	average ☐ measured ☒	830
s_o	Area covered by one cc(STP) monolayer nitrogen	m^2/ml		4.3844

TABLE A.5 (Continued)

t_{t1}	= 46.70 sec.	t_{c_1}	= 52.0 sec.
t_{t2}	= 46.60 sec.	t_{c_2}	= 52.2 sec.
t_{t3}	= 46.60 sec.	t_{c_3}	= 52.4 sec.
$t_{t_{avg.}}$	= 46.63 sec.	$t_{c_{avg.}}$	= 52.20 sec.

Symbol	Measurement or Calculation	Dimension	First Run	Second Run	Third Run
	Inlet pressure of the adsorption gas (N_2)	in.	13	25	
t_t	Soap film transit time for total gas flow	sec.	46.63	41.40	
F_t	Total (He + N_2) flow rate: $F_t = \frac{60}{t_t} v_{meter}$	ml/min	25.747		
F_a	Adsorption gas (N_2) flow rate $F_a = F_t - F_c$	ml/min	2.747		
A_{des}	Area of the desorption peak	counts	420		
v_{cal}	Volume of the injection tube used	ml	.5247		
A_{cal}	Area of the calibration peak	counts	854		
$V_{ads}(R)$	Volume of adsorbed gas $v_{ads(R)} = \frac{A_{des}}{A_{cal}} v_{cal}$	ml	.2580		
v_{ads}	Volume of adsorbed gas corrected to standard temperature pressure: $v_{ads} = v_{ads(R)}{}^f$	ml	.23		

TABLE A.5 (Continued)

Symbol	Measurement or Calculation	Dimension	First Run	Second Run	Third Run
P	Partial pressure of nitrogen $p = \frac{F_a}{F_t} P_T$	mmHg 77.725	77.725		
p/p_o	Relative pressure of nitrogen	.094	.094		X*
	$(p_o - p)$	mmHg 752.275	752.275		
	$v_{ads}(p_o - p)$	ml mmHg 173.023	173.023		
	$\frac{p}{v_{ads}(p_o - p)}$	ml^{-1} .449	.449		y*

*See one-point calculation.

TABLE A.6 ONE-POINT CALCULATION FOR SPECIFIC SURFACE AREA

Symbol	Measurement or Calculation	Dimension	Result
α'	The slope of the BET plot $\alpha' = \frac{y}{x}$	.2/.042	4.762
v_m'	Volume of adsorbed nitrogen for a monolayer: $v_m' = \frac{1}{\alpha'}$	1/4.762	0.21
S	$v_m' s_o$ .21 x 4.3844	m^2	.921
S_s'	Specific surface area of the sample: $S_s' = \frac{v_m' s_o}{w}$ $\frac{.921}{.61054}$	m^2/g $\frac{.921}{.61054}$	$1.508 m^2/gm$

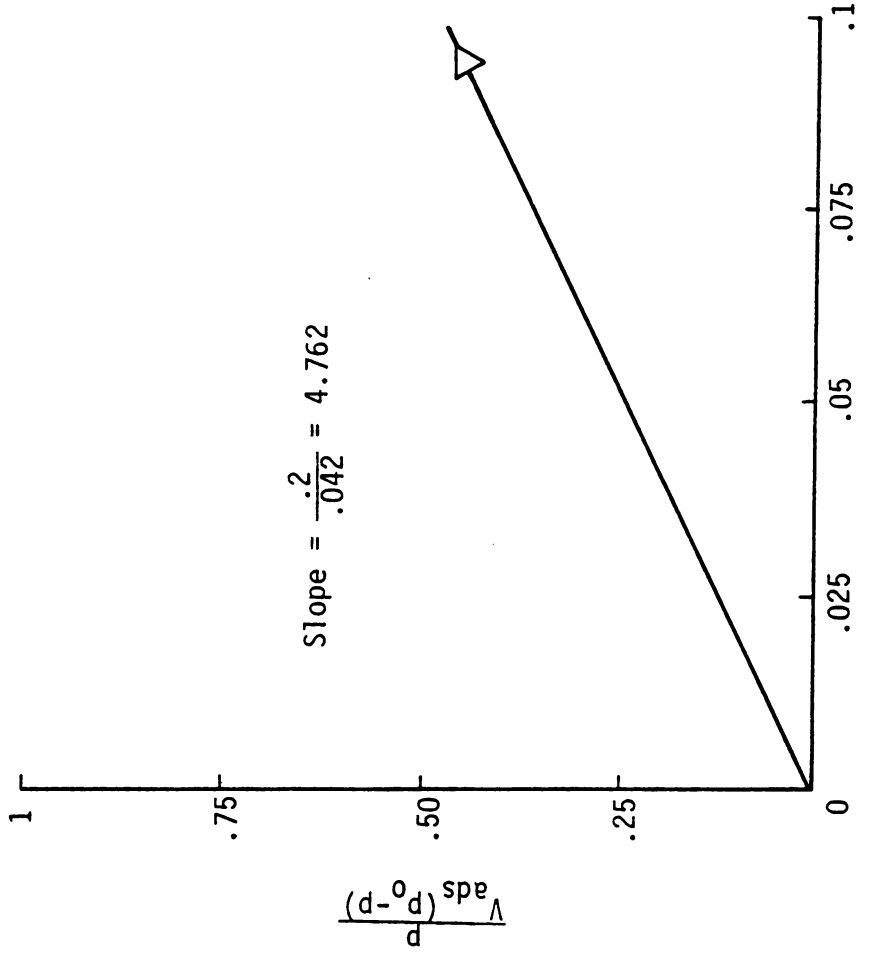

Figure A-1 One point B. E. T. plot.

TABLE A.7
CONSOLIDATION DATA FOR
A KAOLINITE TRIAXIAL
TEST SAMPLE

$\sqrt{t}$ min $^{1/2}$	Δv cm^3
.32	.59
.50	.75
.71	.89
1.22	1.29
1.41	1.39
2.00	1.89
2.83	2.70
3.87	3.79
5.48	5.50
7.87	7.79
10.95	9.93
14.59	11.89
31.00	13.83
34.00	13.95

CU- 8 100% kaolinite sample
consolidation pressure + 3.50 kg/cm^2

TABLE A.8
CONSOLIDATION DATA FOR
A FIBER TRIAXIAL TEST
SAMPLE

$\sqrt{t}$ min$^{1/2}$	Δv cm^3
1	7.26
1.41	9.16
2.83	15.96
3.87	18.66
5.00	21.24
8.49	25.31
12.12	27.05
19.21	28.55
38.25	31.25
42.21	34.05

CD-F 2 100% Fiber sample
Consolidation pressure = 3 kg/cm^2

TABLE B.1 COMPRESSION TEST DATA, SAMPLE C1, 100% FIBERS

Consolidation pressure = 2.402 kg/cm^2

Final water content = 42.13%

x-section area = 1cm^2
Volume of solids = .8831cm^3
Initial volume = 4.9922cm^3

Load (Kg/cm^2)	Change in Height, Δh (cm.)	Change in Volume Δv (cm^3)	Volume of Voids Vv (cm^3)	Void Ratio e	Coefficient of Vol. Compressibility (m_v)† x 10^{-4} cm^2/kg
2.4020	0.0000*	0.0000*	4.1091	4.6530	---
6.3974	1.9558	1.9558	2.1533	2.4383	980.00
14.4519	2.7229	2.7229	1.3862	1.5697	452.64
27.4519	3.0124	3.0124	1.0967	1.2419	240.88
43.8087	3.2334	3.2334	0.8757	0.9916	156.42
59.7905	3.3426	3.3426	0.7665	0.8680	116.67
91.7314	3.4925	3.4925	0.6166	0.6982	78.31
123.7087	3.5636	3.5636	0.5455	0.6177	58.84
171.6723	3.6424	3.6424	0.4667	0.5285	43.10
218.8632	3.7059	3.7059	0.4032	0.4566	34.29
266.0496	3.7287	3.7287	0.3804	0.4308	28.32
313.1678	3.7592	3.7592	0.3499	0.3962	24.23
360.2678	3.7922	3.7922	0.3169	0.3588	21.22

$^\dagger m_v = \frac{\Delta V}{V \cdot \Delta P}$ *Zero reference for 2.4 kg/cm^2 load.

TABLE B.2 COMPRESSION TEST DATA, SAMPLE C2, 54% FIBERS and 46% CLAY BY VOLUME

Consolidation pressure = 2.402 kg/cm^2

Final water content = 21.49%

x-sectional area = $1cm^2$
Volume of solids = $1.1326cm^3$
Initial volume = $3.9190cm^3$

Load (Kg/cm^2)	Change in Height, Δh (cm.)	Change in Volume Δv (cm^3)	Volume of Voids Vv (cm^3)	Void Ratio e	Coefficient of Vol. Compressibility (m_v) x 10^{-4} cm^2/kg
2.4020	0.0000	0.0000	2.7864	2.4602	----
6.3975	.8738	.8738	1.9126	1.6886	558.04
14.4520	1.3437	1.3437	1.4427	1.2738	284.53
26.1406	1.5850	1.5850	1.2014	1.0607	170.37
42.4974	1.7729	1.7729	1.0135	0.8948	112.82
58.4565	1.8821	1.8821	0.9043	0.7984	85.67
90.4565	2.0168	2.0168	0.7696	0.6795	58.44
122.4065	2.0853	2.0853	0.7011	0.6190	44.34
170.3610	2.1692	2.1692	0.6172	0.5449	32.95
217.5428	2.2250	2.2250	0.5614	0.4957	26.38
264.5610	2.2581	2.2581	0.5283	0.4664	21.97
311.8292	2.2911	2.2911	0.4953	0.4373	18.89
358.9199	2.3190	2.3190	0.4674	0.4127	16.59

TABLE B.3 COMPRESSION TEST DATA SAMPLE, C3, 25% FIBERS/75% CLAY BY VOLUME

Conslidation pressure = 2.402 kg/cm^2

Final water content = 20.41%

x-sectional area = 1 cm^2
Volume of solids = 1.6313
Initial volume = 4.5066cm^3

Load (Kg/cm^2)	Change in Height, Δh (cm.)	Change in Volume Δv (cm^3)	Volume of Voids Vv (cm^3)	Void Ratio e	Coefficient of Vol. Compressibility (m_v) x 10^{-4} cm^2/kg
2.4020	0.0000	0.0000	2.8753	1.7626	---
6.4315	0.6985	0.6985	2.1768	1.3344	384.65
14.4519	1.0897	1.0897	1.7856	1.0946	200.66
25.7360	1.3411	1.3411	1.5342	0.9405	127.53
42.0928	1.5443	1.5443	1.3310	0.8159	86.33
58.1109	1.6383	1.6383	1.2370	0.7583	65.25
90.0336	1.7932	1.7932	1.0821	0.6633	45.40
122.0018	1.8847	1.8847	0.9906	0.6072	34.96
169.9563	1.9736	1.9736	0.9017	0.5527	26.13
217.0654	2.0498	2.0498	0.8255	0.5060	21.18
264.1790	2.0904	2.0904	0.7849	0.4812	17.71
311.4654	2.1336	2.1336	0.7417	0.4547	15.31
358.5245	2.1666	2.1666	0.7087	0.4344	13.49

TABLE B.4 COMPRESSION TEST DATA, SAMPLE C4, 100% CLAY

Consolidation pressure = 2.402 kg/cm^2

Final water content = 16.86%

x-sectional area = $1cm^2$

Volume of solids = 2.5962 cm^3

Initial volume = 5.6840 cm^3

100% Clay

Load (Kg/cm^2)	Change in Height, Δh (cm.)	Change in Volume Δv (cm^3)	Volume of Voids Vv (cm^3)	Void Ratio e	Coefficient of Vol. Compressibility (m_v) x 10^{-4} cm^2/kg
2.4020	0.0000	0.0000	3.0878	1.1894	---
6.3975	0.4597	0.4597	2.6281	1.0123	202.41
14.4520	0.7874	0.7874	2.3004	0.8861	114.96
25.6770	0.9728	0.9728	2.1150	0.8147	73.53
42.0338	1.1659	1.1659	1.9219	0.7403	51.75
57.9929	1.2522	1.2522	1.8356	0.7070	39.62
89.9565	1.3919	1.3919	1.6959	0.6532	27.96
121.9065	1.4935	1.4935	1.5943	0.6141	21.98
169.8974	1.6027	1.6027	1.4851	0.5720	16.83
217.0747	1.6764	1.6764	1.4114	0.5436	13.73
264.3520	1.7526	1.7526	1.3352	0.5143	11.77
311.4384	1.7932	1.7932	1.2946	0.4987	10.20
358.4202	1.8440	1.8440	1.2438	0.4791	9.11

TABLE B.5 COMPRESSION TEST DATA, SAMPLE C5 , 100% FIBERS

Consolidation pressure = 1.24 kg/cm^2

Final water content = 93.57%

x-sectional area = 1 in^2 = 6.4516 cm^2
Volume of solids = 5.6558 cm^3
Initial volume = 31.6928 cm^3

Load (Kg/cm^2)	Change in Height, Δh (cm.)	Change in Volume Δv (cm^3)	Volume of Voids Vv (cm^3)	Void Ratio e	Coefficient of Vol. Compressibility (m_v) x 10^{-4} cm^2/kg
1.240	0.0000	0.0000	26.0370	4.6036	---
1.865	0.8128	5.2439	20.7931	3.6764	2647.36
2.489	1.3589	8.7671	17.2699	3.0535	2214.79
3.113	1.6129	10.4058	15.6312	2.7637	1752.98
3.736	1.8313	11.8148	14.2222	2.5146	1493.55
4.961	2.2504	14.5187	11.5183	2.0365	1231.14
7.439	2.5324	16.3380	9.6990	1.7149	831.60
9.916	2.6924	17.3703	8.6667	1.5324	631.72
14.871	2.8905	18.6483	7.3887	1.3064	431.66
19.819	3.0124	19.4348	6.6022	1.1673	330.06

TABLE B.6 COMPRESSION TEST DATA, SAMPLE C6, 100% FIBERS

Consolidation pressure = 6.64 kg/cm^2

Final water content = 57.57%

x-sectional area = 1 in^2 = 6.4516 cm^2
Volume of solids = 5.9156 cm^3
Initial volume = 16.9213 cm^3

Load (Kg/cm^2)	Change in Height, Δh (cm.)	Change in Volume Δv (cm^3)	Volume of Voids Vv (cm^3)	Void Ratio e	Coefficient of Vol. Compressibility (m_v) x 10^{-4} cm^2/kg
6.6442	0.0000	0.0000	11.0057	1.8605	---
9.1228	0.1372	0.8852	10.1205	1.7108	211.05
11.6007	0.3251	2.0974	8.9083	1.5059	250.07
16.5607	0.5004	3.2284	7.7773	1.3147	192.39
21.5123	0.6172	3.9819	7.0238	1.1873	158.27
26.4632	0.6985	4.5064	6.4993	1.0987	134.37
33.7510	0.7899	5.0961	5.9096	0.9990	111.10
41.0952	0.8433	5.4406	5.5651	0.9407	93.32
50.2233	0.9728	6.2761	4.7296	0.7995	85.10

TABLE B.7 COMPRESSION TEST DATA, SAMPLE C7, 100% FIBERS

Consolidation pressure = 1.97 kg/cm^2

Final water content = 59.75%

x-sectional area = 1 in^2 = 6.4516 cm^2
Volume of solids = 8.3247 cm^3
Initial volume = 39.4819 cm^3

Load (Kg/cm^2)	Change in Height, Δh (cm.)	Change in Volume Δv (cm^3)	Volume of Voids Vv (cm^3)	Void Ratio e	Coefficient of Vol. Compressibility (m_v) x 10^{-4} cm^2/kg
1.9713	0.0000	0.0000	31.1572	3.7427	---
4.1089	1.5291	9.8651	21.2921	2.5577	1168.89
6.6442	2.2835	14.7322	16.4250	1.9730	798.51
9.1228	2.6060	16.8129	14.3443	1.7231	595.45
14.0828	2.9743	19.1889	11.9683	1.4377	401.28
19.0344	3.2233	20.7954	10.3618	1.2447	308.68
26.4631	3.3858	21.8438	9.3134	1.1188	225.89
33.7777	3.5738	23.0567	8.1005	0.9731	183.60
41.0811	3.6169	23.3348	7.8224	0.9397	151.11
48.3788	3.7617	24.2689	6.8883	0.8275	132.45
55.6927	3.7897	24.4496	6.7076	0.8057	115.27

TABLE C.1 DIRECT SHEAR TEST DATA, SAMPLE S1

Material: Saturated full length fibers
Dry Density* = 31.77pcf
Water content* = 131.5% Consolidation Pr = 2.83 kg/cm^2

Load (lbs)	Load (kg)	Displacement (in)	Displacment (cm)	Area (cm^2)	Shear Stress (Kg/cm^2)
3.19	1.450	.001	.0025	6.4453	.2249
5.26	2.391	.003	.0076	6.4323	.3717
7.89	3.586	.006	.0152	6.4130	.5592
10.34	4.700	.010	.0254	6.3871	.7359
13.15	5.977	.017	.0432	6.3419	.9425
15.78	7.173	.023	.0584	6.3033	1.1379
18.42	8.373	.032	.0813	6.2451	1.3407
21.62	9.827	.045	.1143	6.1613	1.5949
24.44	11.109	.060	.1524	6.0645	1.8318
26.69	12.132	.075	.1905	5.9677	2.0329
28.19	12.814	.085	.2159	5.9032	2.1707
29.88	13.582	.100	.2540	5.8064	2.3391
27.44	12.473	.100	.2540	5.8064	2.1481
24.25	11.023	.100	.2540	5.8064	1.8984
21.05	9.568	.099	.2515	5.8128	1.6460
18.04	8.200	.098	.2489	5.8194	1.4091
15.41	7.005	.096	.2438	5.8323	1.2011
12.78	5.809	.094	.2388	5.8450	.9938
9.96	4.527	.091	.2311	5.8646	.7719
7.89	3.586	.088	.2235	5.8839	.6095
5.08	2.309	.083	.2108	5.9162	.3903
2.82	1.282	.078	.1981	5.9484	.2155
1.50	.682	.075	.1905	5.9677	.1143
0.0	0.0	.067	.1702	6.0193	0.0
5.82	2.645	.067	.1702	6.0193	.4394
8.64	3.927	.070	.1778	5.9999	.6545
11.46	5.209	.072	.1829	5.9870	.8701
14.66	6.664	.076	.1930	5.9614	1.1179
17.48	7.945	.080	.2032	5.9355	1.3386
20.67	9.395	.085	.2159	5.9032	1.5915
23.68	10.764	.090	.2286	5.8709	1.8334
26.69	12.132	.096	.2438	5.8323	2.0801
29.88	13.582	.104	.2642	5.7805	2.3496
32.14	14.609	.115	.2921	5.7097	2.5586
33.83	15.377	.130	.3302	5.6129	2.7396
34.77	15.805	.140	.3556	5.5484	2.8486
36.46	16.573	.160	.4064	5.4193	3.0581
37.96	17.255	.180	.4572	5.2903	3.2616

TABLE C.1 (Continued)

Load (lbs)	Load (kg)	Displacement (in)	Displacment (cm)	Area (cm^2)	Shear Stress (Kg/cm^2)
39.29	17.859	.200	.5080	5.1613	3.4602
36.28	16.491	.199	.5055	5.1676	3.1912
30.64	13.927	.198	.5029	5.1742	2.6916
22.36	10.164	.193	.4902	5.2065	1.9522
18.79	8.541	.190	.4826	5.2258	1.6344
13.72	6.236	.184	.4674	5.2644	1.1846
10.90	4.955	.180	.4572	5.2903	.9366
7.52	3.418	.176	.4470	5.3162	.6429
3.38	1.536	.168	.4267	5.3678	.2862
0.0	0.0	.153	.3886	5.4646	0.0
6.95	3.159	.153	.3886	5.4646	.5781
9.77	4.441	.155	.3937	5.4516	.8146
12.78	5.809	.158	.4013	5.4323	1.0693
15.79	7.177	.162	.4115	5.4064	1.3275
18.79	8.541	.165	.4191	5.3871	1.5855
21.80	9.909	.170	.4318	5.3548	1.8505
24.81	11.277	.175	.4445	5.3226	2.1187
27.82	12.645	.180	.4572	5.2903	2.3902
30.45	13.841	.185	.4699	5.2581	2.6323
33.46	15.209	.190	.4826	5.2258	2.9104
38.53	17.514	.200	.5080	5.1613	3.3933
40.79	18.541	.210	.5334	5.0968	3.6378
41.54	18.882	.220	.5588	5.0322	3.7522
42.48	19.309	.240	.6096	4.9032	3.9380
43.42	19.736	.260	.6604	4.7742	4.1339
44.17	20.077	.280	.7112	4.6452	4.3221
44.73	20.332	.300	.7620	4.5161	4.5021

Failure assumed at 20% lateral displacement.

TABLE C.2 DIRECT SHEAR TEST DATA, SAMPLE S2

Material: Saturated full length fibers
Dry Density*= 30.45 pcf
Water content*= 140% Consolidation Pr = 3.45 kg/cm^2

Load (lbs)	Load (kg)	Lateral Displacement (in)	Lateral Displacement (cm)	Vertical Displacement (in)	Vertical Displacement (cm)	Area (cm^2)	Shear Stress (kg/cm^2)
3.00	1.364	.001	.0025	0.0	0.0	6.4453	.2116
6.01	2.732	.003	.0076	0.0	0.0	6.4323	.4247
8.27	3.759	.005	.0127	-.001	-.0025	6.4193	.5856
13.53	6.150	.014	.0356	-.002	-.0051	6.3612	.9668
16.16	7.345	.020	.0508	-.004	-.0102	6.3226	1.1617
18.79	8.541	.029	.0737	-.005	-.0127	6.2644	1.3634
21.80	9.909	.039	.0991	-.006	-.0152	6.1999	1.5983
24.25	11.023	.048	.1219	-.007	-.0178	6.1419	1.7947
27.06	12.300	.060	.1524	-.008	-.0203	6.0645	2.0282
29.69	13.495	.075	.1905	-.009	-.0229	5.9677	2.2613
32.70	14.864	.092	.2337	-.010	-.0254	5.8580	2.5374
34.21	15.550	.100	.2540	-.010	-.0254	5.8064	2.6781
35.34	16.064	.110	.2794	-.011	-.0279	5.7419	2.7977
38.15	17.341	.130	.3302	-.012	-.0305	5.6129	3.0895
34.96	15.891	.130	.3302	-.012	-.0305	5.6129	2.8312
28.94	13.155	.129	.3277	-.012	-.0305	5.6192	2.3411
19.54	8.882	.125	.3175	-.013	-.0330	5.6452	1.5734
12.03	5.468	.119	.3023	-.013	-.0330	5.6838	.9620
3.94	1.791	.108	.2743	-.015	-.0381	5.7549	.3112
0.0	0.0	.095	.2413	-.018	-.0457	5.8387	0.0
4.13	1.877	.095	.2413	-.018	-.0457	5.8387	.3215
10.15	4.614	.098	.2489	-.019	-.0483	5.8194	.7929
16.16	7.345	.103	.2616	-.019	-.0483	5.7871	1.2692
21.99	9.995	.109	.2769	-.019	-.0483	5.7483	1.7388
27.82	12.645	.117	.2972	-.019	-.0483	5.6967	2.2197
35.71	16.232	.130	.3302	-.019	-.0483	5.6129	2.8919
40.22	18.282	.145	.3683	-.017	-.0432	5.5161	3.3143
42.10	19.136	.160	.4064	-.016	-.0406	5.4193	3.5311
43.79	19.905	.170	.4318	-.015	-.0381	5.3548	3.7172
44.36	20.164	.178	.4521	-.014	-.0356	5.3033	3.8022
45.11	20.505	.187	.4749	-.013	-.0330	5.2454	3.9091
45.67	20.759	.200	.5080	-.012	-.0305	5.1613	4.0220
41.35	18.795	.199	.5055	-.012	-.0305	5.1676	3.6371
35.34	16.064	.198	.5029	-.013	-.0330	5.1742	3.1046
30.07	13.668	.195	.4953	-.014	-.0356	5.1935	2.6318

TABLE C.2 (Continued)

Load (lbs)	Load (kg)	Lateral Displacement		Vertical Displacement		Area (cm^2)	Shear Stress (kg/cm^2)
		(in)	(cm)	(in	(cm)		
24.81	11.277	.192	.4877	-.015	-.0381	5.2128	2.1633
18.42	8.373	.186	.4724	-.017	-.0432	5.2517	1.5943
11.28	5.127	.178	.4521	-.021	-.0533	5.3033	.9668
5.07	2.305	.170	.4318	-.022	-.0559	5.3548	.4305
.75	.341	.160	.4064	-.023	-.0584	5.4193	.0629
0.0	0.0	.155	.3937	-.024	-.0609	5.4516	0.0
8.27	3.759	.155	.3937	-.025	-.0635	5.4516	.6895
14.28	6.491	.156	.3962	-.025	-.0635	5.4453	1.1920
19.73	8.968	.162	.4115	-.025	-.0635	5.4064	1.6588
25.37	11.532	.169	.4293	-.025	-.0635	5.3612	2.1510
35.15	15.977	.183	.4648	-.023	-.0584	5.2710	3.0311
40.60	18.455	.191	.4851	-.021	-.0533	5.2194	3.5358
45.67	20.759	.200	.5080	-.018	-.0457	5.1613	4.0220

Failure assumed at 20% lateral displacement.
*After consolidation.

TABLE C.3 DIRECT SHEAR TEST DATA, SAMPLE S3

Material: Saturated full length fibers
Dry density*= 32.18 pc
Water content*= 129%
Consolidation Pr = 4.06 kg/cm^2

Load (lbs)	Load (kg)	Lateral Displacement		Vertical Displacement		Area (cm^2)	Shear Stress (kg/cm^2)
		(in)	(cm)	(in	(cm)		
3.00	1.364	.001	.0025	0.0	0.0	6.4453	.2116
8.27	3.759	.006	.0152	-.001	-.0025	6.4130	.5862
13.53	6.150	.015	.0381	-.003	-.0076	6.3548	.9678
18.79	8.541	.026	.0660	-.005	-.0127	6.2839	1.3592
24.25	11.023	.043	.1092	-.008	-.0203	6.1742	1.7853
29.32	13.327	.063	.1600	-.010	-.0254	6.0452	2.2046
34.77	15.805	.085	.2159	-.011	-.0279	5.9032	2.6774
37.59	17.086	.100	.2540	-.013	-.0330	5.8064	2.9426
34.58	15.718	.100	.2540	-.013	-.0330	5.8064	2.7070
29.13	13.241	.099	.2515	-.013	-.0330	5.8128	2.2779
31.20	14.182	.098	.2489	-.013	-.0330	5.8194	2.4370
18.42	8.373	.095	.2413	-.014	-.0356	5.8387	1.4341
13.15	5.977	.091	.2311	-.014	-.0356	5.8646	1.0192
6.39	2.905	.084	.2134	-.015	-.0381	5.9096	.4916
1.88	.855	.076	.1930	-.016	-.0406	5.9614	.1434
0.00	0.0	.068	.1727	-.018	-.0457	6.0129	0.0
7.71	3.505	.070	.1778	-.018	-.0457	5.9999	1.5842
13.72	6.236	.073	.1854	-.018	-.0457	5.9807	1.0427
21.99	9.995	.081	.2057	-.019	-.0483	5.9291	1.6858
28.19	12.814	.089	.2261	-.019	-.0483	5.8773	2.1803
33.83	15.377	.096	.2438	-.019	-.0483	5.8323	2.6365
39.28	17.855	.106	.2692	-.019	-.0483	5.7678	3.0956
43.98	19.991	.130	.3302	-.017	-.0432	5.6129	3.5616
46.62	21.191	.149	.3785	-.015	-.0381	5.4902	3.8598
50.37	22.895	.181	.4597	-.011	-.0279	5.2839	4.3329
56.20	25.545	.190	.4826	-.010	-.0254	5.2258	4.8882
58.64	26.655	.200	.5080	-.009	-.0229	5.1613	5.1644
53.19	24.177	.200	.5080	-.009	-.0229	5.1613	4.6843
43.98	19.991	.199	.5055	-.010	-.0254	5.1676	3.8685
35.71	16.232	.197	.5004	-.011	-.0279	5.1806	3.1332
28.00	12.727	.193	.4902	-.013	-.0330	5.2065	2.4444
21.62	9.827	.188	.4775	-.015	-.0381	5.2388	1.8758
15.79	7.177	.182	.4623	-.017	-.0432	5.2774	1.3599
10.90	4.955	.175	.4445	-.020	-.0508	5.3226	.9309
5.82	2.645	.167	.4242	-.023	-.0584	5.3741	.4922

TABLE C.3 (Continued)

Load (lbs)	Load (kg)	Lateral Displacement		Vertical Displacement		Area (cm^2)	Shear Stress (kg/cm^2)
		(in)	(cm)	(in	(cm)		
3.94	1.791	.150	.3810	-.028	-.0711	5.4839	.3266
9.39	4.268	.152	.3861	-.028	-.0711	5.4709	.7801
17.85	8.114	.158	.4013	-.028	-.0711	5.4323	1.4937
23.31	10.595	.163	.4140	-.027	-.0686	5.4000	1.9620
28.57	12.986	.169	.4293	-.026	-.0660	5.3612	2.4222
38.91	17.686	.183	.4648	-.023	-.0584	5.2710	3.3553
43.98	19.991	.190	.4826	-.021	-.0533	5.2258	3.8254
47.93	21.786	.195	.4953	-.020	-.0508	5.1935	4.1948
54.14	24.609	.210	.5334	-.016	-.0406	5.0968	4.8283
56.39	25.632	.235	.5969	-.010	-.0254	4.9355	5.1934
57.14	25.973	.250	.635	-.007	-.0178	4.8387	5.3678

Failure assumed at 20% lateral displacement

*After consolidation.

TABLE C.4 DIRECT SHEAR TEST DATA, SAMPLE S4

Material: Saturated full length fiber
Dry Density*= 23.47 pcf
water content*= 201%
Consolidation Pr = 1.58 kg/cm^2

Load (lbs)	Load (kg)	Lateral Displacement (in)	Lateral Displacement (cm)	Vertical Displacement (in	Vertical Displacement (cm)	Area (cm^2)	Shear Stress (kg/cm^2)
3.00	1.364	.002	.0051	0.0	0.0	6.4386	.2118
5.83	2.650	.008	.0203	-.002	-.0051	6.4000	.4141
7.89	3.586	.020	.0508	-.004	-.0102	6.3226	.5672
9.39	4.268	.030	.0762	-.006	-.0152	6.2581	.6820
10.90	4.955	.040	.1016	-.007	-.0178	6.1935	.8000
12.03	5.468	.050	.1270	-.009	-.0229	6.1290	.8922
13.53	6.150	.065	.1651	-.010	-.0254	6.0322	1.0195
14.66	6.664	.080	.2032	-.012	-.0305	5.9355	1.1227
15.98	7.264	.100	.2540	-.013	-.0330	5.8064	1.2510
17.10	7.773	.120	.3048	-.014	-.0356	5.6774	1.3691
18.61	8.459	.140	.3556	-.015	-.0381	5.5484	1.5246
19.17	8.714	.150	.3810	-.015	-.0381	5.4839	1.5890
19.73	8.968	.160	.4064	-.015	-.0381	5.4193	1.6548
20.11	9.141	.170	.4318	-.016	-.0406	5.3548	1.7071
20.49	9.314	.180	.4572	-.016	-.0406	5.2903	1.7606
21.05	9.568	.190	.4826	-.016	-.0406	5.2258	1.8309
21.99	9.995	.205	.5207	-.016	-.0406	5.1290	1.9487
22.36	10.164	.220	.5588	-.017	-.0432	5.0322	2.0198
22.74	10.336	.230	.5842	-.017	-.0432	4.9677	2.0806
23.31	10.595	.240	.6096	-.017	-.0432	4.9032	2.1608
23.68	10.764	.250	.6350	-.016	-.0406	4.8387	2.2246
24.25	11.023	.265	.6731	-.016	-.0406	4.7419	2.3246

Failure assumed at 20% lateral displacement.
*After consolidation.

TABLE C.5 DIRECT SHEAR TEST DATA, SAMPLE S5

Material: Saturated full length fibers
Dry Density*= 19.63 psf
Water content*= 253%
Consolidation Pr = .962 kg/cm^2

Load (lbs)	Load (kg)	Lateral Displacement		Vertical Displacement		Area (cm^2)	Shear Stress (kg/cm^2)
		(in)	(cm)	(in)	(cm)		
2.44	1.109	.006	.0512	-.001	-.0025	6.3216	.1754
3.76	1.709	.017	.0432	-.005	-.0127	6.3419	.2695
4.88	2.218	0.28	.0711	-.008	-.0203	6.2710	.3537
5.83	2.650	.042	.1067	-.010	-.0254	6.1806	.4288
7.33	3.332	.063	.1600	-.013	-.0330	6.0452	.5512
8.65	3.932	.083	.2108	-.015	-.0381	5.9162	.6646
9.39	4.268	.100	.2540	-.017	-.0432	5.8064	.7351
10.34	4.700	.120	.3048	-.018	-.0457	5.6774	.8278
10.71	4.868	.135	.3429	-.019	-.0483	5.5806	.8723
11.28	5.127	.150	.3810	-.019	-.0483	5.4839	.9349
11.65	5.295	.160	.4064	-.019	-.0483	5.4193	.9771
12.03	5.468	.170	.4318	-.019	-.0483	5.3548	1.0211
12.41	5.641	.185	.4699	-.020	-.0508	5.2581	1.0728
12.97	5.895	.200	.5080	-.020	-.0508	5.1613	1.1422
13.53	6.150	.220	.5588	-.020	-.0508	5.0322	1.2221
14.28	6.491	.245	.6223	-.021	-.0508	4.8709	1.3326

Failure assumed at 20% lateral displacement.
*After consolidation.

TABLE C.6 DIRECT SHEAR TEST DATA, SAMPLE S6

Material: Saturated full length fibers
Dry Density*= 26.12 psf
Water content*= 174% Consolidation Pr = 2.21 kg/cm^2

Load (lbs)	Load (kg)	Lateral Displacement		Vertical Displacement		Area (cm^2)	Shear Stress (kg/cm^2)
		(in)	(cm)	(in)	(cm)		
2.82	1.282	.001	.0025	0.0	0.0	6.4453	.1989
6.58	2.991	.010	.0254	-.002	-.0051	6.3871	.4683
8.27	3.759	.020	.0508	-.004	-.0102	6.3226	.5945
9.96	4.527	.030	.0762	-.006	-.0152	6.2581	.7234
11.65	5.295	.040	.1016	-.008	-.0203	6.1935	.8549
13.34	6.064	.052	.1321	-.010	-.0254	6.1161	.9915
16.16	7.345	.070	.1778	-.013	-.0330	5.9999	1.2242
17.48	7.945	.080	.2032	-.014	-.0356	5.9355	1.3386
18.61	8.459	.090	.2286	-.016	-.0406	5.8709	1.4408
19.74	8.973	.100	.2540	-.017	-.0432	5.8064	1.5454
21.80	9.909	.120	.3048	-.018	-.0457	5.6774	1.7453
22.93	10.423	.130	.3302	-.019	-.0483	5.6129	1.8569
23.68	10.764	.140	.3556	-.020	-.0508	5.5484	1.9400
24.62	11.191	.150	.3810	-.020	-.0508	5.4839	2.0407
25.56	11.618	.160	.4064	-.021	-.0533	5.4193	2.1438
26.31	11.959	.170	.4318	-.021	-.0533	5.3548	2.2333
26.69	12.132	.181	.4597	-.021	-.0533	5.2839	2.9600
27.82	12.645	.190	.4826	-.021	-.0533	5.2258	2.4197
28.57	12.986	.200	.5080	-.021	-.0533	5.1613	2.5160
29.32	13.327	.215	.5461	-.022	-.0559	5.0645	2.6315
30.64	13.927	.230	.5842	-.022	-.0559	4.9677	2.8035

Failure assumed at 20% lateral displacement.

*After consolidation.

TABLE C.7 DIRECT SHEAR TEST DATA, SAMPLE S7

Material: Saturated full length fibers
Dry Density*= 28.63pcf
Water content*= 153% Consolidation Pr = 3.45 kg/cm^2

Load (lbs)	Load (kg)	Lateral Displacement		Vertical Displacement		Area (cm^2)	Shear Stress (kg/cm^2)
		(in)	(cm)	(in)	(cm)		
6.01	2.732	.004	.0102	0.0	0.0	6.4257	.4252
11.09	5.041	.010	.0254	-.002	-.0051	6.3871	.7892
15.03	6.832	.020	.0508	-.004	-.0102	6.3226	1.0806
17.86	8.118	.030	.0762	-.006	-.0152	6.2581	1.2972
20.11	9.141	.040	.1016	-.008	-.0203	6.1935	1.4759
21.99	9.995	.050	.1270	-.009	-.0229	6.1290	1.6308
23.87	10.850	.060	.1524	-.011	-.0279	6.0645	1.7891
25.56	11.618	.070	.1778	-.011	-.0279	5.9999	1.9364
27.82	12.645	.090	.2286	-.013	-.0330	5.8709	2.1538
29.51	13.414	.100	.2540	-.014	-.0356	5.8064	2.3102
32.14	14.609	.120	.3048	-.016	-.0406	5.6774	2.5732
34.58	15.718	.140	.3556	-.017	-.0432	5.5484	2.8329
36.84	16.745	.160	.4064	-.018	-.0457	5.4193	3.0899
38.90	17.682	.180	.4572	-.019	-.0483	5.2903	3.3423
40.03	18.195	.190	.4826	-.019	-.0483	5.2258	3.4818
41.35	18.795	.200	.5080	-.019	-.0483	5.1613	3.6415
42.29	19.223	.210	.5334	-.019	-.0483	5.0968	3.7716
43.42	19.736	.220	.5588	-.020	-.0508	5.0322	3.9219
45.11	20.505	.235	.5969	-.020	-.0508	4.9355	4.1546
46.43	21.105	.250	.6350	-.019	-.0483	4.8387	4.3617
47.18	21.445	.260	.6604	-.019	-.0483	4.7742	4.4919

Failure assumed at 20% lateral displacement.
*After consolidation.

TABLE C.8 DIRECT SHEAR TEST DATA, SAMPLE S8

Material: Saturated full length fiber sample with no hydrostatic pr.
Dry density*= 22.95 pcf
Water content*= 207% Consolidation Pr = 1.58 kg/cm^2

Load (lbs)	Load (kg)	Lateral Displacement (in)	Lateral Displacement (cm)	Vertical Displacement (in)	Vertical Displacement (cm)	Area (cm^2)	Shear Stress (kg/cm^2)
5.83	2.650	.010	.0254	-.001	-.0025	6.3871	.4149
7.52	3.418	.020	.0508	-.003	-.0076	6.3226	.5406
8.65	3.932	.030	.0762	-.003	-.0076	6.2581	.6283
9.77	4.441	.040	.1016	-.004	-.0102	6.1935	.7170
10.90	4.955	.050	.1270	-.005	-.0127	6.1290	.8085
12.59	5.723	.070	.1778	-.006	-.0152	5.9999	.9538
13.15	5.977	.080	.2032	-.006	-.0152	5.9355	1.0069
13.72	6.236	.090	.2286	-.006	-.0152	5.8709	1.0622
14.47	6.577	.100	.2540	-.006	-.0152	5.8064	1.1327
15.03	6.832	.110	.2794	-.007	-.0178	5.7419	1.1899
15.60	7.091	.120	.3048	-.007	-.0178	5.6774	1.2490
15.98	7.264	.130	.3302	-.007	-.0178	5.6129	1.2942
16.54	7.518	.140	.3556	-.007	-.0178	5.5484	1.3549
16.92	7.691	.150	.3810	-.007	-.0178	5.4839	1.4025
18.04	8.200	.170	.4318	-.007	-.0178	5.3548	1.5313
18.42	8.373	.180	.4572	-.007	-.0178	5.2903	1.5827
19.36	8.800	.200	.5080	-.007	-.0178	5.1613	1.7050
20.30	9.227	.220	.5588	-.007	-.0178	5.0322	1.8336
20.67	9.395	.230	.5842	-.007	-.0178	4.9677	1.8912
21.80	9.909	.250	.6350	-.008	-.0203	4.8387	2.0479
22.36	10.164	.260	.6604	-.007	-.0178	4.7742	2.1289
22.74	10.336	.270	.6858	-.007	-.0178	4.7097	2.1946

Failure assumed at 20% lateral displacement
*After consolidation.

TABLE C.9 DIRECT SHEAR TEST DATA, SAMPLE S9

Material: Saturated full length fibers with no hydrostatic pr.
Dry density*= 27.62 pcf
Water content*= 161% Consolidation Pr = 2.21 kg/cm^2

Load (lbs)	Load (kg)	Lateral Displacement		Vertical Displacement		Area (cm^2)	Shear Stress (kg/cm^2)
		(in)	(cm)	(in)	(cm)		
8.08	3.673	.010	.0254	-.001	-.0025	6.3871	.5751
10.71	4.868	.020	.0508	-.004	-.0102	6.3226	.7699
13.53	6.150	.035	.0889	-.007	-.0178	6.2258	.9878
15.79	7.177	.050	.1270	-.009	-.0229	6.1290	1.1710
17.10	7.773	.060	.1524	-.010	-.0254	6.0645	1.2817
19.36	8.800	.080	.2032	-.012	-.0305	5.9355	1.4826
20.48	9.309	.090	.2286	-.012	-.0305	5.8709	1.5856
21.61	9.823	.100	.2540	-.013	-.0330	5.8064	1.6918
23.49	10.677	.120	.3048	-.014	-.0356	5.6774	1.8806
25.37	11.532	.140	.3556	-.014	-.0356	5.5484	2.0784
26.50	12.045	.155	.3937	-.014	-.0356	5.4516	2.2094
28.19	12.814	.175	.4445	-.015	-.0381	5.3226	2.4074
29.51	13.414	.190	.4826	-.014	-.0356	5.2258	2.5669
30.26	13.755	.200	.5080	-.014	-.0356	5.1613	2.6650
31.01	14.095	.210	.5334	-.014	-.0356	5.0968	2.7655
31.76	14.436	.220	.5588	-.013	-.0330	5.0322	2.8687
32.33	14.695	.230	.5842	-.012	-.0305	4.9677	2.9581
33.08	15.036	.240	.6096	-.011	-.0279	4.9032	3.0666
33.64	15.290	.250	.6350	-.010	-.0254	4.8387	3.1601
34.21	15.550	.260	.6604	-.008	-.0203	4.7742	3.2571

Failure assumed at 20% lateral displacement.

*After consolidation.

TABLE C.10 DIRECT SHEAR TEST DATA, SAMPLE S10

Material: Full length saturated fibers. Test was conducted on this sample after it was oven dried for 24 hours.
Vertical stress = 2.21 kg/cm^2
Dry Density* = 19.81 psf
Water content* = 250% Consolidation Pr = 1.27 kg/cm^2

Load (lbs)	Load (kg)	Lateral Displacement (in)	Lateral Displacement (cm)	Vertical Displacement (in)	Vertical Displacement (cm)	Area (cm^2)	Shear Stress (kg/cm^2)
1.69	.768	.020	.0508	+.001	.0025	6.3226	.1215
3.00	1.364	.040	.1016	+.002	.0051	6.1935	.2202
5.45	2.477	.055	.1397	+.003	.0076	6.0968	.4063
10.33	4.695	.065	.1651	+.003	.0076	6.0322	.7783
22.74	10.336	.070	.1778	+.003	.0076	5.9999	1.7227
39.47	17.941	.075	.1905	+.004	.0102	5.9677	3.0064
71.05	32.295	.083	.2108	+.005	.0127	5.9162	5.4587
85.33	38.786	.090	.2286	+.006	.0152	5.8709	6.6065
93.98	42.718	.100	.2540	+.007	.0178	5.8064	7.3571
97.74	44.427	.120	.3048	+.011	.0279	5.6774	7.8252

Sudden rupture occurred and the lateral load decreased abruptly.
*After consolidation.

TABLE C.11 DIRECT SHEAR TEST DATA, SAMPLE S11

Material: Dry full length fibers
Normal stress = 2.20 kg/cm^2
Dry density*= not available
Water content*= ...%

Consolidation Pr = 2.20 kg/cm^2

Load (lbs)	Load (kg)	Lateral Displacement		Vertical Displacement		Area (cm^2)	Shear Stress (kg/cm^2)
		(in)	(cm)	(in)	(cm)		
4.51	2.045	.003	.0076	-.002	-.0051	6.4323	.3179
7.14	3.245	.007	.0178	-.003	-.0076	6.4064	.5065
9.77	4.441	.011	.0279	-.004	-.0102	6.3807	.6960
12.59	5.723	.016	.0406	-.005	-.0127	6.3485	.9015
15.41	7.005	.022	.0559	-.006	-.0152	6.3096	1.1102
18.23	8.286	.029	.0737	-.007	-.0178	6.2644	1.3227
20.68	9.400	.038	.0965	-.008	-.0203	6.2065	1.5145
23.12	10.509	.052	.1321	-.009	-.0229	6.1161	1.7183
24.25	11.023	.065	.1651	-.010	-.0254	6.0322	1.8274
25.56	11.618	.085	.2159	-.010	-.0254	5.9032	1.9681
27.26	12.391	.112	.2845	-.011	-.0279	5.7289	2.1629
28.19	12.814	.125	.3175	-.011	-.0279	5.6452	2.2699
29.14	13.245	.145	.3683	-.011	-.0279	5.5161	2.4012
30.45	13.841	.165	.4191	-.012	-.0305	5.3871	2.5693
31.39	14.268	.180	.4572	-.012	-.0305	5.2903	2.6970
32.52	14.782	.200	.5080	-.012	-.0305	5.1613	2.8640
34.59	15.723	.220	.5588	-.011	-.0279	5.0322	3.1245
36.09	16.405	.250	.6350	-.010	-.0254	4.8387	3.3904
36.65	16.659	.260	.6604	-.010	-.0254	4.7742	3.4894
37.03	16.832	.270	.6858	-.009	-.0229	4.7097	3.5739
30.83	14.014	.275	.6985	-.009	-.0229	4.6774	2.9961
21.80	9.909	.272	.6909	-.010	-.0254	4.6967	2.1098
12.78	5.809	.268	.6807	-.013	-.0330	4.7226	1.2300
5.83	2.650	.261	.6629	-.017	-.0432	4.7678	.5558
1.50	.682	.252	.6401	-.019	-.0483	4.8257	.1413
0.0	0.0	.248	.6299	.020	-.0508	4.8517	0.0
9.77	4.441	.250	.6350	.020	-.0508	4.8387	.9178
19.17	8.714	.256	.6502	.020	-.0508	4.8001	1.8154
27.44	12.473	.264	.6706	.018	-.0457	4.7483	2.6268
35.34	16.064	.275	.6985	.015	-.0381	4.6774	3.4344
37.78	17.173	.285	.7239	.014	-.0356	4.6129	3.7228

Failure assumed at 20% lateral displacement.
*After consolidation.

TABLE C.12 DIRECT SHEAR TEST DATA, SAMPLE S12

Material: Dry fibers ground to powdered form.

Normal stress = .962 kg/cm^2 Initial void ratio = 5.6267

Dry density*= 14.50 pcf

Water content*= ...% Consolidation Pr = .962 kg/cm^2

Load (lbs)	Load (kg)	Lateral Displacement		Vertical Displacement		Area (cm^2)	Shear Stress (kg/cm^2)
		(in)	(cm)	(in)	(cm)		
2.63	1.196	.003	.0076	0.0	0.0	6.4323	.1859
4.14	1.882	.008	.0203	-.002	-.0051	6.4000	.2941
5.64	2.564	.013	.0330	-.004	-.0102	6.3678	.4027
6.77	3.077	.020	.0508	-.005	-.0127	6.3226	.4867
8.27	3.759	.030	.0762	-.009	-.0229	6.2581	.6007
9.21	4.186	.040	.1016	-.010	-.0254	6.1935	.6759
10.15	4.614	.054	.1372	-.010	-.0254	6.1031	.7560
10.90	4.955	.075	.1905	-.011	-.0279	5.9677	.8303
12.22	5.555	.100	.2540	-.011	-.0279	5.8064	.9567
12.78	5.809	.120	.3048	-.011	-.0279	5.6774	1.0232
13.35	6.068	.140	.3556	-.011	-.0279	5.5484	1.0936
13.91	6.323	.165	.4191	-.011	-.0279	5.3871	1.1737
14.29	6.495	.190	.4826	-.011	-.0279	5.2258	1.2429
14.66	6.664	.200	.5080	-.011	-.0279	5.1613	1.2911
15.04	6.836	.230	.5842	-.011	-.0279	4.9677	1.3761
15.23	6.923	.260	.6604	-.010	-.0254	4.7742	1.4501
15.41	7.005	.285	.7239	-.010	-.0254	4.6129	1.5186
15.60	7.091	.300	.7620	-.010	-.0254	4.5161	1.5702

Failure assumed at 20% lateral displacement.

*After consolidation.

TABLE C.13 DIRECT SHEAR TEST DATA, SAMPLE S13

Material: Dry fiber ground to powdered form
Normal stress = 1.584 kg/cm^2 Initial void ratio = 4.6331
Dry density*= 17.06 pcf
Water content*= ...% Consolidation Pr = 1.584 kg/cm^2

Load (lbs)	Load (kg)	Lateral Displacement		Vertical Displacement		Area (cm^2)	Shear Stress (kg/cm^2)
		(in)	(cm)	(in)	(cm)		
5.64	2.564	.003	.0076	-.001	-.0025	6.4323	.3986
8.46	3.845	.008	.0203	-.002	-.0051	6.4000	.6008
11.09	5.041	.016	.0406	-.003	-.0076	6.3485	.7940
12.97	5.895	.025	.0635	-.004	-.0102	6.2903	.9372
14.66	6.664	.035	.0889	-.005	-.0127	6.2258	1.0704
15.60	7.091	.045	.1143	-.006	-.0152	6.1613	1.1509
16.92	7.691	.060	.1524	-.007	-.0178	6.0645	1.2682
17.67	8.032	.075	.1905	-.007	-.0178	5.9677	1.3459
18.98	8.627	.100	.2540	-.007	-.0178	5.8064	1.4858
19.92	9.055	.125	.3175	-.007	-.0178	5.6452	1.6040
20.86	9.482	.145	.3683	-.007	-.0178	5.5161	1.7189
21.80	9.909	.170	.4318	-.007	-.0178	5.3548	1.8505
22.74	10.336	.200	.5080	-.007	-.0178	5.1613	2.003
23.49	10.677	.220	.5588	-.007	-.0178	5.0322	2.1217
24.44	11.109	.250	.6350	-.006	-.0152	4.8387	2.2959
24.81	11.277	.270	.6858	-.006	-.0152	4.7097	2.3944
25.19	11.450	.290	.7366	-.006	-.0152	4.5806	2.4997
25.56	11.618	.300	.7620	-.006	-.0152	4.5161	2.5726

Failure assumed at 20% lateral displacement.
*After consolidation.

TABLE C.14 DIRECT SHEAR TEST DATA, SAMPLE S14

Material: Dry fibers ground to powdered form.
Normal stress = 2.21 kg/cm^2 Initial void ratio = 4.290
Dry density*= 18.17pcf
Water Content*= ...% Consolidation Pr = 2.21 kg/cm^2

Load (lbs)	Load (kg)	Lateral Displacement		Vertical Displacement		Area (cm^2)	Shear Stress (kg/cm^2)
		(in)	(cm)	(in)	(cm)		
8.64	3.927	.007	.0178	-.001	-.0025	6.4064	.6129
11.09	5.041	.011	.0279	-.003	-.0076	6.3807	.7900
13.72	6.236	.019	.0483	-.004	-.0102	6.3289	.9853
16.35	7.432	.027	.0686	-.006	-.0152	6.2774	1.1839
18.98	8.627	.040	.1016	-.008	-.0203	6.1935	1.3929
20.67	9.395	.050	.1270	-.008	-.0203	6.1290	1.5329
22.74	10.336	.065	.1651	-.009	-.0229	6.0322	1.7135
24.44	11.109	.080	.2032	-.009	-.0229	5.9355	1.8716
25.75	11.705	.090	.2286	-.010	-.0254	5.8709	1.9937
26.50	12.045	.100	.2540	-.010	-.0254	5.8064	2.0744
28.19	12.814	.120	.3048	-.010	-.0254	5.6774	2.2570
29.88	13.582	.140	.3556	-.010	-.0254	5.5484	2.4479
30.64	13.927	.150	.3810	-.009	-.0229	5.4839	2.5396
31.20	14.182	.160	.4064	-.009	-.0229	5.4193	2.6169
32.14	14.609	.175	.4445	-.009	-.0229	5.3226	2.7447
33.08	15.036	.190	.4826	-.009	-.0229	5.2258	2.8773
34.02	15.464	.205	.5207	-.009	-.0229	5.1290	3.0150
35.34	16.064	.225	.5715	-.009	-.0229	4.9999	3.2129
36.47	16.577	.240	.6096	-.009	-.0229	4.9032	3.3809
36.84	16.745	.250	.6350	-.009	-.0229	4.8387	3.4606
37.59	17.086	.262	.6655	-.009	-.0229	4.7612	3.5886
38.15	17.341	.275	.6985	-.008	-.0203	4.6774	3.7074
38.72	17.600	.285	.7239	-.008	-.0203	4.6129	3.8154
39.25	17.841	.300	.7620	-.007	-.0178	4.5161	3.9505

Failure assumed at 20% lateral displacement.
*After consolidation.

TABLE C.15 DIRECT SHEAR TEST DATA, SAMPLE S15

Material: Dry fiber ground to powdered form
Normal stress - 2.83 kg/cm^2 Initial void ratio = 4.0662
Dry density*= 18.97 pcf
Water content*= ...% Consolidation Pr = 2.83 kg/cm^2

Load (lbs)	Load (kg)	Lateral Displacement		Vertical Displacement		Area (cm^2)	Shear Stress (kg/cm^2)
		(in)	(cm)	(in)	(cm)		
6.20	2.818	.003	.0076	0.0	0.0	6.4323	.4381
10.15	4.614	.005	.0127	0.0	0.0	6.4193	.7188
12.78	5.809	.007	.0178	0.0	0.0	6.4064	.9067
15.22	6.918	.011	.0279	-.001	-.0025	6.3807	1.0842
17.67	8.032	.015	.0381	-.002	-.0051	6.3548	1.2639
20.30	9.227	.021	.0533	-.003	-.0076	6.3162	1.4608
22.74	10.336	.028	.0711	-.003	-.0076	6.2710	1.6482
25.18	11.445	.040	.1016	-.004	-.0102	6.1935	1.8479
26.69	12.132	.050	.1270	-.004	-.0102	6.1290	1.9794
28.57	12.986	.065	.1651	-.004	-.0102	6.0322	2.1528
29.70	13.500	.080	.2032	-.005	-.0127	5.9355	2.2745
31.20	14.182	.100	.2540	-.005	-.0127	5.8064	2.4425
32.52	14.782	.120	.3048	-.005	-.0127	5.6774	2.6036
33.27	15.123	.135	.3429	-.005	-.0127	5.5806	2.7099
33.82	15.373	.150	.3810	-.004	-.0102	5.4839	2.8033
34.58	15.718	.165	.4191	-.004	-.0102	5.3871	2.9177
35.52	16.145	.180	.4572	-.004	-.0102	5.2903	3.0518
36.47	16.577	.200	.5080	-.004	-.0102	5.1613	3.2118
37.96	17.255	.220	.5588	-.004	-.0102	5.0322	3.4289
38.91	17.686	.240	.6096	-.004	-.0102	4.9032	3.6070
40.22	18.282	.260	.6604	-.004	-.0102	4.7742	3.8293
41.66	18.936	.280	.7112	-.003	-.0076	4.6452	4.0765
41.73	18.968	.300	.7620	-.003	-.0076	4.5161	4.2000
42.10	19.136	.310	.7874	-.003	-.0076	4.4516	4.2987

Failure assumed at 20% lateral displacement.
*After consolidation.

TABLE C.16 DIREST SHEAR TEST DATA, SAMPLE S16

Material: Dry fiber ground to powdered form

Normal stress = 3.452 kg/cm^2 Initial void ratio - 3.6849

Dry density* =20.51 pcf

Water content* = ...% Consolidation Pr - 3.452 kg/cm^2

Load (lbs)	Load (kg)	Lateral Displacement (in)	Lateral Displacement (cm)	Vertical Displacement (in)	Vertical Displacement (cm)	Area (cm^2)	Shear Stress (kg/cm^2)
6.39	2.905	.002	.0051	0.0	0.0	6.4386	.4512
11.65	5.295	.005	.0127	-.002	-.0051	6.4193	.8249
14.66	6.664	.008	.0203	-.002	-.0051	6.4000	1.0413
17.29	7.859	.010	.0254	-.003	-.0076	6.3871	1.2304
19.92	9.055	.015	.0381	-.004	-.0102	6.3548	1.4249
22.55	10.250	.019	.0483	-.005	-.0127	6.3289	1.6196
25.56	11.618	.025	.0635	-.006	-.0152	6.2903	1.8469
28.19	12.814	.033	.0838	-.007	-.0178	6.2387	2.0539
31.01	14.095	.045	.1143	-.008	-.0203	6.1613	2.2877
33.64	15.291	.060	.1524	-.009	-.0229	6.0645	2.5214
36.28	16.491	.082	.2083	-.010	-.0254	5.9225	2.7845
37.97	17.259	.100	.2540	-.010	-.0254	5.8064	2.9724
39.47	17.941	.120	.3048	-.010	-.0254	5.6774	3.1601
40.78	18.536	.140	.3556	-.011	-.0279	5.5484	3.3408
42.29	19.223	.165	.4191	-.011	-.0279	5.3871	3.5683
43.61	19.823	.190	.4826	-.010	-.0254	5.2258	3.7933
43.98	19.991	.200	.5080	-.010	-.0254	5.1613	3.8732
44.36	20.164	.205	.5207	-.010	-.0254	5.1290	3.9314
45.48	20.673	.230	.5842	-.010	-.0254	4.9677	4.1615
46.42	21.100	.245	.6223	-.010	-.0254	4.8709	4.3318
46.80	21.273	.255	.6477	-.010	-.0254	4.8064	4.4259
47.36	21.527	.270	.6858	-.010	-.0254	4.7097	4.5708
47.74	21.700	.280	.7112	-.010	-.0254	4.6452	4.6715
48.49	22.041	.300	.7620	-.010	-.0254	4.5161	4.8805

Failure assumed at 20% lateral displacement.

*After consolidation.

TABLE C.17 DIRECT SHEAR TEST DATA, SAMPLE S17

Material: Dry fibers ground to powedered form
Normal stress = 4.075 kg/cm^2 Initial void ratio = 3.5256
Dry density*= 21.23 pcf
Water content*= ...% Consolidation Pr = 4.075 kg/cm^2

Load (lbs)	Load (kg)	Lateral Displacement (in)	Lateral Displacement (cm)	Vertical Displacement (in)	Vertical Displacement (cm)	Area (cm^2)	Shear Stress (kg/cm^2)
6.76	3.073	.002	.0051	-.001	-.0025	6.4386	.4773
9.96	4.527	.004	.0102	-.001	-.0025	6.4257	.7045
12.96	5.891	.007	.0178	-.002	-.0051	6.4064	.9195
15.98	7.264	.010	.0254	-.003	-.0076	6.3871	1.1373
18.79	8.541	.013	.0330	-.004	-.0102	6.3678	1.3413
21.80	9.909	.016	.0406	-.006	-.0152	6.3485	1.5608
25.18	11.445	.022	.0559	-.007	-.0178	6.3096	1.8139
28.00	12.727	.027	.0686	-.009	-.0229	6.2774	2.0274
30.64	13.927	.034	.0864	-.010	-.0254	6.2321	2.2347
33.08	15.036	.043	.1092	-.012	-.0305	6.1742	2.4353
36.09	16.405	.059	.1499	-.014	-.0356	6.0709	2.7022
38.72	17.600	.084	.2134	-.015	-.0381	5.9096	2.9782
39.85	18.114	.100	.2540	-.016	-.0406	5.8064	3.1197
41.54	18.882	.124	.3149	-.016	-.0406	5.6518	3.3409
42.48	19.309	.140	.3556	-.016	-.0406	5.5484	3.4801
43.98	19.991	.165	.4191	-.016	-.0406	5.3871	3.7109
44.73	20.332	.180	.4572	-.017	-.0432	5.2903	3.8433
46.24	21.018	.200	.5080	-.017	-.0432	5.1613	4.0722
47.36	21.527	.220	.5588	-.017	-.0432	5.0322	4.2779
48.12	21.873	.235	.5969	-.017	-.0432	4.9355	4.4318
48.30	21.955	.265	.6731	-.017	-.0432	4.7419	4.6300
48.30	21.955	.270	.6858	-.017	-.0432	4.7097	4.6617
48.31	21.959	.275	.6985	-.017	-.0432	4.6774	4.6947
48.31	21.959	.300	.7620	-.017	-.0432	4.5161	4.8624

Failure assumed at 20% lateral displacement.
*After consolidation.

TABLE C.18 DIRECT SHEAR TEST DATA, SAMPLE S18

Material: Dry fibers ground to powdered form
Normal stress = 4.686 kg/cm^2 Initial void ratio = 3.2845
Dry density*= 22.43 pcf
Water content*= ...% Consolidation Pr = 4.686 kg/cm^2

Load (lbs)	Load (kg)	Lateral Displacement		Vertical Displacement		Area (cm^2)	Shear Stress (kg/cm^2)
		(in)	(cm)	(in)	(cm)		
7.14	3.245	.002	.0051	0.0	0.0	6.4386	.5040
13.72	6.236	.004	.0102	0.0	0.0	6.4257	.9705
19.74	8.973	.007	.0178	-.001	-.0025	6.4064	1.4006
25.56	11.618	.011	.0279	-.002	-.0051	6.3807	1.8208
31.20	14.182	.016	.0406	-.003	-.0076	6.3485	2.2339
34.02	15.464	.020	.0508	-.004	-.0102	6.3226	2.4458
36.84	16.745	.025	.0635	-.004	-.0102	6.2903	2.6620
39.47	17.941	.030	.0762	-.005	-.0127	6.2581	2.8668
42.85	19.477	.040	.1016	-.006	-.0152	6.1935	3.1447
46.99	21.359	.060	.1524	-.007	-.0178	6.0645	3.5219
48.49	22.041	.070	.1778	-.007	-.0178	5.9999	3.6736
50.37	22.895	.085	.2159	-.007	-.0178	5.9032	3.8784
52.26	23.755	.100	.2540	-.007	-.0178	5.8064	4.0912
54.32	24.691	.120	.3048	-.007	-.0178	5.6774	4.3490
55.64	25.291	.140	.3556	-.007	-.0178	5.5484	4.5583
57.14	25.973	.160	.4064	-.007	-.0178	5.4193	4.7927
57.89	26.314	.170	.4318	-.007	-.0178	5.3548	4.9141
58.65	26.659	.180	.4572	-.007	-.0178	5.2903	5.0392
60.71	27.595	.200	.5080	-.007	-.0178	5.1613	5.3465
63.16	28.709	.230	.5842	-.006	-.0152	4.9677	5.7791
65.03	29.559	.250	.6350	-.006	-.0152	4.8387	6.1089
66.73	30.332	.270	.6858	-.006	-.0152	4.7097	6.4403
68.42	31.100	.290	.7366	-.005	-.0127	4.5806	6.7895
69.36	31.527	.300	.7620	-.005	-.0127	4.5161	6.9810

Failure assumed at 20% lateral displacement.
*After consolidation.

TABLE C.19 DIRECT SHEAR TEST DATA, SAMPLE S19

Material: Dry fibers ground to powdered form

Normal stress - 6.550 kg/cm^2 Initial void ratio = 2.9808

Dry density*= 24.14 pcf

Water content*= ...% Consolidation Pr = 6.550 kg/cm^2

Load (lbs)	Load (kg)	Lateral Displacement		Vertical Displacement		Area (cm^2)	Shear Stress (kg/cm^2)
		(in)	(cm)	(in)	(cm)		
17.85	8.114	.004	.0102	-.001	.0025	6.4257	1.2627
37.21	16.914	.013	.0330	-.005	.0127	6.3678	2.6562
51.12	23.236	.025	.0635	-.006	.0152	6.2903	3.6939
53.38	24.264	.029	.0737	-.006	.0152	6.2644	3.8733
56.10	25.500	.033	.0838	-.007	.0178	6.2387	4.0874
58.45	26.568	.039	.0991	-.007	.0178	6.1999	4.2852
61.27	27.850	.047	.1194	-.008	.0203	6.1483	4.5297
63.72	28.964	.057	.1448	-.009	.0229	6.0838	4.7608
66.16	30.073	.072	.1829	-.009	.0229	5.9870	5.0230
67.66	30.755	.085	.2159	-.010	.0254	5.9032	5.2099
69.92	31.782	.100	.2540	-.010	.0254	5.8064	5.4736
71.99	32.723	.115	.2921	-.010	.0254	5.7097	5.7311
73.87	33.577	.130	.3302	-.010	.0254	5.6129	5.9821
75.75	34.432	.145	.3683	-.010	.0254	5.5161	6.2421
77.25	35.114	.160	.4064	-.010	.0254	5.4193	6.4794
78.94	35.882	.175	.4445	-.010	.0254	5.3226	6.7414
80.07	36.395	.185	.4699	-.009	.0229	5.2581	6.9217
81.58	37.082	.200	.5080	-.009	.0229	5.1613	7.1846
83.45	37.932	.220	.5588	-.010	.0254	5.0322	7.5379
85.71	38.959	.240	.6096	-.009	.0229	4.9032	7.9456
86.84	39.473	.255	.6477	-.009	.0229	4.8064	8.2126
88.15	40.068	.270	.6858	-.009	.0229	4.7097	8.5075
89.47	40.668	.285	.7239	-.009	.0229	4.6129	8.8161
90.60	41.182	.300	.7620	-.009	.0229	4.5161	9.1189

Failure assumed at 20% lateral displacement.

*After consolidation.

TABLE C.20 DIRECT SHEAR TEST DATA, SAMPLE S20

Material: Saturated fibers, ground to powdered form
Normal stress = 1.584 kg/cm^2
Dry density*= 24.89 pcf
Water content*= 185%
Consolidation Pr = 1.584 kg/cm^2

Load (lbs)	Load (kg)	Lateral Displacement		Vertical Displacement		Area (cm^2)	Shear Stress (kg/cm^2)
		(in)	(cm)	(in)	(cm)		
3.01	1.368	.003	.0076	-.002	-.0051	6.4323	.2127
6.01	2.732	.008	.0203	-.001	-.0025	6.4000	.4269
12.03	5.468	.012	.0305	-.001	-.0025	6.3741	.8578
14.66	6.664	.017	.0432	-.001	-.0025	6.3419	1.0508
17.48	7.945	.028	.0711	-.002	-.0051	6.2710	1.2669
19.73	8.968	.055	.1397	-.002	-.0051	6.0968	1.4709
20.30	9.227	.070	.1778	-.002	-.0051	5.9999	1.5379
21.05	9.568	.100	.2540	-.001	-.0025	5.8064	1.6478
21.62	9.827	.115	.2921	-.001	-.0025	5.7097	1.7211
22.36	10.164	.140	.3556	-.001	-.0025	5.5484	1.8319
23.12	10.509	.160	.4064	0.0	0.0	5.4193	1.9392
23.68	10.764	.180	.4572	0.0	0.0	5.2903	2.0347
24.44	11.109	.200	.5080	0.0	0.0	5.1613	2.1524
25.00	11.364	.220	.5588	-.001	-.0025	5.0322	2.2583
25.56	11.618	.240	.6096	-.001	-.0025	4.9032	2.3695
56.50	12.045	.260	.6604	+.001	+.0025	4.7742	2.5229
27.06	12.300	.290	.7366	+.002	+.0051	4.5806	2.6852
27.44	12.473	.300	.762	+.002	+.0051	4.5161	2.7619

Failure assumed at 20% lateral displacement.
*After consolidation.

TABLE C.21 DIRECT SHEAR TEST DATA, SAMPLE S21

Material: Saturated fibers ground to powdered form
Normal stress = 2.206 kg/cm^2
Dry density*= 27.83 pcf
Water content*= 159%
Consolidation Pr = 2.206 kg/cm^2

Load (lbs)	Load (kg)	Lateral Displacement (in)	Lateral Displacement (cm)	Vertical Displacement (in)	Vertical Displacement (cm)	Area (cm^2)	Shear Stress (kg/cm^2)
5.45	2.477	.002	.0051	0.0	0.0	6.4386	.3847
8.27	3.759	.007	.0178	-.002	-.0051	6.4064	.5868
11.27	5.123	.014	.0356	-.003	-.0076	6.3612	.8054
14.09	6.405	.024	.0609	-.004	-.0102	6.2969	1.0172
16.72	7.600	.035	.0889	-.005	-.0127	6.2258	1.2207
19.73	8.968	.050	.1270	-.006	-.0152	6.1290	1.4632
22.55	10.250	.070	.1778	-.007	-.0178	5.9999	1.7084
24.24	11.018	.085	.2159	-.008	-.0203	5.9032	1.8664
25.56	11.618	.100	.2540	-.008	-.0203	5.8064	2.0009
26.69	12.132	.115	2.921	-.008	-.0203	5.7097	2.1248
27.44	12.473	.130	.3302	-.008	-.0203	5.6129	2.2222
28.75	13.068	.150	.3810	-.008	-.0203	5.4839	2.3829
29.69	13.495	.170	.4318	-.008	-.0203	5.3548	2.5202
30.64	13.927	.190	.4826	-.007	-.0178	5.2258	2.6650
31.01	14.095	.200	.5080	-.007	-.0178	5.1613	2.7309
31.76	14.436	.215	.5461	-.006	-.0152	5.0645	2.8504
32.70	14.864	.240	.6096	-.004	-.0102	4.9037	3.0315
33.08	15.036	.250	.6350	-.004	-.0102	4.8387	3.1074
33.64	15.291	.265	.6731	-.002	-.0051	4.7419	3.2247
33.83	15.377	.285	.7239	0.0	0.0	4.6129	3.3335
34.21	15.55	.300	.7620	0.0	0.0	4.5161	3.4432

Failure assumed at 20% lateral displacement.
*After consolidation.

TABLE C.22 DIRECT SHEAR TEST DATA, SAMPLE S22

Material: Saturated fiber ground to powdered form.

Normal stress - 2.830 kg/cm^2

Dry density*= 26.04 pcf

Water content*= 175%

Consolidation Pr = 2.830 kg.cm^2

Load (lbs)	Load (kg)	Lateral Displacement (in)	Lateral Displacement (cm)	Vertical Displacement (in)	Vertical Displacement (cm)	Area (cm^2)	Shear Stress (kg/cm^2)
6.76	3.073	.002	.0051	0.0	0.0	6.4386	.4773
9.77	4.441	.005	.0127	0.0	0.0	6.4193	.6918
12.40	5.636	.009	.0229	0.0	0.0	6.3934	.8815
15.22	6.918	.015	.0381	-.001	-.0025	6.3548	1.0886
18.04	8.200	.025	.0635	-.002	-.0051	6.2903	1.3036
23.30	10.591	.047	.1194	-.002	-.0051	6.1483	1.7226
26.12	11.873	.063	.1600	-.003	-.0076	6.0452	1.9640
28.38	12.900	.080	.2032	-.003	-.0076	5.9355	2.1734
30.45	13.841	.100	.2540	-.003	-.0076	5.8064	2.3837
32.33	14.695	.120	.3048	-.003	-.0076	5.6774	2.5883
34.21	15.550	.144	.3658	-.002	-.0051	5.5225	2.8157
35.34	16.064	.160	.4064	-.002	-.0051	5.4193	2.9642
36.46	16.573	.175	.4445	-.002	-.0051	5.3226	3.1137
37.59	17.086	.200	.5080	-.002	-.0051	5.1613	3.3104
38.91	17.686	.210	.5334	-.002	-.0051	5.0968	3.4700
40.60	18.455	.230	.5842	-.001	-.0025	4.9677	3.7150
41.16	18.709	.245	.6223	0.0	0.0	4.8709	3.8409
41.92	19.055	.260	.6604	+.001	+.0025	4.7742	3.9912
42.66	19.391	.270	.6858	+.003	+.0076	4.7097	4.1172
43.04	19.564	.280	.7112	+.004	+.0102	4.6452	4.2117
43.98	19.991	.300	.7620	+.006	+.0152	4.5161	4.4266
44.36	20.164	.310	.7874	+.008	+.0203	4.4516	4.5296
44.54	20.245	.320	.8128	+.009	+.0229	4.3871	4.6147

Failure assumed at 20% lateral displacement.

*After consolidation.

TABLE C.23 DIRECT SHEAR TEST DATA, SAMPLE S23

Material: Saturated fibers ground to powdered form
Normal stress = 4.075 kg/cm^2
Dry density*= 28.12 pcf
Water content*= 157%
Consolidation Pr = 4.075 kg/cm^2

Load (lbs)	Load (kg)	Lateral Displacement		Vertical Displacement		Area (cm^2)	Shear Stress (kg/cm^2)
		(in)	(cm)	(in)	(cm)		
6.01	2.732	.003	.0076	0.0	0.0	6.4323	.4247
8.83	4.014	.006	.0152	-.001	-.0025	6.4130	.6259
11.65	5.295	.009	.0229	-.001	-.0025	6,3934	.8282
14.66	6.664	.014	.0356	-.002	-.0051	6.3612	1.0476
17.48	7.945	.020	.0508	-.002	-.0051	6.3226	1.2566
20.30	9.227	.027	.0686	-.003	-.0076	6.2774	.14699
22.93	10.423	.035	.0889	-.004	-.0102	6.2258	1.6742
25.94	11.791	.044	.1118	-.004	-.0102	6.1676	1.9118
28.38	12.900	.055	.1397	-.005	-.0127	6.0968	2.1159
31.01	14.095	.068	.1727	-.006	-.0152	6.0129	2.3441
33.83	15.377	.083	.2108	-.006	-.0152	5.9162	2.5991
36.28	16.491	.100	.2540	-.006	-.0152	5.8064	2.8401
37.21	16.914	.110	.2794	-.006	-.0152	5.7419	2.9457
38.72	17.600	.120	.3048	-.006	-.0152	5.6774	3.1000
41.16	18.709	.140	.3556	-.006	-.0152	5.5484	3.3720
42.10	19.136	.155	.3937	-.006	-.0152	5.4516	3.5102
43.98	19.991	.174	.4419	-.007	-.0152	5.3292	3.7512
46.62	21.191	.200	.5080	-.007	-.0178	5.1613	4.1057
48.12	21.873	.220	.5588	-.007	-.0178	5.0322	4.3466
49.62	22.555	.240	.6096	-.007	-.0178	4.9032	4.6000
51.32	23.327	.260	.6604	-.007	-.0178	4.7742	4.8861
54.88	24.945	.300	.7620	-.007	-.0178	4.5161	5.5236
55.82	25.373	.310	.7874	-.007	-.0178	4.4516	5.6997
56.39	25.632	.320	.8182	-.007	-.0178	4.3734	5.8609

Failure assumed at 20% lateral displacement.
*After consolidation.

TABLE C.24 DIRECT SHEAR TEST DATA, SAMPLE 24

Material: Saturated fibers ground to powdered form.
Normal stress = 6.55 kg/cm^2
Dry density*= 35.07 pcf
Water content*= 112%
Consolidation Pr = 6.55 kg/cm^2

Load (lbs)	Load (kg)	Lateral Displacement (in)	Lateral Displacement (cm)	Vertical Displacement (in)	Vertical Displacement (cm)	Area (cm^2)	Shear Stress (kg/cm^2)
6.39	2.905	.002	.0051	0.0	0.0	6.4386	.4512
16.35	7.432	.004	.0102	0.0	0.0	6.4257	1.1566
22.56	10.255	.006	.0152	0.0	0.0	6.4130	1.5991
28.38	12.900	.010	.0254	-.006	-.0157	6.3871	2.0197
31.20	14.182	.012	.0305	-.001	-.0025	6.3741	2.2249
37.22	16.918	.017	.0432	-.002	-.0051	6.3419	2.6677
42.85	19.477	.024	.0610	-.002	-.0051	6.2967	3.0932
46.62	21.191	.030	.0762	-.003	-.0076	6.2581	3.3862
51.88	23.582	.040	.1016	-.003	-.0076	6.1935	3.8075
56.39	25.632	.052	.1321	-.003	-.0076	6.1161	4.1909
58.83	26.741	.060	.1524	-.003	-.0076	6.0645	4.4094
61.09	27.768	.068	.1727	-.003	-.0076	6.0129	4.6181
63.15	28.705	.080	.2032	-.003	-.0076	5.9355	4.8362
65.41	29.732	.090	.2286	-.003	-.0076	5.8709	5.0643
68.04	30.927	.100	.2540	-.003	-.0076	5.8064	5.3264
71.42	32.464	.120	.3048	-.003	-.0076	5.6774	5.7181
73.87	33.577	.137	.3480	-.002	-.0051	5.5677	6.0307
75.94	34.518	.153	.3886	-.002	-.0051	5.4646	6.3167
77.25	35.114	.165	.4191	-.002	-.0051	5.3871	6.5182
79.51	36.141	.185	.4699	-.001	-.0025	5.2581	6.8734
81.58	37.082	.200	.5080	0.0	0.0	5.1613	7.1846
84.21	38.277	.233	.5918	+.003	+.0076	4.9484	7.7352
85.71	38.959	.260	.6604	+.005	+.0127	4.7742	8.1603

Failure assumed at 20% lateral displacement.
*After consolidation.

TABLE C.25 DIRECT SHEAR TEST DATA, SAMPLE S25

Material: Saturated fibers ground to powdered form.
Normal stress = 5.304 kg/cm^2
Dry density*= 31.71 pcf
Water content*= 132%
Consolidation Pr = 5.304 kg/cm^2

Load (lbs)	Load (kg)	Lateral Displacement (in)	Lateral Displacement (cm)	Vertical Displacement (in)	Vertical Displacement (cm)	Area (cm^2)	Shear Stress (kg/cm^2)
6.20	2.818	.003	.0076	0.0	0.0	6.4323	.4381
18.23	8.286	.009	.0229	-.001	-.0025	6.3934	1.2960
23.49	10.677	.015	.0381	-.002	-.0051	6.3548	1.6801
28.75	13.068	.024	.0610	-.003	-.0076	6.2967	2.0754
33.83	15.377	.035	.0889	-.004	-.0102	6.2258	2.4699
39.28	17.855	.050	.1270	-.005	-.0127	6.1290	2.9132
43.98	19.991	.068	.1727	-.005	-.0127	6.0129	3.3247
46.99	21.359	.080	.2032	-.005	-.0127	5.9355	3.5985
49.06	22.300	.090	.2286	-.005	-.0127	5.8709	3.7984
50.56	22.982	.100	.2540	-.005	-.0127	5.8064	3.9580
54.13	24.605	.120	.3048	-.005	-.0127	5.6774	4.3339
56.95	25.886	.140	.3556	-.005	-.0127	5.5484	4.6655
58.83	26.741	.155	.3937	-.005	-.0127	5.4516	4.9052
60.52	27.509	.177	.4496	-.004	-.0102	5.3096	5.1810
62.40	28.364	.185	.4699	-.004	-.0102	5.2581	5.3943
64.28	29.218	.200	.5080	-.004	-.0102	5.1613	5.6610
66.91	30.414	.222	.5639	-.004	-.0102	5.0193	6.0594
68.23	31.014	.235	.5969	-.003	-.0076	4.9355	6.2839
69.36	31.527	.250	.6350	-.002	-.0051	4.8387	6.5156
71.24	32.382	2.70	.6858	-.001	-.0025	4.7097	6.8756
72.93	33.150	.290	.7366	0.0	0.0	4.5806	7.2370
74.06	33.664	.300	.7620	+.001	+.0025	4.5161	7.4542
75.18	34.173	.315	.8001	+.001	+.0025	4.4193	7.7327

Failure assumed at 20% lateral displacement.
*After consolidation.

TABLE D.1 TRIAXIAL TEST DATA, SAMPLE CU-1
KAOLINITE

Consolidation pressure = 2.0 kg/cm^2
Angle between direction of compression and horizontal = 90°
σ_{1_f} = 3.634 kg/cm^2 A_f = .23
σ_{3_f} = 1.520 kg/cm^2 Water content* = 29.21%
U_f = .48 kg/cm^2 Dry density* = 93.21 pcf

Load (kg)	Displacement (cm)	Pore Pressure (kg/cm^2)	Axial Strain (%)	$\bar{\sigma}_1$ (kg/cm^2)	$\bar{\sigma}_3$ (kg/cm^2)
0.0	0.0	0.0	0.0	2.00	2.00
1.17	.05842	.01	0.756	2.099	1.99
6.31	.11938	.10	1.546	2.485	1.90
10.72	.16764	.25	2.171	2.739	1.75
15.27	.27432	.50	3.552	2.899	1.50
16.88	.33528	.55	4.341	2.973	1.45
18.20	.39116	.60	5.064	3.029	1.40
20.55	.51308	.61	6.644	3.199	1.39
21.87	.60198	.61	7.795	3.291	1.39
22.75	.65786	.60	8.518	3.362	1.40
23.64	.73152	.55	9.472	3.468	1.45
24.81	.83566	.55	10.820	3.536	1.45
25.10	.88392	.50	11.445	3.595	1.50
25.69	.98298	.48	12.728	3.634	1.52
25.84	1.04648	.46	13.550	3.646	1.54
25.84	1.12776	.43	14.603	3.650	1.57
24.52	1.34366	.33	17.398	3.579	1.67
23.93	1.43510	.34	18.582	3.497	1.66
21.58	1.52908	.33	19.799	3.302	1.67
20.55	1.57480	.34	20.391	3.202	1.66

$\bar{\sigma}_1$ and $\bar{\sigma}_3$ equal the major and minor effective principal stresses, respectively. Failure taken at maximum deviator stress or at 20% axial strain.

*Water content and dry density after consolidation.

TABLE D.2 TRIAXIAL TEST DATA, SAMPLE CU-2
KAOLINITE

Consolidation pressure = 4.0 kg/cm^2
Angle between direction of compression and horizonatal = 90°
σ_{1_f} = 5.219 kg/cm^2 A_f = .55
σ_{3_f} = 2.52 kg/cm^2 Water content = 28.28%
U_f = 1.48 kg/cm^2 Dry density = 94.65 pcf

Load (kg)	Displacement (cm)	Pore Pressure (kg/cm^2)	Axial Strain (%)	$\bar{\sigma}_1$ (kg/cm^2)	$\bar{\sigma}_3$ (kg/cm^2)
0.0	0.0	0.0	0.0	4.00	4.00
1.71	.0025	0.0	.032	4.162	4.00
4.57	.0178	.01	.231	4.422	3.99
4.43	.0736	0.0	.954	4.416	4.00
4.29	.1041	-.04	1.349	4.441	4.04
5.00	.1829	0.0	2.370	4.463	4.00
7.43	.2184	.10	2.830	4.585	3.90
14.14	.2438	.04	3.159	4.946	3.60
17.00	.2667	.60	3.456	4.957	3.40
20.71	.3149	.93	4.080	4.982	3.07
24.14	.3860	1.21	5.003	4.965	2.79
25.43	.4165	1.29	5.397	4.992	2.71
27.43	.4826	1.48	6.254	4.958	2.52
29.71	.5766	1.50	7.472	5.108	2.50
30.71	.6426	1.48	8.327	5.189	2.52
31.43	.7391	1.49	9.577	5.205	2.51
31.71	.7925	1.48	10.269	5.219	2.52
31.71	.8356	1.49	10.828	5.192	2.51
31.57	.8839	1.50	11.454	5.151	2.50
30.57	1.0236	1.39	13.264	5.124	2.61

$\bar{\sigma}_1$ and $\bar{\sigma}_3$ equal the major and minor effective principal stresses, respectively. Failure taken at maximum deviator stress or at 20% axial strain.

*Water content and dry density after consolidation.

TABLE D.3 TRIAXIAL TEST DATA, SAMPLE CU-3
KAOLINITE

Consolidation pressure = 5.50 kg/cm^2
Angle between direction of compression and horizontal = 90°
σ_{1_f} = 5.409 kg/cm^2 U_f = 3.06 kg/cm^2
A_f = 1.03
σ_{3_f} = 2.440 kg/cm^2 Water content = 27.85%
Dry density = 95.20 pcf

Load (kg)	Displacement (cm)	Pore Pressure (kg/cm^2)	Axial Strain (%)	$\bar{\sigma}_1$ (kg/cm^2)	$\bar{\sigma}_3$ (kg/cm^2)
0.0	0.0	0.0	0.0	5.500	5.50
1.28	.0102	.20	.141	5.450	5.30
6.71	.0254	.52	.352	5.764	4.98
9.57	.0432	.80	.598	5.817	4.70
11.28	.0584	1.00	.810	5.812	4.50
12.85	.0813	1.24	1.127	5.751	4.26
14.85	.1143	1.60	1.586	5.616	3.90
16.71	.1524	1.94	2.114	5.480	3.56
19.00	.2235	2.38	3.101	5.281	3.12
20.14	.2642	2.58	3.664	5.198	2.92
21.57	.3124	2.73	4.334	5.191	2.77
22.85	.3759	2.88	5.215	5.162	2.62
24.14	.4343	2.98	6.025	5.182	2.52
25.14	.4801	3.01	6.659	5.244	2.49
26.28	.5486	3.05	7.611	5.301	2.45
27.14	.6071	3.06	8.421	5.357	2.44
27.85	.6604	3.06	9.161	5.409	2.44
27.57	.7671	3.03	10.641	5.361	2.47
25.57	.8839	2.94	12.262	5.194	2.56
20.43	.9627	2.90	13.354	4.677	2.60

$\bar{\sigma}_1$ and $\bar{\sigma}_3$ equal the major and minor effective principal stresses, respectively. Failure taken at maximum deviator stress or at 20% axial strain.

*Water content and dry density after consolidation.

TABLE D.4 TRIAXIAL TEST DATA, SAMPLE CU-4
KAOLINITE

Consolidation pre-sure - 1.50 kg/cm^2
Angle between direction of compression and horizontal = 90°

σ_{1_f} = 2.561 kg/cm^2 U_f = .46 kg/cm^2

σ_{3_f} = 1.040 kg/cm^2 A_f = .30

Water content = 31.05%
Dry density = 90.71 pcf

Load (kg)	Displacement (cm)	Pore Pressure (kg/cm^2)	Axial Strain (%)	$\bar{\sigma}_1$ (kg/cm^2)	$\bar{\sigma}_3$ (kg/cm^2)
0.00	0.0000	0.00	0.000	1.500	1.50
2.00	.0127	0.00	.158	1.691	1.50
3.58	.0178	.04	.222	1.802	1.46
5.58	.0279	.14	.348	1.893	1.36
7.00	.0432	.20	.538	1.967	1.30
9.43	.0965	.35	1.203	2.042	1.15
12.00	.1905	.47	2.374	2.153	1.03
13.29	.2718	.49	3.388	2.239	1.01
14.00	.3251	.50	4.052	2.286	1.00
15.15	.4242	.50	5.287	2.375	1.00
16.15	.5588	.47	6.965	2.469	1.03
16.72	.6274	.43	7.819	2.546	1.07
17.00	.6604	.47	8.231	2.524	1.03
17.43	.7366	.45	9.181	2.566	1.05
17.58	.7798	.46	9.719	2.561	1.04
17.65	.8788	.42	10.954	2.585	1.08
17.79	.9804	.41	12.220	2.585	1.09
17.77	1.1227	.37	13.993	2.594	1.13
17.29	1.2598	.36	15.703	2.536	1.14
16.72	1.3386	.35	16.684	2.484	1.15

$\bar{\sigma}_1$ and $\bar{\sigma}_3$ equal the major and minor effective principal stresses, respectively. Failure taken at maximum deviator stress or at 20% axial strain.

*Water content and dry density after consolidation.

TABLE D.5 TRIAXIAL TEST DATA, SAMPLE CU-5
KAOLINITE

Consolidation pressure = 6.50 kg/cm^2
Angle between direction of compression and horizontal = 90°
σ_{1_f} = 8.184 kg/cm^2 A_f = .59
σ_{3_f} = 4.040 kg/cm^2 Water content = 26.45%
Dry density = 97.21 pcf
U_f = 2.46 kg/cm^2

Load (kg)	Displacement (cm)	Pore Pressure (kg/cm^2)	Axial Strain (%)	$\bar{\sigma}_1$ (kg/cm^2)	$\bar{\sigma}_3$ (kg/cm^2)
0.0	0.0000	0.00	0.000	6.500	6.50
1.43	.0203	.04	.271	6.613	6.46
3.57	.0483	.10	.644	6.781	6.40
8.57	.0605	.20	.806	7.214	6.30
16.71	.0787	.44	1.050	7.838	6.06
20.00	.0965	.61	1.287	8.013	5.89
23.57	.1194	.85	1.592	8.144	5.65
27.85	.1600	1.24	2.134	8.191	5.26
30.00	.1879	1.44	2.507	8.205	5.06
33.57	.2438	1.80	3.253	8.193	4.70
37.43	.3149	2.13	4.201	8.226	4.37
39.85	.3861	2.33	5.149	8.235	4.17
41.14	.5004	2.45	6.674	8.179	4.05
41.57	.5563	2.47	7.419	8.169	4.03
41.93	.6071	2.46	8.097	8.184	4.04
42.14	.6655	2.46	8.877	8.169	4.04
42.28	.7341	2.42	9.791	8.182	4.08
42.00	.8890	2.34	11.858	8.141	4.16
41.14	1.0135	2.29	13.518	8.035	4.21
40.14	1.0769	2.23	14.365	7.966	4.27

$\bar{\sigma}_1$ and $\bar{\sigma}_3$ equal the major and minor effective principal stresses, respectively. Failure taken at maximum deviator stress or at 20% axial strain.

*Water content and dry density after consolidation.

TABLE D.6 TRIAXIAL TEST DATA, SAMPLE CU-6
KAOLINITE

Consolidation pressure = 6.50 kg/cm^2
Angle between direction of compression and horizontal = 90°

σ_{1_f} = 8.176 kg/cm^2 A_f = .62

σ_{3_f} = 3.790 kg/cm^2 Water content = 29.40%
Dry density = 92.95 pcf

U_f = 2.71 kg/cm^2

Load (kg)	Displacement (cm)	Pore Pressure (kg/cm^2)	Axial Strain (%)	$\bar{\sigma}_1$ (kg/cm^2)	$\bar{\sigma}_3$ (kg/cm^2)
0.0	0.0	0.00	0.00	6.500	6.50
2.14	.0102	.04	.138	6.690	6.46
4.28	.0203	.09	.276	6.871	6.41
9.28	.0254	.16	.346	7.337	6.34
13.57	.0330	.29	.449	7.667	6.21
16.42	.0406	.38	.553	7.882	6.12
21.42	.0533	.64	7.26	8.155	5.86
24.28	.0660	.82	.898	8.276	5.68
27.14	.0787	1.00	1.071	8.397	5.50
30.00	.0965	1.22	1.313	8.474	5.28
32.85	.1168	1.47	1.589	8.518	5.03
34.71	.1321	1.61	1.797	8.567	4.89
37.14	.1575	1.80	2.143	8.622	4.70
39.99	.2438	2.30	3.318	8.372	4.20
41.57	.3277	2.53	4.458	8.256	3.97
42.85	.4293	2.68	5.840	8.174	3.82
43.62	.5004	2.71	6.808	8.176	3.79
44.28	.6096	2.72	8.294	8.161	3.78
43.85	.7087	2.70	9.642	8.075	3.80
34.28	.8001	2.58	10.886	7.216	3.92

$\bar{\sigma}_1$ and $\bar{\sigma}_3$ equal the major and minor effective principal stresses, respectively. Failure taken at maximum deviator stress or at 20% axial strain.

*Water content and dry density after consolidation.

TABLE D.7 TRIAXIAL TEST DATA, SAMPLE CU-7
KAOLINITE

Consolidation pressure = 2.50 kg/cm^2
Angle between direction of compression and horizontal = 90°

σ_{1_f} = 2.848 kg/cm^2 A_f = .79

σ_{3_f} = 1.170 kg/cm^2 Water content = 33.78%
Dry density = 87.26 pcf

U_f = 1.33 kg/cm^2

Load (kg)	Displacement (cm)	Pore Pressure (kg/cm^2)	Axial Strain (%)	$\bar{\sigma}_1$ (kg/cm^2)	$\bar{\sigma}_3$ (kg/cm^2)
0.00	0.0000	0.00	0.000	2.50	2.50
1.43	.0254	.05	.340	2.594	2.45
5.72	.0356	.18	.477	2.895	2.32
7.15	.0432	.25	.579	2.968	2.25
10.15	.0787	.50	1.056	3.014	2.00
12.86	.1549	.89	2.077	2.882	1.61
14.29	.2311	1.04	3.098	2.859	1.46
15.43	.3200	1.18	4.290	2.812	1.32
16.01	.3734	1.22	5.005	2.817	1.28
16.86	..4851	1.30	6.503	2.792	1.20
17.29	.5410	1.30	7.252	2.820	1.20
17.79	.6223	1.32	8.342	2.828	1.18
18.15	.6833	1.32	9.161	2.845	1.18
18.43	.7569	1.32	10.147	2.853	1.18
18.61	.8052	1.33	10.793	2.847	1.17
18.72	.8433	1.33	11.304	2.848	1.17
18.75	.8788	1.35	11.781	2.822	1.15
18.15	.9703	1.34	13.007	2.755	1.16
15.72	1.0338	1.32	13.858	2.548	1.18
15.01	1.0465	1.31	14.028	2.493	1.19

$\bar{\sigma}_1$ and $\bar{\sigma}_3$ equal the major and minor effective principal stresses, respectively. Failure taken at maximum deviator stress or at 20% axial strain.

*Water content and dry density after consolidation.

TABLE D.8 TRIAXIAL TEST DATA, SAMPLE CU-8
KAOLINITE

Consolidation pressure - 3.50 kg/cm^2
Angle between direction of compression and horizontal = 90°

σ_{1_f} = 3.627 kg/cm^2 A_f = .93

σ_{3_f} = 1.700 kg/cm^2 Water content = 33.58%
Dry density = 87.49 pcf

U_f = 1.80 kg/cm^2

Load (kg)	Displacement (cm)	Pore Pressure (kg/cm^2)	Axial Strain (%)	$\bar{\sigma}_1$ (kg/cm^2)	$\bar{\sigma}_3$ (kg/cm^2)
0.00	0.0000	0.00	0.000	3.500	3.50
2.72	.0228	.01	.313	3.737	3.49
5.57	.0254	.10	.347	3.905	3.40
8.43	.0356	.23	.487	4.034	3.27
11.86	.0533	.45	.730	4.123	3.05
14.14	.0787	.68	1.078	4.093	2.82
17.00	.1295	1.00	1.773	4.021	2.50
18.43	.1702	1.16	2.329	3.979	2.34
19.86	.2311	1.37	3.164	3.882	2.13
20.86	.2921	1.50	3.998	3.824	2.00
21.57	.3581	1.61	4.902	3.757	1.89
22.00	.3962	1.67	5.423	3.725	1.83
22.43	.4623	1.72	6.327	3.693	1.78
22.86	.5537	1.81	7.579	3.614	1.69
23.00	.5842	1.80	7.996	3.627	1.70
23.10	.6401	1.83	8.761	3.589	1.67
23.11	.7036	1.87	9.630	3.532	1.63
22.86	.8103	1.90	11.090	3.450	1.60
21.43	.9576	1.90	13.107	3.295	1.60
19.86	1.0719	1.93	14.671	3.114	1.57

$\bar{\sigma}_1$ and $\bar{\sigma}_3$ equal the major and minor effective principal stresses, respectively. Failure taken at maximum deviator stress or at 20% axial strain.

*Water content and dry density after consolidation.

TABLE D.9 TRIAXIAL TEST DATA, SAMPLE CU-9
KAOLINITE

Consolidation pressure - 4.50 kg/cm^2
Angle between direction of compression and horizontal = 90°

σ_{1_f} = 4.500 kg/cm^2 A_f = 1.0

σ_{3_f} = 2.210 kg/cm^2 Water content = 32.33%
Dry density = 88.91 pcf

U_f = 2.29 kg/cm^2

Load (kg)	Displacement (cm)	Pore Pressure (kg/cm^2)	Axial Strain (%)	$\bar{\sigma}_1$ (kg/cm^2)	$\bar{\sigma}_3$ (kg/cm^2)
0.00	0.0000	0.00	0.000	4.500	4.50
4.71	.0038	.11	.053	4.884	4.39
9.00	.0127	.32	.177	5.122	4.18
11.86	.0279	.58	.389	5.158	3.92
14.71	.0533	.86	.742	5.171	3.64
16.86	.0823	1.18	1.144	5.068	3.32
17.57	.0965	1.27	1.342	5.047	3.23
18.29	.1118	1.37	1.554	5.018	3.13
19.00	.1270	1.48	1.766	4.978	3.02
19.71	.1499	1.59	2.084	4.933	2.91
21.14	.2083	1.80	2.896	4.852	2.70
21.86	.2515	1.95	3.497	4.762	2.55
22.29	.2921	2.04	4.062	4.702	2.46
22.57	.3302	2.10	4.592	4.658	2.40
23.14	.4013	2.21	5.581	4.580	2.29
23.39	.4749	2.29	6.605	4.500	2.21
23.43	.5080	2.30	7.064	4.483	2.20
23.43	.5486	2.31	7.629	4.463	2.19
21.57	.7289	2.37	10.138	4.162	2.13
19.71	.8229	2.40	11.444	3.929	2.10

$\bar{\sigma}_1$ and $\bar{\sigma}_3$ equal the major and minor effective principal stresses, respectively. Failure taken at maximum deviator stress or at 20% axial strain.

*Water content and dry density after consolidation.

TABLE D.10 TRIAXIAL TEST DATA, SAMPLE CU-FC1
75% KAOLINITE/25% FIBER BY VOLUME

Consolidation pressure = 3.0 kg/cm^2
Angle between direction of compression and horizontal = 90°

σ_{1_f} = 3.958 kg/cm^2 A_f = .65

σ_{3_f} = 1.200 kg/cm^2 Water content = 46.71%

U_f = 1.800 kg/cm^2 Dry density = 70.16 pcf

Load (kg)	Displacement (cm)	Pore Pressure (kg/cm^2)	Axial Strain (%)	$\bar{\sigma}_1$ (kg/cm^2)	$\bar{\sigma}_3$ (kg/cm^2)
0.00	0.0000	0.00	0.000	3.000	3.00
3.71	.0254	0.10	.331	3.385	2.90
8.00	.0406	.30	.529	3.745	2.70
10.85	.0686	.54	.894	3.872	2.46
12.28	.0864	.69	1.126	3.904	2.31
15.14	.1448	.98	1.887	3.972	2.02
16.57	.1829	1.14	2.384	3.984	1.86
18.00	.2337	1.29	3.046	4.002	1.71
19.43	.2946	1.42	3.841	4.034	1.58
20.14	.3327	1.50	4.337	4.019	1.50
21.57	.4445	1.63	5.794	4.039	1.37
22.29	.5309	1.71	6.919	4.016	1.29
22.71	.5944	1.76	7.747	3.992	1.24
23.00	.6680	1.80	8.707	3.958	1.20
23.33	.7950	1.88	10.363	3.867	1.12
23.46	.8890	1.90	11.588	3.825	1.10
23.57	.9322	1.91	12.151	3.809	1.09
23.71	1.0058	1.95	13.110	3.756	1.05
23.85	1.1176	2.00	14.568	3.676	1.00
24.86	1.3792	2.10	17.978	3.577	.90

$\bar{\sigma}_1$ and $\bar{\sigma}_3$ equal the major and minor effective principal stresses, respectively. Failure taken at maximum deviator stress or at 20% axial strain.

*Water content and dry density after consolidation.

TABLE D.11 TRIAXIAL TEST DATA, SAMPLE CU-FC2
75% KAOLINITE/25% FIBER BY VOLUME

Consolidation pressure = 4.50 kg/cm^2
Angle between direction of compression and horizontal = 90°

σ_{1_f} = 5.898 kg/cm^2 A_f = .64

σ_{3_f} = 1.96 kg/cm^2 Water content = 45.29%
Dry density = 70.50 pcf

U_f = 2.54 kg/cm^2

Load (kg)	Displacement (cm)	Pore Pressure (kg/cm^2)	Axial Strain (%)	$\bar{\sigma}_1$ (kg/cm^2)	$\bar{\sigma}_3$ (kg/cm^2)
0.00	0.0000	0.00	0.000	4.500	4.50
4.14	.0229	.08	.307	4.890	4.42
7.00	.0483	.15	.647	5.143	4.35
9.86	.0533	.22	.715	5.396	4.28
14.14	.0660	.38	.886	5.718	4.12
17.00	.0813	.53	1.090	5.887	3.97
19.85	.1041	.77	1.397	5.962	3.73
21.28	.1168	.90	1.567	5.988	3.60
24.14	.1524	1.19	2.044	6.006	3.31
27.00	.1981	1.46	2.657	6.038	3.04
29.14	.2413	1.69	3.237	6.026	2.81
31.57	.3023	1.91	4.054	6.044	2.59
33.43	.3683	2.10	4.940	6.024	2.40
34.85	.4343	2.24	5.826	6.003	2.26
36.28	.5105	2.38	6.848	5.974	2.12
37.00	.5639	2.44	7.564	5.960	2.06
37.71	.6299	2.54	8.449	5.898	1.96
38.71	.8357	2.70	11.209	5.719	1.80
39.07	1.0973	2.85	14.718	5.449	1.65
39.07	1.2624	2.95	16.932	5.252	1.55

$\bar{\sigma}_1$ and $\bar{\sigma}_3$ equal the major and minor effective principal stresses, respectively. Failure taken at maximum deviator stress or at 20% axial strain.

*Water content and dry density after consolidation.

TABLE D.12 TRIAXIAL TEST DATA, SAMPLE CU-FC3
75% KAOLINITE/25% FIBER BY VOLUME

Consolidation pressure = 2.00 kg/cm^2
Angle between direction of compression and horizontal = 90°

σ_{1_f} = 2.882 kg/cm^2 A_f = .58

σ_{3_f} = .77 kg/cm^2 Water content = 51.05%

U_f = 1.23 kg/cm^2 Dry density = 66.90 pcf

Load (kg)	Displacement (cm)	Pore Pressure (kg/cm2)	Axial Strain (%)	$\bar{\sigma}_1$ (kg/cm^2)	$\bar{\sigma}_3$ (kg/cm^2)
0.00	0.0000	0.00	0.000	2.000	2.00
4.43	.0102	.10	.147	2.469	1.90
7.29	.0381	.28	.549	2.654	1.72
10.15	.0762	.53	1.099	2.765	1.47
11.58	.1499	.55	2.163	2.801	1.34
13.01	.2134	.80	3.079	2.826	1.20
14.43	.3073	.90	4.436	2.879	1.10
15.00	.3454	.95	4.986	2.888	1.05
15.43	.3810	.99	5.499	2.891	1.01
16.15	.4521	1.02	6.526	2.927	.98
16.57	.5029	1.08	7.259	2.903	.92
16.93	.5588	1.09	8.066	2.917	.91
17.29	.6223	1.11	8.983	2.919	.89
17.72	.6909	1.12	9.973	2.937	.88
18.01	.7315	1.14	10.559	2.937	.86
18.29	.8128	1.17	11.732	2.913	.83
18.72	.9347	1.20	13.492	2.888	.80
18.93	.9906	1.21	14.299	2.883	.79
19.29	1.0465	1.23	15.106	2.882	.77
19.58	1.1455	1.25	16.535	2.858	.75

$\bar{\sigma}_1$ and $\bar{\sigma}_3$ equal the major and minor effective principal stresses, respectively. Failure taken at maximum deviator stress or at 20% axial strain.

*Water content and dry density after consolidation.

TABLE D.13 TRIAXIAL TEST DATA, SAMPLE CU-FC4
75% KAOLINITE/25% FIBER BY VOLUME

Consolidation pressure = 6.00 kg/cm^2
Angle between direction of compression and horizontal = 90°

σ_{1_f} = 7.279 kg/cm^2 A_f = .73

σ_{3_f} = 2.52 kg/cm^2 Water content = 40.51%
Dry density = 75.44 pcf

U_f = 3.48 kg/cm^2

Load (kg)	Displacement (cm)	Pore Pressure (kg/cm^2)	Axial Strain (%)	$\bar{\sigma}_1$ (kg/cm^2)	$\bar{\sigma}_3$ (kg/cm^2)
0.00	0.0000	0.00	0.000	6.000	6.00
3.57	.0203	.05	.265	6.415	5.95
6.43	.0279	.12	.364	6.715	5.88
10.71	.0457	.35	.596	7.039	5.65
13.57	.0635	.59	.828	7.166	5.41
16.43	.0838	.84	1.093	7.280	5.16
19.28	.1118	1.15	1.457	7.329	4.85
23.71	.1600	1.60	2.086	7.429	4.40
26.43	.1981	1.90	2.582	7.459	4.10
29.43	.2515	2.22	3.277	7.494	3.78
32.29	.3124	2.50	4.072	7.542	3.50
35.00	.3886	2.78	5.066	7.555	3.22
36.43	.4343	2.90	5.662	7.583	3.10
37.85	.4851	3.05	6.324	7.575	2.95
39.29	.5842	3.26	7.615	7.476	2.74
40.00	.6756	3.48	8.807	7.279	2.52
40.71	.8001	3.58	10.429	7.178	2.42
41.71	.9652	3.72	12.581	7.037	2.28
42.86	1.1887	3.95	15.496	6.776	2.05
43.86	1.3767	4.14	17.946	6.555	1.86

$\bar{\sigma}_1$ and $\bar{\sigma}_3$ equal the major and minor effective principal stresses, respectively. Failure taken at maximum deviator stress or at 20% axial strain.

*Water content and dry density after consolidation.

TABLE D.14 TRIAXIAL TEST DATA, SAMPLE CU-CF1
54% FIBER/46% KAOLINITE BY VOLUME

Consolidation pressure = 3.00 kg/cm^2
Angle between direction of compression and horizontal = 90°

σ_{1_f} = 4.202 kg/cm^2

σ_{3_f} = .94 kg/cm^2

U_f = 2.06 kg/cm^2

A_f = .63

Water content - 54.28%
Dry density = 60.36 pcf

Load (kg)	Displacement (cm)	Pore Pressure (kg/cm^2)	Axial Strain (%)	$\bar{\sigma}_1$ (kg/cm^2)	$\bar{\sigma}_3$ (kg/cm^2)
0.00	0.0000	0.00	0.000	3.000	3.00
8.28	.0381	.18	.513	3.689	2.82
14.00	.0864	.50	1.164	3.961	2.50
18.71	.1575	.81	2.122	4.124	2.19
24.43	.2972	1.20	4.004	4.277	1.80
26.57	.3759	1.35	5.065	4.314	1.65
28.85	.4902	1.53	6.605	4.315	1.47
30.85	.6172	1.65	8.316	4.337	1.35
32.00	.7163	1.71	9.651	4.343	1.29
32.43	.7620	1.74	10.267	4.333	1.26
33.28	.8611	1.80	11.602	4.307	1.20
33.85	.9373	1.83	12.628	4.293	1.17
34.64	1.0262	1.89	13.826	4.262	1.11
35.00	1.1049	1.91	14.887	4.236	1.09
35.28	1.1532	1.94	15.537	4.207	1.06
35.18	1.2446	2.00	16.769	4.092	1.00
36.90	1.3437	2.00	18.104	4.191	1.00
37.93	1.4453	2.02	19.473	4.175	.95
38.62	1.4859	2.06	20.021	4.202	.94
39.13	1.5215	2.08	20.499	4.205	.92

$\bar{\sigma}_1$ and $\bar{\sigma}_3$ equal the major and minor effective principal stresses, respectively. Failure taken at maximum deviator stress or at 20% axial strain.

*Water content and dry density after consolidation.

TABLE D.15 TRIAXIAL TEST DATA, SAMPLE CU-CF2
54% FIBER/46% KAOLINITE BY VOLUME

Consolidation pressure = 4.00 kg/cm^2
Angle between direction of compression and horizontal = 90°

σ_{1_f} = 5.668 kg/cm^2 A_f = .63

σ_{3_f} = 1.140 kg/cm^2 Water content = 59.85%

U_f = 2.86 kg/cm^2 Dry density = 57.35 pcf

Load (kg)	Displacement (cm)	Pore Pressure (kg/cm^2)	Axial Strain (%)	$\bar{\sigma}_1$ (kg/cm^2)	$\bar{\sigma}_3$ (kg/cm^2)
0.00	0.0000	0.00	0.000	4.000	4.00
5.28	.0102	.03	.139	4.579	3.97
11.00	.0432	.22	.592	5.043	3.78
13.85	.0787	.40	1.080	5.182	3.60
16.00	.1067	.54	1.463	5.281	3.46
19.57	.1676	.88	2.299	5.328	3.12
23.57	.2642	1.34	3.623	5.283	2.66
26.43	.3581	1.65	4.911	5.252	2.35
29.43	.4749	1.93	6.514	5.247	2.07
31.28	.5791	2.11	7.942	5.216	1.89
32.57	.6706	2.24	9.196	5.176	1.76
34.21	.7976	2.38	10.938	5.139	1.62
35.25	.8382	2.40	11.495	5.203	1.60
36.62	.8890	2.45	12.192	5.264	1.55
39.37	1.0058	2.55	13.794	5.369	1.45
42.47	1.1328	2.65	15.536	5.493	1.35
44.88	1.2395	2.71	16.999	5.592	1.29
46.94	1.3309	2.79	18.253	5.641	1.21
49.01	1.4579	2.86	19.994	5.668	1.14
49.18	1.4834	2.87	20.343	5.654	1.13

$\bar{\sigma}_1$ and $\bar{\sigma}_3$ equal the major and minor effective principal stresses, respectively. Failure taken at maximum deviator stress or at 20% axial strain.

*Water content and dry density after consolidation.

TABLE D.16 TRIAXIAL TEST DATA, SAMPLE CU-CF3
54% FIBER/46% KAOLINITE BY VOLUME

Consolidation pressure = 6.00 kg/cm^2
Angle between direction of compression and horizontal = 90°

σ_{1_f} = 8.659 kg/cm^2 A_f = .61
σ_{3_f} = 1.770 kg/cm^2 Water content - 56.06%
Dry density = 64.92 pcf
U_f = 4.23 kg/cm^2

Load (kg)	Displacement (cm)	Pore Pressure (kg/cm^2)	Axial Strain (%)	$\bar{\sigma}_1$ (kg/cm^2)	$\bar{\sigma}_3$ (kg/cm^2)
0.00	0.0000	0.00	0.000	6.000	6.00
4.00	.0254	.08	.354	6.474	5.92
9.71	.0356	.19	.495	7.152	5.81
15.43	.0572	.40	.796	7.727	5.60
20.57	.0914	.72	1.274	8.101	5.28
26.14	.1448	1.27	2.017	8.288	4.73
31.53	.2209	1.98	3.078	8.266	4.02
44.25	.3073	2.64	4.281	9.245	3.36
49.41	.4140	3.09	5.767	9.379	2.91
52.51	.5156	3.40	7.182	9.371	2.60
55.26	.6172	3.61	8.598	9.407	2.39
57.67	.7569	3.80	10.544	9.367	2.20
58.70	.8712	3.92	12.136	9.246	2.08
59.73	1.0008	4.00	13.940	9.142	2.00
60.08	1.0617	4.03	14.789	9.083	1.97
60.08	1.1303	4.07	15.745	8.963	1.93
60.77	1.2319	4.12	17.160	8.874	1.88
61.45	1.3411	4.18	18.681	8.762	1.82
61.97	1.4351	4.23	19.991	8.659	1.77
62.14	1.4681	4.25	20.450	8.618	1.75

$\bar{\sigma}_1$ and $\bar{\sigma}_3$ equal the major and minor effective principal stresses, respectively. Failure taken at maximum deviator stress or at 20% axial strain.

*Water content and dry density after consolidation.

The following tests were not carried up to assumed 20% strain.

TABLE D.17 TRIAXIAL TEST DATA, SAMPLE CU-CF4
54% FIBER/46% KAOLINITE BY VOLUME

Consolidation pressure = 1.50 kg/cm^2
Angle between direction of compression and horizontal = 90°

σ_{1_f} = --- kg/cm^2 A_f = ---

σ_{3_f} = --- kg/cm^2 Water content = 64.82%
Dry density = 41.18 pcf

U_f = --- kg/cm^2

TABLE D.18 TRIAXIAL TEST DATA, SAMPLE CU-CF5
54% FIBER/46% KAOLINITE BY VOLUME

Consolidation pressure = 3.00 kg/cm^2
Angle between direction of compression and horizontal = 90°

σ_{1_f} = --- kg/cm^2 A_f = ---

σ_{3_f} = --- kg/cm^2 Water content = 64.42%
Dry density = 41.33 pcf

U_f = --- kg/cm^2

The following tests were not carried up to assumed 20% strain

TABLE D.19 TRIAXIAL TEST DATA, SAMPLE CU-CF6
54% FIBERS/46% KAOLINITE BY VOLUME

Consolidation pressure = 4.00 kg/cm^2
Angle between direction of compression and horizontal = 90°

σ_{1_f} = --- kg/cm^2 A_f = ---

σ_{3_f} = --- kg/cm^2 Water content = 58.56%
Dry density = 43.59 pcf

U_f = --- kg/cm^2

TABLE D.20 TRIAXIAL TEST DATA, SAMPLE CU-CF7
54% FIBERS/46% KAOLINITE BY VOLUME

Consolidation pressure = 5.00 kg/cm^2
Angle between direction of compression and horizontal = 90°

σ_{1_f} = --- kg/cm^2 A_f = ---

σ_{3_f} = --- kg/cm^2 Water content = 58.11%
Dry density = 43.78 pcf

U_f = --- kg/cm^2

TABLE D.21 TRIAXIAL TEST DATA, SAMPLE CD-FC1
25% FIBER/75% KAOLINITE BY VOLUME

Consolidation pressure = 4.00 kg/cm^2
Angle between direction of compression and horizontal = 90°

σ_{1_f} = 10.806 kg/cm^2 at 20% strain
σ_{3_f} = 4.00 kg/cm^2

Water content = 38.73%
Dry density = 75.69 pcf
Volume after consolidation = 72.60cm^3

Load (kg)	Displacement (cm)	Volume Change (cm^3)	Axial Strain (%)	$\bar{\sigma}_1$ (kg/cm^2)	$\bar{\sigma}_3$ (kg/cm^2)
0.00	0.0000	0.00	0.000	4.000	4.00
7.42	.01778	.15	.236	4.771	4.00
11.71	.0483	.22	.639	5.213	4.00
16.28	.0914	.35	1.212	5.680	4.00
22.28	.1626	.56	2.154	6.284	4.00
27.00	.2286	.72	3.029	6.749	4.00
29.43	.2642	.81	3.499	6.986	4.00
33.44	.3175	.98	4.207	7.376	4.00
45.83	.4115	1.27	5.452	8.585	4.00
51.68	.5232	1.51	6.933	9.107	4.00
56.49	.6350	1.76	8.413	9.512	4.00
60.63	.7468	1.99	9.894	9.839	4.00
62.34	.8001	2.10	10.600	9.967	4.00
64.75	.8890	2.27	11.778	10.130	4.00
67.51	.9982	2.45	13.226	10.303	4.00
69.91	1.0998	2.69	14.572	10.448	4.00
72.32	1.1913	2.89	15.783	10.594	4.00
74.04	1.2954	3.06	17.163	10.657	4.00
76.11	1.3963	3.22	18.50	10.748	4.00
78.17	1.5095	3.38	20.10	10.810	4.00

$\bar{\sigma}_1$ and $\bar{\sigma}_3$ equal the major and minor effective principal stresses, respectively. Failure taken at maximum deviator stress or at 20% axial strain.

*Water content and dry density after consolidation.

TABLE D.22 TRIAXIAL TEST DATA, SAMPLE CD-FC2
25% FIBER/75% KAOLINITE BY VOLUME

Consolidation pressure = 2.50 kg/cm^2
Angle between direction of compression and horizontal = 90°

σ_{1_f} = 7.782 kg/cm^2
σ_{3_f} = 2.500 kg/cm^2

Water content = 42.44%
Dry density = 73.47 pcf
Volume after consolidation = 59.28cm^3

Load (kg)	Displacement (cm)	Volume Change (cm^3)	Axial Strain (%)	$\bar{\sigma}_1$ (kg/cm^2)	$\bar{\sigma}_3$ (kg/cm^2)
0.00	0.0000	0.00	0.000	2.500	2.50
7.00	.0254	.06	.357	3.337	2.50
8.57	.0483	.10	.679	3.522	2.50
10.71	.0939	.25	1.322	3.773	2.50
13.43	.1702	.50	2.394	4.086	2.50
17.00	.2819	.89	3.966	4.488	2.50
19.57	.3734	1.19	5.252	4.769	2.50
21.14	.4267	1.38	6.002	4.940	2.50
23.85	.5334	1.70	7.503	5.224	2.50
25.86	.6147	1.97	8.647	5.431	2.50
28.71	.7366	2.31	10.362	5.712	2.50
30.85	.8306	2.60	11.684	5.918	2.50
32.71	.9144	2.84	12.863	6.091	2.50
34.00	.9754	3.00	13.720	6.206	2.50
36.00	1.0566	3.20	14.864	6.386	2.50
37.28	1.1252	3.35	15.829	6.489	2.50
40.71	1.2268	3.59	17.258	6.801	2.50
47.24	1.3437	3.80	18.901	7.409	2.50
49.65	1.3894	3.90	19.545	7.628	2.50
51.37	1.4224	3.97	20.009	7.782	2.50

$\bar{\sigma}_1$ and $\bar{\sigma}_3$ equal the major and minor effective principal stresses, respectively. Failure taken at maximum deviator stress or at 20% axial strain.

*Water content and dry density after consolidation.

TABLE D.23 TRIAXIAL TEST DATA, SAMPLE CD-FC3
25% FIBERS/75% KAOLINITE BY VOLUME

Consolidation pressure = 1.50 kg/cm^2
Angle between direction of compression and horizontal - 90°

σ_{1_f} = 3.873 kg/cm^2
σ_{3_f} = 1.50 kg/cm^2

Water content = 51.84%
Dry density = 66.39 pcf
Volume after consolidation = 70.59cm^3

Load (kg)	Displacement (cm)	Volume Change (cm^3)	Axial Strain (%)	$\bar{\sigma}_1$ (kg/cm^2)	$\bar{\sigma}_3$ (kg/cm^2)
0.00	0.0000	0.00	0.000	1.500	1.50
2.17	0.0152	.01	0.208	1.725	1.50
4.74	0.0660	.18	0.900	1.989	1.50
6.31	0.1193	.34	1.628	2.148	1.50
7.60	0.1727	.51	2.355	2.277	1.50
9.74	0.2794	.90	3.809	2.486	1.50
11.45	0.3785	1.25	5.159	2.648	1.50
13.31	0.4953	1.63	6.753	2.820	1.50
14.74	0.5892	1.91	8.034	2.947	1.50
15.88	0.6807	2.20	9.281	3.045	1.50
17.74	0.8128	2.55	11.081	3.200	1.50
19.31	0.9271	2.90	12.639	3.328	1.50
20.88	1.0617	3.25	14.475	3.445	1.50
22.16	1.1557	3.45	15.756	3.539	1.50
23.31	1.2319	3.61	16.795	3.624	1.50
24.17	1.2877	3.76	17.557	3.687	1.50
25.03	1.3512	3.90	18.423	3.746	1.50
25.88	1.4122	4.05	19.254	3.803	1.50
26.31	1.4351	4.09	19.566	3.834	1.50
26.88	1.4681	4.12	20.01	3.873	1.50

$\bar{\sigma}_1$ and $\bar{\sigma}_3$ equal the major and minor effective principal stresses, respectively. Failure taken at maximum deviator stress or at 20% axial strain.

*Water content and dry density after consolidation.

TABLE D.24 TRIAXIAL TEST DATA, SAMPLE CD-CF1
54% FIBER/46% KAOLINITE BY VOLUME

Consolidation pressure = 4.50 kg/cm^2
Angle between direction of compression and horizontal = 90°

σ_{1_f} = 12.372 kg/cm^2
σ_{3_f} = 4.50 kg/cm^2

Water content = 48.96%
Dry density = 63.06 pcf
Volume after consolidation = 67.04 cm^3

Load (kg)	Displacement (cm)	Volume Change (cm^3)	Axial Strain (%)	$\bar{\sigma}_1$ (kg/cm^2)	$\bar{\sigma}_3$ (kg/cm^2)
0.00	0.0000	0.00	0.000	4.500	4.50
5.86	.0127	.03	.177	5.128	4.50
10.29	.0394	.10	.547	5.599	4.50
16.15	.1016	.31	1.412	6.216	4.50
18.43	.1321	.41	1.836	6.453	4.50
23.00	.2007	.69	2.789	6.924	4.50
25.86	.2464	.88	3.425	7.215	4.50
29.29	.3048	1.10	4.237	7.559	4.50
34.15	.3962	1.45	5.508	8.039	4.50
43.74	.4902	1.79	6.815	8.993	4.50
51.65	.5817	2.10	8.086	9.758	4.50
55.43	.6731	2.42	9.357	10.093	4.50
58.53	.7442	2.65	10.346	10.362	4.50
61.28	.8179	2.89	11.369	10.590	4.50
64.72	.9042	3.18	12.570	10.874	4.50
70.22	1.0541	3.60	14.654	11.295	4.50
73.67	1.1379	3.85	15.818	11.559	4.50
77.45	1.2344	4.11	17.160	11.833	4.50
81.23	1.3335	4.39	18.538	12.098	4.50
85.36	1.4376	4.63	19.985	12.372	4.50

$\bar{\sigma}_1$ and $\bar{\sigma}_3$ equal the major and minor effective principal stresses, respectively. Failure taken at maximum deviator stress or at 20% axial strain.

*Water content and dry density after consolidation.

TABLE D.25 TRIAXIAL TEST DATA, SAMPLE CD-CF2
54% FIBER/46% KAOLINITE BY VOLUME

Consolidation pressure = 3.50 kg/cm^2
Angle between direction of compression and horizontal = 90°

σ_{1_f} = 10.060 kg/cm^2
σ_{3_f} = 3.50 kg/cm^2

Water Content = 54.85%
Dry density = 59.05 pcf
Volume after consolidation = 70.98cm^3

Load (kg)	Displacement (cm)	Volume Change (cm^3)	Axial Strain (%)	$\bar{\sigma}_1$ (kg/cm^2)	$\bar{\sigma}_3$ (kg/cm^2)
0.00	0.0000	0.00	0.000	3.500	3.50
5.57	.0152	.03	.203	4.088	3.50
9.71	.0457	.15	.609	4.523	3.05
14.00	.0965	.38	1.286	4.969	3.05
18.00	.1549	.60	2.064	5.381	3.50
22.86	.2388	.96	3.179	5.874	3.50
27.00	.3226	1.31	4.296	6.285	3.50
30.86	.4064	1.65	5.413	6.662	3.50
34.86	.4978	2.00	6.631	7.043	3.50
41.23	.5893	2.32	7.848	7.655	3.50
51.90	.7391	2.86	9.844	8.658	3.50
54.99	.8433	3.19	11.231	8.907	3.50
59.12	.9829	3.51	13.092	9.218	3.50
61.87	1.0820	3.88	14.411	9.426	3.50
64.63	1.1760	4.10	15.663	9.620	3.50
66.35	1.2522	4.30	16.678	9.726	3.50
68.75	1.3462	4.51	17.929	9.874	3.50
70.47	1.4249	4.70	18.978	9.969	3.50
71.51	1.4605	4.79	19.452	10.035	3.50
72.19	1.5011	4.87	19.993	10.060	3.50

$\bar{\sigma}_1$ and $\bar{\sigma}_3$ equal the major and minor effective principal stresses, respectively. Failure taken at maximum deviator stress or at 20% axial strain.

*Water content and dry density after consolidation.

TABLE D.26 TRIAXIAL TEST DATA, SAMPLE CD-CF3
54% FIBERS/46% KAOLINITE BY VOLUME

Consolidation pressure = 2.50 kg/cm^2
Angle between direction of compression and horizontal = 90°

σ_{1_f} = 8.126 kg/cm^2
σ_{3_f} = 2.50 kg/cm^2

Water content = 56.77%
Dry density = 59.24 pcf
Volume after consolidation = 66.09 cm^3

Load (kg)	Displacement (cm)	Volume Change (cm^3)	Axial Strain (%)	$\bar{\sigma}_1$ (kg/cm^2)	$\bar{\sigma}_3$ (kg/cm^2)
0.00	0.0000	0.00	0.000	2.500	2.50
7.86	0.0228	.10	0.312	3.370	2.50
11.43	0.0812	.25	1.109	3.758	2.50
16.43	0.1879	.53	2.566	4.289	2.50
19.29	0.2616	.77	3.571	4.587	2.50
22.86	0.3632	1.08	4.958	4.948	2.50
26.72	0.4775	1.40	6.518	5.329	2.50
28.15	0.5283	1.59	7.211	5.467	2.50
31.58	0.6273	1.90	8.563	5.796	2.50
33.86	0.7035	2.10	9.603	6.005	2.50
39.84	0.8280	2.50	11.302	6.572	2.50
46.03	0.9398	2.80	12.827	7.146	2.50
48.44	1.0210	3.20	13.937	7.357	2.50
49.47	1.0591	3.15	14.457	7.427	2.50
50.84	1.1277	3.30	15.393	7.519	2.50
52.56	1.1963	3.50	16.329	7.648	2.50
55.66	1.3030	3.75	17.785	7.879	2.50
57.72	1.3817	3.95	18.860	8.032	2.50
59.10	1.4478	4.12	19.761	8.107	2.50
59.44	1.4655	4.15	20.00	8.126	2.50

$\bar{\sigma}_1$ and $\bar{\sigma}_3$ equal the major and minor effective principal stresses, respectively. Failure taken at maximum deviator stress or at 20% axial strain.

*Water content and dry density after consolidation.

TABLE D.27 TRIAXIAL TEST DATA, SAMPLE CD-F1
ALL FIBER

Consolidation pressure = 1.50 kg/cm^2
Angle between direction of compression and horizontal = 90°

σ_{1_f} = 5.032 kg/cm^2
σ_{3_f} = 1.500 kg/cm^2

Water content = 144.57%
Dry density = 29.09 pcf
Volume after consolidation = 58.70cm^3

Load (kg)	Displacement (cm)	Volume Change (cm^3)	Axial Strain (%)	$\bar{\sigma}_1$ (kg/cm^2)	$\bar{\sigma}_3$ (kg/cm^2)
0.00	0.0000	0.00	0.000	1.500	1.50
2.14	.0152	.10	.238	1.733	1.50
3.57	.0305	.21	.476	1.889	1.50
4.28	.0457	.34	.714	1.966	1.50
5.71	.0838	.62	1.309	2.121	1.50
7.14	.1372	1.09	2.142	2.277	1.50
8.57	.2083	1.65	3.253	2.431	1.50
10.71	.3175	2.65	4.958	2.663	1.50
11.43	.3581	3.00	5.593	2.741	1.50
13.14	.4547	3.80	7.100	2.924	1.50
14.57	.5359	4.46	8.369	3.076	1.50
16.57	.6375	5.30	9.956	3.289	1.50
18.28	.7188	6.00	11.226	3.472	1.50
20.43	.8153	6.74	12.733	3.697	1.50
24.43	.9779	8.05	15.272	4.117	1.50
26.71	1.0592	8.60	16.541	4.349	1.50
29.28	1.1430	9.22	17.850	4.613	1.50
30.00	1.1709	9.42	18.286	4.685	1.50
32.86	1.2649	10.22	19.754	4.983	1.50
33.57	1.2878	10.40	20.112	5.055	1.50

$\bar{\sigma}_1$ and $\bar{\sigma}_3$ equal the major and minor effective principal stresses, respectively. Failure taken at maximum deviator stress or at 20% axial strain.

*Water content and dry density after consolidation.

TABLE D.28 TRIAXIAL TEST DATA, SAMPLE CD-F2
ALL FIBER

Consolidation pressure = 3.00 kg/cm^2
Angle between direction of compression and horizontal = 90°

σ_{1_f} = 10.858 kg/cm^2
σ_{3_f} = 3.00 kg.cm^2

Water content = 113.22%
Dry density = 35.02 pcf
Volume after consolidation = 61.16 cm^3

Load (kg)	Displacement (cm)	Volume Change (cm^3)	Axial Strain (%)	$\bar{\sigma}_1$ (kg/cm^2)	$\bar{\sigma}_3$ (kg/cm^2)
0.00	0.0000	0.00	0.000	3.000	3.00
1.86	.0076	.10	.117	3.198	3.00
4.72	.0229	.14	.351	3.502	3.00
7.57	.0457	.22	.702	3.803	3.00
10.43	.0813	.40	1.248	4.104	3.00
14.72	.1600	.85	2.457	4.550	3.00
17.57	.2235	1.22	3.432	4.843	3.00
20.57	.2870	1.58	4.407	5.149	3.00
23.72	.3607	1.95	5.538	5.464	3.00
26.14	.4166	2.26	6.397	5.705	3.00
29.00	.4877	2.62	7.488	5.984	3.00
31.86	.5512	2.97	8.464	6.264	3.00
35.00	.6223	3.30	9.556	6.563	3.00
46.53	.7645	4.10	11.740	7.687	3.00
54.10	.8357	4.38	12.832	8.408	3.00
60.98	.9728	5.20	14.939	9.036	3.00
63.39	1.0211	5.50	15.679	9.254	3.00
71.30	1.1506	6.35	17.669	9.975	3.00
77.15	1.2446	7.03	19.112	10.508	3.00
83.00	1.3386	7.98	20.55	11.075	3.00

$\bar{\sigma}_1$ and $\bar{\sigma}_3$ equal the major and minor effective principal stresses, respectively. Failure taken at maximum deviator stress or at 20% axial strain.

*Water content and dry density after consolidation.

TABLE D.29 TRIAXIAL TEST DATA, SAMPLE CD-F3
ALL FIBERS

Consolidation pressure = 4.50 kg/cm^2
Angle between direction of compression and horizontal = 90°

σ_{1_f} = 13.74 kg/cm^2

σ_{3_f} = 4.50 kg/cm^2

Water content = 100.17%
Dry density = 35.23 pcf
Volume after consolidation = 63.87cm^3

Load (kg)	Displacement (cm)	Volume Change (cm^3)	Axial Strain (%)	$\bar{\sigma}_1$ (kg/cm^2)	$\bar{\sigma}_3$ (kg/cm^2)
0.00	0.0000	0.00	0.000	4.500	4.50
3.29	.0102	.05	.161	4.824	4.50
10.43	.0330	.10	.524	5.526	4.50
16.15	.0686	.21	1.088	6.082	4.50
19.00	.0991	.30	1.571	6.355	4.50
21.86	.1346	.42	2.135	6.625	4.50
26.43	.2083	.70	3.304	7.050	4.50
30.43	.2642	.95	4.190	7.421	4.50
34.00	.3251	1.20	5.157	7.744	4.50
37.24	.3886	1.47	6.165	8.030	4.50
53.07	.5029	1.99	7.978	9.475	4.50
57.54	.5639	2.25	8.945	9.859	4.50
64.76	.6807	2.80	10.798	10.463	4.50
71.30	.7899	3.30	12.531	10.990	4.50
78.18	.8890	3.78	14.102	11.545	4.50
86.09	1.0008	4.34	15.875	12.169	4.50
91.94	1.0846	4.73	17.205	12.614	4.50
100.54	1.1888	5.26	18.857	13.275	4.50
104.67	1.2369	5.51	19.620	13.588	4.50
108.79	1.2852	5.76	20.388	13.896	4.50

$\bar{\sigma}_1$ and $\bar{\sigma}_3$ equal the major and minor effective principal stresses, respectively. Failure taken at maximum deviator stress or at 20% axial strain.

*Water content and dry density after consolidation.

TABLE D.30 TRIAXIAL TEST DATA, SAMPLE CD-F4
ALL FIBERS

Consolidation pressure = 3.00 kg/cm^2
Angle between direction of compression and horizontal = 90°

σ_{1_f} = 9.123 kg/cm^2
σ_{3_f} = 3 kg/cm^2

Water content = 118.81%
Dry density = 31.36 pcf
Volume after consolidation = 62.84cm^3

Load (kg)	Displacement (cm)	Volume Change (cm^3)	Axial Strain (%)	$\bar{\sigma}_1$ (kg/cm^2)	$\bar{\sigma}_3$ (kg/cm^2)
0.00	0.0000	0.00	0.000	3.000	3.00
4.86	.0178	.08	.289	3.474	3.00
7.86	.0483	.22	.785	3.765	3.00
9.86	.0889	.44	1.447	3.957	3.00
12.14	.1448	.75	2.356	4.173	3.00
15.72	.2362	.90	3.844	4.499	3.00
18.57	.2870	1.07	4.671	4.761	3.00
21.43	.3556	1.40	5.787	5.019	3.00
22.72	.3886	1.55	6.324	5.134	3.00
27.14	.4902	1.80	7.978	5.514	3.00
30.00	.5588	2.15	9.094	5.761	3.00
32.57	.6223	2.47	10.127	5.981	3.00
37.29	.7315	3.10	11.905	6.379	3.00
44.09	.8204	3.61	13.352	6.964	3.00
55.62	.9322	4.00	15.171	7.928	3.00
58.20	.9906	4.60	16.121	8.151	3.00
62.32	1.0643	5.02	17.320	8.476	3.00
65.08	1.1227	5.33	18.271	8.683	3.00
70.07	1.2141	5.85	19.759	9.063	3.00
72.99	1.2675	6.15	20.627	9.280	3.00

$\bar{\sigma}_1$ and $\bar{\sigma}_3$ equal the major and minor effective principal stresses, respectively. Failure taken at maximum deviator stress or at 20% axial strain.

*Water content and dry density after consolidation.

TABLE D.31 TRIAXIAL TEST DATA, SAMPLE CD-F5
ALL FIBERS

Consolidation pressure = 4.50 kg/cm^2
Angle between direction of compression and horizontal = 90°

$_1f$ = 13.152 kg/cm^2
$_3f$ = 4.500 kg/cm^2

Water content - 96.65%
Dry density = 33.99 pcf*
Volume after consolidation = 64.04 cm^3

Load (kg)	Displacement (cm)	Volume Change (cm^3)	Axial Strain (%)	$\bar{\sigma}_1$ (kg/cm^2)	$\bar{\sigma}_3$ (kg/cm^2)
0.00	0.0000	0.00	0.000	4.500	4.50
5.57	.0203	.06	.336	5.024	4.50
8.57	.0432	.15	.715	5.305	4.50
11.57	.0787	.29	1.303	5.582	4.50
13.28	.1016	.40	1.682	5.739	4.50
16.28	.1448	.60	2.396	6.013	4.50
18.00	.1676	.73	2.774	6.170	4.50
21.71	.2261	1.01	3.741	6.503	4.50
26.28	.2997	1.40	4.960	6.909	4.50
31.00	.3734	1.85	6.179	7.326	4.50
36.25	.4470	2.24	7.398	7.782	4.50
51.73	.5461	2.81	9.038	9.143	4.50
59.64	.6680	3.50	11.056	9.794	4.50
66.17	.7391	3.98	12.233	10.342	4.50
71.33	.8229	4.36	13.620	10.738	4.50
75.81	.8839	4.69	14.629	11.088	4.50
83.37	.9855	5.24	16.311	11.669	4.50
90.25	1.0668	5.66	17.656	12.191	4.50
101.95	1.1938	6.34	19.758	13.066	4.50
104.01	1.2192	6.49	20.178	13.216	4.50

$\bar{\sigma}_1$ and $\bar{\sigma}_3$ equal the major and minor effective principal stresses, respectively. Failure taken at maximum deviator stress or at 20% axial strain.

*Water content and dry density after consolidation.

TABLE D.32 TRIAXIAL TEST DATA, SAMPLE CD-F6
ALL FIBERS

Consolidation pressure = 1.50 kg/cm^2
Angle between direction of compression and horizontal = 90°

σ_{1_f} = 4.991 kg/cm^2 at
σ_{3_f} = 1.50 kg/cm^2

Water content = 150.22%
Dry density = 27.69 pcf
Volume after consolidation = 70.37cm^3

Load (kg)	Displacement (cm)	Volume Change (cm^3)	Axial Strain (%)	$\bar{\sigma}_1$ (kg/cm^2)	$\bar{\sigma}_3$ (kg/cm^2)
0.00	0.0000	0.00	0.000	1.500	1.50
2.57	.0229	.20	.364	1.729	1.50
4.14	.0635	.58	1.011	1.869	1.50
6.43	.1498	1.40	2.387	2.071	1.50
7.43	.1430	1.79	3.075	2.159	1.50
9.00	.2616	2.45	4.167	2.297	1.50
10.43	.3251	3.07	5.178	2.423	1.50
12.29	.4115	3.89	6.554	2.585	1.50
14.00	.4851	4.57	7.727	2.733	1.50
15.29	.5334	5.02	8.496	2.844	1.50
17.14	.6019	5.61	9.588	3.003	1.50
18.72	.6655	6.19	10.599	3.137	1.50
21.14	.7493	6.90	11.935	3.342	1.50
23.72	.8306	7.60	13.229	3.559	1.50
27.14	.9398	8.55	14.968	3.844	1.50
30.72	1.0389	9.40	16.547	4.140	1.50
33.43	1.1125	10.10	17.719	4.366	1.50
35.86	1.1709	10.60	18.650	4.565	1.50
39.22	1.2344	11.18	19.662	4.843	1.50
44.04	1.2827	11.57	20.430	5.242	1.50

$\bar{\sigma}_1$ and $\bar{\sigma}_3$ equal the major and minor effective principal stresses, respectively. Failure taken at maximum deviator stress or at 20% axial strain.

*Water content and dry density after consolidation.

TABLE D.33 TRIAXIAL TEST DATA, SAMPLE CU-F1
ALL FIBERS

Consolidation pressure = 2.50 kg/cm^2
Angle between direction of compression and horizontal = 90°

σ_{1_f} = 4.950 kg/cm^2 at 15 1/2 % strain Water content = 143.29%
Dry density = 28.88 pcf

σ_{3_f} = 0.0 kg/cm^2 at 15 1/2 % strain

Load (kg)	Displacement (cm)	Pore Pressure (kg/cm^2)	Axial Strain (%)	$\bar{\sigma}_1$ (kg/cm^2)	$\bar{\sigma}_3$ (kg/cm^2)
0.00	0.0000	0.00	0.000	2.500	2.50
6.29	.0330	.10	.514	2.989	2.40
8.43	.0559	.15	.869	3.138	2.35
9.86	.0813	.24	1.265	3.178	2.26
11.29	.1041	.32	1.621	3.227	2.18
12.71	.1295	.42	2.016	3.254	2.08
14.14	.1549	.50	2.412	3.301	2.00
16.28	.1956	.63	3.044	3.358	1.87
19.14	.2489	.94	3.874	3.295	1.56
22.00	.3048	1.04	4.744	3.436	1.46
24.86	.3632	1.24	5.654	3.470	1.26
29.43	.4749	1.59	7.393	3.479	.91
32.71	.5563	1.85	8.658	3.466	.65
39.79	.7289	2.20	11.347	3.626	.30
48.39	.8382	2.38	13.047	4.087	.12
54.24	.9195	2.45	14.312	4.431	.05
56.99	1.0008	2.50	15.577	4.536	0.00
59.05	1.0566	2.50	16.447	4.652	0.00
62.04	1.1557	2.51	17.989	4.786	-.01
64.56	1.1989	2.51	18.661	4.950	-.01

$\bar{\sigma}_1$ and $\bar{\sigma}_3$ equal the major and minor effective principal stresses, respectively. Failure taken at maximum deviator stress or at 20% axial strain.

*Water content and dry density after consolidation.

TABLE D.34 TRIAXIAL TEST DATA, SAMPLE CU-F2
ALL FIBERS

Consolidation pressure = 0.50 kg/cm^2
Angle between direction of compression and horizontal = 90°

σ_{1_f} = 1.126 kg/cm^2
σ_{3_f} = 0.34 kg/cm^2
U_f = 0.16 kg/cm^2

A_f = 0.20
Water content = 246.88%
Dry density = 19.10 pcf

Load (kg)	Displacement (cm)	Pore Pressure (kg/cm^2)	Axial Strain (%)	$\bar{\sigma}_1$ (kg/cm^2)	$\bar{\sigma}_3$ (kg/cm^2)
0.00	0.0000	0.00	0.00	0.500	0.50
3.00	.0831	.05	1.08	.648	.45
5.30	.1956	.10	2.55	.745	.40
6.80	.2883	.13	3.76	.807	.37
7.90	.4473	.14	5.84	.858	.36
8.90	.5743	.14	7.49	.911	.36
9.50	.7061	.14	9.22	.937	.36
10.00	.8529	.15	11.13	.944	.35
11.40	.9896	.15	12.92	1.014	.35
12.10	1.1094	.15	14.48	1.042	.35
12.90	1.2842	.15	16.76	1.068	.35
13.80	1.4089	.15	18.39	1.103	.35
14.70	1.5336	.16	20.02	1.126	.34
15.90	1.6584	.16	21.65	1.173	.34

$\bar{\sigma}_1$ and $\bar{\sigma}_3$ equal the major and minor effective principal stresses, respectively. Failure taken at maximum deviator stress or at 20% axial strain.

*Water content and dry density after consolidation.

TABLE D.35 TRIAXIAL TEST DATA, SAMPLE CU-F3
ALL FIBERS

Consolidation pressure = 0.50 kg/cm^2
Angle between direction of compression and horizontal = 90°

σ_{1_f} = .773 kg/cm^2
σ_{3_f} = 0.00 kg/cm^2
U_f = .50 kg/cm^2
A_f = 0.65
Water content = 299.61%
Dry density = 16.90 pcf

Load (kg)	Displacement (cm)	Pore Pressure (kg/cm^2)	Axial Strain %	$\bar{\sigma}_1$ (kg/cm^2)	$\bar{\sigma}_3$ (kg/cm^2)
0.00	0.0000	0.00	0.00	0.500	0.50
3.00	0.1194	0.24	1.51	0.436	0.26
5.00	.2032	0.36	2.57	0.430	0.14
6.30	.2896	0.44	3.67	0.421	0.06
7.00	.4039	0.48	5.12	0.416	0.02
8.70	.5410	0.50	6.85	0.483	0.00
9.60	.6731	0.50	8.53	0.523	0.00
10.50	.8433	0.50	10.68	0.559	0.00
11.60	.9855	0.50	12.48	0.605	0.00
12.70	1.1481	0.50	14.54	0.646	0.00
14.00	1.3132	0.50	16.64	0.695	0.00
15.10	1.4453	0.50	18.31	0.735	0.00
15.70	1.5240	0.50	19.31	0.755	0.00
16.90	1.6485	0.50	20.88	0.796	0.00

$\bar{\sigma}_1$ and $\bar{\sigma}_3$ equal the major and minor effective principal stresses, respectively. Failure taken at maximum deviator stress or at 20% axial strain.

*Water content and dry density after consolidation.

TABLE D.36 TRIAXIAL TEST DATA, SAMPLE CU-F4, ALL FIBERS

Consolidation pressure = 3.50 kg/cm^2
Angle between direction of compression and horizontal = 90°

σ_{1_f} = 4.738 kg/cm^2 A_f = 0.72 kg/cm^2
σ_{3_f} = .39 kg/cm^2 Water content = 158.53%
U_f = 3.11 kg/cm^2 Dry density = 30.15 pcf

Load (kg)	Displacement (cm)	Pore Pressure (kg/cm2)	Axial Strain (%)	$\bar{\sigma}_1$ (kg/cm^2)	$\bar{\sigma}_3$ (kg/cm^2)
0.00	0.0000	0.00	0.00	3.500	3.50
4.15	.0625	0.00	.88	3.793	3.50
15.25	.2035	.27	2.87	4.283	3.23
21.45	.3914	.53	5.52	4.413	2.97
29.20	.5088	.84	7.18	4.590	2.66
36.60	.6495	1.20	9.16	4.668	2.30
43.30	.7747	1.54	10.93	4.707	1.96
49.30	.8687	1.90	12.26	4.681	1.60
55.30	.9939	2.20	14.02	4.686	13.0
60.50	1.0879	2.50	15.35	4.647	1.00
65.50	1.1816	2.71	16.67	4.677	.79
69.20	1.2756	2.90	18.00	4.641	.60
73.20	1.3304	3.02	18.77	4.715	.48
76.30	1.4166	3.11	19.99	4.738	.39
77.60	1.4478	3.15	20.43	4.748	.35

$\bar{\sigma}_1$ and $\bar{\sigma}_3$ equal the major and minor effective principal stresses, respectively. Failure taken at maximum deviator stress or at 20% axial strain.

*Water content and dry density after consolidation.

TABLE D.37 TRIAXIAL TEST DATA, SAMPLE CU-F5, ALL FIBERS

Consolidation pressure = 1.0 kg/cm^2
Angle between direction of compression and horizontal = 90°

σ_{1_f} = 1.715 kg/cm^2 A_f = .58

σ_{3_f} = 0.0 kg/cm^2 Water content = 234.4%

U_f = 1.00 kg/cm^2 Dry density = 20.86 pcf

Load (kg)	Displacement (cm)	Pore Pressure (kg/cm^2)	Axial Strain (%)	$\bar{\sigma}_1$ (kg/cm^2)	$\bar{\sigma}_3$ (kg/cm^2)
0.00	0.0000	0.00	0.00	0.000	0.00
1.60	.0127	.12	.16	.976	.88
7.80	.0973	.39	1.25	1.071	.61
12.80	.2113	.63	2.70	1.116	.37
15.90	.3297	.80	4.22	1.112	.20
17.80	.4226	.91	5.41	1.098	.09
19.00	.5072	.92	6.50	1.144	.08
21.00	.5958	.96	7.63	1.201	.04
22.20	.7102	.98	9.10	1.228	.02
23.90	.8242	.99	10.56	1.290	.01
25.50	.9721	1.00	12.46	1.336	0.00
27.00	1.0990	1.00	14.08	1.388	0.00
29.40	1.2088	1.00	15.49	1.488	0.00
32.00	1.3526	1.00	17.33	1.584	0.00
34.00	1.4752	1.00	18.91	1.651	0.00
36.90	1.6104	1.00	20.64	1.753	0.00

$\bar{\sigma}_1$ and $\bar{\sigma}_3$ equal the major and minor effective principal stresses, respectively. Failure taken at maximum deviator stress or at 20% axial strain.

*Water content and dry density after consolidation.

TABLE D.38 TRIAXIAL TEST DATA, SAMPLE CU-F6, ALL FIBERS

Consolidation pressure = 1.00 kg/cm^2
Angle between direction of compression and horizontal = 90°

σ_{1_f} = 1.340 kg/cm^2 A_f = .75

σ_{3_f} = 0.0 kg/cm^2 Water content = n.a.%

U_f = 1.00 kg/cm^2 Dry density = n.a. pcf

Load (kg)	Displacement (cm)	Pore Pressure (kg/cm^2)	Axial Strain (%)	$\bar{\sigma}_1$ (kg/cm^2)	$\bar{\sigma}_3$ (kg/cm^2)
0.00	0.0000	0.00	0.00	1.000	1.00
5.00	.0257	.07	.32	1.267	.93
7.10	.0686	.24	.87	1.236	.76
8.20	.1407	.39	1.79	1.154	.61
9.10	.2057	.49	2.61	1.109	.51
10.10	.2400	.58	3.05	1.082	.42
11.50	.3053	.66	3.88	1.087	.34
12.04	.3635	.72	4.62	1.079	.28
13.00	.4219	.75	5.37	1.081	.25
13.20	.4800	.80	6.11	1.038	.20
14.00	.4973	.86	6.33	1.026	.14
15.00	.5898	.87	7.53	1.067	.13
16.00	.6515	.87	8.29	1.122	.13
16.20	.7236	.88	9.21	1.114	.12
16.80	.7922	.92	10.08	1.101	.08
18.80	.9294	.95	11.82	1.170	.05
20.00	1.0668	.98	13.57	1.188	.02
21.20	1.2586	1.00	16.02	1.203	0.00
22.80	1.3716	1.00	17.45	1.272	0.00
24.80	1.5773	1.00	20.07	1.340	0.00

$\bar{\sigma}_1$ and $\bar{\sigma}_3$ equal the major and minor effective principal stresses, respectively. Failure taken at maximum deviator stress or at 20% axial strain.

*Water content and dry density after consolidation.

TABLE D.39 TRIAXIAL TEST DATA, SAMPLE CU-F7
ALL FIBERS

Consolidation pressure = 2.03 kg/cm^2
Angle between direction of compression and horizontal = 90°

σ_{1_f} = 4.032 kg/cm^2
σ_{3_f} = .02 kg/cm^2
U_f = 2.01 kg/cm^2

A_f = 0.50
Water content = 169.81%
Initial dry density = 29.70 pcf

Load (kg)	Displacement (cm)	Pore Pressure (kg/cm^2)	Axial Strain (%)	$\bar{\sigma}_1$ (kg/cm^2)	$\bar{\sigma}_3$ (kg/cm^2)
0.00	0.0000	0.00	0.000	2.03	2.03
2.87	0.0813	0.00	.05	2.459	2.03
4.30	0.0914	0.02	.024	2.652	2.01
6.45	0.1168	0.08	.73	2.906	1.95
8.60	0.1524	0.12	1.42	3.179	1.91
10.03	0.1626	0.19	1.61	3.317	1.84
11.46	0.1727	0.25	1.81	3.465	1.78
13.61	0.1930	0.43	2.20	3.593	1.60
15.05	0.2159	0.58	2.64	3.644	1.45
17.20	0.2565	0.80	3.42	3.717	1.23
19.35	0.3175	1.02	4.60	3.773	1.01
21.50	0.3988	1.25	6.16	3.800	0.78
24.36	0.5613	1.58	9.30	3.758	0.45
25.79	0.6579	1.71	11.15	3.750	0.32
27.23	0.7518	1.82	12.96	3.758	0.21
28.66	0.8484	1.90	14.82	3.785	0.13
30.09	0.9296	1.94	16.39	3.856	0.09
31.53	1.0135	1.99	18.00	3.910	0.04
32.96	1.0897	2.01	19.47	3.993	0.02
34.39	1.1582	2.02	20.79	4.089	0.01

$\bar{\sigma}_1$ and $\bar{\sigma}_3$ equal the major and minor effective principal stresses, respectively. Failure tkane at maximum deviator stress or at 20% axial strain.

*Water content and dry density after consolidation.